

**Functional, Structural and Molecular Investigations
into Experimental Type-1 and Type-2 Diabetes-
induced Cardiomyopathy**

By

Alicia D'Souza

A thesis submitted in partial fulfilment for the requirements of the degree of Doctor of
Philosophy at the University of Central Lancashire

February 2011

DECLARATION

I declare that while registered as a candidate for the research degree, I have not been a registered candidate or enrolled student for another award of the University or other academic or professional institution. No material contained in the thesis has been used in any other submission for an academic award and is solely my own work.

ABSTRACT

Epidemiological studies have implicated that hyperglycemia (HG), even in the absence of overt diabetes mellitus (DM) may elicit adverse cardiac outcomes including diastolic dysfunction and heart failure (HF), possibly due in part to structural remodelling of the myocardium. This study investigated the relationship between HG, left ventricle (LV) remodelling and underlying molecular events at 2 ends of the spectrum of glucose (dys)metabolic states- in prediabetes and in overt chronic type 2 DM (T2DM) using the spontaneously diabetic Goto-Kakizaki (GK) rat as a model of prediabetes that progresses to overt T2DM. LV isolations from 2 and 18-month old male Goto-Kakizaki (GK) rats and age-matched male Wistar controls grouped on the basis of age, fasting plasma glucose and following an oral glucose tolerance test (OGTT) into prediabetic and chronic mild T2DM groups were used to assess remodelling changes and underlying transforming Growth Factor β 1 (TGF β 1) activity, pro-hypertrophic Akt-p70S6K signalling and gene expression profile of the ECM and Ca²⁺ mediators using histological, immunohistochemical, immunoblotting and quantitative gene expression analyses and compared to age-matched Wistar control rats. LV remodelling in the prediabetic GK rat presented with marked hypertrophy of cardiomyocytes and increased ECM deposition that altogether translated into increased heart size in the absence of ultrastructural changes or fibre disarray. Molecular derangements underlying this phenotype included upregulated TGF β 1 transcription and activity, recapitulation of foetal gene phenotype markers B-type natriuretic peptide (BNP) and α -skeletal actin (α SKA), activation of the Akt-p70S6K pathway and altered gene expression profile of key components (collagen 1 α , fibronectin) and modulators i.e matrix metalloproteinases (MMP) 2 and 9, connective tissue growth factor (CTGF) of the ECM. Chronic mild T2DM produced prominent LV hypertrophy in GK rats, underscored by increased myocyte size and LV wall thickness, expression of natriuretic peptides (Atrial natriuretic peptide (ANP) and BNP) and Akt phosphorylation. In the absence of caspase-3 mediated apoptosis, fibrosis proliferation in the GK LV paralleled increased transcriptional and biologically active pro-fibrogenic TGF β 1 in the LV with upregulated mRNA abundance for key ECM components such as fibronectin, collagen type(s) 1 and 3 α and regulators including MMP 2 and 9, and their tissue inhibitor (TIMP) 4, connexin 43 (Cx43) and integrin α 5. Ageing GK rats also presented with altered mRNA expression for cardiac sarcoplasmic reticulum Ca²⁺ATPase 2a (SERCA2a), Na⁺/Ca²⁺ exchanger and the L-type Ca²⁺ channels which may contribute to the altered Ca²⁺ transient kinetics previously observed in this model at 18 months of age (unpaired *t*

test, $p < 0.05$ vs. age-matched Wistar control for all parameters). The present results support the clinical relevance and suitability of the GK model of human disease in aiding definition of the mechanisms of ventricular decompensation in HF of diabetic origin. Additionally, this study demonstrates that a milieu dominated by chronic mild HG can produce a hypertrophic myopathy that recapitulates several aspects of the failing heart. Data concerning molecular signalling cascades and ECM phenotype may be particularly significant as targeting features of structural remodelling may delay onset and severity of myocardial complications.

TABLE OF CONTENTS

DECLARATION	I
ABSTRACT	II
TABLE OF CONTENTS	III
LIST OF TABLES AND FIGURES	IV
ACKNOWLEDGEMENTS	V
ABBREVIATIONS	VI
FOREWORD	VII

1. GENERAL INTRODUCTION

1.1 The functional anatomy of the mammalian heart.....	1
1.1.1 The extracellular matrix.....	3
1.1.2 The cardiomyocyte.....	6
1.1.3 Mechanical events of the cardiac cycle.....	11
1.2 Heart failure.....	14
1.2.1 Pathophysiology of the failing heart.....	15
1.2.2 Molecular signature of cardiac structural remodelling.....	19
1.2.3 Transforming growth factor β 1 in remodelling and failure.....	23
1.3 Diabetes Mellitus.....	26
1.3.1 Influence of diabetes on heart failure risk and outcomes.....	29
1.3.2 Relationship between hyperglycemia and heart failure.....	32
1.3.3 Animal Models of Diabetes Mellitus.....	34
1.3.4 Aims and scope of developmental experiments.....	37

2. METHODS

2.1 Experimental design.....	40
2.2 Experimental models.....	40
2.3 Sample collection.....	41
2.4 Histology.....	41
2.4.1 Immunohistochemistry.....	42
2.4.2 Immunofluorescence labelling and confocal laser scanning microscopy.....	43
2.4.3 Electron microscopy.....	44
2.5 Functional studies in the STZ-induced type 1 diabetic rat.....	45
2.5.1 Measurement of left ventricle action potential.....	46
2.5.2 Isolation of ventricular myocytes.....	46
2.5.3 Measurement of contraction in isolated myocytes.....	47
2.5.4 Measurement of intracellular calcium transients in isolated myocytes.....	47
2.6 Transforming growth factor β 1 immunoassay.....	48
2.7 Western blotting.....	50

2.8 mRNA quantification by quantitative real time PCR.....	54
2.9 Statistical analysis.....	58
3. DEVELOPMENTAL EXPERIMENTS: LEFT VENTRICLE MORPHOLOGY AND MYOCYTE FUNCTION IN THE STREPTOZOTOCIN-INDUCED TYPE 1 DIABETIC RAT	
3.1 Abstract.....	59
3.2 Assessment of cardiomyocyte contractile function and intracellular calcium transients in the STZ-induced diabetic rat	
3.2.1 Introduction.....	60
3.2.2 Methods.....	61
3.2.3 Results.....	61
3.2.4 Discussion.....	65
3.3 Association of diabetes with histopathological changes in the left ventricle	
3.3.1 Introduction.....	69
3.3.2 Methods.....	70
3.3.3 Results.....	70
3.3.4 Discussion.....	74
3.4 The story so far.....	78
3.4.1 Cardiac complications in Prediabetes- Overview of the status quo.....	79
3.4.2 Physiological relevance of the Goto-Kakizaki rat model.....	82
3.4.3 Aims and scope of the study.....	82
4. LEFT VENTRICLE STRUCTURAL REMODELLING IN THE PREDIABETIC GK RAT	
4.1 Abstract.....	85
4.2 Introduction.....	86
4.3 Materials and methods.....	87
4.4 Results.....	88
4.5 Discussion.....	102
5. LEFT VENTRICLE STRUCTURAL REMODELLING IN CHRONIC T2DM IN THE GK RAT	
5.1 Abstract.....	107
5.2 Introduction.....	108
5.3 Materials and Methods.....	109
5.4 Results.....	109
5.5 Discussion.....	122
6. IMPACT OF AGE ON STRUCTURAL REMODELLING IN THE LEFT VENTRICLE	
6.1 Introduction.....	128
6.2 Methods.....	128
6.3 Results.....	128
6.4 Discussion.....	135

7. GENERAL DISCUSSION	
7.1 Perspectives.....	137
7.2 Limitations and future scope of the study.....	140
7.3 Concluding remarks.....	144
BIBLIOGRAPHY.....	VIII
COMMUNICATIONS.....	IX

LIST OF TABLES**CHAPTER 2**

- Table 2.1 List of antibodies used in the study
- Table 2.2 List of PCR primers used in the study

CHAPTER 3

- Table 3.1 Glucometry and gravimetry data obtained 6-7 weeks post STZ-administration
- Table 3.2 Contractility in ventricular cardiomyocytes
- Table 3.3 $[Ca^{2+}]_i$ transient kinetics
- Table 3.4 Studies correlating dysglycemia and heart failure

CHAPTER 4

- Table 4.1 General characteristics of control and GK rats at 8 weeks
- Table 4.2 Total and active TGF β 1 in plasma of control and GK rats

LIST OF FIGURES AND ILLUSTRATIONS**CHAPTER 1**

- Figure 1.1 The mammalian heart
- Figure 1.2 Components of the extracellular matrix
- Figure 1.3 Functional anatomy of ventricular cardiomyocytes
- Figure 1.4 Mechanical events of the cardiac cycle
- Figure 1.5 Heart failure pathogenesis
- Figure 1.6 Cardiac Hypertrophy
- Figure 1.7 Functional interactions of HG with TGF β signalling that underlie *in vitro* cellular hypertrophy

CHAPTER 2

- Figure 2.1 Standard calibration curve for TGF β 1
- Figure 2.2 Typical Tris-HCl gel after electrophoretic transfer
- Figure 2.3 Representative scan of exposed film showing PVDF membrane and proteins detected by ECL
- Figure 2.4 Representative RTqPCR validation methodology

CHAPTER 3

- Figure 3.1 Ventricular action potentials
- Figure 3.2 Ventricular cardiomyocyte contractility
- Figure 3.3 Representative fast time-base recording of Ca^{2+} transients in control and STZ-treated ventricular myocytes
- Figure 3.4 Histopathology of the left ventricle
- Figure 3.5 Myocyte diameter in diabetes
- Figure 3.6 Investigation of collagenous matrix deposition
- Figure 3.7 Myocyte apoptosis

CHAPTER 4

- Figure 4.1 Glucometry data
- Figure 4.2 Left ventricle hypertrophy and myocyte ultrastructure
- Figure 4.3 Collagenous matrix proliferation
- Figure 4.4 TGF β 1 protein level and expression
- Figure 4.5 Gene expression profile of the extracellular matrix
- Figure 4.6 Expression of biomarkers for cardiac hypertrophy
- Figure 4.7 Activation of Akt-p70S6K signalling

CHAPTER 5

- Figure 5.1 Oral glucose tolerance test
- Figure 5.2 Structural remodelling of the LV in chronic mild T2DM
- Figure 5.3 TGF β 1 protein levels and expression
- Figure 5.4 Transcriptional profile of the LV in chronic mild T2DM
- Figure 5.5 Akt-p70S6K signalling

CHAPTER 6

- Figure 6.1 Age-dependent structural remodelling in the LV
- Figure 6.2 Age-related effects on LV TGF β 1 concentration
- Figure 6.3 Effect of age on Akt and p70S6K phosphorylation in the LV

ACKNOWLEDGEMENTS

It is a pleasure to convey sincere thanks to the many people who have made this thesis possible.

I cannot overstate my gratitude to Professor Jaipaul Singh - Ph.D. supervisor, friend, philosopher and guide. During my time at UCLAN and through our many travels, he has been a constant source of sound advice, great company and terrific ideas. His mentorship has been paramount in providing a well-rounded research experience and has encouraged me to grow as an experimentalist and an independent thinker. For everything you have done for me Jai, I thank you.

Many, many thanks are due to several academics with whom I have had the good fortune of working with during my research and study. I am especially grateful to Professors Chris Howarth and Ernest Adeghate from the United Arab Emirates University (UAEU), Professor Mark Boyett, Drs. Halina Dobryznski and Joseph Yanni from the University of Manchester, Dr. Keshore Bidasee from the University of Nebraska Medical Centre (UNMC), Professor Robert Lea and Drs. Niall Woods and Steven Beeton from UCLAN. I also owe special thanks to Prof. Keith Bagnall from UAEU for his encouragement and insight.

Collectively and individually, I am indebted to good friends and student colleagues from UCLAN as well as other institutions for providing a stimulating environment to learn and grow. I am especially grateful to Banu Abdallah, Basel Arafat, Rakesh Tekade, Rachel Stevens, Kanar Fadhil, Shakil Patel, Glenda Melling, Hajira Faki, Olaf Bayer and Helen Godfrey for the emotional support and camaraderie they have so willingly provided, especially through the difficult times. The co-operation of Mey Al Kitbi from UAEU, Agnes Constantino, Chun-Hong Shao and Caronda Moore from UNMC is also gratefully acknowledged.

I am also immensely grateful to the technical and support staff at UCLAN, particularly to Sal Tracy, Elizabeth Green, Sujata Patel, Tony Dickon and Christine Woodcock for several favours bestowed. The kind assistance of Anwar Qureshi and Saeed Tariq from UAEU also deserves particular mention.

Most of all, I wish to express my deep and sincere thanks to my family and especially my parents, Aloysius and Jacintha D'Souza for their absolute confidence, unflinching love, support and encouragement. To them I dedicate this thesis.

ABBREVIATIONS

[Ca ²⁺] _i	Intracellular calcium transient
αSKA	α-Skeletal actin
ACCORD	Action to Control Cardiovascular Risk in Diabetes (study)
ANP	Atrial natriuretic peptide
APD	Action potential duration
APD ₅₀	Action potential duration at 50% repolarization
ATLAS	Assessment of Treatment with Lisinopril and Survival (study)
ATPase	Adenosine triphosphatase
AV	Atrioventricular
BNP	B-type natriuretic peptide
BPM	Beats per minute
BSA	Bovine serum albumin
BW	Body weight
cAMP	Cyclic adenosine monophosphate
cDNA	Complementary deoxyribonucleic acid
CHD	Coronary heart disease
CHF	Congestive heart failure
CHS	Cardiovascular health study
Ca _v	Voltage gated Ca ²⁺ channels
Col1α	Collagen Type 1α
Col3α	Collagen Type 3α
CTGF	Connective tissue growth factor
CVD	Cardiovascular disease
Cx43	Connexin 43
DCM	Diabetic cardiomyopathy
DM	Diabetes mellitus
EC coupling	Excitation-contraction coupling
ECG	Electrocardiogram
ECM	Extracellular matrix

EDTA	Ethylenediaminetetraacetic acid
EDV	End diastolic volume
ELISA	Enzyme-linked immunosorbent assay
EPICAL	Epidémiologie de l'Insuffisance Cardiaque Avancée en Lorraine (study)
EPIC	The European Prospective Investigation into Cancer and Nutrition (study)
FFPE	Formalin fixed paraffin embedded
FITC	Fluorescein Isothiocyanate
GTT	Glucose tolerance test
GK rat	Goto-Kakizaki rat
H&E	Hematoxylin and Eosin
HbA1c	Glycated haemoglobin
HEPES	(4-(2-hydroxyethyl)-1-piperazineethanesulfonic acid
HF	Heart failure
HG	Hyperglycemia
HRP	Horse radish peroxidase
HW	Heart weight
Hz,	Hertz
IFG	Impaired fasting glucose
IGT	Impaired glucose tolerance
IR	Insulin resistance
LV	Left ventricle
LVEF	Left ventricle ejection fraction
LVW	Left ventricle weight
MESA	Multi ethnic study of atherosclerosis
MHC	Myosin heavy chain
MI	Myocardial infarction
MMP	Matrix metalloproteinase
MTOR	Mammalian target of rapamycin
NCX	Sodium calcium exchanger

OGTT	Oral glucose tolerance test
OLETF	Otsuka long evans tokushima fatty
OPTIMAAL	Optimal Therapy in Myocardial Infarction with the Angiotensin II Antagonist Losartan
PBS	Phosphate buffered saline
PI3-K	Phosphatidylinositol 3-kinase
Plb	Phospholamban
PVDF	Polyvinylidene difluoride
RAAS	Renin angiotensin aldeosterone system
RCL	Resting cell length
RESOLVD	Randomized Evaluation of Strategies for Left Ventricular Dysfunction
RNA	Ribonucleic acid
RTqPCR	Quantitative real time polymerase chain reaction
RyR	Ryanodine receptor
SA	Sinoatrial
SERCA2a	Sarcoendoplasmic reticulum Ca ²⁺ ATPase 2a
Smad	“sma”(Caenorhabditis elegans protein) + “Mad” mothers against decapentaplegic
SOLVD	Study of Left Ventricle Dysfunction
SR	Sarcoplasmic reticulum
STZ	Streptozotocin
T1DM	Type 1 diabetes mellitus
T2DM	Type 2 diabetes mellitus
TGFβ1	Transforming growth factor β1
TIMP	Tissue inhibitor of matrix metalloproteinase
Tm	Tropomyosin
TNF	Tumour necrosis factor
TnT, TnI, TnC	Troponin T, Troponin I, Troponin C
UKPDS	United Kingdom prospective diabetes study
V	Volts

ABBREVIATIONS

VI

V-HeFT-II

Vasodilator-Heart Failure Trial- II

WHO

World health organisation

FOREWORD

Understanding the integrative biology of the failing heart in dysglycemic states at genetic, molecular and cellular levels is an important focus of current research efforts. Although DCM and its consequences on myocardial structure and function has been the subject of extensive enquiry, the role of hyperglycemia (HG) in HF pathogenesis by way of structural remodelling is still ambiguous. In investigating the relationship between HG and its potential contribution to HF pathogenesis in the relative absence of traditional cardiovascular risk factors, the approach to the study was 2 pronged by design. First, the effects of HG on myocyte contractility and remodelling in the ventricle were assessed using the well established STZ-type 1 model of DM. While the results demonstrated that HG may indeed result in altered contractile kinetics and structural remodelling in the LV, the clinical relevance of the study left much to be desired, especially given recently drawn correlations between prediabetes and adverse cardiac outcomes. Thus, following this ‘developmental’ study, the nature of remodelling changes in dysglycemia and cogent molecular events were further investigated using the GK rat, a non-obese, non hypertensive model that develops mild T2DM following a prediabetic phase.

In effect, chapter one introduces the relevant functional anatomy of the mammalian heart, the significance of remodelling changes in HF pathogenesis, reviews the biological basis of the link between DM, HG and HF and presents the rationale for the developmental experiments. The second chapter details preliminary experiments on myocyte contractility and remodelling in the STZ-induced model and the clinical motivation for future experimentation in the GK rat. In the subsequent chapters, ventricular remodelling and underlying molecular profile were explored further in prediabetes and overt chronic T2DM. As such, each section is dealt with separately for clarity but areas of common integration are signposted in the final chapter. In its entirety, by focussing on the role of HG alone, this work represents an attempt to simplify a complex problem and identifies several avenues for future research.

CHAPTER 1

GENERAL INTRODUCTION

For it is the heart by whose virtue and pulse the blood is moved, perfected, made apt to nourish and is preserved from corruption and coagulation It is indeed the fountain of life, the source of all action.'

William Harvey (1578-1697)

1.1 The Functional Anatomy of the Mammalian Heart

The mammalian heart is a four-chambered muscular organ situated in the anterior mediastinum, immediately posterior to the sternum and encapsulated by the pericardium. Its pumping ability is central to the functioning of the circulatory system wherein blood is pumped through a network of blood vessels namely arteries, veins, arterioles, venules and capillaries. These blood vessels can be subdivided into a pulmonary circuit carrying blood to and from gas exchange surfaces of the lungs and a systemic circuit through which blood is transported to and from the rest of the body (Sherwood, 2008).

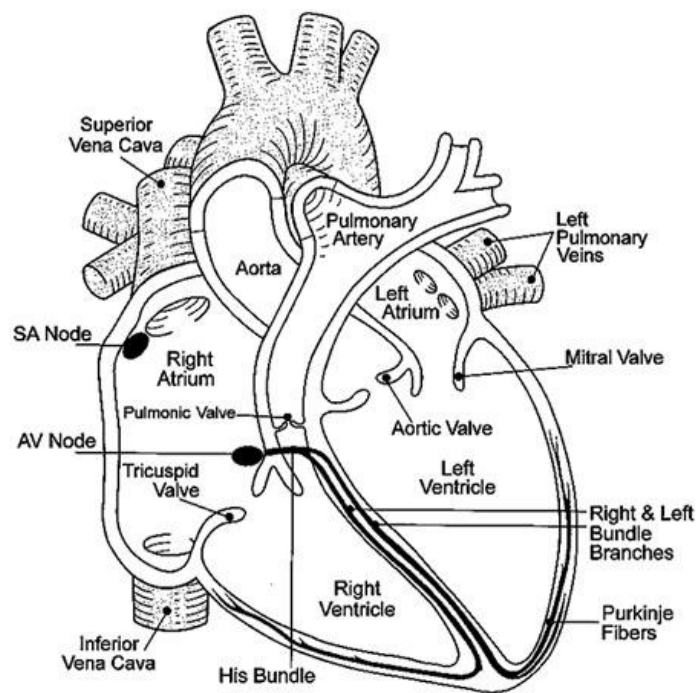


Fig 1.1: The mammalian heart. Components are described in the text.

(Image courtesy www.beyondbiology.org)

As given in Figure (Fig) 1, the right and left atria and the right and left ventricles make up the four chambers of the mammalian heart. Two chambers of the heart may be associated with each circuit; the right atrium receives blood from the systemic circuit

through the superior vena cava and the inferior vena cava and allows inflow into the right ventricle passing through the right atrioventricular (AV) or tricuspid valve. Blood is then pumped into the pulmonary circuit eventually being collected by the left atrium and emptied into the LV through the left AV or bicuspid valve. Semilunar valves are situated between the ventricles and the major blood vessels of the heart and open and close passively due to pressure gradients. Blood pumped from the right atrium into the pulmonary trunk passes through the pulmonary valve and blood leaves the left ventricle through the aortic valve into the ascending aorta. The atria are separated by the interatrial septum and the ventricles by a much thicker interventricular septum that houses electrical conduction tissue. Innervation of the heart is by both vagal and sympathetic fibres. The SA node and the atria are predominantly innervated by the right vagus whereas the left vagus nerve supplies the AV node and the bundle of His (Vander *et al.*, 2007). The myocardium in the ventricles is only sparsely innervated by vagal efferents. Although rhythmic contraction of the heart is initiated in the SA node, cardiac function is mediated by neural activation. Release of noradrenaline by sympathetic nerves and subsequent activation of beta adrenergic receptors result in positive chronotropy, inotropy and dromotropy whereas parasympathetic stimulation brings about opposite effects, secreting acetylcholine that acts on muscarinic receptors. The cardiac action potential that initiates contraction is generated in the sinoatrial (SA) node and spreads through the atria before converging upon the AV node for distribution to the ventricles by the specialised Bundle of His, right and left bundle branches and Purkinje fibre network (Koeppen and Stanton, 2008).

The walls of the atria are thinner than those of the ventricles, particularly the LV whose wall is 3-4 times thicker than the right ventricle at a corresponding position (Vander *et al.*, 2007). The wall of the heart is typically described to be made up of 3 layers; the outer epicardium (visceral pericardium) is a serous membrane consisting of an exposed mesothelium and a layer of smooth connective tissue that is attached to the myocardium (Koeppen and Stanton, 2008). The inner surfaces of the heart (including the valves) are lined by the endocardium that consists of squamous epithelial cells continuous with the endothelium of blood vessels. The myocardium is the middle muscular wall of the heart that forms both atria and ventricles. This layer encompasses several types of cells including atrial and ventricular contractile 'working' myocytes that comprise muscle fibres, nodal cells, purkinje fibres, smooth muscle cells and fibroblasts (Koeppen and Stanton, 2008). Cardiac myocytes account for 70% to 75% of the myocardium by cell volume but only 25% to 30% by cell number (Miner and Miller, 2006). Cardiac

fibroblasts that synthesize proteins of the ECM are the most abundant cell type of the myocardium

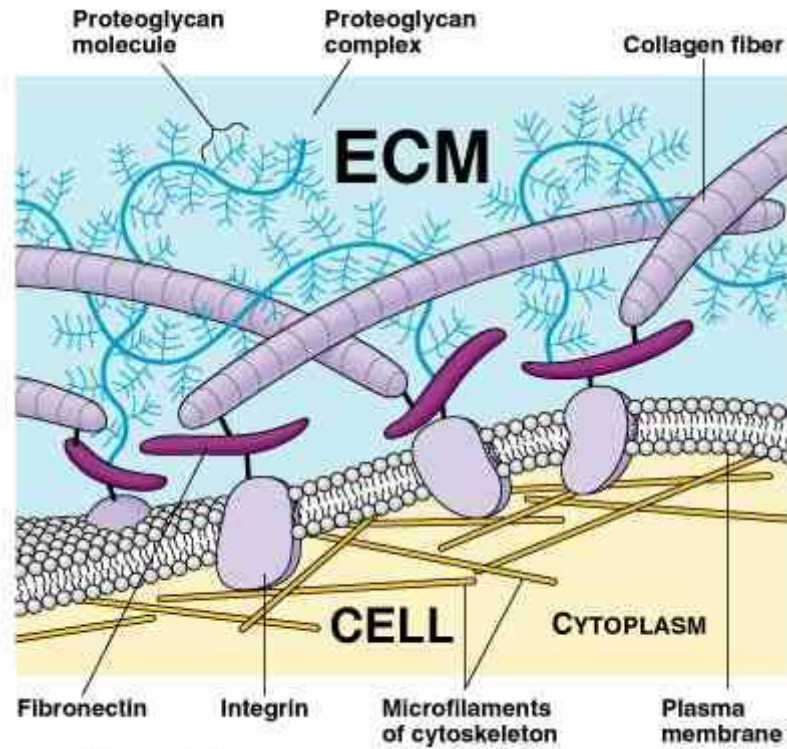
1.1.1 The Extracellular Matrix

The muscle fibre array of the myocardium is surrounded and interspersed by the ECM, a fibrillar, highly differentiated structure consisting of an organised hierarchy of connective tissue that provides structural support and functional integrity to the heart. The ECM is broadly differentiated into an epimysium encircling the endo- and epicardium, a perimysium that groups myofibrils into bundles and an endomysium that surrounds individual myocytes and provides connection to the vasculature (Fedak *et al.*, 2005). It comprises of a complex network of structural proteins (collagen and elastic fibres) and adhesive proteins (fibronectin, laminin) within a hydrated proteoglycan and glycosaminoglycan-rich milieu (Graham *et al.*, 2008). Coiled fibers of the ECM act to store energy produced during systole, and hence relengthening of cardiac myocytes during diastole (Miner and Miller, 2006). Apart from the provision of a structural network that translates developed force in individual myocytes into regular synchronous contraction and passive stiffness, the ECM also functions to prevent myocyte slippage, overstretch and interstitial oedema. Once considered an inert physical scaffolding, ongoing research has established diverse roles of the ECM in transmembrane signalling, MAPK activation, growth factor mediation, cytoskeletal rearrangement, modulation of cell phenotype among other regulatory roles in hypertrophy and ontogenic development (Fedak *et al.*, 2005; Graham *et al.*, 2008; Bowers *et al.*, 2010; Hutchinson *et al.*, 2010). Transmembrane mechanoreceptors known as integrins constitute another important feature of the ECM that transduces mechanical forces and changes in ECM structure, through signals from the extracellular compartment to the cytoskeleton and vice versa. Integrins consist of two different chains, α (120±150 kDa) and β (110±190 kDa), linked by non covalent bounds. They modulate signals instigated by ionic channels, hormone receptors and growth factors, and participate in various transduction processes including those concerned with cell motility, division, differentiation and programmed death (Spinale, 2007; Graham *et al.*, 2008; Bowers *et al.*, 2010).

The ECM is a dynamic entity and component proteins are maintained by a finely controlled homeostatic balance between deposition and degradation. Different families of MMPs that favour or inhibit matrix degradation, regulate the ECM in both normal and pathological conditions. Collagenases (MMP1) cleave collagens in fragments which

in turn constitute the substrate of proteases including the gelatinases (MMP2, MMP9) that are responsible for the degradation of type IV collagen and fibronectin (Bowers *et al.*, 2010). These zinc-dependent enzymes are regulated by a class of proteins called TIMPs. The ability to synthesize ECM components differs among cells in the heart and varies depending upon the inciting stimulus; myocytes produce type IV and VI collagens, laminin and proteoglycans. Collagen type(s) I and III and fibronectin, as well as MMPs are synthesised by the surrounding fibroblasts (Banerjee *et al.* 2006; 2007). Integrin activation also induces the synthesis of collagens and gelatinases, which regulate the synthesis and type of ECM proteins (Spinale, 2007). Modulation of these various components regulates mechanical, chemical and electrical signalling between cells (Miner and Miller, 2006).

(A)



(B)

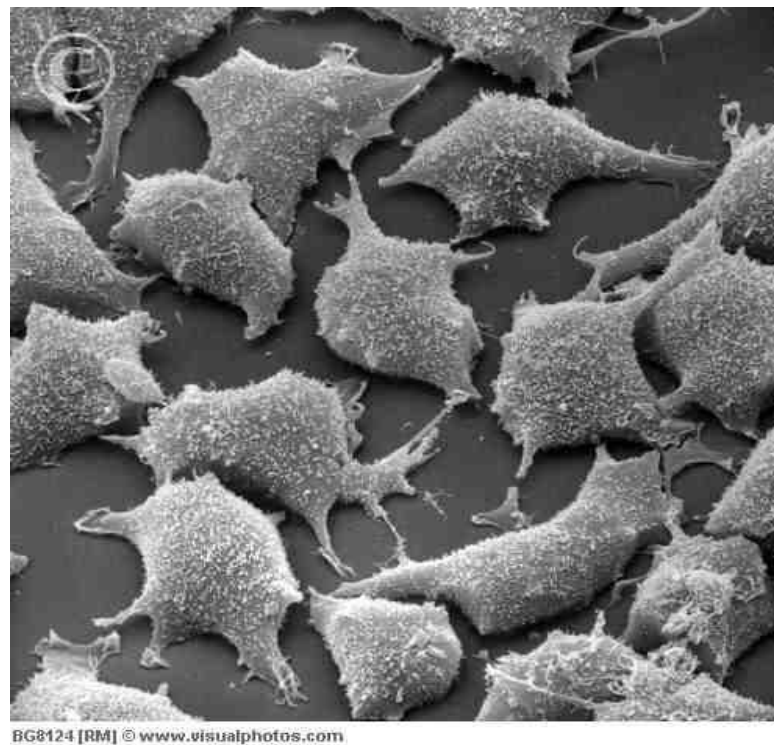


Fig 1.2 Components of the extracellular matrix. Interaction between different cell types (A). Electron micrograph of human fibroblast cells (B). Magnification X28, 000. Image A from www.visualphotos.com, B from <http://www.dr-jacques-imbeau.com/index.html>

1.1.2 The Cardiomyocyte

A ventricular myocyte is an elongated cell containing contractile myofibrils that give it a striated appearance (Fig 1.2 A). Ventricular myocytes are typically uni-nucleated, have a variable branching morphology, extensive capillary supply and are connected to adjacent cardiomyocytes at blunt ends by specialised intercalated discs. The intercalated discs of neighbouring cells are physically connected by types of cell junction i.e. gap junctions and desmosomes that together orchestrate and integrate cardiac electro-mechanical activity. As a result, the entire myocardium functions as a single unit known as a 'syncytium' with a single contraction of the atria followed by a single contraction of the ventricles (Vander *et al.*, 2001).

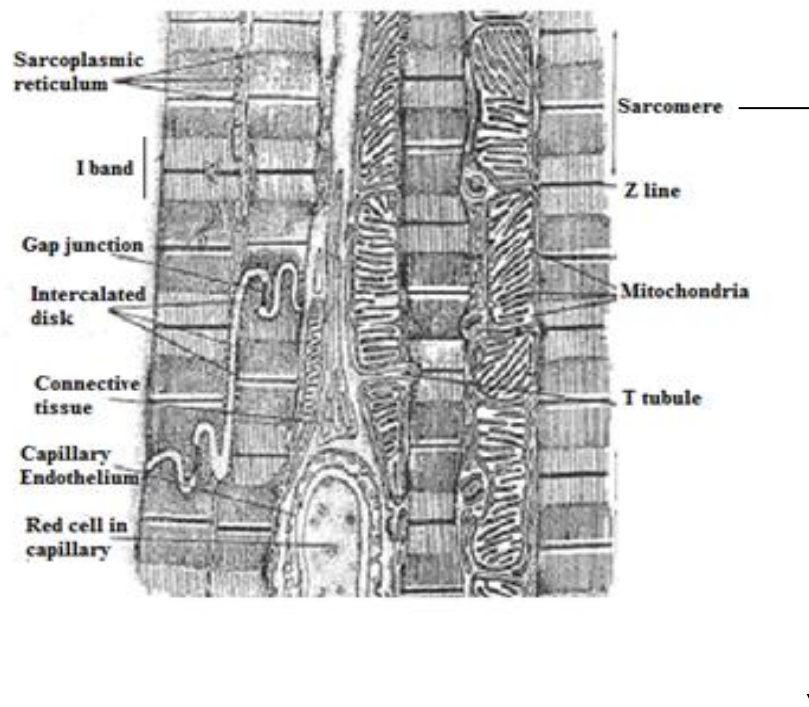
An exquisitely specialised cardiac microanatomy coordinates the processes of orderly spread of action potentials, contraction of cardiac chambers and the pumping action of the heart. Similar in many respects to skeletal muscle cells, the fundamental contractile unit within the myocyte is the sarcomere containing interdigitating thick and thin filaments of the contractile apparatus, namely the proteins actin, myosin, the troponin complex and tropomyosin (Tm). Three proteins, Troponin T, I and C (TnT, TnI, TnC) make up the thin filament complex and together mediate the extent of crossbridge formation whilst contributing to the structural integrity of the sarcomere (Fig 1.2 B, Sherwood, 2008) (Koeppen and Stanton, 2008). Within the cardiomyocyte, each myofibril is surrounded by the sarcoplasmic reticulum (SR), a highly organised Ca^{2+} handling organelle made up of membranous tubules that regulate cytosolic Ca^{2+} flux in conjunction with key sarcoplasmic proteins namely SERCA, the regulatory protein of SERCA- phospholamban (Plb), and the Ca^{2+} release channels (Fig 1.2 B). Another specialised component of the cardiomyocyte is the sarcolemma, a lipid bilayer combination of the plasma membrane and the basement membrane that contains membrane receptors, pumps and channels that regulate contractility. The sarcolemma forms the intercalated disks and penetrates deep into the cell to form the Transverse 'T' tubular system that bring in close proximity ion channels and the SR calcium handling proteins, thus playing a pivotal role in cell contractility (Vander *et al.*, 2001) (Fig 1.2 A, 1.2 C). Integrins are interwoven throughout the sarcolemma and form an important collagen-integrin-cytoskeletal relation.

Nodal cells differ morphologically from contractile myocytes, being smaller in size with fewer contractile elements and gap junctions that appear more dispersed; a feature that accommodates protection from hyperpolarisation in the SA node and a slowing of conduction in the AV node. The latter feature works to ensure sequential contraction of

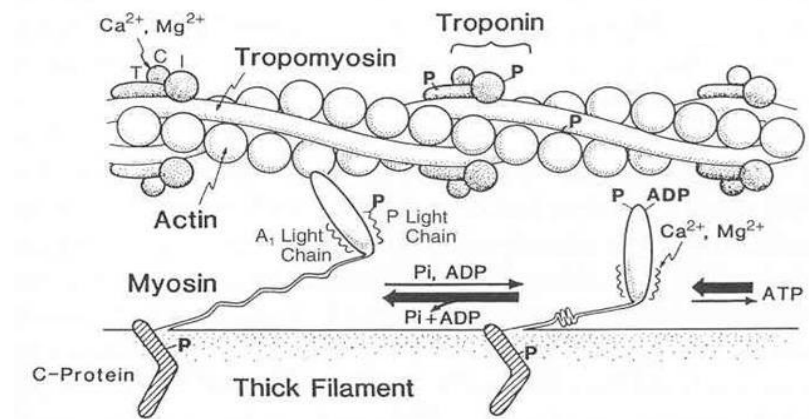
atria and ventricles. By contrast, gap junctions (made up of Connexins, notably 40 and 43) are abundant in cells of the His-Purkinje system allowing for rapid conduction of electrical impulses (Walker and Spinale, 1999).

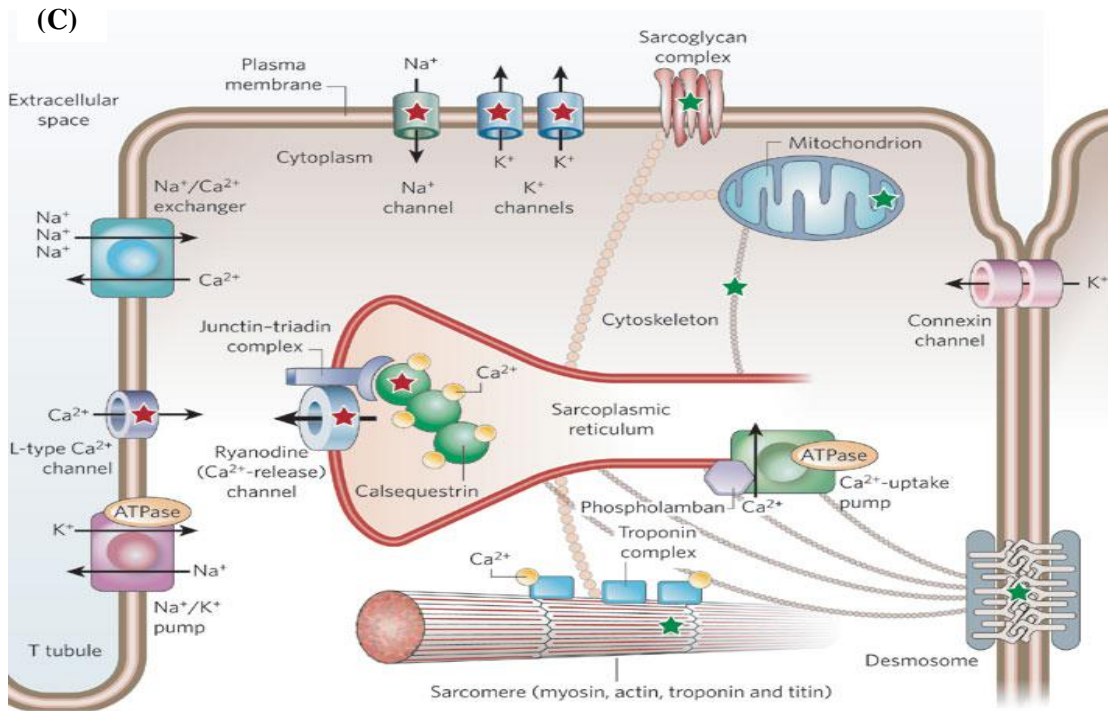
Fig 1.3: Functional anatomy of ventricular cardiomyocytes. Representation of EM micrograph detailing cardiomyocyte architecture (A). Cardiac myofilaments in cross bridge cycle underlying muscle contraction (B). Protein complexes and intracellular organelles involved in cardiac excitation–contraction coupling are illustrated (C) Red stars indicate proteins encoded by genes that are mutated in primary arrhythmia syndromes; many of these proteins form part of macromolecular complexes, so mutations in several genes could be responsible for these syndromes. Green stars indicate protein complexes in which mutations in multiple genes cause cardiomyopathies often associated with arrhythmias; these complexes include the sarcomere (in hypertrophic cardiomyopathy), the desmosome (in arrhythmic right ventricular cardiomyopathy), and the cytoskeleton, sarcoglycan complex and mitochondrion (in dilated cardiomyopathy). Typical ventricular myocyte action potential resulting from sarcolemmal protein interactions (D). Structure-function relationships between the elements in the figure and further descriptions of each component are summarized in the text. Image courtesy: (A) Koeppen and Stanton, 2008; (B) available via http://www.ccbm.jhu.edu/doc/courses/BME_580_682; (C) Knollmann and Roden, 2008; (D) Adapted from Vander *et al.*, 2007

(A)

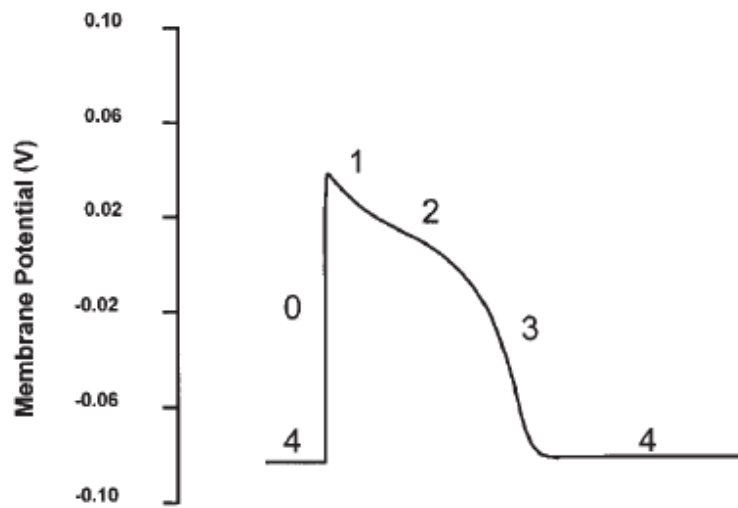


(B)





(D)



A more complete appreciation of the functional anatomy of myocyte ultrastructure comes from placing in it the context of (ventricular) myocyte contraction and relaxation. Grossly oversimplified, these processes are described as follows:

At the resting membrane potential (corresponding to phase 4 of the action potential, Fig 1.2 D) the sarcolemma is only permeable to K^+ , a condition maintained by the combined activities of the inward K^+ rectifier, Na^+/K^+ ATPase and the Na^+/Ca^{2+} exchanger operating in forward mode (Fig 1.2 C, 1.2 D). Depolarisation of the plasma membrane beyond an inherent threshold voltage results in the activation of voltage gated Na^+ and Ca^{2+} channels. Opening of fast Na^+ channels results in the rapid upstroke characteristic of phase 0 of the action potential whereas the subsequent inward current that maintains the plateau of the action potential is primarily due to Ca influx via L-type Ca^{2+} channels, with Na^+/Ca^{2+} exchanger playing a minor role. Rapid inactivation of the fast Na^+ channels (2-10 ms) and a transient net outward current of K^+ along the electrochemical gradient contributes to an early, brief repolarisation (notch) during phase 1 of the action potential (Fig 1.2 D). The small influx of Ca^{2+} that enters the cell after initial depolarisation triggers Ca^{2+} release from the SR by activating SR Ca^{2+} release channels culminating in a transient rise in cytosolic free calcium concentration to micromolar concentrations (10 μ M/litre) from a resting (diastolic) nanomolar concentration (100 nanomoles/L). A central feature of this process is the gating of the SR Ca^{2+} release channels by ryanodine receptors (RyR) located within terminal cisternae of the SR. This 'calcium-induced calcium release', activates the contractile machinery and initiates contraction in the myocyte by a mechanism termed Excitation-Contraction coupling (EC coupling) (Vander *et al.*, 2001).

Under resting conditions, lower intracellular Ca^{2+} favours the shift of the Tn-Tm complex towards the outer grooves of the actin filament and thereby blocks actin-myosin interaction. Rise in Ca^{2+} concentrations during the action potential and subsequent binding to TnC strengthens TnC-TnI interaction and detaches TnI from the actin molecule by a conformational shift of the Tn-Tm complex, enabling crossbridge formation (Fig 1.2 B). The available literature suggests that thin filament activation is achieved by the movement of Tm over the surface of actin and this motion permits force generation and shortening. After crossbridge formation, i.e. the attachment of the myosin head of the thick filament to the actin molecules of the thin filament, the myosin head changes conformation 'pivoting' towards the M-line, with concomitant ATP

hydrolysis to ADP that generates force causing the thin filament to slide over the thick filament and the sarcomere to shorten, altogether resulting in contraction. Binding of adenosine triphosphate (ATP) to the myosin head causes detachment of cross-bridges and (re)exposure of active sites making possible interaction with another cross-bridge (Fig 1.2B). This highly dynamic phenomenon termed the 'sliding filament theory' moves the filaments approximately 10 nm with an average velocity of 0.98 $\mu\text{m/s}$ (Koeppen and Stanton, 2008). Factors such as SR Ca^{2+} release, sensitivity of the myofilaments to Ca^{2+} , number of crossbridges formed, duration of the action potential and ATP stores appear to decisively affect cardiomyocyte contraction. Following contraction, relaxation and is achieved by the removal of Ca^{2+} (that activates myofilaments) from the cytosol by cellular Ca^{2+} transport systems. This phase corresponds to repolarisation or phase 3 of the action potential, wherein decay of the calcium transient occurs due to the reuptake of Ca^{2+} into the SR by SERCA and the extrusion of Ca^{2+} from the myocyte, primarily by the $\text{Na}^+/\text{Ca}^{2+}$ exchanger (Fig 1.2 C, 1.2 D). This phase is characterised by the closure of sarcolemmal Ca^{2+} channels and increased K^+ conductance through the (slow and rapid) delayed rectifier K^+ currents corresponding to a negative change in membrane potential. When membrane potential is restored to -80 to -85 mV, conductance is limited to the inward rectifier K^+ channels that together set the resting membrane potential (phase 4) (Walker and Spinale 1999; Vander *et al* 2007).

1.1.3 Mechanical events of the cardiac cycle

The cardiac cycle consists of alternate periods of systole (contraction and emptying) and diastole (relaxation and filling) in the atria and ventricles. Contraction results from the spread of the action potential across the heart whereas relaxation follows the subsequent repolarisation of the myocardium. In the text below, as one full cardiac cycle that begins and ends with ventricular diastole is described (Fig 1.3). The terms systole and diastole are used to indicate events in the ventricle and only activity in the left side of the heart is described. These are identical to those on the right side, with the exception of lower pressures in the right side of the heart (Sherwood, 2008).

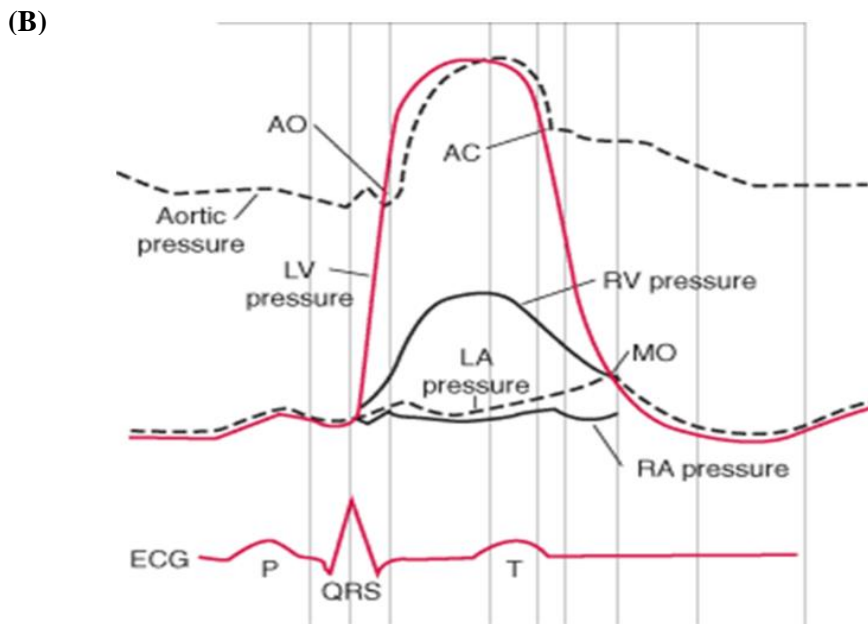
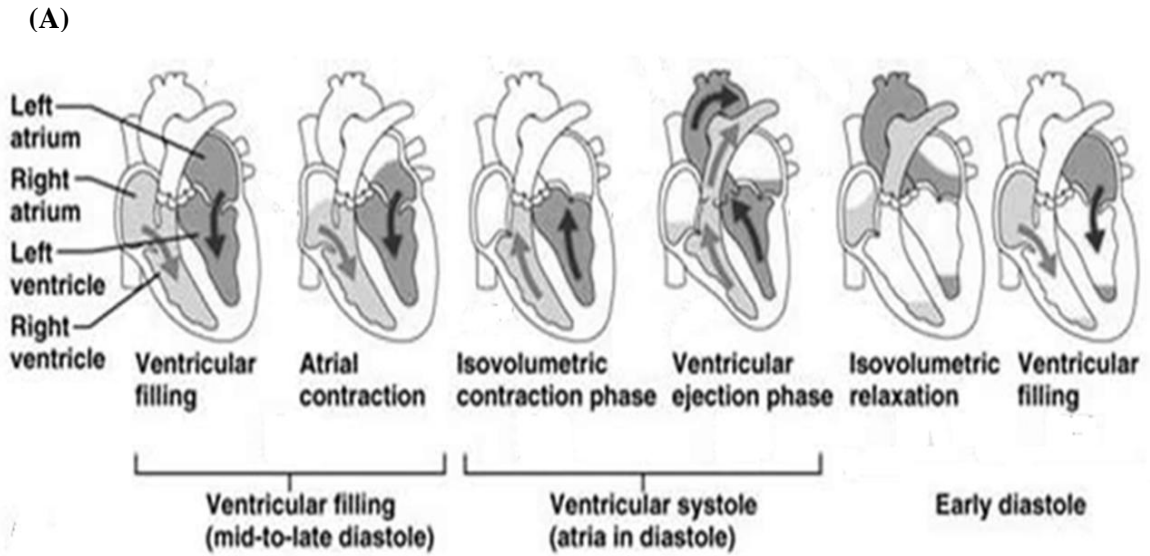


Fig 1.3: Mechanical events of the cardiac cycle. Currently accepted time frames of systole and diastole (A). The physiological phases of cardiac cycle that include isovolumic contraction, ejection, isovolumic relaxation rapid and slow filling, and atrial contraction are shown. Measurements of intravascular pressure in the aorta, LV, left atrium (LA), and LV volume that underlie the phases of the cardiac cycle, together with their impact on the mitral and aortic valves and the corresponding ventricular electrocardiogram (ECG). Aortic flow occurs between the 2 intervals that define ejection. AO: Aortic valve opens; AC: Aortic valve closes; MO: Mitral valve opens. (Images adapted from www.merckmanual.org)

As given in Fig 1.3, beginning at mid ventricular diastole, where the atrium is also in diastole, there is a continuous inflow of blood from the venous system into the atrium and hence a pressure differential. During this phase, the AV valve is open and passive ventricular filling results in a rising ventricular volume. This stage corresponds to the TP interval on the ECG. The next phase, late ventricular diastole, the SA node reaches threshold and fires and is detectable on the ECG as the P wave as the impulse spreads throughout the atria. This atrial depolarisation results in atrial contraction, squeezing blood into the ventricle. Although ventricular pressure rises simultaneously with rise in atrial pressure from this additional volume of blood added to the ventricle, the AV valve remains open throughout atrial contraction as pressure in the atria slightly exceeds that in the ventricle. During the next stage, where ventricular diastole ends, atrial contraction and ventricular filling are completed and the volume of blood, also known as end diastolic volume (EDV) averages at about 135 ml (Sherwood, 2008). During the next phase that sees the onset of ventricular excitation and ventricular systole, the impulse after atrial excitation travels to the AV node and the His-Purkinje system to depolarise the ventricle, represented on the ECG as the QRS complex. The modest delay between the QRS complex and the actual onset of ventricular systole is the time required for the EC coupling process. Atrial repolarisation and ventricular depolarisation occur simultaneously, so the atria are in diastole throughout ventricular systole. With the onset of ventricular contraction, ventricular pressure exceeds atrial pressure and the backward pressure gradient forces the AV valve closed. During the next phase, Isovolumetric ventricular contraction, the AV valves and the aortic valves are closed, and hence blood does not enter or leave the ventricle and ventricular pressure continues to rise as the volume remains constant. When the ventricular pressure exceeds aortic pressure, the aortic valve opens and ejection of blood begins. The aortic pressure curve continues to rise as blood is pumped into the aorta faster than that being drained into smaller vessels. The T wave on the ECG signifies the end of ventricular systole and as the ventricles start to relax, on repolarisation, ventricular pressure falls below aortic pressure resulting in the closure of the aortic valve. At this point, synonymous with isovolumetric ventricular relaxation, the AV valve is not yet open, as ventricular pressure still exceeds atrial pressure. When ventricular pressure falls below atrial pressure, the AV valves open and ventricular filling occurs again. Subsequently, the phase continues as described into late ventricular diastole, where the SA node fires again and the cardiac cycle continues.

1.2 Heart Failure

Congestive HF (CHF) or simply HF has been defined as ‘a complex clinical syndrome that can result from any structural or functional cardiac disorder that impairs the ability of the ventricle to fill with or eject blood’ (Dokken, 2008). Classification into systolic and diastolic dysfunction has further emphasized the functional distinction between abnormalities in contraction and relaxation. Systolic heart failure arises from a compromise in the contractility of the heart and is defined as a left ventricular ejection fraction (LVEF) of <45%. Diastolic dysfunction is a consequence of impaired relaxation and abnormal ventricular filling (Gutierrez and Blanchard, 2004). Moreover, recent years have seen the recognition and confirmation of the clinical syndrome of HF with preserved LV ejection fraction, often accompanied by diastolic dysfunction and a prognosis similar to ‘classical’ systolic HF (Owan *et al.*, 2006)

HF susceptibility is greatly increased in patients with diabetes mellitus (DM), metabolic syndrome, hypertension, ischemic events, history of cardiomyopathy and on use of cardiotoxins (e.g. cocaine, alcohol) (Francis, 2001). The condition is supremely debilitating and is known to reduce self reported quality of life more than most other chronic medical conditions (Gill *et al.*, 2009) including arthritis or chronic lung disease (Hobbs *et al.*, 2002). Sudden cardiac death is responsible for at least half of deaths although many succumb to progressive pump failure and congestion (Swedberg *et al.*, 2005). Most patients have signs and symptoms of fluid overload and pulmonary congestion including ascites, edema, dyspnea, orthopnea, and paroxysmal nocturnal dyspnea. Outside congestive symptoms, patients often present with signs of low cardiac output, including fatigue, effort intolerance, cachexia, and renal hypoperfusion (Hobbs and Boyle, 2010). Deaths from end-organ failure due to insufficient systemic organ perfusion are not uncommon, particularly to the kidneys. Occurrence of renal dysfunction, cachexia, valvular regurgitation, ventricular arrhythmias, lower LVEF, high catecholamine and BNP levels, low serum sodium level, hypocholesterolemia, and marked LV dilation are all considered indicators of poor prognosis (Hobbs and Boyle, 2010). Patients with combined systolic and diastolic LV dysfunction also have a worse prognosis than patients with either in isolation (Hansen *et al.*, 2001).

Presently, HF prevalence is on the rise as populations age, western diets predominate, cardiac disease from infectious aetiologies are overcome and the rate of acute mortality from ischemic events subside owing to dramatic improvements in sanitation, preventive

and interventional medicine (Jessup and Brozena, 2004; Benjamin and Schneider, 2005; Gill *et al.*, 2009). Combining recent data on incidence and survival, the British Heart Foundation estimates that at least 4% of all deaths in the UK are due to HF (www.heartstats.org). The incidence and prevalence of HF increases steeply with age, the average age of first diagnosis being 76 years (Hobbs *et al.*, 2002). Surveys in the UK and elsewhere show that 10-20% of the very elderly have HF. In 2008, of the 8650 registered deaths in England and Wales attributed to HF, 97% were in the 65 and over age group (Wells and Gordon, 2008). Needless to say, HF is also a major burden on healthcare expenditure. In this regard, a 2009 estimate was that HF directly accounted for 1.9% of total NHS spending in the UK with 69% being on hospitalisations and indirectly via long term nursing care costs and secondary admissions for a further equivalent of 2% of NHS expenditure (Gill *et al.*, 2009). In 2008-9 there were 58,849 admissions for HF in England alone, resulting in 740,697 bed days and 106,808 finished consultant episodes (www.heartstats.org). Mortality rates associated with HF are astronomical, at around 80% in men within 6 years of diagnosis, a prognosis worse than most forms of cancer, with almost 40% of those diagnosed dying within a year (National horizon scanning centre clinical guidelines, 2010).

1.2.1 Pathophysiology of the failing heart

Myocyte contractile dysfunction

The traditional construct has viewed HF as a functional disorder, precipitated by impaired LV pump performance in response to increased hemodynamic burden of the heart and associated defects in myocyte contractility (Houser and Marguiles, 2003). HF is associated with a multitude of cellular and molecular defects that culminate in electrophysiological dysfunction, depressed myocyte contractility, fatal arrhythmias and pump failure (Kumar and Clark, 2009). Numerous studies have suggested that failing human cardiac myocytes undergo several changes that might be expected to lead to a progressive loss of contractile function, including decreased α -myosin heavy chain (MHC) gene expression with a concomitant increase in β MHC expression, progressive loss of myofilaments in cardiac myocytes and alterations in cytoskeletal proteins (Schaper *et al.*, 1991; Nuebauer *et al.*, 1995; Lowes *et al.*, 1997; Gupta *et al.*, 2000). In addition to these changes and the desensitization of adrenergic regulation, substantial evidence indicates that depressed myocyte contractility results from EC coupling alterations. These include slowed Ca^{2+} reuptake as a result of reduced SERCA2a

expression and upregulated NCX exchanger in compensation, increased RyR2 phosphorylation and ensuing increase in SR Ca^{2+} leak (Gupta *et al.*, 2000). Moreover, an increased Na^+ influx and intracellular Na^+ accumulation, that increases internal Ca^{2+} and SR Ca^{2+} load has also been previously documented (Pieske and Houser, 2003). Recent studies have indicated that a loss of t-tubules may occur in HF, leading to the anatomic and functional dissociation between electrical activation of the sarcolemma and release of SR Ca^{2+} (Wasserstrom *et al.*, 2009). It is postulated that this process results in the isolation of increasing numbers of Ca^{2+} release units from the the L-type Ca^{2+} channel, and activation by Ca^{2+} diffusion from neighboring Ca^{2+} release units rather than by Ca^{2+} channels (Song *et al.*, 2006). The ensuing delay in activation of the RyRs may cause a poorly coordinated release of Ca^{2+} along the cell length, leaving a highly fractionated cellular wavefront during Ca^{2+} release altogether contributing to reduced rates of calcium cycling and diminished cellular contractile performance in CHF (Wasserstrom *et al.*, 2009).

The idea that myocyte contractility is depressed in the failing heart is supported by many, but not all, (Gupta *et al.*, 2000) studies. Current or previously used HF treatments that increase contractility, primarily by increasing cAMP, have generally increased mortality (Houser and Marguiles, 2003). Similarly, a recent study has reported that that maintaining myocyte contractility after myocardial ischemia (MI), by increasing Ca^{2+} influx, depresses rather than improves cardiac pump function by reducing myocyte number (Zhang *et al.*, 2010). It is generally agreed upon that contractile properties can be similar in normal and failing muscles under basal conditions but rate-related contractile reserve is absent or significantly reduced in failing human myocardium. Several studies have described that at least in the end-stage failing human heart, basal contractility is well preserved but "contractility reserve" i.e. the ability to increase contractility with heart rate or sympathetic stimulation is severely depressed. Such alterations may underlie the poor pumping function, reduced exercise capacity and tachycardia intolerance of the failing human heart (Scrutinio *et al.*, 2000; Gudjonsson *et al.*, 2002; Houser and Marguiles, 2003)

Reduced pump performance of the failing heart may not exclusively be the result of fundamental defects in myocyte contractile properties. Other important factors include geometric remodelling and ECM alterations, cell death (apoptosis), altered vascular structure and reactivity, abnormal energy utilization and neurohormonal disturbances that can also contribute to the progression of HF (Swynghedauw, 1999) at least under

certain conditions and may do so independent of defective myocyte contractility (Fedak *et al.*, 2005). Most importantly, contrasting the traditional view that contractile failure leads to overt HF, today the HF pathophysiology paradigm has shifted towards the notion that the systolic and diastolic dysfunction are consequences of a structural increase in ventricular chamber volume (Swynghedauw *et al.*, 2010). This is related to changes in ventricular geometry that places the heart at a considerable mechanical disadvantage, independent of any functional changes at the cellular level. Several studies detailing the natural history of HF have shown that progressive LV remodelling is directly related to future deterioration in LV performance and a less favorable clinical course in HF patients (Cohn *et al.*, 1995; Douglas *et al.*, 1989; Vasan *et al.*, 1997; Mann, 1999). Conversely, preventing the progression of HF by slowing or reversing the remodelling process is today an important target of therapy. The chronic effects of therapies on surrogate measures of remodelling including changes in ejection fraction, LV end-diastolic and end-systolic volumes have been assessed in large randomised studies and serve as a guide to the remodelling process. Given the potential central importance of LV remodelling in the progression of HF, the following section outlines putative cellular and molecular mechanisms underlying this process.

Cardiac Structural Remodelling

Structural and functional integrity of the heart is orchestrated by a fine balance between several neurohormonal and hemodynamic influences. Disruptions in this ‘fine tuning’ (e.g. in duress or injury) activate a complex, progressive process of diverse adaptive responses at transcriptional, molecular, cellular and functional levels that allow the heart to adjust to new working conditions and can be collectively termed ‘remodelling’. For the intents and purposes of this work, cardiac remodelling may be broadly defined as alterations in cardiac structure resulting from altered hemodynamic load and/or cardiac injury. While remodelling may be physiological or pathological and by extension adaptive or maladaptive, in the present context the above definition excludes all aspects gestational or developmental as well as favourable remodelling that follows intensive exercise and is restricted to acquired structural rearrangement in the left myocardium.

Cardiac remodelling is a common denominator in the aetiology of several primary cardiovascular diseases notably DM, coronary atherosclerosis, hypertension, cardiomyopathy, and myocarditis (Swynghedauw, 1999). As shown in Fig 1.4, HF may be viewed as a progressive disorder that is initiated in response to an index event (that

may be acute i.e. MI, chronic i.e. DM or hereditary) that results in a loss/damage of functioning myocytes or alternatively produces a decline in the ability of the heart to function as a pump. Irrespective of the inciting event, several neurohormonal and inflammatory pathways are activated, including the renin–angiotensin–aldosterone system (RAAS), the adrenergic system, inflammatory cytokine systems and a host of other autocrine and paracrine events as compensatory mechanisms to maintain stroke volume at a reduced ejection fraction (Packer, 1992; Fedak *et al.*, 2005). Thus far, a multitude of proteins including norepinephrine, angiotensin II, endothelin, aldosterone, TGF β 1, tumor necrosis factor α (TNF α) have been implicated in to disease progression of the failing heart (Maytin and Colucci, 2002; Fedak *et al.*, 2005; Swynghedauw *et al.*, 2010). These processes are initially compensatory and beneficial, and in most instances, patients remain asymptomatic or minimally symptomatic following the initial decline in pumping capacity of the heart, or will develop symptoms only after the dysfunction has been present for some time (Maytin and Colucci, 2002). As such, the index event produces remodelling of the LV frequently along one of two patterns: hypertrophy or dilation. Myocardial hypertrophy associated remodelling results in increased LV mass without any effects on LV volume in a process termed ‘concentric remodelling’ that is associated with preserved function as the ventricle is capable of generating greater force and higher pressure. The onset of LV dilation is characterised by ‘eccentric remodelling’ and substantial increases in intraventricular volume with comparable increases in LV mass that represents a compensatory response to augment cardiac output in the face of diminished contractile function. Eventually, functional demands override physiological compensatory mechanisms. It follows that the hypertrophic reserve of the myocardium is met; LV dilation progresses without appreciable increases in LV mass and in accordance with the Law of Laplace induces excessive wall stresses known to be typically antecedent to overt HF (Swynghedauw, 1999) (Fig 1.4). Self-sustaining neurohormonal and cytokine input becomes deleterious in the long term and the overexpression of the portfolio of bioactive molecules are known to contribute to disease progression independently of hemodynamic status by exerting direct cardiotoxic effects. Targeting neurohormonal input is therefore the basis of current HF treatment. Altogether, the triggers that stimulate the development of HF and varied and diverse and sustained LV remodelling is associated with a poor prognosis, gradual myocardial deterioration and a critical step towards transition to *decompensatio cordis*. However, it is important to appreciate that cardiac remodelling is a biological adaptive processes

triggered by environmental stress, and the onset of HF represents the limits of said adaptation.

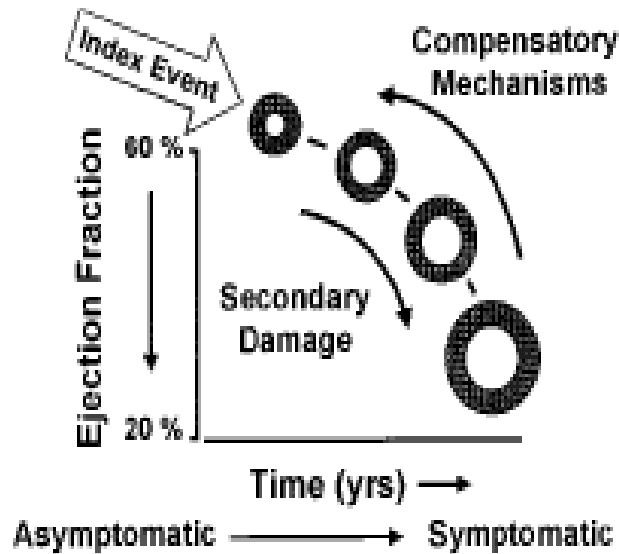


Fig 1.4: Heart failure pathogenesis. Currently accepted schema of HF development and progression states that HF begins in response to an index event that produces an initial decline in pumping capacity of the heart following which a variety of compensatory mechanisms are activated to restore homeostatic CV function, including the adrenergic nervous system, the renin angiotensin system, and the cytokine system. Although beneficial in the short term, sustained activation of these systems can lead to worsening LV remodelling and cardiac decompensation that underscores the transition to symptomatic HF. (Image courtesy Mann *et al.*, 2009)

1.2.2 Molecular signature of cardiac structural remodelling

Cardiac remodelling occurs in response to cues generated by mechano-sensors (Connexins, integrins) that couple cellular signalling pathways to altered or mechanical stress/ injury. Where the nature and extent of signals that are transiently activated are far from fully understood, it is accepted that the myocardial response to injury or altered mechanical load involves profound alterations in gene expression including the activation of those that are normally involved in embryogenesis, also known as the foetal gene program (Swynghedauw, 1999). In the context of MI-induced cardiac remodelling alone, genome-wide analyses have revealed significant coordinated changes in over 1400 genes early and 125 genes late in the infarct zone, and nearly 600 genes early and 100 genes late in the non-infarct zone (LaFramboise *et al.*, 2005).

Foetal gene reprogramming, characteristic of pathological remodelling frequently involves an upregulation of fetal isoforms of genes whose products regulate cardiac

contractility and Ca^{2+} handling and paralleled by a down-regulation of their adult isoforms (i.e., up-regulation of β -MHC vs. down-regulation of α -MHC) and often includes decreased SERCA2a and increased NCX expression (Hilfiker-Kleiner *et al.*, 2006). Another important feature of the foetal gene phenotype markedly expressed in the remodelled myocardium is that of the natriuretic peptides ANP and BNP, often detectable in the circulation where they are used as an indirect marker for myocardial injury/overload (Lukowicz *et al.*, 2005). These transcriptional changes culminate in several molecular and cellular alterations that characterise myocardial remodelling. For the purposes of this work, they are broadly categorised into those that occur in the myocyte and changes that occur in the volume and composition of the ECM.

Within the myocyte, in addition to the functional changes described in the previous section, the remodelling process is invariably associated with sarcomeric reorganisation; Dilation of the heart is associated with myocyte re-lengthening, mediated by the generation of new sarcomeres in series and an enhancement of the length-to width ratio whereas a hypertrophic phenotype is the result parallel addition of new sarcomeres. At the molecular levels, hypertrophy appears to be characterized by increased expression of adult isoforms of sarcomeric genes (i.e., α MHC, cardiac α SKA) and is often concomitant with increased natriuretic peptide synthesis (Hilfiker-Kleiner *et al.*, 2006). Furthermore, biomechanical stretch signalling, altered redox states and pathological stimuli including HG and TGF β 1 may induce the activation of the phosphatidylinositol 3-kinase (PI3-K)/protein kinase B (Akt)-p70S6K, and/or activation of extracellular signal-regulated kinases (ERK) which co-ordinate the hypertrophic response (Selvetella *et al.*, 2004, Wu and Derynck, 2009).

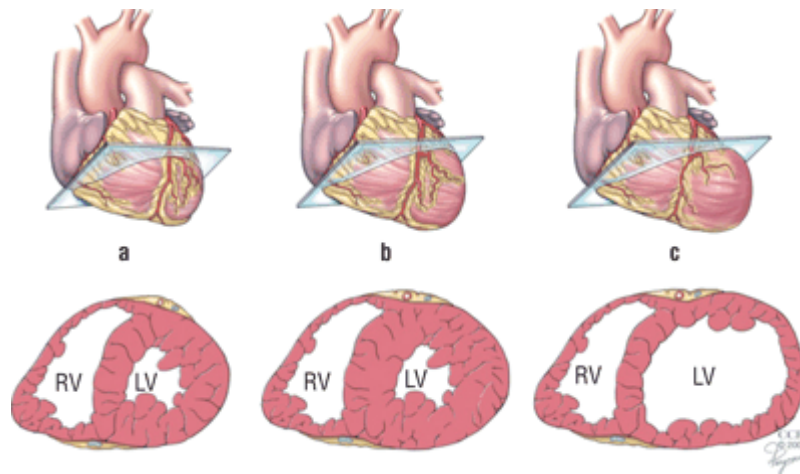


Fig 1.6: Cardiac Hypertrophy. Left and Right Ventricles (LV and RV) in cross section. a, normal; b, concentric hypertrophy; and c, eccentric hypertrophy. Image adapted from Albert *et al.*, 2004.

Much experimental evidence suggests that the gradual loss of myocytes through necrotic and apoptotic cell death contributes to progressive and LV remodelling and cardiac dysfunction in the failing heart (Sabbah 2000; Wenker *et al.*, 2003; Foo *et al.*, 2005). Particularly in relation to apoptosis, this point of view has received increasing support with the recognition that DNA damage characteristic of apoptotic cell death occurs in myocytes from failing hearts (Sabbah, 2000). Apoptotic events are characterised by the activation of caspase-8 and subsequently procaspase-3, an event initiated by the activation of cell surface death receptors (e.g., Fas/FasL). On activation, caspase-3 activates downstream proapoptotic effector proteins such as Bax and Bad and subsequently the release of cytochrome *c* and other apoptogens from mitochondria (Hilfiker-Kleiner *et al.*, 2006). Additionally, caspases may also cleave myocardial contractile proteins and promote systolic dysfunction. Therefore, treatment with caspase inhibitors after myocardial infarction has been shown to preserve myocardial contractile proteins, reduce systolic dysfunction, and attenuate adverse ventricular remodelling and reduce infarct size after MI (Chandrashekar *et al.*, 2004). Despite the undeniable intrinsic appeal of programmed cell death as a potentially important mechanism for disease progression in the failing heart, a definitive role for cell death has not been established on account of several considerations including: 1. As catecholamines can provoke apoptosis, there is the possible overestimation of myocyte apoptosis frequency

assessed in explanted hearts obtained from patients awaiting cardiac transplantation, many of whom receive inotropic support (Narula *et al.*, 1996; Olivetti *et al.*, 1997). 2. Data concerning myocyte cell death in mild to moderate HF is not forthcoming, casting doubt over whether apoptosis contributes to failure or whether it is a phenomenon that is observed only in end-stage HF. 3. There is considerable disparity in the published literature over estimates of apoptotic processes, ranging from 0.003%/year to clinically unrealistic estimates of '5% to 35% (estimated myocyte loss > 100%/year) (Mann, 1999). These inconsistencies in findings may be attributable to varying inclusion criteria amongst studies. For e.g. a study examining the zone of infarction may report significantly greater apoptotic myocytes opposed to another examining non infarcted hearts and/or a milder pathology. Thus, it is difficult to definitively ascertain whether myocyte cell loss is an important contributor to HF pathogenesis, occurs early and continually in HF or, instead, only in end-stage hearts.

Outside changes in the myocyte, structural remodelling in the myocardium is associated with alterations in the structure and function of the ECM. Indeed, ECM deposition is a widely recognized alteration in the failing heart and the notion that progressive fibrosis underlies LV dilatation and HF progression has been engendered by several experimental and clinical studies (Cohn, 1995; Mann, 1999; Maytin and Colucci, 2002; Fedak *et al.*, 2005, Miner and Miller, 2006; Bowers *et al.*, 2010). In pathological conditions, the ECM can be temporarily remodeled, reversibly remodeled or fully adapt to the changes in biomechanical load. However, prolonged overload results in detrimental collagen deposition that can render the heart electrically and structurally heterogenous, result in excessive diastolic stiffness (Van Heerebeek *et al.*, 2008) and/or induce LV dilatation altogether resulting in overt HF. Particular emphasis is given to the collagenolytic MMPs and their inhibitors, the TIMPs in underlying LV dilatation. The balance of proteolytic and antiproteolytic activity appears to be an important determinant of the rate of ventricular enlargement. The general view is that disruption of this balance results in progressive MMP activation leading to degradation of the ECM, myocyte slippage, thinning of the ventricular wall, and ventricular dilation that occurs in end stage HF (Swynghedauw, 1999; Maytin and Colucci, 2006; Yan *et al.*, 2009). In support of this stance, pharmacologic MMP inhibition in a pacing-induced animal model of HF improved LV dimensions and performance when administered early in the remodelling process (Spinale *et al.*, 1999). Chronic pharmacologic inhibition of MMP activity in rats with HF of hypertensive origin resulted in an attenuation of ventricular

dilation and dysfunction that was sustained throughout the 4 months of therapy (Peterson *et al.*, 1999). Similarly, targeted deletion of MMPs has been shown to limit maladaptive remodelling in experimental models (Matsusaka *et al.*, 2006) altogether indicating the potential therapeutic relevance of MMP inhibition which may be exploited in the near future. Studies employing transgenic mice clearly show the role of MMPs and TIMPs in mediating the preservation of normal cardiac geometry and function, and are consistent with less deleterious cardiac remodelling in animal models treated with pharmacological MMP inhibitors (Graham and Trafford, 2007).

1.2.3 TGF β 1 in Cardiac Remodelling and Failure

In recent years, a central role for TGF β 1 in the remodelling myocardium has come to light, given consistent myocardial upregulation in experimental models of MI and HF, and frequently in patients with dilated or hypertrophic cardiomyopathy (Dobaczewski *et al.*, 2010). TGF β 1 is the most prevalent isoform of the TGF β s, a family of pleiotropic cytokines which are implicated in a wide variety of cell functions, including regulation of inflammation, ECM deposition, cell proliferation, differentiation and growth. The activating stimuli for TGF β 1 are varied, including reactive oxygen species, integrin-mediated interactions and also MMP's 2 and 9, a phenomenon that couples matrix degradation with activation of a molecule that primarily mediates matrix integrity and stability (Annes *et al.*, 2003). Beyond homeostatic roles, TGF β 1 mediates phenotype and function of several cell types crucial in tissue injury and repair processes including fibroblasts. In addition to enhancing ECM synthesis from fibroblasts, it exerts potent matrix-preserving actions by suppressing the activity of the MMPs and by inducing synthesis of TIMPs (Schiller *et al.*, 2004). TGF β 1 is a key upstream effector of CTGF, a fibrogenic mediator that acts in concert with TGF β to promote persistent fibrosis (Leask and Abraham, 2004). The hypertrophic effects of TGF β 1 stimulation on cardiomyocytes may be by TGF β 1-mediated synthesis of fetal contractile proteins (Parker *et al.*, 1990). Alternatively and of particular importance, a recent *invitro* study elegantly demonstrated the ability of HG to induce hypertrophy in fibroblasts and epithelial cells (Wu *et al.*, 2009) and implicated a central role for TGF β 1 signalling in this process (Fig 1.5). It was demonstrated that blocking the kinase activity of the T β RI receptor or loss of its expression prevented the hypertrophic effects of HG. The authors proposed that exposure of cells to HG induced a rapid increase in cell surface levels of the TGF β receptors, T β RI and T β RII, and a rapid activation of TGF β ligand by MMP2 and MMP9. The consequent autocrine TGF β signalling in response to glucose led to

activation of pro-hypertrophic Akt-TOR pathway. As such, blocking MMP2/MMP9 (by transfection of cells with siRNA specific for MMP2 or MMP9) or TGF- β -induced TOR activation (by administering rapamycin) inhibited high glucose-induced cell hypertrophy. However, whether this mechanism holds true *in vivo* and in the context of the cardiomyocyte has not been established.

Although there is substantial evidence indicating that TGF β 1 mRNA and protein induction is upregulated in the remodelling myocardium, direct evidence of increased activity is still lacking (Dobaczewski *et al.*, 2010) and *in vivo* effects of TGF β 1 in promoting the myocardial fibrotic and hypertrophic response are supported by overexpression experiments in transgenic mice (Rosenkranz 2002, Dobaczewski *et al.*, 2010). Targeting regulatory mechanisms of ECM homeostasis that precede transition to HF remains a vital goal in HF management. As TGF β 1 levels often reflect the development of cardiac remodelling (Villar *et al.*, 2009) the TGF β 1 system is a promising therapeutic target for myocardial infarction and for cardiomyopathic conditions such as diabetic cardiomyopathy that are associated with fibrosis and hypertrophy. Also late, but not early, TGF β blockade has been demonstrated to attenuate remodelling in experimental MI and TGF β inhibition through administration of inhibitory peptides (Hermida *et al.*, 2009), or neutralizing antibodies (Kuwahara *et al.*, 2002), has prevented the development of cardiac fibrosis in experimental pressure overload.

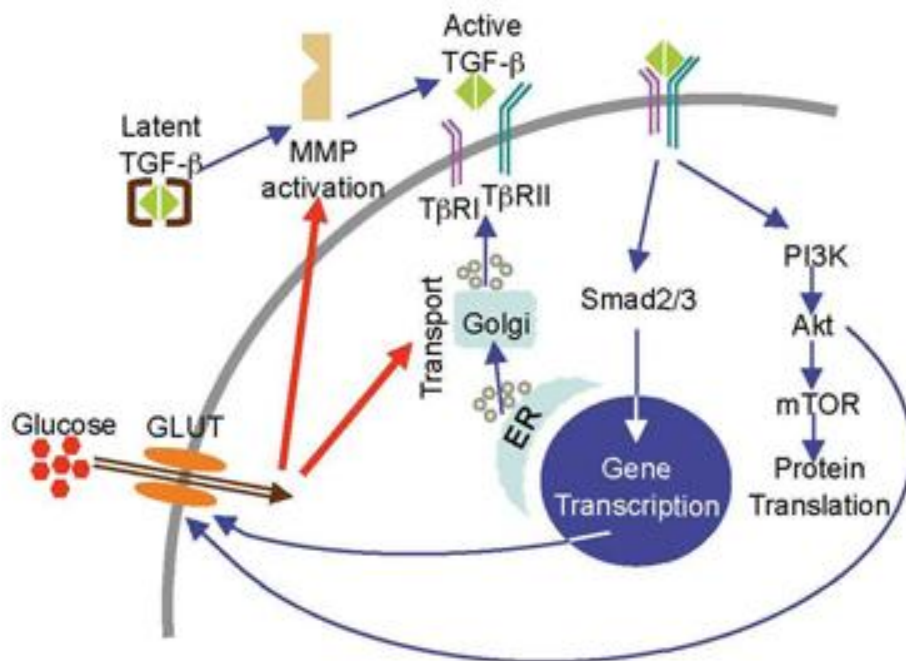


Fig 1.5: Functional interactions of HG with TGFβ signalling that underlie *in vitro* cellular hypertrophy in epithelial cells. HG-induced cell hypertrophy required functional TβRI signalling and rapid induction of TGFβ signalling including Smad (Smad, “sma” (Caenorhabditis elegans protein) + “Mad” mothers against decapentaplegic) activation and MMP-dependent mediation of latent TGFβ, altogether leading to activation of the Akt-TOR pathway and increased cell size. Image courtesy Wu and Derynck, 2009.

In précis, structural remodelling pathognomonic of HF is characterised by alterations in cardiomyocyte phenotype with re-expression of a fetal gene program, defective EC coupling, disturbed intracellular Ca^{2+} handling, and ECM aberrations. These findings have been reproduced *in vitro* and in experimental model systems and are produced in response to several stimuli known to be associated with pathologic remodelling, including mechanical strain, catecholamines, angiotensin, endothelin, peptide growth factors like TGFβ1, inflammatory cytokines, and oxidative stress.

Knowledge and understanding of the mechanisms underlying HF has developed steadily over the last century. Once considered an edematous disorder, 40 years ago a hemodynamic derangement and today a principally neurohormonal event, the central dogma of HF onset and progression has evolved considerably. However, a unifying mechanism underlying HF pathogenesis is still elusive and there is still considerable uncertainty of the exact nature of the disease, defaulting to the analysis of its parts from various perspectives. In this regard, where numerous drug and nondrug strategies have

been developed over the last 20 years, based on the prevailing mechanistic understanding at the time, many efforts to correct fluid retention, stimulate the inotropic state of the heart, and modulate neurohormonal systems have not predictably improved the condition of HF patients (Lionetti and Recchia, 2010). The complexities and intricacies of the field and the challenges encountered in translational study are outside the scope of this thesis but were effectively emphasised in a 2002 editorial stating ‘Nearly 1,000 new drugs and devices have been developed for the treatment of HF during the past 20 years, but only 9 have received regulatory approval and are being used in the clinical setting’ (Packer, 2002). Unfortunately, almost a decade later, the editorial comment is still highly topical.

What cannot be contested is the impact of DM towards HF pathogenesis. CHF and DM commonly coexist and each condition appears to increase the likelihood of developing the other. Their synergistic influence in the same patient markedly increases the risk of morbidity and mortality and complicates therapeutic intervention (McDonald *et al.*, 2008; Van Melle *et al.*, 2010). In the next section, epidemiological overlap and fascinating intersection between these 2 common conditions is addressed. However, for the purposes of the present work, text is limited to the contribution of DM towards HF pathogenesis

1.3 Diabetes Mellitus

The importance of studying DM is illustrated by the fact that it is a disease of epidemiological impact, being one of five leading causes of death in most developed countries (Bandyopadhyay, 2006). The estimated prevalence rate for DM in 2010 was 285 million, projected to affect 438 million people by 2030 (Diabetes UK, 2010). The epidemic of DM is accompanied by the scourge of CVD. With morbidity and mortality rates reaching epic proportions, the disease today represents one of the greatest medical and socio-economic challenges for this century.

Clinical Presentation of Diabetes Mellitus

DM is a progressive, debilitating disease characterised by HG and glucose intolerance due to insulin deficiency, impaired effectiveness of insulin action or both (Kumar and Clark, 2009). Current diagnosis of the disease is based on glucose levels (WHO, 2006); random venous plasma glucose levels above 11.1mmol/L on two occasions and/or fasting plasma glucose ≥ 7 mmol/l (126 mg/dL) is required for a diagnosis of DM. A two-hour blood glucose ≥ 11.1 mmol/L (200 mg/dL) on administration of an OGTT (2 hour venous plasma glucose after ingestion of 75 g oral glucose load) compared to

normal glucose tolerance value of <7.8 mmol/L is used to further confirm DM. Other signs and symptoms include polydipsia, polyphagia and unexplained weight loss.

On the basis of aetiology, natural history and clinical presentation of the disorder, the disease is classified into type 1 (T1DM) and type 2 DM (T2DM). T1DM, previously known as juvenile-onset DM ranks as one of the most common childhood diseases in developed nations and comprises $<10\%$ of all cases of DM. The causative factors of T1DM continue to be under some speculation and a genetic vulnerability has been suggested (Horst *et al.*, 1997). The prevailing concept is that T1DM, also known as 'Insulin Dependent Diabetes Mellitus' results from a cellular-mediated autoimmune destruction of pancreatic islet β cells that is strongly associated with the major histocompatibility complex resulting in loss of insulin production that is restored, up to a point by immunosuppression (Parving *et al.*, 1999). Despite several advances in the field, T1DM is currently refractory to prevention, barring toxic immunosuppression (Mordes *et al.*, 2008). T2DM, previously known as Non Insulin Dependent Diabetes Mellitus, accounts for 90-95 % of diabetic individuals (Zimmet and Alberti, 2006). The disorder is characterised by HG due to an impairment of insulin-mediated glucose uptake, i.e. insulin resistance (IR) or a defective secretion of insulin by pancreatic β cells. As age advances, insulin secretion tends to decline. In this respect it is noteworthy that most diagnoses of T2DM are made after the age of 40 years although the age of onset maybe several years earlier (Kannel and McGee, 1979). Factors initiating T2DM are multi-factorial, cumulative and are usually related to obesity, and decreased physical activity altogether accelerated by genetic predisposition. These alterations increase insulin resistance and in concert with progressive β cell failure, resulting in rising glycemia in the nondiabetic range. In recent years, it has become apparent that being non-diabetic does necessarily imply normoglycemia. An interim condition termed 'prediabetes' that presages the onset of T2DM has been identified wherein glucose levels are elevated but do not meet the current criteria that define diabetes (Bergman, 2009). The term prediabetes is used interchangeably with impaired fasting glucose (IFG) and/or impaired glucose tolerance (IGT), both of which are associated with IR, IFG being primarily due to hepatic insulin resistance and IGT related to IR in muscle (Nathan *et al.*, 2007). IFG is currently defined as an elevated fasting plasma glucose of 100-125 mg/dl (5.6-7.0 mmol/l) and IGT as a 2-hour glucose value between 140-199 mg/dl (7.8-11.1 mmol/l) on OGTT. Although the transition from these early metabolic abnormalities to overt diabetes may take many years, current estimates indicate that up to 70% of individuals with these prediabetic states eventually develop DM and as many

as 83% of individuals with IGT may develop the disease over a lifetime unless changes occur in diet and level of activity (Nathan *et al.*, 2007). It is noteworthy that the absolute glucose concentration that clearly distinguished normal from abnormal glucose tolerance has not been established and the current literature advocates the acknowledgement of a ‘continuum of risk’ opposed to a specific value (Nathan *et al.*, 2007; Cefalu and Watson, 2008; Bergman *et al.*, 2009). Independent studies have reported strong associations between normal FPG levels and the incidence of diabetes, suggesting that diabetes risk increases with fasting glucose levels even within the normal range (Shaw *et al.*, 2000; Nichols *et al.*, 2008). Taking this into account, the speculation has arisen that mild diabetes may not differ substantially from IGT and by extension that that IFG differs from “normal” glucose tolerance at least at the upper limits of the fasting range (Bergman *et al.*, 2009). Finally, the term ‘dysglycemia’ has been coined to describe a state of plasma glucose at which adverse outcomes are likely to occur (Schainberg *et al.*, 2010).

The Burden of Cardiovascular Disease in Diabetes Mellitus

Cardiovascular disease (CVD) refers to dysfunction of the heart and/or the blood vessels, or the blood itself (Marso and Stern, 2003) and includes the clinical manifestations of microvascular and macrovascular disease, coronary heart disease (CHD), stroke, and peripheral vascular disease. CVD is a major cause of death and disability in people with DM, accounting for 44% of fatalities in people with T1DM and 52% in people with T2DM (Diabetes UK, 2010). CVD accounts for up to 80 % premature mortality associated with DM and in the UK, diabetes is second only to smoking as the leading cause of CVD (British Medical Association, 2004). DM has been established as a major independent risk factor for CVD in current risk assessment algorithms such as the Framingham risk score, the New Zealand risk calculator and the British Guidelines (Cameron and Cruikshank, 2007). Diabetic patients frequently show signs of accelerated atherosclerosis, undergo acute coronary syndromes, MI with peripheral artery disease and stroke (Spinetti *et al.*, 2008). Compared with a non diabetic individual, a person with T2DM has a 2-4 fold increased risk of dying from MI or stroke and a 10-15 fold increased risk of a lower extremity amputation (Peter *et al.*, 2008). Diabetic patients also have an adverse course following MI, with high rates of post infarct failure and death (Goodfellow, 1997).

1.3.1 Influence of Diabetes Mellitus on Heart Failure Risk and Outcomes

While CHD is the most common cardiac manifestation in patients with DM, several epidemiological studies have provided clear evidence of the negative influence of diabetes on the prevalence, severity and prognosis of HF (Zimmet and Alberti, 2006). The 2005 ‘Guideline Update for the Diagnosis and Management of Chronic Heart Failure in the Adult’ of the American College of Cardiology/American Heart Association designated patients with DM as having stage ‘A’ HF in recognition of the disease as an important precursor for HF and an independent risk factor for death in HF patients (Hunt *et al.*, 2005).

The first demonstration of an increased risk of HF in patients with DM was reported by Kannel and colleagues in 1979, based on data obtained from 20 years follow-up of the Framingham cohort, wherein a 2.4-fold increase in the incidence of HF in diabetic men and a 5.1-fold increase in diabetic women was reported, independent of age, hypertension, dyslipidaemia, obesity and CHD (Kannel *et al.*, 1974). Since then other large population-based studies have yielded similar results. These include the Cardiovascular Health Study (CHS) (Gottdeiner *et al.*, 2000), the Strong Heart Study (SHS) (Devereux *et al.*, 2000) and the Multi-Ethnic Study of Atherosclerosis (MESA) (Bertoni *et al.*, 2006) that have observed correlations between DM and increased incident HF and also markers of HF risk including LV mass, volume and systolic dysfunction. Cross sectional studies have reiterated these findings, frequently reporting an unusually high prevalence of HF in diabetic patients. A report by Nichols *et al.*, (2001) noted 12% of Type 2 diabetic patients with HF at entry, with an annual incidence of 3.3%. In a similar study of 2737 elderly patients over 43 months, the incidence of HF was vastly higher in diabetic (39%) compared with non-diabetic (23%) patients (Aronow *et al.*, 1999). As expected, subgroup analyses of randomised studies have shown that, that diabetic patients are over-represented in large HF trial populations; 26% of patients in the Prevention arm of the Studies of Left Ventricular Dysfunction (SOLVD) clinical trial were diabetic (The SOLVD Investigators, 1991). Similarly, 19% of ATLAS (Assessment of Treatment with Lisinopril and Survival) study patients were diagnosed with DM (Komadja *et al.*, 1994). Finally, in the V-HeFT-II, trial (Vasodilator-Heart Failure Trial) (Cohn *et al.*, 1986), RESOLVD (Randomized Evaluation of Strategies for Left Ventricular Dysfunction) (McKelvie *et al.*, 1999) and Epidémiologie de l'Insuffisance Cardiaque Avancée en Lorraine (EPICAL) (Zannad *et al.*, 1999) trials diabetic patients represented 20%, 27% and 26% of the population

respectively. Overall, recent estimates indicate that the prevalence of HF in diabetic patients is 12%, rising to 22% in those over the age of 64 years, significantly higher than the 4-6% prevalence in age-matched control populations (Asghar *et al.*, 2009). In 2003, up to a third of all HF hospital admittances were diabetic and conversely, DM has a prevalence of 30% in patients with HF and the disease may be up to four times as prevalent in patients with newly diagnosed HF (Bauters *et al.*, 2003). Finally, diabetic patients are also more likely than non-diabetic patients to develop HF following MI, despite comparable infarct sizes (Mak *et al.*, 1997)

Diabetic Cardiomyopathy in Heart failure Pathogenesis

The association of DM with increased HF risk can be broadly grouped into two main categories, namely CHD and DCM. Although the common final pathway for both CHD and DCM is HF, the latter is the focus of this thesis. A heightened cardiovascular mortality rate in diabetics is accountable in part, to an accelerated atherosclerosis and microvascular dysfunction coupled with augmented thrombogenicity, procoagulability and activation of systemic inflammation culminating in atherothrombotic CHD, diabetic microangiopathy, small artery endothelial dysfunction and increased arterial stiffness. However, HF in DM patients may also have a non-thrombotic/ischemic aetiology with the disease resulting in a distinct metabolic cardiomyopathy. The concept of DCM was first introduced by Rubler *et al.*, (1972), and has subsequently been widely used by epidemiologists and clinicians. Its pathogenesis is underscored by a combination of structural (hypertrophic and fibrotic) remodelling of the myocardium and diastolic dysfunction that precedes systolic failure and overt CHF (Grossman and Messerli, 1996; Bracken *et al.*, 2003).

Evidence substantiating the existence of DCM arises from numerous clinical trials and epidemiological studies implicating structural changes within the myocardium that impair function as a consequence of the disease and its (dys)metabolic milieu, independent of other cardiac co-morbidities (Galderisi *et al.*, 1991; Ishihara *et al.*, 2001; Marwick, 2006; Fox *et al.*, 2007; Sack, 2009). Increased LV diastolic stiffness is often the earliest manifestation of DM-induced LV dysfunction and frequently becomes the main functional deficit of the diabetic heart. Hence HF often presents with normal LVEF (Van Heerebeek *et al.*, 2008) but reduced diastolic compliance is known to modify ischaemic LV dysfunction, as is evident from the reduced LV remodelling and increased incidence of HF after acute myocardial infarction in patients with DM (Stone

et al., 1989; Solomon *et al.*, 2002). Several studies in diabetic populations have reported echocardiographic changes consistent with diastolic dysfunction and LV hypertrophy that precedes the onset of systolic dysfunction. Increased LV wall thickness, LV mass index, impairment of early diastolic filling, prolongation of isovolumetric relaxation, increased atrial filling and increased numbers of supraventricular premature beats, an age-related decline in ejection fraction, and an age-related increase in diastolic diameter are frequently reported in diabetic patients and portend an increased risk for the subsequent development of HF, particularly in the presence of coexisting hypertension (Liu *et al.*, 2001; Bell, 2003; Schannwell *et al.* 2002; Fang *et al.*, 2004; Boudina and Abel, 2007; Dokken, 2008). Echocardiography measurements have revealed that these complications can occur in ‘uncomplicated’ T1DM without clinically apparent macrovascular or microvascular complications and that 30% of patients with well controlled T2DM may have diastolic dysfunction (Boudina and Abel, 2007). In the same vein, data collected utilizing Flow and Doppler methods suggest traditional techniques may have underestimated this figure, further indicating a 40% to 60% prevalence of diastolic dysfunction in community surveys and in smaller studies of individuals with type 1 and type 2 diabetes without overt CHD (Poirier *et al.*, 2001; Redfield *et al.*, 2003; DiBonito *et al.*, 2005; Galderisi *et al.*, 2006). These findings have been confirmed in the laboratory where experimental DCM models demonstrate structural remodelling and abnormalities in diastolic LV function, with or without systolic LV dysfunction. Most studies have been performed in isolated perfused hearts and reveal depressed cardiac function (Sidell *et al.*, 2002; Mazumdar *et al.*, 2004; Boudina *et al.*, 2005; Buchanan *et al.*, 2005). *In vivo* work in rodent models has provided evidence for systolic and diastolic dysfunction by echocardiography (Zhou *et al.*, 2000; Semeniuk *et al.*, 2002). At the cellular level, these abnormalities have been associated with myocyte hypertrophy, fibrosis proliferation and contractile dysfunction of isolated myocytes (Fang *et al.*, 2004; Marwick, 2006; Asghar *et al.*, 2009).

While the existence of DCM as a distinct clinical entity might be conceptually agreed upon and many structural and functional manifestations characterised, its origins are incompletely understood. Several putative mechanisms have been proposed including microangiopathy and cardiac autonomic neuropathy, the metabolic derangements of HG, IR/hyperinsulinemia and their adverse sequelae including depletion of glucose transporter 4, increased free fatty acids, advanced glycation end products and reactive oxygen species, dysfunctional Ca^{2+} homeostasis, that synergistically predispose to the detriment of cardiac structure and function (Dhalla *et al.*, 1998; Kajstura *et al.*, 2001;

Brownlee *et al.*, 2005; Boudina and Abel, 2010). Evidence indicating the involvement and relative contribution of these abnormalities in the development of DCM is still largely equivocal. Where further description of each underlying cause is outside the remit of this report, emphasis in this work is placed on the singular role of HG in the myocardial complications of DM.

1.3.2 Relation between Hyperglycemia and Heart Failure

HG- the *sine qua non* for a diagnosis of DM, the target for antidiabetic therapy and (together with glycated haemoglobin {HbA1c}) the principal marker of glucose control (Schainberg *et al.*, 2010), is an important factor that increases the risk for the development of CV events in general and HF in particular in patients with DM (Bauters *et al.*, 2003; Anselmino *et al.*, 2010). The significance of HG in HF pathogenesis is perhaps better appreciated against a background of clinical trial data. In this context, the level of HbA1c, as a measure of cumulative glycemic burden, is an important marker of increased risk. In an epidemiological analysis of the United Kingdom Prospective Diabetes Study (UKPDS), for each 1% rise in HbA1c, a 14% rise was shown in the risk for MI, a 12% rise in the risk for stroke, and a 16% rise in the risk for HF (Stratton *et al.*, 2000). In the Strong heart study, T2DM was associated with LV enlargement and decreased myocardial function, where the extent and frequency of diastolic dysfunction was directly proportional to A1c level (Devereux *et al.* 2000). In a Danish study of MI survivors with DM and HF, each 1% increase in HbA1c above 5% over a 2.5-year follow-up period resulted in a 24% increase in mortality (Gustafsson *et al.*, 2007). Preliminary data from an ongoing study in Scotland demonstrated that 1% increase in HbA1c was independently linked to a 19% increase in incident HF after controlling for mean arterial pressure and use of anti-diabetic drugs such as thiazolidinediones (Wong *et al.*, 2010). A number of mechanisms have been postulated by which HG can contribute to the development and progression of DCM and HF. Diastolic dysfunction in DCM is thought to be the result of HG-induced structural remodelling characterised by myocellular hypertrophy and apoptotic cell death, alterations in myocardial Ca²⁺ handling and ECM modifications, leading to increased ventricular stiffness and impaired relaxation (Bell, 2003; Asghar *et al.*, 2009; Boudina and Abel, 2010). Experimental studies indicate that cardiac efficiency is decreased in diabetes because of increased fatty acid utilization, which leads to an increased production of ROS. The increase in HG-mediated oxidative stress in diabetic hearts has been found to alter mitochondrial function, decrease NO levels, worsen endothelial function, and induce myocardial injury through stimulation of inflammatory mediators

resulting in cardiomyocyte contractile dysfunction and altered Ca^{2+} homeostasis (Dhalla *et al.*, 1998; Kajstura *et al.*, 2001; Brownlee *et al.*, 2005; Boudina and Abel, 2010).

Compelling epidemiological and experimental evidence notwithstanding, the role of HG *per se* in HF pathogenesis is still controversial and several factors potentially contribute to the contention: A significant proportion of what is known about the underlying aetiology of DCM is based on scattered data obtained from several animal models and considerable inconsistency exists in the demonstration of cardinal manifestations of the disease including myocyte contractile dysfunction and structural remodelling (Asghar *et al.*, 2009). In the interpretation of experimental results, differences in animal models examined are another major consideration. Moreover, because DM develops at varying tempos in these models, it is important to bear in mind that studies performed in animals before the onset of DM may reflect changes that are secondary to other risk factors (e.g. underlying obesity), and studies performed after the onset of DM may reflect the added effects of HG of various durations. Thus despite numerous studies of experimental diabetes, there are varying degrees of disparity in the exposition of the ‘hallmark’ characteristics of DCM (addressed further in Chapter 3).

DM is a multifaceted disease that often clusters with the metabolic syndrome (especially obesity and hypertension). Hence it is a challenge to de-tangle the importance of contributory insults to the myocardium and distinct delineation of the syndrome from other cardiac risk factors is not always feasible in clinical studies (Sack, 2009). The extensive overlap between DM, hypertension, and ischemic heart disease also makes it difficult to tease out the degree of myocardial dysfunction that is caused by the metabolic syndrome, *per se*. Caution is advised in the interpretation of clinical trial/epidemiological study data as conclusions sometimes tend to be drawn from small, heterogeneous populations using indices with known limitations. These include non-adjustment for accepted confounding factors such as diastolic dysfunction or LVEF and short follow up times (Held *et al.*, 2007; Van Melle *et al.*, 2010). Moreover, despite strong associations between increasing dysglycemia and CV risk it has not been clearly demonstrated that lowering of blood glucose improves in HF prognosis/ delays HF onset patients with T2DM (Goldfine and Beckman, 2008). Where glycemetic control is expected to eliminate morbidity and mortality in DM, recent trials have demonstrated that very tight control of glucose in patients with diabetes (with or without episodes of hypoglycemia) may not improve mortality, and may, in fact, increase it (DCCT research group, 1993; Nathan *et al.*, 2005; Gerstein *et al.*, 2008). Results for some outcomes, such as all-cause and cardiovascular mortality have varied significantly

across trials. For instance, the UKPDS metformin trial reported that tight glycemic control reduced mortality risks (UKPDS study group, 1999). In stark contrast, the ACCORD (Action to Control Cardiovascular Risk in Diabetes) trial reported that stringent glycemic control increased these risks (ACCORD study group, 2008). Possible explanations for the increased mortality risk with tight control in the ACCORD trial included the adverse effects from hypoglycaemia or the anti-diabetic insulin sensitizer rosiglitazone and **chance**. (!) (Montori and Fernández-Balsells, 2009).

1.3.3 Animal models of Diabetes Mellitus

A significant part of the current understanding of the pathophysiology and pathogenesis of cardiac disease in DM can be attributed to experimentation in the rodent model system. The rodent model shares many phenotypic similarities to human disease and meaningful correlates can be drawn in metabolism and physiology. With regard to the influence of DM on cardiac structure and function, rat models have been effectively used to study structural phenotypes, physiology of altered energy flux and storage, insulin secretion and action and numerous other metabolic parameters (McNeill, 1999; Kahn, 2005). Considering the limitations of invasive testing in human tissues and ethical and logistical constraints herewith, rat models provide invaluable opportunities to study detailed molecular mechanisms underlying the pathophysiology of diabetes in controlled conditions accounting for microbiological, chemical, genetic and environmental factors. Other advantages include relatively short generation intervals, adaptability to invasive testing and other economic considerations. Rat models mimicking physiological and pathological states unique to each diabetes subtype have been developed to investigate inherent etiopathologic heterogeneities. Spontaneous models of type 1 DM include BB (bio breeding) rat and the Long Evans Tokushima lean rat, whereas the Otsuka Long-Evans Tokushima Fatty (OLETF) rat and Israeli sand rat are examples of monogenic models of obesity and diabetes. The rat models utilized in this study are described below.

The Streptozotocin-induced type 1 diabetic rat model

Chemically induced type-1 diabetes is by far the most common model of animal DM and frequently involves administration of agents that produce the desired pathology by producing toxic effects on the beta cells of the pancreas. Alloxan and Streptozotocin

(STZ) are widely used diabetogenic agents owing to their specific action on β cells resulting in lesions that quite accurately resemble β cell destruction characteristic of T1DM and the sustenance of a relatively permanent diseased state to enable investigation of chronic effects of DM (Lenzen, 2008). Compared to alloxan (cyclic urea analog), STZ is reported to have a greater specificity to β cells, a longer half life and is associated with lower mortality rates (Lenzen, 2008), making it the agent of choice for chemical induction of experimental diabetes in this study. The antimicrobial STZ [2-deoxy-2(3-methyl-3-nitrosourea)1-D-glucopyranose], is a product of *Streptomyces achromogens* and has been used as a chemotherapeutic alkylating agent. Declared diabetogenic in 1963, by Rakieta *et al.*, (1963) STZ results in a metabolic milieu characterised by insulinopenia termed 'STZ-diabetes' resulting from targeted β cell necrosis via processes of methylation, free radical generation and NO production. Post administration, the GLUT-2 transporter transports STZ into pancreatic cells wherein it generates highly reactive carbonium ions (CH^3+) that alkylate and fragment DNA bases along a defined sequence of events. DNA damage results in the activation and overstimulation of the pro-survival, cell repair nuclear enzyme poly(ADP-ribose) polymerase and concomitant reduction in β cell NAD^+ and ATP stores. This alteration in redox states and histological changes in the affected cells ultimately result in β cell necrosis. Other supplementary hypotheses in the diabetogenic potential of STZ include its ability to act as an intracellular nitric oxide (NO) donor, generating 3',5'-cyclic guanosine monophosphate (cGMP) and NO that participate in DNA damage by inhibiting aconitase (Turk *et al.*, 1993). Finally, the participation of STZ in xanthine metabolism has been associated with increases in ROS that may further accelerate cell death and inhibition of insulin synthesis (Nukatsuka *et al.*, 1990). In aggregate, these mechanisms result in deficits in insulin biosynthesis, glucose-induced insulin secretion and glucose transport and metabolism culminating in diabetes that resembles human hyperglycemic nonketotic DM (Weir *et al.*, 1981).

The GK rat

The GK rat is a non-obese, spontaneously T2DM model obtained by the selective breeding of mildly glucose-intolerant Wistar rats, repeated over several generations (Goto *et al.*, 1975). The pathogenesis of diabetes in the GK rat includes reduced pancreatic β cell mass (upto 50%) and pancreatic insulin stores, an impaired insulin secretion in response to glucose both *in vivo* and in isolated pancreata, IR in adipose tissue, muscle and liver, moderate but stable fasting HG and late complications

manifesting as nephropathy and neuropathy (Ostenson *et al.* 1993; Yashushi *et al.*, 2007; Howarth *et al.*, 2007). T2DM in the GK rat is speculated to be polygenic, and six independent genetic loci have been identified to be involved in the disease (Gaugier *et al.*, 2006). GK rats have a stable, inheritable form of T2DM and do not develop marked obesity, hypertension or hyperlipidemia (Portha *et al.*, 1991; Zhou *et al.* 1995; Begum and Ragolia, 1998; Yashushi *et al.*, 2007; Darmellah *et al.*, 2007).

1.3.4 Aims and Scope of Developmental Experiments

To summarise the concepts presented in this section, independent of CHD, diabetic patients appear to have an increased risk of developing HF. Although this phenomenon is strongly correlated with increasing HG, the convoluted nature of the disease, ambiguous clinical data and inconsistencies in experimental results emphasise a need to re-examine cardiac effects of HG and its potential contribution to DCM in order to formulate independent observations and draw concrete conclusions. This was the rationale for ‘developmental’ experiments presented in this thesis. The main mechanical defects of DCM (encompassing reduced contractility, prolonged relaxation, and decreased compliance) are associated with impaired contractile function at the level of the cardiomyocyte and/or LV remodelling changes (Fang *et al.*, 2004; Asghar *et al.*, 2009).

The following hypotheses were tested in the developmental phase of this study using the the STZ-induced rat model of DM.

1. A milieu dominated by HG can produce impairments in myocyte contractility and altered $[Ca^{2+}]_i$ handling.
2. LV Structural remodelling occurs as a result of uncontrolled HG, characterised principally by myocyte hypertrophy, ECM proliferation and apoptotic cell death.

CHAPTER 2

MATERIALS AND METHODS

2.1 Experimental design: Developmental experiments assessing myocyte contractility and remodelling changes were conducted in STZ-induced T1 diabetic rats and age-matched Wistar controls. Subsequently, in one set of experiments, cellular and molecular reorganisation of the myocardium in prediabetes was studied in young adult GK rats at 8 weeks of age. Next, the effect of chronic overt (mild) T2DM on the same variables was evaluated in aged animals at 18 months of age. For each experiment, there was a diabetic/prediabetic group and a normoglycemic Wistar control group matched for age. Focus was on the LV as it is recognised as the primary target of apoptotic and remodelling changes, especially in the ageing heart (Kwak *et al.*, 2006).

2.2 Experimental models: The project received the relevant ethical clearance from the Ethics Committee at the University of Central Lancashire. All procedures conformed to the 'UK Animals (Scientific Procedures) Act 1986'. Animals were housed in groups under institutional regulations at standard vivarium conditions, granted free access to water and commercial chow (unless specifically indicated) and exposed to a 12 hr light/12 hr dark cycle. Rats were monitored throughout the experimental period for any signs of distress.

2.2.1 Streptozotocin induction: For experiments described in Chapter 3, 10 Male Wistar rats (initial body weight 100-150 gm) were given a single intraperitoneal injection of 60 mg/kg body weight Streptozotocin (Sigma, S-0130) dissolved in 0.1 M citrate buffer solution (0.1 M citric acid, 0.1M sodium citrate in distilled water, pH 4.5). An equivalent volume of citrate buffer solution was administered to 10 healthy age-matched Wistar controls. 2-4 days following STZ-administration and prior to experimentation at 6-7 weeks, blood glucose was assessed using a glucose meter (One Touch II glucose meter, Lifescan inc) to confirm DM after an overnight fast.

2.2.2 GK model of prediabetes and T2DM: Young adult male GK rats and age-matched Wistar controls with initial body weights of 150-180 gm were obtained from a commercial colony (Taconic, USA). Aged GK rats were 18 months old and weighed approximately 413 gm. No spontaneous deaths were recorded in the colony at this age. Prediabetes in the young group (n=8) and overt DM in the aged GK rats (n=8) was confirmed by measuring fasting blood glucose as described for the STZ-rats. Additionally, an OGTT was administered in GK rats and age-matched controls (n=8 for both old and young groups) to assess glucose tolerance. In brief, after an overnight fast, animals were injected intraperitoneally with 6 g glucose /kg bodyweight. Blood glucose was measured using a glucometer (One Touch II glucose meter, Lifescan inc) at time zero, 30, 60 and 120 min after glucose injection.

2.3 Sample collection: Animals were weighed throughout the study period and before termination of the experiment at six-seven weeks for the STZ-treated rat group, eight weeks for young (prediabetic) GK rat group and at eighteen months for the aged GK rat group and respective age-matched male Wistar controls for all cohorts. Animals were humanely killed by cervical dislocation and hearts rapidly removed by midsternal incision. Blood was collected from bifurcation at the aorta in tubes containing 25 mM Ethylenediaminetetraacetic acid (EDTA) and rapidly put on ice following centrifugation at 3,000 rpm for 5 min. Plasma was removed, transferred to a new tube, and spun again at 12,000 rpm for 5 min to remove residual red blood cells and platelets. Samples were stored at -70°C until use. After the excision of the heart, the great vessels were trimmed off and blood was removed by opening atrial and ventricular chambers, and heart weight was recorded. Subsequently, the atria were dissected along the atrio-ventricular groove and the coronary arteries cut perpendicular to their course for assessment of atherosclerotic lesions. The LV was isolated and the weight (inclusive of the septum) was determined. In a subset of hearts from both the GK groups (n=4), wall thickness was estimated by cross-sectioning midway between the apex and the coronary groove by averaging 10 equally spaced measurements from sections of the LV representing the portion halfway between the base and the apex of the heart. These determinations were restricted to the LV free wall. In all groups of animals, the LV free wall was then dissected radially to obtain tissue fragments extending from the endocardial to the epicardial surface. These samples were then immersed in a drop of freezing medium (OCT, BDH), frozen in liquid N² for RNA/protein assays and stored at -70°C or processed for light/electron/confocal microscopy as follows:

2.4 Histology: Tissue samples were fixed in 10% formalin, dehydrated with ethanol and embedded in paraffin using previously described methods (Bilim *et al.*, 2008). Paraffin embedded LV samples were sectioned at 4 µm, deparaffinised in HistoClear (Sigma Aldrich), de-hydrated in a graded alcohol series (50, 70, 80, 95 and 100% Ethanol), re-hydrated and stained with the hematoxylin and eosin stain (H&E) for general examination and with Masson's trichrome stain for the determination of ECM deposition according to established methods (Luna *et al.*, 1968; Shishido *et al.*, 2003). In the GK rat groups, sections were also stained with Picrosirius red that highlights myocardial collagen. H&E, Masson's trichrome and Picrosirius-red stained sections were visualized by light microscopy using an objective with a calibrated magnification of 400X. Sampling fields were captured digitally into a computer database via a high

resolution colour camera (Carl Zeiss) coupled to an objective lens attached to the microscope (Zeiss, Germany). Images were analyzed with a freely available computer-assisted colour image analysis system (NIH ImageJ 1.37 V (Bethesda, MD, USA)). The program was calibrated using a calibration slide (GRATICULES LTD) traceable to national standards (National Physical Laboratory, Teddington, Middlesex, UK). Visual fields encompassed 2816 X 1880 square pixels with a resolution of 15.88 pixels/micron (area = 0.02099 mm²). For all quantitative assessments a minimum of 4 separate regions of the LV/animal encompassing the entire thickness of the wall were examined in order to ensure that results would be representative of the entire tissue.

Extent of ECM proliferation in the LV was morphometrically assessed using methods described by Farah *et al.*, (2009). This procedure involved the application of colour segmentation to digitized images of sections stained with Massons' trichrome that specifically stained the ECM green or with Picrosirius red that stained collagen fibres red. Using Image J programmed to highlight shades of a specified colour (green or red) on stained sections based on operator's threshold settings, collagen area fraction (percent fibrosis) was calculated as the ratio of the area of fibrotic tissue to total myocardial tissue area. The measured total tissue area within each field was further corrected for white non-tissue spaces by a similar method of demarcation to provide a corrected area of true myocardial tissue. 35-40 systematically selected fields (encompassing approximately 0.7-0.8 mm²) per experimental group were included in the analysis.

2.4.1 Immunohistochemistry: To investigate the contribution of mild diabetes towards activation of the apoptotic pathway, activity of caspase-3, the prime effector of cardiomyocyte apoptosis, was estimated using a commercially available caspase-3 detection kit (Apoptosis Marker: Signal Stain Cleaved Caspase-3 (Asp175) IHC detection kit, Cell Signalling Technology) and manufacturers' instructions. Caspases have been previously described as 'cysteine-dependent aspartate specific proteases functioning as endonucleases integral in the final execution of nuclei and cell death' (Kwak *et al.*, 2006). A critical step in the execution of the apoptotic program eliciting DNA fragmentation is cleavage of caspase-3 into 19 and 17 kDa fragments.

Briefly, formalin fixed paraffin embedded (FFPE) sections were deparaffinized in HistoClear (Sigma Aldrich, H2779) and rehydrated in graded alcohol series whereas frozen sections were allowed to equilibrate for 5 minutes at room temperature before

being post-fixed with 10% neutral buffered formalin. Endogenous peroxidase was inhibited using 0.3% H₂O₂ in methanol. Epitope retrieval in the FFPE sections was accomplished by heating the sections in 10mM citrate buffer (0.1 M Citric Acid, 0.1 M NaCitrate, dihydrate 10 mM, pH 6) for 20 minutes using a conventional microwave oven. Following antigen retrieval, FFPE sections were allowed to cool for 20 min before the reaction was stopped in running distilled water. Prior to the application of the primary antibody, nonimmune goat serum was applied as a protein block. Sections were incubated overnight at 4°C with prediluted polyclonal rabbit anti-active caspase 3 antibody, washed in 2 changes of PBS for 10 minutes each (that specifically recognizes the large fragment (17/19 kD) of activated, but not full length caspase-3) then incubated for 30 min in biotinylated (prediluted) goat anti-rabbit IgG. Sections were then washed in PBS and incubated with horseradish peroxidase (HRP)-streptavidin for 30 min. The antibody complex was visualized using H₂O₂ as a substrate and diaminobenzidine as chromogen. The development of the immunohistochemical staining was monitored by microscopy. Finally, slides were rinsed in running tap water, counterstained with Mayers' Hematoxylin (Sigma Aldrich, MHS16) for 1 minute, dehydrated through a series of ethanols to HistoClear, and coverslipped with Permount (Fisher Scientific, Norcross, GA). A semiquantitative estimation of apoptotic cells as an average of 35-40 LV fields/group defined as cleaved-caspase-3 positive cells/area (mm²) was carried out by Image J using photomicrographs imaged at X400 and utilization of a plugin known as DeadEasy Caspase that is based on a mathematical algorithm for object recognition and custom designed for the quantification of cleaved caspase-3 mediated apoptosis (Forero *et al.*, 2009).

2.4.2 Immunofluorescent labelling and confocal laser scanning microscopy

Paraffin sections were processed for immunofluorescence microscopy. Briefly, sections were deparaffinised in HistoClear (Sigma Aldrich) and dehydrated through a series of alcohols before antigen retrieval as described above. Sections were then blocked in 1.5% normal goat serum (NGS), incubated overnight in either Fluorescein isothiocyanate (FITC)-conjugated Lectin (Sigma Aldrich) at a concentration of 1µg/µl or αSKA (Abcam, 1:50). For αSKA labelling, tissues were further incubated with FITC-conjugated anti-mouse IgG (Sigma Aldrich) at a dilution of 1:200 for 2 hours at room temperature. Post labelling, sections were washed with PBS three times and mounted in Fluoromount (Sigma Aldrich). Slides were examined using a laser scanning confocal microscope (LSM 510, Carl Zeiss, UK) equipped for detection of FITC (excitation

bandpass 450–490 nm, emission low-pass 515 nm) and subjective material captured as 512 x 512 pixel images (magnification X400) collected at constant settings wherever applicable. Image J was used to measure either cell size or fluorescent intensity/unit area. Specificity of staining patterns was established by replacement of primary antibody/ Fluorescent probe with 1.5% normal goat serum in PBS and background fluorescence thus determined.

Cell size measurement by Lectin labelling: Lectin labelling clearly defined individual cardiomyocytes. To compare size, the short axis diameter of individual myocytes was measured thrice on transverse sections by drawing a point to point perpendicular line with Image J and averaging obtained values.

Fluorescent intensity measurement for anti- α SKA labelling:

Sections to be compared were immunolabelled under identical experimental conditions on the same day. Digital images for each experimental group were at the same settings for gain and threshold. All random scans of myocardial tissue from control and diabetic groups were recorded at the same photo multiplier tube setting of 450–500, pinhole aperture setting of 50 μ m, and at the same laser voltage setting of 20 mW. Confocal settings were: laser power 10%, iris 2.0 and gain around 950 (variable between experiments but constant for each experimental group). Fluorescent signal quantification of anti- α SKA labelled sections was achieved by transforming confocal micrographs in gray luminance values ranging from 0 (corresponding to black) to 255 (corresponding to white) and splitting into RGB channels on Image J. The green channel was used to calculate fluorescence intensity, evaluated as the sum of pixel intensity values. The total fluorescence intensity within each field was inferred and the value obtained was subtracted from the background, i.e. Signal detected using the negative control stained in tandem. This corrected value for pixel intensity in the image was then expressed as labelling intensity/unit area of field (512x512 pixels). Values were averaged for each section and given as mean+SEM value for control and GK groups.

2.4.3 Electron Microscopy: Freshly isolated LV samples from 2 month old Wistar and GK rats were cut to 2 mm x 2 mm size, transferred into Karnovsky's fixative (16% paraformaldehyde, 50% EM grade glutaraldehyde, 0.1 M sodium phosphate buffer) at pH 7.2 in 7 ml glass vials and allowed to rotate on a rota mixer for 4-5 hours at room temperature. Samples were washed in 0.1M phosphate buffer 3 times for 15 minutes

each and stored at 4°C until further processing. Postfixation procedures included adding 1 ml of 1% osmium tetroxide buffered in 0.1 M sodium cacodylate and allowed to mix for one hour at room temperature on a rotamixer, following washing in distilled water and dehydration in graded ethanol series as follows: 15 minutes each in 30%, 50%, 70%, 80%, 90%, ethanol, and 2 changes in absolute ethanol and propylene oxide. Tissues were then embedded using flat molds, in resin of the following composition: Agar 100 epoxy resin, 24 ml; Dodecenylsuccinic anhydride, 16ml, Methyl nadic anhydride, 10 ml and Tri(Dimethylaminomethyl phenol, 1.2 ml; Polymerization was done at 60°C for 24 hours. Semithin sections, (1 μ m thick) were cut with glass knives from randomly chosen blocks and stained with Toluidine blue for examination by light microscopy. Five blocks with both transverse and longitudinally directed myocytes were chosen from each experimental group. Tissues which were abnormal by light microscopic examination were excluded from ultrastructural studies. Semithin sections stained with methylene blue were examined in the light microscope and appropriate areas were chosen for preparing ultrathin sections. Thin sections were cut with diamond knife (DuPont) on LKB III ultratome from the same 5 blocks and picked up on mesh copper grids. The sections were stained with saturated uranyl acetate solution in 50 percent ethanol for 15 minutes and lead citrate solution for two minutes. Ultrathin sections were examined under a JEM 1010 electron microscope at an accelerating voltage of 60 kV. Electron micrographs were printed on 8 x 10 inch photographic paper at various magnifications.

2.5 Functional studies in the STZ-induced type 1 diabetic rat

Solutions and Reagents

1. The cell isolation solution (Physiological salt solution) was composed of the following (in mM): 130.0, NaCl (VWR, 102415-R); 5.4, KCl (VWR, 1019842); 1.4, MgCl₂ (VWR, 220933-M), 0.4 NaH₂PO₄ (VWR, 102494-C); 5, 4-(2-hydroxyethyl)-1-piperazineethanesulfonic acid (HEPES) (Sigma, C-0780); 10, glucose; 20, taurine (Sigma, T-0625) and 10 creatine (Sigma, T-0780) set to pH 7.3 (Orion pH meter, 920-A) with 4M NaOH (VWR, 10252).
2. Normal Tyrode solution (Cell perfusion solution) was made up of (in mM): 140, NaCl; 5, KCl; 1, MgCl₂.6H₂O (VWR, 101494-V); 10, glucose; 5, 4-(2-hydroxyethyl)-1-piperazineethanesulfonic acid; 1, CaCl₂ set to pH 7.4 with 4 M NaOH.

2.5.1 Measurement of Left Ventricular Action Potential

Five STZ-treated rats and age-matched Wistar controls were humanely killed by decapitation and the hearts rapidly excised, perfused in a retrograde fashion at constant flow (8 ml/gm/heart/min) in Langendorff mode with Normal Tyrode solution continuously bubbled with oxygen and at 37°C (physiological temperature). When the isolated heart preparation stabilized to contract regularly at 300 beats per minute (BPM), extracellular ventricular action potentials were recorded using a purpose built suction electrode in accordance with methods that have been previously described (Howarth *et al.*, 2007). Recordings were collected at 400 Hz, amplified (ML136 Bioamp, ADInstruments, Castle Hill, New South Wales, Australia) and visualised by interfacing with a PC via Powerlab (PL410, ADInstruments). Data analysis was carried out using ADInstruments software version 4.21 (ADInstruments). Action potential duration (APD) was analyzed using IDL software (IDL research Systems, Boulder, CO). APD₅₀ was measured as the time taken for 50 % repolarization

2.5.2 Isolation of Ventricular Myocytes:

Ventricular myocytes were isolated from 5 STZ-treated and 6 control rats by methods that have been previously described for studies of contractility and $[Ca^{2+}]_i$ transients (Howarth *et al.*, 2007). Briefly, after the completion of action potential recordings described above, hearts were perfused with a Ca^{2+} free isolation solution that contained Ethylene glycol tetraacetic acid (0.01 mM), following which the heart was perfused with a physiological salt solution containing 0.05 mmol/L Ca^{2+} , 0.75 mg/mL collagenase (type 1; Worthington Biochemical Corp., Lakewood, NJ, USA) and 0.075 mg/ml protease (type X1V; Sigma, Taufkirchen, Germany). The last solution was re-circulated to expose the heart to the enzymes for duration of 6 min. After, perfusion with the enzyme, the heart was removed from the perfusion apparatus; the ventricles were excised, minced and gently agitated at 300 oscillations/min in a 5ml collagenase solution supplemented with 1% Bovine Serum Albumin (BSA). Cells were filtered at through gauze (300 μ m aperture, Cadish precision meshes, Finchley, London) and suspended in isolation solution. The filtrate was centrifuged at 400 rpm for 1 minute, supernatant removed and cell pellet resuspended in physiological salt solution containing 0.75 mM Ca^{2+} . The process was repeated 4 times and isolated myocytes from the 2nd and 3rd repetition(s) were stored at 4°C until use at a period not exceeding 1-2 hours.

2.5.3 Measurement of contraction in isolated ventricular myocytes

Freshly isolated ventricular myocytes were allowed to settle on the glass bottom of a Perspex chamber mounted on the stage of an inverted microscope (Axiovert35, Zeiss, Germany) with a 40X objective lens and were superfused at 3-5 ml/min with a HEPES-based Tyrodes solution maintained at 35-37°C using a power driven magnetic micro pump (Cole parmer instruments, London) and a heating system coupled to a temperature controller (Medical systems corp., USA). Myocytes were field stimulated at 1Hz (S88 stimulator, Grass-Telefactor, USA) using 2 platinum electrodes positioned at either side of the chamber. Shortening was measured as an index of contractility using a video edge detection system. (VED-114, Crystal Biotech, Northborough, MA, USA) and data was acquired and analysed using SignalAverager (version 6.16, Cambridge Electronic Design, Cambridge, UK). The degree of shortening (expressed as a percentage of resting cell length) and the time to peak shortening and time from peak shortening to half-relaxation were recorded.

2.5.4 Measurement of intracellular calcium transients in isolated ventricular myocytes

$[Ca^{2+}]_i$ transients were measured by previously described methods (Howarth *et al.*, 2007). To briefly summarize, cardiomyocytes were loaded with a fluorescent indicator fura-2-AM (Molecular probes, Leiden, The Netherlands) by adding 6.25 ul of a 1.0 mM stock of fura-2-AM dissolved in dimethyl sulfoxide to a 2.5 ml solution containing freshly isolated myocytes resulting in a final fura-2-AM solution of 2.5 μ M/L. The cells were then gently agitated for 10 min at RT, following which they were centrifuged at 400 rpm for 1 minute, resuspended in normal tyrodes solution and incubated for 30 min. Following loading of the fluorescent indicator, $[Ca^{2+}]_i$ transients were measured by exposing the myocytes to light at 340 nm and 380 nm in an alternate fashion using a monochromator (Cairn Research, Faversham, UK) that switched between the 2 wavelengths every 2 ms. A photomultiplier tube recorded fluorescence emission at 510 nm and the ratio of emission at the 2 excitation wavelengths (340/380 ratio) was determined as an index of $[Ca^{2+}]_i$. The amplitude of the Ca^{2+} transient was recorded along with a time course of $[Ca^{2+}]_i$ analysis, including time to peak and the time from peak to half-relaxation of the $[Ca^{2+}]_i$ transient. Decay of the transient was measured as time from the peak amplitude of the transient to half its decay. Finally, the rate of decay was obtained by plotting a gradient on the decay of the $[Ca^{2+}]_i$ transient. Data were collected and analysed using Signal Averager.

2.6 Transforming growth factor β 1 Immunoassay

Protein extraction

LV samples from 3 Wistar controls and 3 GK rats (at 2 and 18 months) were weighed and homogenised in the following buffer (ELISA kit manufacturers recommendation): 0.5% Triton X-100, 2 μ g/ml Aprotinin (Sigma Aldrich, A6013) in PBS (concentration in mmol/L- NaCl: 137, KCl: 2.7, Na₂HPO₄ 10, KH₂PO₄: 1.76, pH 7.4). Homogenate was sonicated and centrifuged at 14,000 g for 1 minute at 4°C. The supernatant was aliquotted into tubes on ice and was further assayed for protein concentration or stored at -80°C

Modified Lowry protein assay

Protein concentration in LV tissue homogenate was assayed by the modified Lowry method described previously (Lowry *et al.*, 1951). The linearity range for protein detection is given as 1-1,500 μ g/ml. Briefly, protein in samples or BSA standards was reacted with 1% cupric sulfate and 2% Sodium potassium tartate in an alkaline solution of 1N NaOH and 2% Na₂CO₃, which resulted in formation of a tetradentate copper-protein complex. This complex further reduced a 2N Folin-Ciocalteu Reagent added to samples/ standards to produce a blue colored, water-soluble product. Absorbance of the latter was measured at 750 nm with a microplate reader (Micro Quant, Biotech Instruments). Five standards, 0, 1, 2.5, 10 and 20 were diluted from a 20 μ g/ μ l stock solution to produce a standard curve.

Detection of Total and active Transforming growth factor β 1 by Enzyme-Linked ImmunoSorbent Assay (ELISA):

Endogenous TGF β 1 in plasma and LV homogenates (extracted as described above) from control and GK animals was assayed using TGF β 1 Emax Immunoassay system (Promega, Madison, WI) and manufacturer's protocol. The TGF β 1 Emax ImmunoAssay System is an ELISA designed to detect biologically active and/or total TGF β 1 in an antibody sandwich format and typically demonstrates \leq 3% cross reactivity with other TGF β 1 isoforms (e.g. TGF β 2/3).

Following this protocol, flat bottomed 96-well plates were coated with TGF β 1 monoclonal antibody in freshly prepared carbonate coating buffer (0.025M sodium bicarbonate, 0.025M sodium carbonate, pH 9.7) at a dilution of 1:1000 and incubated overnight at 4°C. Nonspecific binding was blocked by adding diluted TGF β Block 5X

Buffer (manufacturer supplied) and incubation at 37°C for 35 minutes, following which plates were washed once with Tris buffered saline-tween Wash buffer (20mM Tris-HCl (pH 7.6) 150 mM NaCl 0.05% (v/v) Tween 20). All subsequent washes were conducted with the same buffer. Standards were prepared in duplicate by diluting the manufacturer's supplied 1 µg/ml TGFβ1 standard to produce a standard curve from 0-1000pg/ml (0, 15.6, 31, 62, 125, 250, 500, 1000 pg/ml) as given in Figure 2.1.

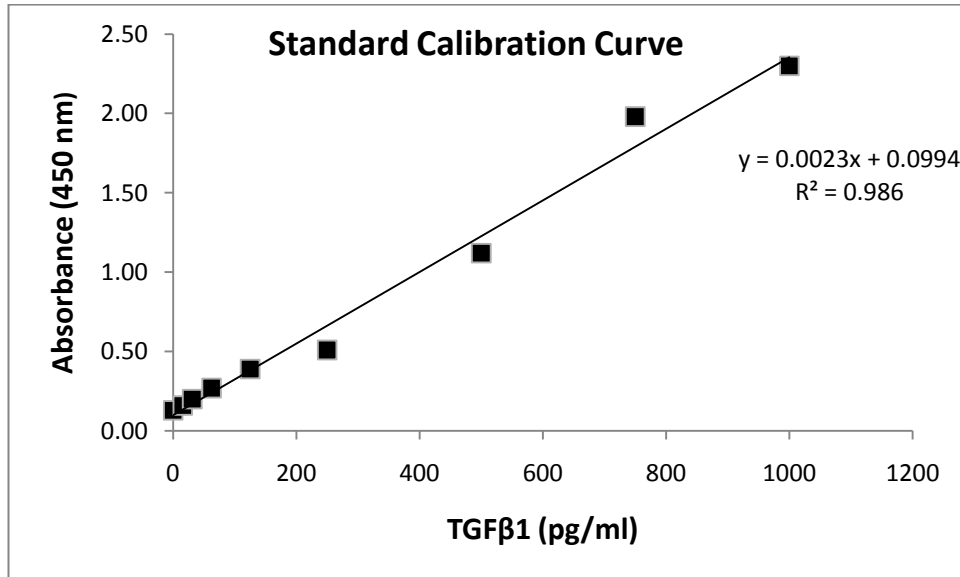


Fig 2.1: Standard calibration curve for TGFβ1

To assay total *and* active TGFβ1, plasma samples or centrifuged supernatant from LV sample homogenate were divided into 2 equal fractions. One fraction was acid-treated to activate total TGFβ1 per manufacturer's instructions. Briefly, either plasma or LV homogenate diluted 1:5 in Dulbecco's PBS were acidified to pH 2.6 by adding 1N HCl/50µl of sample. Following incubation for 15 minutes at room temperature, samples were neutralized to pH 7.6 by adding 1N NaOH/50 µl sample. This method is based on the premise that acid treatment releases the active TGFβ1 molecule from the latent complex present in the sample fractions. As such, the fraction of the samples without acid treatment represented endogenous levels of biologically active TGFβ1 whereas acid-treated fractions represented the total TGFβ1 in the sample. Subsequently, a volume of 100 µl of acid treated and/or naturally processed samples were added to coated well plates and incubated for 90 minutes at room temperature. Optimal sample concentrations were established by testing a dilution series. As such, plasma samples were diluted 1:16 and LV homogenate was diluted 1:2 in the provided Sample Buffer. After washing 5 times, the amount of specifically bound polyclonal antibody was

detected by adding 100 μ l of provided polyclonal anti-TGF β 1 (at a dilution of 1:1000) to each well and incubation for 2 hours at room temperature. TGF β HRP Conjugate was added at a dilution of 1:100 to each well and incubated for 2 hours. The unbound conjugate was removed by washing five times, and samples were incubated with 100 μ l of provided chromogenic substrate (TMB One Solution) for 15 minutes at room temperature to produce a blue colour in the wells. Acidification of samples by adding 100 μ l of 1N HCl changed colour to yellow. The color change was measured at 450 nm using a microplate reader (Anthos Hill, Biochrome Ltd, UK). The amount of active TGF β 1 in the samples was proportional to the color generated in the oxidation-reduction reaction. Total and active levels of TGF β 1 in LV samples and Plasma were analysed in duplicate. The results in pg/ml were obtained by extrapolation from standard curve expressed as ratio of Active:Total TGF β 1 for plasma samples and pg/mg of total protein for LV homogenate samples.

2.7 Western Blotting

The contribution of mild HG in Prediabetes and overt mild T2DM towards levels and activation of Akt and downstream signalling to p70S6K (that mediates the hypertrophic response) was investigated by western blotting. Western blotting, also known as immunoblotting is a technique that involves separation of proteins using SDS-PAGE followed by protein immobilisation of polyvinylidene fluoride (PVDF) or nitrocellulose membranes (Burnette, 1981).

Protein extraction: Frozen LV samples from 2 and 18 month old GK and age-matched control rats were washed in ice-cold PBS, minced with a sterile blade and sonicated after homogenisation on ice in a buffer containing 250 mM KCl, 20 mM Imidazole, 2.5 mM Dithiothreitol, 0.3 M Sucrose, Phosphatase 1, pH 7.2. Lysates were then centrifuged at 14000 g for one minute following which the supernatant was collected, aliquotted and stored at -70°C or used for determination of protein content by the Modified Lowry assay described in section 2.6.

Sodium dodecyl sulfate polyacrylamide gel electrophoresis (SDS PAGE) and electroblotting: Dithiothreitol in gel dissociation medium (62.5 mM Tris-base, 6% SDS, 20% glycerol, and 0.002% bromophenol blue at a concentration of 10mg/ml was added to lysate containing 50 μ g/ μ l extracted LV protein to give a final volume of 30 μ l and the mixture was centrifuged for 10 seconds at 130 g. Next, samples were placed in a boiling water bath for 15 minutes and following brief centrifugation for 10 seconds at 130 g were loaded onto commercially available 4-15% Tris-HCl gels (Bio-Rad

Laboratories, Hercules, CA, USA) run at 150V for 140 min in a running buffer comprising 250 mM Glycine, 25mM Tris-base, 0.1% (w/v) SDS in dH₂O at pH 8.3. Prestained molecular weight markers (Prestained SDS-PAGE Standards, broad range', Bio-Rad Laboratories, Hercules, CA, USA). Electrophoretic transfer of proteins onto methanol-activated 'Immobilon' polyvinylidene fluoride (PVDF) membranes (Millipore) was achieved using a semi-dry transfer apparatus (Bio-Rad Laboratories, Hercules, CA, USA) and buffer containing 10 mM 3-[cyclohexylamino]-1-propane sulfonic acid, 10% methanol, 0.1% (w/v) SDS in dH₂O, pH 9 adjusted with NaOH. Electroblotting was carried out at 0.3 A (constant amperage) for 2 hours at 4°C. Electrophoretic transfer was indicated by the complete transfer of prestained molecular weight markers, following which gels were stained with gentle agitation in Coomassie blue and finally destained in a solution of 7.5% glacial acetic acid and 10% absolute ethanol in distilled water for 2 hours with constant agitation. Stained gels were placed on a white surface and photographed under white lights to document the consistency of protein loading (Fig 2.2).

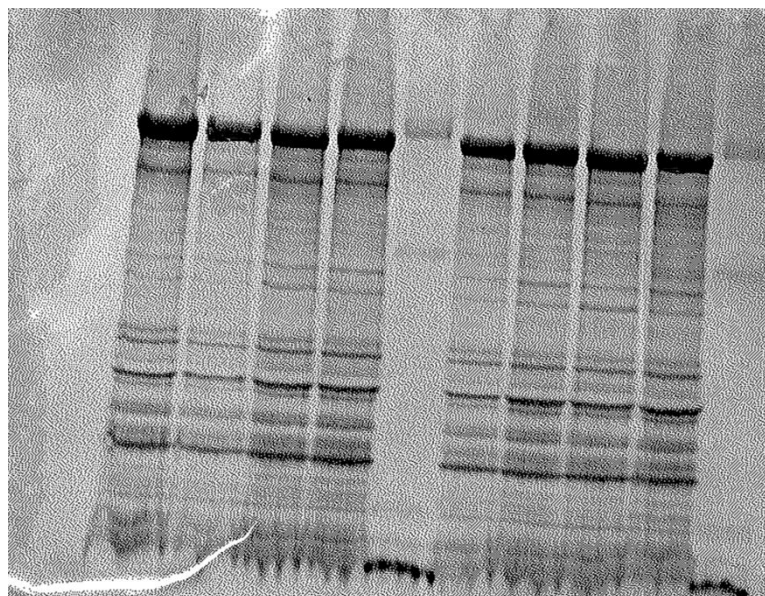


Fig 2.2: Typical Tris-HCl gel after electrophoretic transfer. Gel was destained and photographed after staining with Coomassie blue to highlight protein loading

Antibodies and densitometry: PVDF membranes were probed with antibodies given in Table 2.1 as follows: 1. Primary antibody and anti- β actin as a loading control (1:1000 in 0.5% BSA in PBS) overnight at 4°C. 2. Secondary antibody, (1:2000 in 0.5% BSA in PBS) for one hour at room temperature. 3. 2ml Enhanced Chemiluminescence (ECL) reagent mix from ECLTM Western Blot Detection Reagents

(GE Healthcare) (1:1 mix of Amersham reagents 1 and 2) and exposure to film (Blue ultra autorad film 8x10, Double emulsion blue, ISC BioExpress) for 30 seconds. Multiple exposures ensured the desired intensity was achieved. Sizes of the immunodetected proteins were verified by standard molecular weight markers and β actin that served as a loading control. The ECL method is based on the emission of light during the Horeseradish peroxidise (HRP)- and hydrogen peroxide-catalyzed oxidation of luminol. The emitted light is then captured on film. After each step membranes were rinsed in several changes of washing buffer (TBS + 1% Tween 20, pH 7.4) at 10 minutes each.

Table 2.1: List of antibodies used in the study indicating catalogue number and dilution

	Antibody	Source and catalogue number	Dilution
1	Mouse monoclonal anti Alpha skeletal actin	Abcam (ab74245)	1:50
2	Goat FITC-conjugated anti mouse IgG	Sigma Aldrich (M0659)	1:200
3	Mouse monoclonal anti-Akt	Cell Signalling (2967)	1:1000
4	Rabbit polyclonal anti phosphorylated Akt (Ser 2771)	Cell Signalling (9271)	1:1000
5	Rabbit polyclonal anti p70S6K	Cell Signalling (9202)	1:1000
6	Rabbit polyclonal anti phosphorylated p70S6K (Thr 389)	Cell Signalling (9205)	1:1000
7	Goat polyclonal anti beta actin (Actin 1-19)-HRP	Santa Cruz Biotechnology (sc 1616)	1:2000
8	bovine anti mouse IgG-HRP	Santa Cruz Biotechnology (sc2371)	1:2000
9	donkey anti rabbit IgG-HRP	Santa Cruz Biotechnology (sc2305)	1:2000
10	donkey anti goat IgG-HRP	Santa Cruz Biotechnology (sc2304)	1:2000

Exposed film was scanned (Fig 2.3) and proteins imaged by densitometry using the ‘Gel Analysis’ method on Image J which provides reproducible estimates of protein concentration in terms of relative band intensity, by quantifying optical density (pixels) of selected areas and semi-automated correction for background noise. Data were computed and quantified in densitometry units (area x pixel density). This value was then normalized to band intensity of loading control (β actin). Finally, normalized values are presented in graphs as ratio of phosphorylated target protein: total target protein. Membranes were stripped (with buffer made containing 15 gm glycine, 1 gm SDS, 10 ml Tween 2 in 1L of distilled water, pH 2.2) and reprobod by steps 1, 2 and 3 outlined above. Experiments for each protein measured were conducted in triplicate.

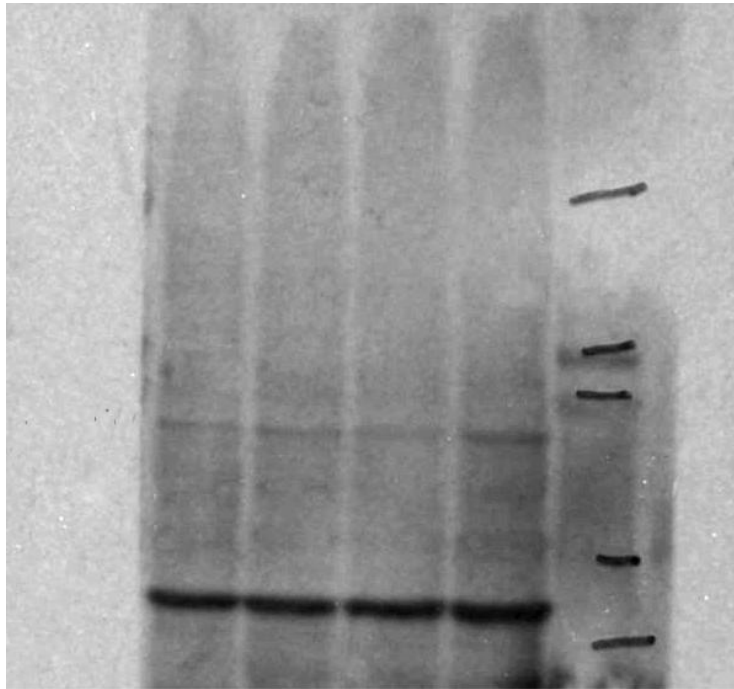


Fig 2.3: Representative scan of exposed film showing PVDF membrane and proteins detected by ECL. The film is of a western blot with bands showing phosphorylated p70S6K protein and β -actin serving as a loading control for quantification purposes in Wistar control LV at 2 weeks. The molecular weight markers are visible on the left and were highlighted with a felt tip marker

2.8 mRNA quantification by Quantitative Reverse transcriptase Polymerase chain reaction

Reverse transcription (RT) followed by quantitative polymerase chain reaction (qPCR) is a sensitive method for mRNA quantification. In comparison to more traditional approaches such as Northern blot, dot blot and in situ hybridisation, RTqPCR assays are most commonly used methods for characterizing or confirming patterns of gene expression and comparing mRNA levels in sample populations. In this study, ‘real time’ RTqPCR assays were used for the quantification of mRNA expression of several target genes using the two-step SYBR green I RT-PCR protocols. RTqPCR follows the general principle of PCR, a key differentiating factor being that the amplified DNA is detected as the reaction progresses in *real time* compared to standard PCR, where the product of the reaction is detected at its end. The experimental design, primer sequences, experimental conditions and techniques detailed below have been previously carefully validated (Tellez *et al.*, 2006; Yanni *et al.*, 2010). Very briefly, the process involved the extraction of RNA from frozen samples, reverse transcription of RNA into complementary DNA (cDNA) using reverse transcriptase and the random hexamer priming method and use of the resulting cDNA as a template for subsequent PCR amplification using primers (given in Table 2.2) specific for genes of interest followed by automated detection and quantification of amplification products.

mRNA isolation and generation of cDNA

For isolation and purification of mRNA, frozen LV samples were cut into 20 μm sections on a cryostat. Total RNA was isolated from sections using Qiagen muscle RNA extraction procedure and manufacturer’s instructions (Qiagen, Hilden, Germany). In summary, this process involved the addition of β -mercaptoethanol to provided ‘RLT’ buffer followed by homogenisation of samples on ice and addition of proteinase K to digest proteins in tissue. Next, the samples were centrifuged at 13000 rpm for 5 minutes and supernatant dissolved in β -mercaptoethanol-‘RLT’ mix and vortexed. This step is a modification of the original protocol and by increasing salt concentration in the homogenate, led to more reliable yields. After addition of 100% ethanol and vortexing, the samples were applied to the Qiagen-provided columns in aliquots, centrifuged for 15 seconds at 13000 rpm for after each aliquot and flow through decanted. DNase was then diluted in the provided buffer and added to the columns and left to digest for one

hour at room temperature. After 3 rounds of centrifugation and addition of 'RW' buffer, the column was dried and eluted by addition of Millipore H₂O and spinning down. A second elution resulted in a final volume of roughly 90µl that was left to precipitate overnight at -20C. After spinning for 30 minutes at 13000 rpm in the cold, resulting RNA was ethanol precipitated and pellets dissolved in 6-10µl, Diethylpyrocarbonate-treated (RNase free) water. The RNA concentration was then measured with a Nanodrop ND-1000 spectrophotometer (Nanodrop Technologies, USA).

The isolated RNA (and resulting cDNA) samples from different rats were kept separate, i.e. the samples were not pooled. 125 ng of total RNA from each sample was reverse transcribed with Superscript III reverse transcriptase (Invitrogen) in a 20 µl reaction according to the manufacturer's instructions, using random hexamer priming. In précis, to each 8 µl of RNA, 2 µl a solution made up of Hexamers/ deoxyribonucleotide triphosphate in buffer containing manufacturer provided RT buffer, 25 mM MgCl₂ 0.1M DTT and Superscript III reverse transcriptase and heated to 65°C for 10 min. The tubes were then transferred onto ice immediately for 3 minutes and subsequently, 10 µl of the RT/buffer master was added ice, following incubation at 25 °C for 10 min in the PCR machine, for first priming, 50 °C for 50 min, for further synthesis and 85 °C for 15 min, to stop the reaction. Aliquots of the resulting cDNA were diluted 10-fold in water for direct use in qPCR.

Quantitative PCR: RTqPCR was performed using an ABI Prism 7900 HT Sequence Detection System (Applied Biosystems, Foster, USA). The size of qPCR products and specificity of primers were previously tested in our laboratory by running samples on 2 % agarose gels containing ethidium bromide and visualised by ultraviolet light. Commercially available primers gave amplicons of similar size. The reaction mixture was comprised of 1 µl of cDNA, 900 nM forward primer, 900 nM reverse primer or 1x Qiagen assay, 1x SYBR Green Master Mix (Applied Biosystems) and DNase-free water and the final volume was 10 µl. All samples were run in triplicate. The reaction conditions were: denaturation step of 95°C for 10 min, 40 cycles of amplification and quantification steps of 95°C for 30 s, 60°C for 30 s and 72°C for 1 min. The melt curve conditions were: 95°C for 15 s, 60°C for 15 s and 95°C for 15 s. The technical validity of the PCR assay setup was assessed by examining RNA amplification data. Fig 2.4 illustrates representative data obtained with the primers. By running a melting curve after the PCR reaction, the desired amplicon was differentiated from other non-specific

products. Dissociation curves were examined to rule out formation of contaminants or Primer-dimers (Fig 2.4 B).

Table 2.2: List of primers used in the study

Target transcript	Species	Qiagen catalogue number
CTGF	Rat	QT00182021
BNP	Rat	QT00183225
Elastin	Rat	QT01575924
Fibronectin 1	Rat	QT00179333
Integrin alpha 1	Rat	QT00193172
Integrin alpha 5	Rat	QT00431053
Integrin beta 1 (fibronectin receptor beta)	Rat	QT00187656
Matrix metalloproteinase 2	Rat	QT00996254
Matrix metalloproteinase 9	Rat	QT00178290
ANP	Rat	QT00366170
Procollagen, type III, alpha 1	Rat	QT01083537
Transforming growth factor β 1	Rat	QT00190953
Vimentin	Rat	QT00178724
GAPDH	Rat	QT00199633
NCX	Rat	QT01592451
SERCA2a	Rat	QT01082508
Ca _v 1.2	Rat	QT01571822
Ca _v 1.3	Rat	QT00194306
RyR2 (ryanodine receptor)	Rat	QT02348003
Pln_1 (phospholamban)	Rat	QT01290058
Collagen type 1	Rat	QT01621417
Tumour necrosis factor alpha	Rat	QT00178717

Connexin 43 primers were custom designed with Primer 3[®] software provided by the Whitehead Institute for Biomedical Research, Cambridge, MA, USA and were of the following sequence

Forward primer: 5'-GGAATGCAAGAGAGGTTGAAAG-3'

Reverse primer: 5'-GGCATTGGAGAACTGGTAGA-3'

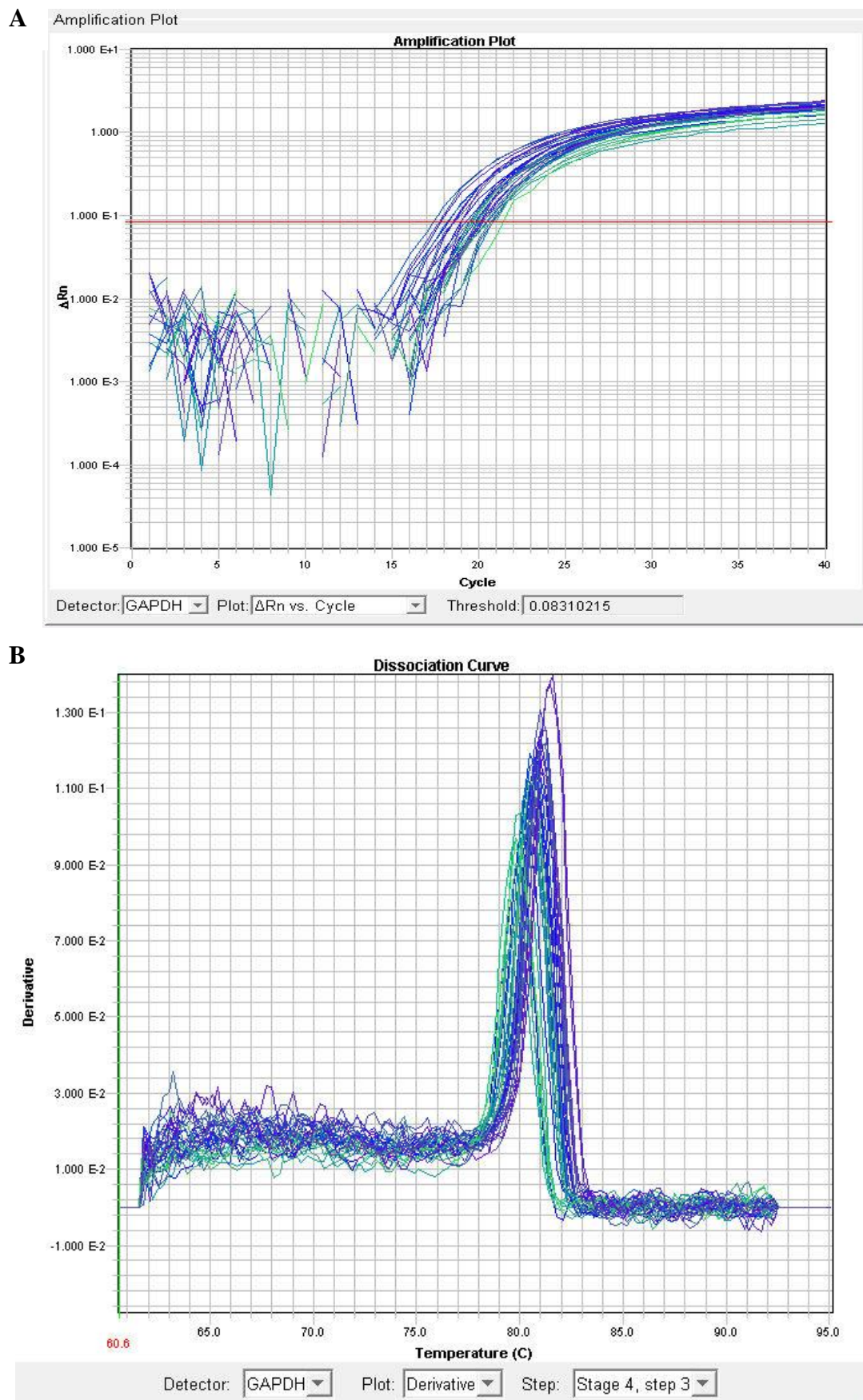


Fig 2.4: Representative RTqPCR validation methodology. GAPDH rtqPCR amplification (A) and dissociation (melting) curve (B), exemplify the protocol used to validate each primer set (Rat GAPDH in figure) and experimental conditions.

Gene Expression Analyses

The cycle threshold (Ct) is the number of cycles required for fluorescent signal to exceed background levels, and is inversely proportional to the amount of target nucleic acid in the sample. In the present study, gene expression was analysed using SDS 2.1.1 software (Applied Biosystems) by a double standardisation method known as the modified $2^{-\Delta\Delta Ct}$ method that adjusts for PCR efficiency differences (Skern *et al.*, 2005). This mathematical model calculates changes in gene expression as a comparison of the Ct values of the samples of interest with a control or calibrator. The Ct values of both the calibrator and the samples of interest are then normalized to an appropriate endogenous housekeeping gene. GAPDH was chosen as the housekeeping gene in the present study as its amplification efficiency has been previously determined in our laboratory to be approximately equal to that of other PCR targets of this study (This is a requirement for $2^{-\Delta\Delta Ct}$ calculation validity). To analyse gene expression, for each run, ratios relative to the calibrator (reference standard sample) were determined based on the respective delta Cts and an average efficiency value was obtained. These ratios were then averaged over all three runs and related to the average content of GAPDH cDNA in each sample to correct for variations in input RNA. The expression levels were represented graphically as corrected value of mRNA abundance relative to average GAPDH content.

2.9 Statistical Analysis

Differences in fasting blood glucose and blood glucose on GTT administration, quantified histology data, RTqPCR-determined relative abundance, TGF β 1 protein levels by ELISA and band intensities from Western Blot between control and diabetic (or prediabetic) groups were compared by unpaired Student's *t*- test using SPSS for Windows v17.0 (SPSS Inc., Chicago, IL, USA). Data in graphs are represented as mean+SEM of 3 or more independent experiments or as indicated. A value of $p < 0.05$ was considered statistically significant. Two-way ANOVAs were conducted to determine differences for ageing and dysglycemia effects and are described in Chapter 7. The level of significance was set at $p < 0.05$

CHAPTER 3

DEVELOPMENTAL EXPERIMENTS

ASSESSMENT OF CARDIOMYOCYTE CONTRACTILE FUNCTION AND STRUCTURAL REMODELLING IN THE LEFT VENTRICLE OF THE STREPTOZOTOCIN- INDUCED TYPE 1 DIABETIC RAT

3.1 Abstract: HF in DM is a major cause of premature morbidity and mortality but the underlying mechanisms are elusive and treatment remains empirical. This chapter represents a set of preliminary experiments in the investigation of the role of HG in diabetic heart disease with primary reference to assessments of cardiomyocyte contractile function and histopathological changes in the LV of STZ-treated type 1 diabetic male Wistar rats compared to age-matched male Wistar controls. Six-seven weeks following STZ-administration (60 mg/kg body weight) ventricular action potentials were measured in the isolated, spontaneously beating Langendorff perfused rat heart. Contraction and $[Ca^{2+}]_i$ were measured in electrically stimulated ventricular myocytes by a Video edge detection system. In another set of experiments, a portion of the LV underwent processing for histological studies employing the Haematoxylin and Eosin stain, labelling with FITC-conjugated Lectin and the Masson's trichrome stain for determination of myocyte size and quantitative assessment of fibrosis respectively. Immunohistochemical studies were conducted to assess the contribution of diabetes towards activation of apoptotic pathways mediated by caspase-3. STZ-treated rats presented with significantly higher blood glucose values relative to controls ($p < 0.01$). Measurements of ventricular action potential indicated that resting heart rate and duration of the action potential was slightly reduced in the STZ-treated rats compared to controls. When electrically stimulated at 1 Hz, contractility was depressed in myocytes from diabetic rats and also exhibited prolonged time(s) for contraction and relaxation ($p < 0.05$). Alterations in $[Ca^{2+}]_i$ homeostasis manifested as prolonged time to peak and prolonged rate of decay of the Ca^{2+} transient in diabetic myocytes relative to controls. LV morphology was also severely altered by DM. Morphometric analysis indicated significant increments in fibrous tissue proliferation, and smaller myocyte transverse diameter. In relation to the latter, the heart was atrophied in type-1 DM as STZ-treated animals presented with lower heart weights and heart weight to body weight ratios relative to controls ($p < 0.01$). In STZ-treated LV, the pathology frequently manifested as focal scarring, myofibrillar loss, vacuolisation and large clusters of cells showing histological signs of apoptosis. Activity of cleaved caspase-3 was also significantly increased in the STZ-treated group ($p < 0.05$). The results of the study indicate that STZ-induced type-1 DM results in the development of a cardiac disease characterised by LV histopathological changes and functional abnormalities manifesting as altered Ca^{2+} homeostasis and contractility in the cardiomyocyte. These findings are consistent with a dominant influence of HG and underlying alterations in insulin action.

3.2 Assessment of Cardiomyocyte Contractile Function and Intracellular Calcium Transients in the Streptozotocin-Induced Type 1 Diabetic Rat Heart

3.2.1 Introduction

Clinical and experimental evidence indicates that the myopathic changes in DM are associated with impairments in contractile force generation, reduced wall compliance, abnormal filling and delayed relaxation of cardiac muscle (Dhalla *et al.* 1985; Ren & Davidoff, 1997; Choi *et al.* 2002; Boudina and Abel, 2007). Experimentally, these defects have been assessed in several species with variations in method, treatment times and as a consequence, variable results. With STZ-induced diabetic animal models, functional deficit has previously been assessed in the intact animal, the isolated perfused heart, papillary muscle preparations and isolated cardiac myocytes. The use of cardiomyocytes is particularly useful as it allows the investigation of contraction and $[Ca^{2+}]_i$ transient kinetics without the confounding effects of hormones and metabolites that are common in *in vivo* studies and changes in perfusion rates that invariably occur in intact hearts. The STZ-induced type 1 diabetic rat has been widely used as a model of DCM. Cardiac rhythm disturbance is reported to be a cardinal feature of DCM in the STZ-treated rat (Zhang *et al.*, 2008). By extension, alterations in the amplitude and time course of contraction and relaxation have been frequently reported in myocytes from STZ-treated rats (Yu *et al.* 1994; Okayama *et al.* 1994; Ren & Davidoff, 1997; Howarth *et al.* 2001; Choi *et al.* 2002).

Nevertheless, substantial discrepancy exists in the published literature regarding parameters of contractile dysfunction in chemically induced type 1 DM, wherein isolated cardiomyocytes from STZ-induced diabetic hearts have been reported to have depressed (Yu *et al.* 1994; Okayama *et al.* 1994; Ren & Davidoff, 1997; Choi *et al.* 2002) elevated (Howarth *et al.* 2001) and conversely unaltered (Tamada *et al.*, 1998; Ishitani *et al.*, 2001) contractile kinetics. Blighted mechanical performance in the diabetic heart has been previously attributed, at least in part to underlying defects in $[Ca^{2+}]_i$ homeostasis (Pierce and Russell, 1997; Choi, 2002; Bracken *et al.*, 2003; Zhang *et al.*, 2008). However, there is limited consensus in results from studies of $[Ca^{2+}]_i$ homeostasis performed on isolated cardiomyocytes as resting Ca^{2+} has been shown to be decreased (Norby *et al.*, 2002; Ozdemir *et al.*, 2005; Yaras *et al.*, 2005), increased (Howarth *et al.*, 2005; Howarth and Qureshi, 2006), or unchanged (Howarth *et al.*, 2002; Howarth *et al.*, 2004). Similarly, conflicting observations of the amplitude of the Ca^{2+} transient also abound, being reported as decreased (Yaras *et al.*, 2003; Kotsanas *et*

al., 2000; Bracken *et al.*, 2004), increased (Howarth *et al.*, 2005), or unchanged (Singh *et al.*, 2006). It is possible that the inconsistency in experimental findings for these parameters is due to differences in duration of the disease in conjunction with experimental conditions (e.g., different stimulation frequencies, voltage, times and temperatures) (Zhang *et al.*, 2008). Thus, experiments were conducted to independently identify the contribution of HG towards experiments contractile characteristics and calcium homeostasis in ventricular myocytes from STZ-induced type 1 diabetic rats and age-matched controls 6-7 weeks post STZ-induction.

3.2.2 Methods

As given in Chapter 2

3.2.3 Results

1. Evaluation of experimental model

General Characteristics of STZ-treated rats and age-matched Wistar controls are represented in Table 3.1. Following 6-7 weeks of treatment, it was observed that the STZ-induced diabetic rats weighed significantly less than age-matched controls ($p<0.05$). Heart weights (HW) were also significantly lower ($p<0.01$) along with a reduction in the HW/BW ratio ($P<0.05$). At sacrifice, plasma glucose levels were approximately 2.41-fold higher in diabetic animals than non diabetic counterparts, in accord with previously published glucometry values at similar time points (Singh *et al.*, 2006; Cosyns *et al.*, 2007).

Table 3.1: Glucometry and Gravimetry data obtained at 15 weeks post STZ-administration. Data are given as mean \pm SEM, * $p<0.05$, ** $p<0.01$

Animals	Fasting Blood Glucose (mg/dL)	BW (g)	HW (g)	HW/BW ratio (g/100g body weight)
Controls (n= 5)	89 \pm 3.56	301 \pm 16.31	0.94 \pm 0.05	0.31 \pm 0.02
STZ-treated (n=6)	305 \pm 7.48**	232 \pm 11.07*	0.55 \pm 0.03**	0.24 \pm 0.11*

1. Left ventricular action potential

Figure 3.1 A represents typical records of left ventricular action potentials in control and STZ-treated hearts. Summarised data for mean heart rate and time from threshold of action potential to 50% repolarisation (APD50) are given in 3.1 B and C respectively. The results indicated that STZ-treated rats have slightly lower heart rates compared to controls (190 ± 5.83 vs. 173 ± 1.33 bpm) as well as increased action potential duration (32.83 ± 1.90 vs. 37.91 ± 2.53 ms) However, the differences did not reach statistical significance in either case ($p>0.05$).

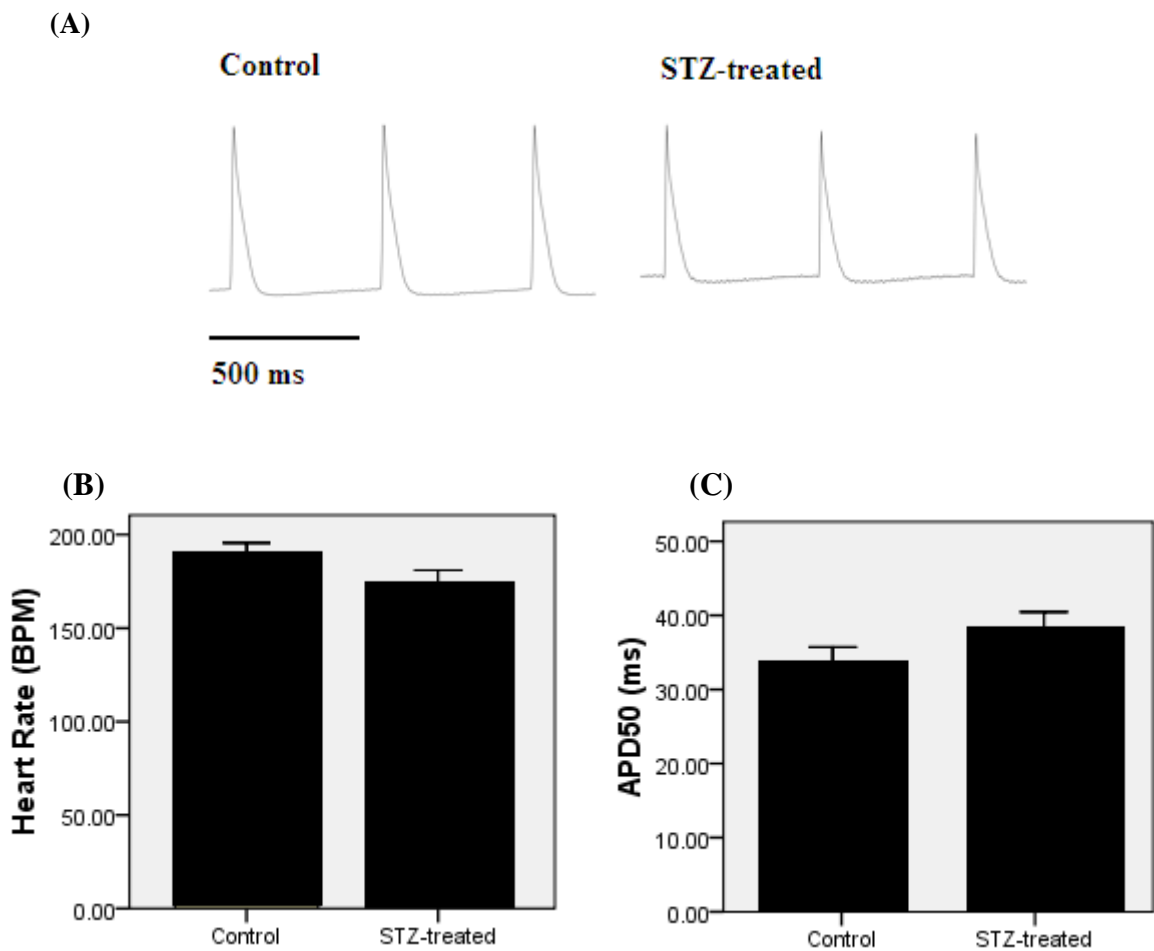
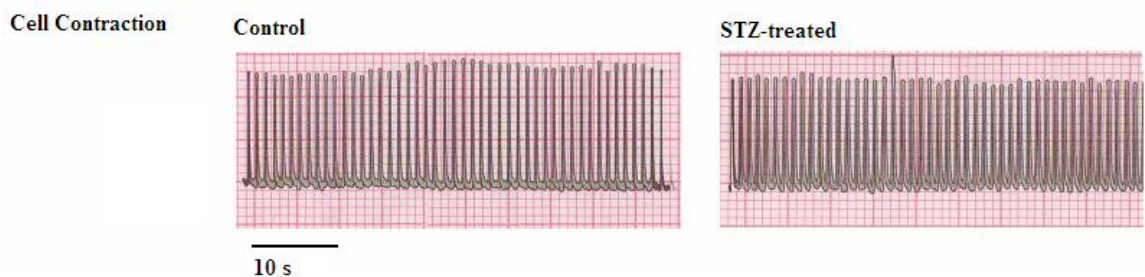


Fig 3.1: Ventricular action potentials. Typical recordings of left ventricular action potentials (A), Spontaneous heart rate [beats/minute, (bpm)] from control and STZ-treated rats (B) and time from threshold of action potential to 50% repolarisation (APD50). Data are representative of 5 independent preparations and given as mean+SEM; n=5 for each group

3. Ventricular Myocyte Contractility:

Fig 3.2 A represents a typical trace showing cell contraction. Fast time-base recordings of contraction in ventricular myocytes stimulated 1Hz are depicted in 3.2 B. Table 3.2 describes amplitude and time course of shortening in myocytes from control and STZ-treated rats. No significant differences were found in resting cell length (RCL) between the 2 groups, but peak amplitude of shortening (expressed as a % of RCL) was significantly reduced by STZ treatment ($p < 0.01$). In comparison with their control counterparts, diabetic rats also displayed a slower time course of shortening i.e. increased time to peak shortening and time to 50% relaxation ($p < 0.05$).

A



B

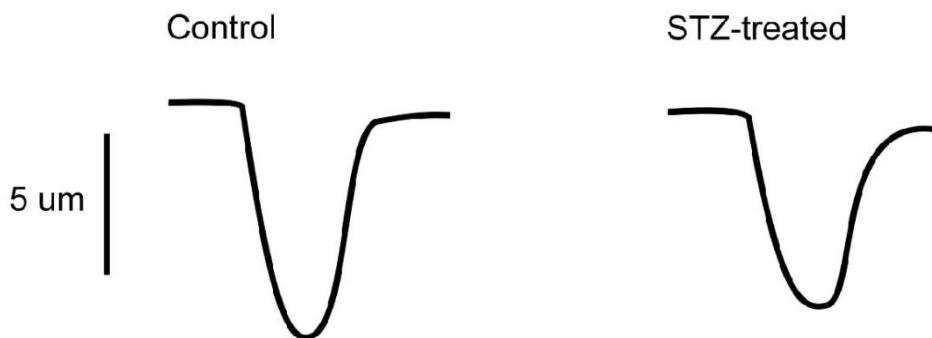


Fig 3.2: Ventricular cardiomyocyte contractility. Representative traces of shortening in Control and STZ-treated ventricular myocytes (**A**). Representative fast time-base recording of unloaded shortening in control and STZ-treated ventricular myocytes (**B**). Traces are typical of 29-33 myocytes isolated from hearts of 5-6 rats.

Table 3.2: Contractility in ventricular cardiomyocytes. Mean data showing effect of 1 mM Ca^{2+} on the amplitude, time to peak shortening and time to half relaxation in electrically stimulated (1 Hz, 50 V, 1 ms pulse width) and superfused (35–37°C) ventricular myocytes of age-matched control and diabetic rat hearts (n=5-6). Figures in brackets represent number of cells * $p < 0.05$, ** $p < 0.01$, unpaired students-t test.

MEASURED PARAMETERS	CONTROL	STZ-TREATED
Resting cell length (μm)	103.57 \pm 2.85 (33)	97.55 \pm 3.29
Peak amplitude shortening (% resting cell length)	5.82 \pm 0.34 (33)	3.86 \pm 0.23 (33)**
Time to peak shortening (ms)	112.47 \pm 5.01 (16)	129.39 \pm 5.99 (19)*
Time to half relaxation (ms)	40.71 \pm 2.09 (16)	48.47 \pm 2.90 (19)*

5. Calcium homeostasis in ventricular myocytes

Representative fast time-base recordings of Ca^{2+} transients in ventricular myocytes from control and STZ-treated rats are given in Fig 3.3. Data describing amplitude and time course of Ca^{2+} transients in cells from STZ-treated and control rats are summarized in Table 3.3. The results showed that STZ-treatment did not result in a statistically significant difference in peak or resting $[\text{Ca}^{2+}]_i$ between groups. However, the kinetics of the Ca^{2+} transient were slower for diabetic rats (increased time to peak $[\text{Ca}^{2+}]_i$ and time constant of Ca^{2+} transient decay; $p < 0.05$).

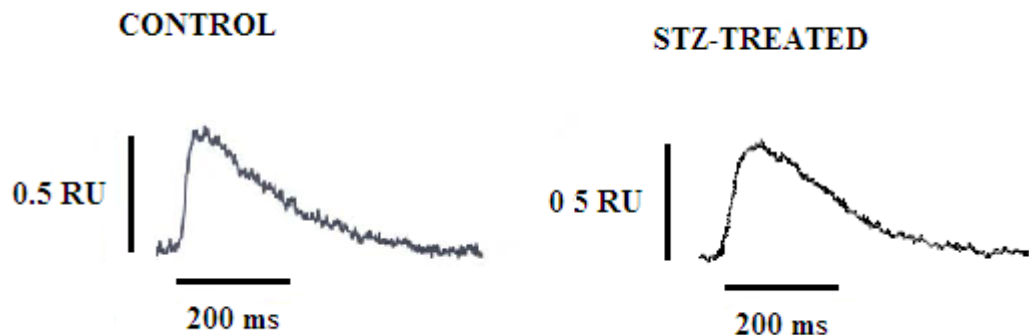


Fig 3.3: Representative fast time-base recording of Ca^{2+} transients in control and STZ-treated ventricular myocytes. RU: ratio units. Traces are typical of 29-33 myocytes isolated from hearts of 5-6 rats.

Table 3.3: $[Ca^{2+}]_i$ transient kinetics. Data showing effect of 1 mM Ca^{2+} on the amplitude, time to peak, and time to half relaxation of Ca^{2+} transients in electrically stimulated (1 Hz, 50 V, 1 ms pulse width) and superfused (35–37°C) ventricular myocytes of age-matched control and diabetic rat hearts (n=5-6). Values are mean \pm SEM and figures in brackets represent number of cells * $p < 0.05$, ** $p < 0.01$, unpaired students-t test

Measured Parameters	Control	STZ-Treated
Resting Fura-2 (Fluorescent ratio units)	1.63 \pm 0.25 (23)	1.56 \pm 0.18 (21)
Ca²⁺ transient amplitude (Fluorescent ratio units)	0.37 \pm 0.04 (23)	0.33 \pm 0.03 (21)
Time to peak calcium transient (ms)	77.16 \pm 3.5 (23)	89.53 \pm 2.54 (21)*
Rate of Ca²⁺ decay (ratio units/s)	0.75 \pm 0.02 (23)	0.57 \pm 0.02 (21)**

3.2.4 Discussion

Various clinical and experimental studies have demonstrated alterations in the rate and force of cardiac contraction in diabetes that are likely to be key events mediating the adverse effects of diabetes on cardiac performance (Schaffer *et al.*, 1989; Ren and Davidoff 1997; Ren and Bode, 2000). The present study has demonstrated intrinsic defects in contractile function in ventricular myocytes of STZ-treated diabetic rats independent of any overt hormonal/vascular effects which is congruent with clinical findings of the existence of a diabetes-specific cardiomyopathy independent of atherosclerosis, vascular, or valvular diseases in human T1DM (Rubler *et al.*, 1972; Kannel *et al.*, 1974; Galderisi *et al.*, 1991; Choi *et al.*, 2002).

The principal findings of this study are summarised as follows: Firstly, 6-7 weeks post STZ-administration, rats presented with significantly greater blood glucose levels and showed significantly less body and heart weight gain compared to age-matched controls. Second, No statistically significant differences were found in resting heart rate in STZ-induced diabetic rats, although contractility was depressed and time course(s) of contraction and relaxation at physiological conditions were prolonged in in myocytes

from diabetic rats. Third, These impairments in mechanical function may be due in part to alterations in $[Ca^{2+}]_i$ homeostasis that manifested as prolonged time to peak and prolonged rate of decay of the Ca^{2+} transient in diabetic myocytes relative to controls.

Overt mechanical abnormalities in diabetes characterised by altered duration and rate of ventricular contraction and relaxation have been observed in intact working hearts (Davidoff *et al.*, 1990), isolated papillary muscle (Fein *et al.*, 1980; Ren *et al.*, 1998) and isolated ventricular myocytes (Ren and Davidoff, 1997) with the severity of dysfunction generally increasing with duration of the disease. In this study, the finding that STZ-induced diabetes resulted in depressed contractility i.e. lower peak amplitude and altered time-course of shortening in STZ-treated ventricular myocytes is in agreement with previous studies, albeit under different conditions (Choi *et al.*, 2002; Noda *et al.*, 1993; Ren and Davidoff, 1997). At the molecular level, such alterations in chronotropic and inotropic parameters have been hypothesised to be an offshoot of deranged expression and/or function of several sarcolemmal membrane receptors and other key proteins involved in regulating/maintaining intracellular ionic homeostasis (Bidasee *et al.*, 2004). Specifically, alterations in $[Ca^{2+}]_i$, the major regulator of cardiac contractility are appreciated as key mechanisms underlying diabetic cardiac dysfunction (Zhang *et al.*, 2008) although, as noted previously, experimental findings are inconsistent. Disturbed Ca^{2+} homeostasis in DM may alter cardiac function by mechanisms including a reduced activity of the ATPases, decreased ability of the SR to take up calcium, and reduced activities of other exchangers such as Na^+/Ca^{2+} exchanger and SERCA (Boudina and Abel, 2007). Although the present study did not examine the critical systems that regulate $[Ca^{2+}]_i$, it is feasible that altered $[Ca^{2+}]_i$ kinetics observed in myocytes from STZ-induced diabetic rats may be indicative of disturbed electrically stimulated $[Ca^{2+}]_i$ release and extrusion. In this study, myocytes from STZ-treated rats had unchanged resting $[Ca^{2+}]_i$ level, and Ca^{2+} transient amplitude, despite showing reduced contractility relative to controls. These results are consistent with some previous studies (Howarth *et al.*, 2002; 2004; Zhang, 2008) performed on isolated cardiomyocytes at identical conditions (35–37°C and 1 Hz). In contrast, results from other studies showed a reduced Ca^{2+} transient amplitude or peak $[Ca^{2+}]_i$ (Lagadic-Grossman *et al.*, 1996; Kotsanas *et al.*, 2000; Yaras *et al.*, 2005), but it should be noted that the experiments in question were performed at lower temperatures (21–25°C) and different stimulation frequencies (0.2–0.5 Hz).

The lower contractility in diabetic myocytes may be further attributable to a reduced myofilament Ca^{2+} responsiveness/sensitivity, which has been reported in diabetic heart (Pierce and Dhalla, 1985; Metzger *et al.*, 1999; Ren and Bode, 2000). This mechanism is speculated to be related to decreased cardiac myosin Ca^{2+} -ATPase activity, which is noted as a feature of both chemically induced and genetic diabetes (Ren and Bode, 2000). Previous studies in STZ-treated rats have documented impaired activity of SERCA and/or other Ca^{2+} -regulating proteins such as $\text{Na}^+/\text{Ca}^{2+}$ exchanger (Russ *et al.*, 1991; Chattou *et al.*, 1999; Ren and Bode, 2000). It is likely that these impairments may underscore the defects in $[\text{Ca}^{2+}]_i$ clearing and subsequently result in the prolonged time course of cardiac contraction and relaxation observed in the STZ-induced diabetic myocytes relative to controls. While it is impossible to definitively establish the relationship between reduced rate of the decay in the Ca^{2+} transient and slowed mechanical relaxation, the findings of this study are supplemented by previous work suggesting that mechanical relaxation is intrinsically slower in diabetic animals and is exacerbated by the reduced rate of decrease of $[\text{Ca}^{2+}]_i$ (Zhang *et al.*, 2008). Moreover, myocytes from STZ-treated rats presented with a slightly prolonged APD, which could possibly result in the slower kinetics of the Ca^{2+} transient as it is well known that the rate of return of $[\text{Ca}^{2+}]_i$ to resting levels is decreased by sustained depolarization, an effect that is partly due to inhibition of Ca^{2+} extrusion by the sodium calcium exchanger (NCX) (Zhang *et al.*, 2008). In explanation of the changes observed in the time course of contraction, duration of shortening and relaxation in this study, parallels can be drawn with previous work in chemically-induced diabetic models that has attributed the lower rate of shortening with diabetes-induced shifts in contractile protein isoforms, notably the redistribution of myosin isozymes from the fast type (V_1) to the slow type (V_3) (Baum *et al.*, 1989; Dillmann, 1989; Metzger, 1999; Ren and Bode, 2000). Lastly, a reduction in mitochondrial respiration and pyruvate dehydrogenase activity in the diabetic heart may result in a depressed rate of ATP production that could further compromise cardiac contractile mechanics in DM (Yu *et al.*, 1997; Ren and Bode, 2000).

In conclusion, this study has demonstrated that experimental DM results in altered mechanical function and cellular Ca^{2+} homeostasis in the isolated ventricular myocyte. Where altered Ca^{2+} transport has been thoroughly investigated at cellular, molecular and genetic levels, less is known about the contribution of ventricular remodelling and alterations in contractile proteins in DCM towards functional deficit. The findings discussed in this chapter suggest that cardiac dysfunction in STZ-induced diabetes is

likely to be attributable to changes at the single-cell level, i.e. altered EC-coupling mechanics. However, distinct from subcellular alterations, ventricular remodelling in DM may also significantly contribute to overt functional deficit (Zhang *et al.*, 2008). Although some features of cardiac remodelling in DM may be in dispute, a large body of evidence associates hyperplasia of myocardial ECM and myocytes with abnormalities in systolic and prominently, diastolic function that are also reiterated in clinical and experimental heart failure. In the context of the latter, cardiac remodelling is known to be a critical factor in the transition from compensated to decompensated states. However, the same features divide opinion in experimental DM and reported findings of the nature, severity and extent of cardiac remodelling in DM are considerably divergent. As such, features of ventricular remodelling are assessed in the next section to determine the scope of cardiac changes (myocyte and non-myocyte remodelling) in experimental diabetes that may predispose to a decline in cardiac pump function.

3.3 Association of Diabetes with Histopathological Changes in the Left Ventricle:

3.3.1 Introduction

Myocardial structural remodelling been the focus of several studies investigating diabetic cardiomyopathy (DCM) in rodent, murine, canine, and primate models of the disease (Asghar *et al.*, 2009) that report a cascade of myocardial changes including fibrosis (Syrový and Hodný, 1992), alterations in myocyte size and microcirculatory abnormalities such as the thickening of the endothelial basal lamina (Hamby *et al.*, 1974; Wang *et al.*, 2006). These changes are believed to result from metabolic abnormalities and subcellular defects resulting as a reactionary response of the myocardium to HG (Fein, 1996; Depre *et al.*, 2000; Cai *et al.*, 2000). The latter is also known to evoke abnormal gene expression and cardiac cell death by both apoptosis and necrosis (Cai *et al.*, 2000) as the disease progresses untreated.

However, there are substantial discrepancies in inferences drawn regarding the onset, severity and nature of pathological alteration in experimental studies (Asghar *et al.*, 2009); These run the gamut from absence of detectable changes (Regan *et al.*, 1981) to severe myocytolysis and contracture band formation (Jackson *et al.*, 1985), with some studies demonstrating significant changes within the first week of disease induction (Reinila and Akerblom, 1984). Contrastingly, in other studies structural manifestations of the disease were only apparent after 6 and 12 weeks (Thompson, 1988). Where common findings in biopsies of the diabetic heart are interstitial fibrosis and myocyte hypertrophy, in some cases further examination revealed a regional heterogeneity with areas showing no increase in ECM deposition (Wang *et al.*, 2006). With regard to cardiomyocyte size, contrasting studies in the same model of the disease (e.g. STZ-induced diabetic rats) demonstrate both hypertrophy (Xia *et al.*, 2007) and atrophy (Nemoto *et al.*, 2006, Bilim 2008).

As mentioned previously, it is important to appreciate the valid interpretation of experimental evidence on structural remodelling in DCM is confounded by factors such as the diabetogen, differences in the severity and duration of DM, the simultaneous presence of experimental hypertension or the subjective nature of the experimental design focussing upon one component of the tissue (Thompson, 1988). As such, the present study was undertaken in order to assess and confirm the development of LV histopathological changes induced by HG in the rat heart, 6-7 weeks post-STZ administration.

3.3.2 Methods

As given in Chapter 3

3.3.3 Results

1. Histopathology of the LV myocardium

Visual analysis of the stained sections by light microscopy revealed general disorganization of myocardial architecture characterized by thinner fibres, disarray of myofibres and scarcity of myofibrils in the STZ-diabetic group compared to Wistar controls (Fig 3.4).

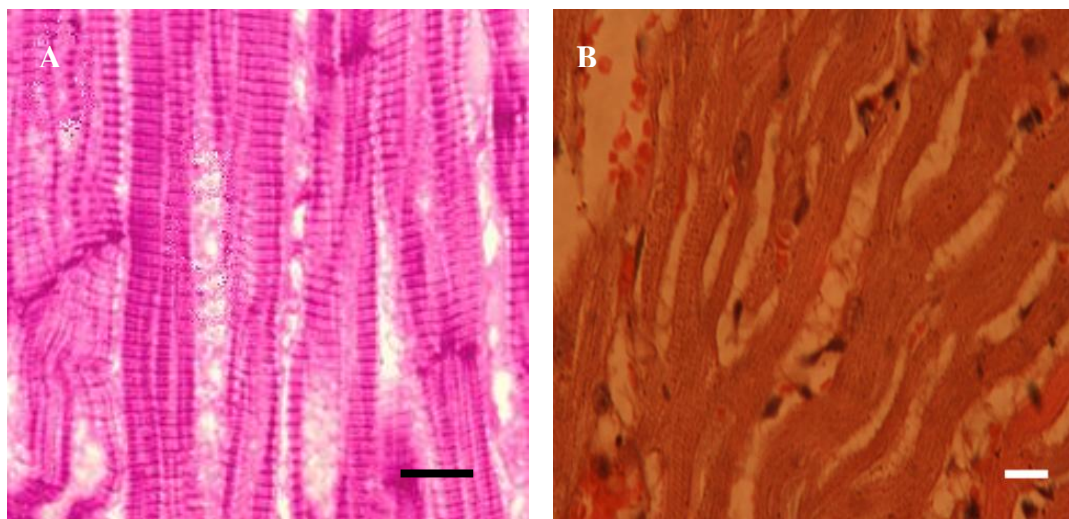


Fig 3.4: Histopathology of the LV. Representative light micrographs showing H & E stain. In control LV muscle fibres are well organized (**A**). In contrast, diabetic LV frequently demonstrated architectural distortion along with a disordered and irregular pattern of myofibrillar arrangement and thinner fibres (**B**). Occasionally, diabetic LV also presented with spongy and vacuolated cytoplasm reminiscent of impending apoptotic cell death (ref, B, arrows). Photomicrographs are typical of 55-60 fields/experimental group consisting of 5 animals per group. The bar in the right photomicrograph indicates 20 μm and 10 μm on the left .

2. Myocyte Diameter

The effects of STZ-induced diabetes on myocyte diameter in the LV are represented in Figure 3.5. Image analysis of FITC-conjugated lectin stained sections revealed a change in cardiomyocyte width in the diabetic group (C). Compared to age-matched controls (A), myocyte diameter was significantly smaller in the STZ-treated rats (B) (9.93 ± 0.26 vs. 9.11 ± 0.25 μm , $p < 0.05$).

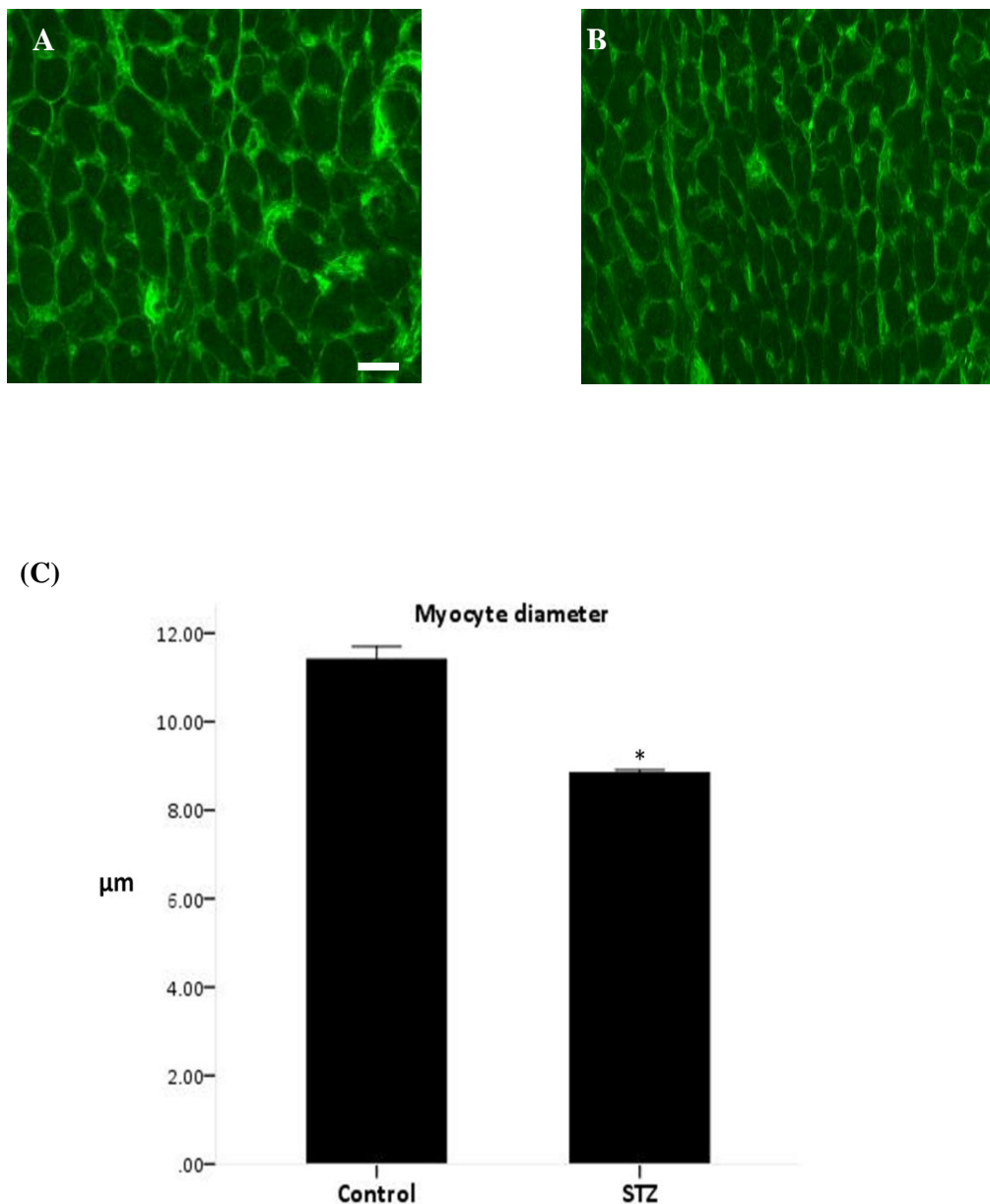


Figure 3.5: Myocyte diameter. Representative light micrographs showing FITC-conjugated Lectin staining. Myocytes in the STZ-treated group (B) appeared smaller

than age-matched controls (A). Original magnification X 200; Photomicrographs are typical of 25-35 fields/experimental group consisting of 5-9 animals per group. The bar in the lower right photomicrograph indicates 10 μm , and accounts for all micrographs. Cardiomyocyte transverse diameter (μm) measured by image analysis (C). * $p < 0.05$, vs. respective control, unpaired t test, $n = 48-51$ myocytes.

3. Myocardial fibrosis

When compared to respective controls, STZ-induced rats demonstrated increased ECM deposition in both interstitial and perivascular regions, as evidenced by Masson's trichrome staining (Fig 3.5). Quantitatively, area of interstitial fibrosis was significantly greater in STZ-treated rats compared to age-matched controls occupying $5.05 \pm 0.44\%$ vs. $3.51 \pm 0.44\%$ ($p < 0.05$) of the myocardial area analysed, representing an approximate 43.8% increase (Fig 2.6).

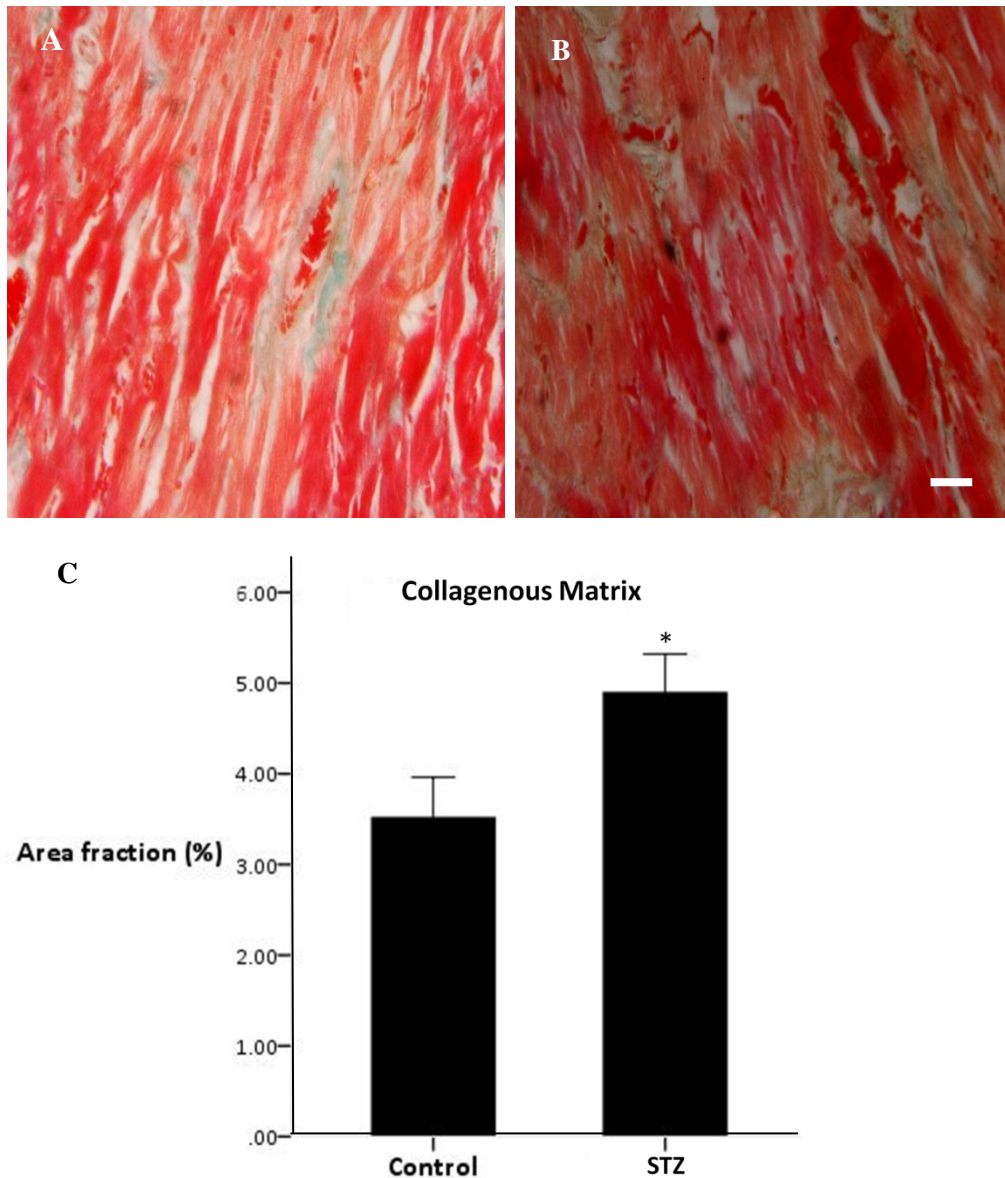


Fig 3.6: Investigation of collagenous matrix deposition. Representative light photomicrographs of Masson's Trichrome stained myocardial sections. Sections from

STZ-treated (B) rats developed greater extents of fibrosis deposition (green staining) in interstitial and perivascular regions relative to respective controls (A). Original Magnification X400, Photomicrographs are typical of 37-41 fields/experimental group consisting of 5-9 animals per group. Scale bar indicates 20 μm . Interstitial ECM deposition in left ventricular myocardium (C) * $p < 0.05$ vs. control. Unpaired t test.

4. Apoptosis: Diabetes has been associated with cardiac myocyte loss through apoptotic mechanisms (Adegate, 2004). Also, in STZ-treated diabetic LV, H&E stained sections occasionally demonstrated signs of end stage apoptosis, manifesting as condensation of nuclei and cell shrinkage (Fig 2.7). Therefore, the contribution of diabetes in the activation of caspase-3, a key effector of the apoptotic process, was assessed. Immunohistochemical staining for cleaved (active) caspase-3 showed a significant increase in immunoreactivity in the hearts of STZ-treated diabetic rats compared to age-matched controls (Fig 2.7 D) (1.86 ± 1.30 in control LV vs. 8.56 ± 7.92 positive cells/ mm^2 in STZ-treated LV, $p < 0.05$)

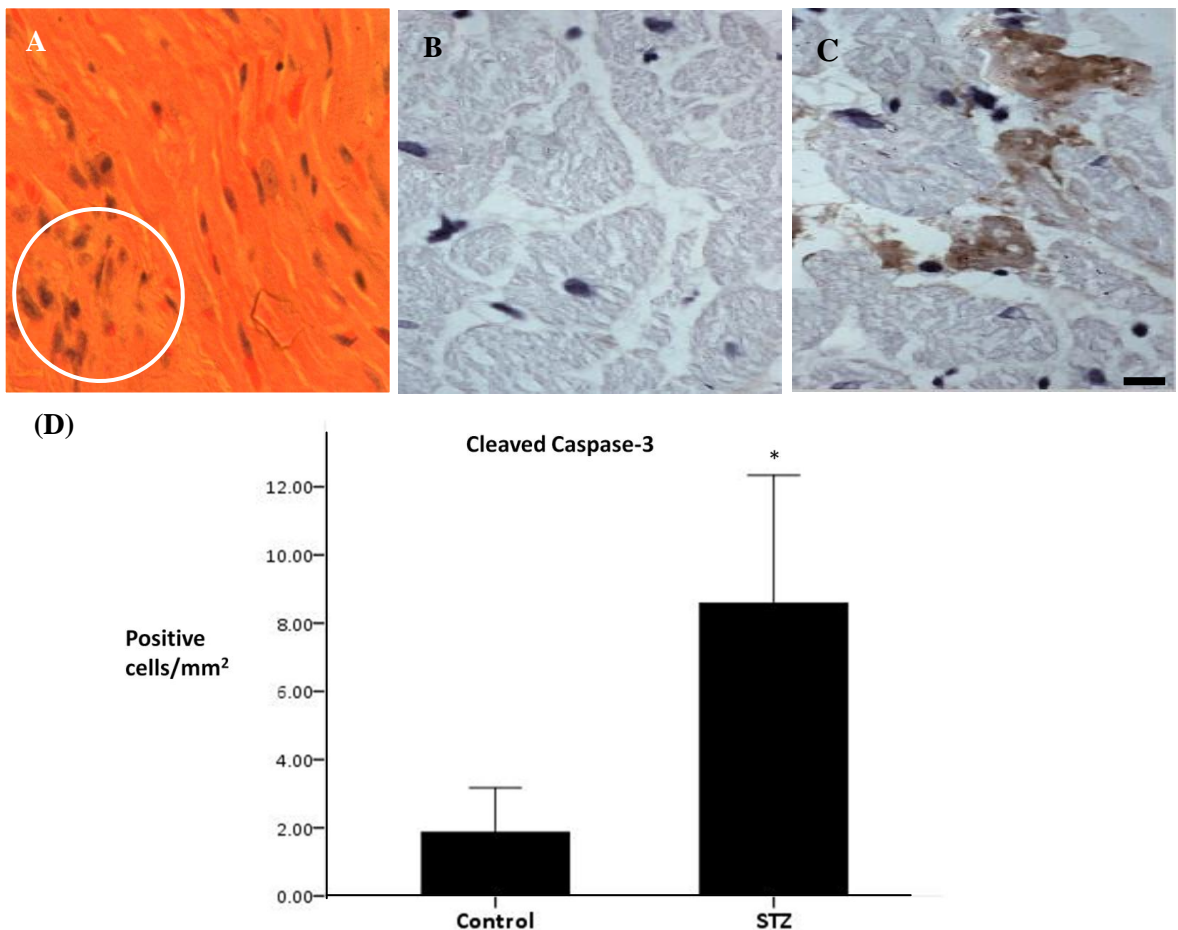


Fig 3.7: Myocyte apoptosis. STZ-treated LV, H&E stain (A). In the STZ-treated rats clusters of cells showed signs of end stage apoptosis (A , circle) characterized by condensation of nuclei and cell shrinkage. Active Caspase 3-positive myocytes (brown staining) in the left ventricle of control (B) and STZ-treated rats (C). Original magnification X 400, Photomicrographs are typical of 10-15 fields/experimental group consisting of 5-6 animals per group. The bar in the left photomicrograph indicates 20

µm, and accounts for all micrographs. Sections are counterstained with Haematoxylin (blue). Semi-quantitative analysis of cleaved caspase-3 labeling (D). Results indicated increased active caspase-3 labelling in STZ LV compared to age-matched wistar controls. (n= 5-9, results expressed as mean+S.E.M, * $p < 0.05$ vs. control, unpaired t test)

2.3.4 Discussion

The chemically-induced diabetic rat is a well documented model for the study of diabetic complications arising from HG and in this study STZ-treatment produced a constellation of characteristics that mimics (severe) clinical type-1 diabetes. The experimental design and duration resulted in a stable population of insulin-deficient animals for the intervals studied.

A notable finding was that STZ-induction resulted in significant cardiac atrophy characterised by loss of heart weight, reductions in heart weight to body weight ratios, and reduced cardiomyocyte diameter, in accordance with previous studies (Kawaguchi *et al.*, 1999; Nemoto *et al.*, 2006; Bilim *et al.*, 2008). The mechanisms underlying cardiac atrophy in this model have not been identified although a role of nutrient deficiency as been suggested (Savabi *et al.*, 1992; Nemoto *et al.*, 2006). As heart size is reported to be sensitive to nutritional status, calorie deprivation in the diabetic rats as an offshoot of metabolic disturbance in diabetes and energy production shift from glucose utilization towards β -oxidation of free fatty acids may have brought about the observed phenotype (Rodrigues *et al.*, 1998; Nemoto *et al.*, 2006). However, previous studies examining the differences between atrophic remodelling in STZ-diabetic and food-restricted, malnourished rats demonstrated divergent features of LV remodelling as well as nutritional status between the two (Savabi *et al.*, 1992; Nemoto *et al.*, 2006). Alternatively, cardiac atrophy may be attributed to severe insulinopenia in STZ-treated rats. Among various signalling pathways, the role of insulin, a potent anabolic hormone and its key downstream effector Akt is particularly implicated in the regulation of body and organ size in several species ranging from *C.elegans* and *Drosophila* to mammals and in multiple organs including the heart (Abel, 2005). Indeed a previous report has correlated myocardial atrophy with decreased Akt phosphorylation in STZ-treated rats, an effect that may be modulated by signalling to mTOR and p70S6K downstream of Akt (Bilim *et al.*, 2008). The kinase mTOR is noted as a key positive regulator of protein synthesis and cell growth transducing signals from growth factors, nutrients and energy status. Once activated mTOR influences translation machinery and protein synthesis by TORC1-dependent phosphorylation of ribosomal S6 Kinases (Bertrand *et al.*, 2008), Activated p70S6K phosphorylates ribosomal S6 protein that regulates translation of the

5'TOP mRNAs that encode several translation factors and ribosomal proteins (Alessi *et al.*, 1998). As such upregulation/ activation of Akt, mTOR and p70S6K have been associated with mesangial cell and glomerular hypertrophy in STZ-induced diabetes (Sakaguchi *et al.*, 2006; Yang *et al.*, 2007).

Another important component of the pathological alterations observed in this study was the diffuse ECM deposition in STZ treated LV interstitium. This finding is in agreement with previous reports wherein long standing diabetes was observed to exaggerate LV remodelling whilst increasing perivascular and interstitial fibrosis (Thompson, 1988; Kita *et al.*, 1991; Riva *et al.*, 1998). Despite some conflicting observations, collagen deposition and ECM alterations in experimental models of diabetes, are accepted as structural hallmarks of diabetic heart as well as other target organs of diabetic complications (Ban and Twigg, 2008; Brownlee *et al.*, 1988; Brownlee, 2001). Production of fibrosis is an adaptive response of the heart to pathophysiological stimuli and various mechanisms have been suggested via which chronic HG and its downstream biochemical pathways contribute towards posttranslational modification of the ECM, thereby increasing turnover and predisposing towards pathological remodelling. The increased matrix turnover in the diabetic milieu is also hypothesized to be a result of increased TGF β 1 activity, altered activity of collagen degrading MMPs, or upregulation of collagen mRNA expression (Tschope *et al.*, 2004). Remodelling of the extracellular matrix is also regulated by profibrotic acting peptides (e.g., angiotensin II, aldosterone, endothelin) concentrations of which have been previously discussed as altered in diabetes (Tschope *et al.*, 2004; Ban and Twigg, 2008). Regardless of the underlying mechanisms, morphological and biochemical consequences of ECM proliferation are known to be directly related to loss of function in the myocardium and this non-myocyte remodelling process is known a significant role in the decline of cardiac pump function in DM (DeTombe, 1997) by adverse effects on ventricular compliance.

Cell death, as a consequence of myocardial abnormalities, can evoke a series of pathological changes in the myocardium including a loss of contractile tissue, compensatory hypertrophy of myocardial cells, and reparative fibrosis and has been considered one of the major contributing factors for various cardiomyopathies and HF (Sharma *et al.*, 2007). In particular, the loss of myocardial cells through the highly regulated process of apoptosis occurring during cardiac remodelling in a failing heart is suspected to play a critical role in the transition from compensated hypertrophy to heart

failure by causing a reduction in the relative myofibrillar mass, resulting in cardiac dysfunction (Dhalla *et al.*, 1996; Cook *et al.*, 1999; De Moissac *et al.*, 2000). Diabetes induced cell death has been observed in multiple organs *in vivo* in both clinical and experimental settings and in endothelial cells *in vitro* (Cai and Kang, 2002). Moreover, Rota *et al.* have (2006) described the influence of HG and secondary metabolic disturbances in the induction of apoptosis, as a potential cause of HF in experimental DM. Similarly, several reports have shown that inhibition of myocardial cell death by antioxidants or inhibitors of apoptosis-specific signalling pathways leading to a significant prevention of DCM (Cai and Kang, 2003). In the present study, immunohistochemical quantification of cleaved caspase-3 indicated there was a significant increase in caspase-3 labeling indices in STZ-rats compared to age-matched controls. These observations are in agreement with a previous study that has reported apoptotic cell death in STZ-treated rats and cultured myocytes in response to hyperglycemia at levels analogous to the present study (Cai and Kang, 2003). In the same study, insulin supplementation, further confirmed that the observed effects were a result of HG and not a direct effect of the β cell toxin STZ, as has been argued previously (Cai and Kang, 2003). Insulin is a predominant protective component of the GIK metabolic cocktail (Diaz *et al.*, 1998) administered to attenuate myocardial reperfusion injury, including apoptosis and exerts significant cardioprotection in patients with AMI who are receiving reperfusion (Jonassen *et al.*, 2000). Furthermore, in cultured neonatal rat cardiac myocytes, administration of insulin alone at reoxygenation reduced apoptotic myocardial cells exposed to hypoxia/reoxygenation (Gao *et al.*, 2002). Several signalling pathways have been implicated in the anti-apoptotic effect of insulin, notably signalling via the PI3-K/Akt axis. On the basis of these findings, it can be speculated that loss of the protective, cell-survival effects of insulin and its downstream effectors in diabetes may contribute to the cardiomyocyte apoptosis observed in this study. It is notable that the incidence of apoptotic myocytes in all groups was very low. In this sense, previous work in transgenic mice that express a conditionally active caspase exclusively in the myocardium has demonstrated that chronically elevated but very low levels of myocyte apoptosis play a vital role in HF by predisposing towards dilated cardiomyopathy (Wencker *et al.*, 2003). Moreover, at the risk of making further interspecies comparisons, low frequency of cardiac myocyte apoptosis in failing human hearts has been implied in the pathogenesis of HF (Olivetti *et al.*, 1997; Saraste *et al.*, 1999; Guerra *et al.*, 1999).

In conclusion, this study was conducted in order to assess structural remodelling changes in the LV as a result of uncontrolled DM. The results have indicated that HG can produce marked alterations in myocardial architecture and the expression of a cardiomyopathic phenotype characterised by fibrosis proliferation, apoptotic cell death and atrophy of cardiomyocytes. Together, with altered contractility in ventricular cardiomyocytes, these alterations likely represent the cellular correlates of the prolonged relaxation and decreased compliance that characterises LV diastolic dysfunction in diabetes. (Galderisi *et al.* 1991, Ren *et al.* 1997, Ren & Bode 2000).

3.4 The Story So Far

At first blush, preliminary experiments indicate that LV dysfunction in DM may be due in part at least, to HG-induced alterations in ventricular structural remodelling and myocyte contractility both of which may contribute to diastolic dysfunction and are frequent features of the failing heart. However, certain caveats merit consideration in the interpretation of this, or any study utilizing chemically-induced models of Type 1 DM. These include results being potentially confounded by the fact that STZ is a general toxin which can cause other abnormalities in addition to diabetes mellitus (e.g. hypothyroidism) which may contribute to the phenotype (National heart lung and blood institute working group, 1998). STZ has also been reported to directly induce defects in myocyte contractility *via* an oxidative stress and p38-MAP kinase-dependent mechanism (Wold and Ren, 2004). Moreover, the relevance of this experimental model, to human DM leaves much to be desired, especially in relation to T2DM that epidemiologically represents the bulk of cardiac complications. In this respect, the phenotype described in the developmental study resembles very poorly controlled T1DM and one extreme of the metabolic profile that is very rarely encountered in clinical practise given current standards of care. Where T2DM is frequently diagnosed after the first CV event (Schainberg *et al.*, 2010), and complications most prominent in the ageing diabetic, short study periods typical of experimental protocols utilizing the STZ-induced T1DM rat model are neither realistic nor desirable. Indeed, age is regarded as a major risk factor underlying CHF incidence in DM. Advances in the therapeutic management of DM and CHF and general improvement in living conditions has accentuated the phenomenon; In the 65 years and older age group, of the incidental cases of CHF, 22% of men and 24% of women were diabetic between 1990 and 1994 compared to 15% and 18%, respectively, 20 years earlier) (Verny, 2007). Another key issue in experimentation with the STZ-rat model is that it presents impediments in the study of the modifications in glucose metabolism that precede clinical DM. At present, the clinical research environment is becoming increasingly reflective of the fact the myocardial complications of DM may begin in response to elevated HG that is *below* the range defined for a diagnosis of T2DM and the significance of the prediabetic phase herein. This situation is briefly discussed in the following section.

3.4.1 Cardiac Complications in Prediabetes: Overview of the status quo

Several studies, summarised in Table 3.4, have reinforced the concept that incidence of CV events including HF risk can be correlated with the degree of glucose elevation and not by the presence or absence of DM *per se*. Additionally, the Australian Diabetes, Obesity, and Lifestyle Study (AusDiab), the largest national diabetes population prevalence survey employing an OGTT in more than 11,000 adults over 25 years of age in Australia found that 65% of all cardiovascular disease deaths occurred in people who not only had known DM and newly diagnosed DM, but also IFG or IGT at baseline. The study further indicated that a significant proportion of CVD deaths occur in people with abnormal glucose metabolism (Barr *et al.*, 2007). The authors have postulated that “strategies to prevent premature mortality and particularly CVD death need to be targeted not only to people with diabetes but also to people with milder forms of abnormal glucose metabolism” (Barr *et al.*, 2007). Supporting the AusDiab study, an earlier metaregression analysis of published data by Coutinho *et al.*, from 20 studies of 95,783 individuals followed for 12.4 years has shown the progressive relationship between glucose levels and cardiovascular risk extends below the diabetic threshold and “that dysglycemia is a cardiovascular risk factor” (Coutinho *et al.*, 1999). As such, it appears that glucose intolerance and IFG that presage the development of T2DM are not only indications of risk for progression to DM, but also to have independent pathophysiologic significance that includes mortality, macrovascular complications including MI or stroke. Specifically with respect to cardiac disease, glucose intolerance and IR have been associated with LV hypertrophy (Bianchi *et al.*, 2008), concentric remodelling and diastolic dysfunction (Fujita *et al.*, 2007; Schneider *et al.*, 2010). Thus, from an epidemiological stance, there is a basis to suggest that dysglycemia may reflect a risk for HF even in the absence of overt DM.

Epidemiology aside, the factors underlying the association between dysglycemic states and CVD, especially HF, have not been extensively studied. Most importantly, the benefit of primary prevention of HF pathogenesis associated with glucose lowering in prediabetes based on current definitions has not been established as of this writing. Clinical studies are also rarely without inherent limitations, often failing to describe the potential role of intercurrent events such as acute coronary syndromes or even changes in blood pressure accounting for subsequent hospitalization for HF. Moreover, dysglycemia is often described as associated with a diffuse and aggressive form of coronary artery disease, which could potentially lead to myocardial injury and failure. A

diversity of potential mechanisms of adverse cardiac consequences with glucose intolerance have been reported, the general opinion being that the mechanisms by which diastolic dysfunction may occur in patients with IGT appear to be similar to those operating in DM (Fujita *et al.*, 2007). Thus, where the direct effects of HG have been implicated, at present there are more questions than answers regarding pathogenesis and pathophysiology. The natural history of DM heart function by Doppler echocardiography is limited, because most patients do not have a prediabetic study, and receive treatments in the full-blown stage of DM or after having diabetes complications (Bergman 2010). Because glucose intolerance may affect over 9 million adults in the UK (Diabetes UK, 2010), has been referred to as ‘The Silent Pandemic’ in the popular media (The Press and Journal, 2009) and may increase the lifetime risk of HF substantially, associations between these common and potentially co-morbid conditions are of interest and clinical relevance.

Table 3.4: Studies correlating dysglycemia and HF. MESA: Multi-ethnic study of atherosclerosis. Table adapted from Schainberg *et al.*, 2010

Study	Design	Subjects	Results
UKPDS 35 (Stratton <i>et al.</i> , 2000)	Prospective observational study	n=4,585 patients (white, asian, Indian, afro-caribbean)	Incidence of clinical complications significantly associated with glycemia. No risk threshold for any point. 16% rise in HF risk with 1% A1c rise
EPIC Norfolk (Khaw <i>et al.</i> , 2004)	Epidemiological study 6 year follow-up	n=10,000 (45-79 years)	21% increase in CV events for each 1% rise in A1c>5%. Increase in CHD event by 40% and 25% in mortality for each 1% A1c> 7%
OPTIMAAL study group (Gustaffson <i>et al.</i> , 2007)	Clinical trial comparing ACE inhibitors Losartan and captopril	n= 2,841 (baseline HbA1c) Dm patients that survived MI complicated by HF	Each 1% increase in A1c>5% over 2.5 year follow up increased mortality by 24%
FUNGATA study (Tominaga <i>et al.</i> , 1999)	Cohort population	7 year follow up	IGT was a risk factor but IFG was not
MESA	Population-based sample	n= 6,814 men and women from ethnic groups (white, Hispanic, African American and Chinese)	Differences in LV mass index, volumes and function detected amongst IFG and DM vs. normoglycemia. Ethnicity modified the association

Held and colleagues (2007)	ONTARGET and TRANSCEND cohorts (both randomized controlled trials)	ONTARGET; n=25620 TRANSCEND n=5,926. people with a high risk of CVD with/without DM. 2.4 year follow up	FPG was a significant independent risk factor for incident CHF and combined endpoint of CHF/CV death that persisted after adjustment of DM status
Ingelsson <i>et al.</i> , (2005)	Prospective population-based cohort	n=1,187 swedish men \geq 70 years	Abnormal 2-h postload glucose response was an independent CHF predictor
Nielsen and Lange (2005)	Data extracted from the Veterans Affairs electronic medical record systems	n=20,810 nondiabetic males (predominantly)	Increasing glucose below DM range independently associated with greater HF incidence
Reykjavik study (Thrainsdottir <i>et al.</i> , (2005)	Population-based cohort	n=19,381	Strong association between dysglycemia, prevalent CHF and incident morbidity and mortality during 21.3 yr follow up after traditional risk factor adjustment

As such, there is an urgent need to for appropriate animal models that provide the least ambiguous answers to allow a better understanding of the processes that lead to diabetic cardiac dysfunction. The OLETF rat is an animal model of congenital DM by selective mating. Using the OLETF model, the serial changes in LV filling dynamics histopathology and metabolic disorders, such as HG, myocardial collagen accumulation during the process of DM progression beginning in prediabetes have been evaluated. In the OLETF rat, an increased deposition of collagen in the myocardium and a reduced peak velocity and prolonged deceleration time of early transmitral flow was observed during the pre-stage of T2DM (Mizushige *et al.*, 2000). Nonetheless, the role of HG alone in underlying the reported complications is not clear as in addition to complications induced by HG, the OLETF rat has the added impact of complications due to dyslipidemia and hence is perhaps better suited to studies of the metabolic syndrome opposed to uncomplicated DM.. Furthermore, there is a gender bias with T2DM observed in most (86%), but not all, male rats of this strain, which may further obscure interpretation (Kawano *et al.* 1991, 1992; Yamamoto *et al.* 1999).

Where the pathophysiological relevance of the STZ and OLETF rat to delineating cardiac effects of a milieu dominated by HG is in question, the quest may be more fruitful when pursued in the Goto-Kakizaki (GK) rat.

3.4.2 Physiological relevance of the Goto-Kakizaki Rat model

The GK rat is a non-obese, spontaneously T2DM model obtained by the selective breeding of mildly glucose-intolerant Wistar rats, repeated over several generations (Goto *et al.*, 1975). The pathogenesis of diabetes in the GK rat includes reduced pancreatic β cell mass (upto 50%) and pancreatic insulin stores, an impaired insulin secretion in response to glucose both *in vivo* and in isolated pancreata, IR in adipose tissue, muscle and liver, moderate but stable fasting HG and late complications manifesting as nephropathy and neuropathy (Ostenson *et al.* 1993; Yashushi *et al.*, 2007; Howarth *et al.*, 2007). T2DM in the GK rat is speculated to be polygenic, and six independent genetic loci have been identified to be involved in the disease (Gaugier *et al.*, 2006). From the colony utilized in the present study, all animals were known to exhibit DM and IGT after 10 weeks of age. Thus during the first 8-9 weeks, the animals may be considered prediabetic and thus present a valuable opportunity to study initial pathophysiological changes in the myocardium that precede the onset of DM. Furthermore, GK rats have a stable, inheritable form of T2DM and do not develop marked obesity, hypertension or hyperlipidemia (Portha *et al.*, 1991; Zhou *et al.* 1995; Begum and Ragolia, 1998; Yashushi *et al.*, 2007; Darmellah *et al.*, 2007). This makes it a particularly useful model to studying cardiac effects of DM alone, excluding the confounding effects of obesity and/or hypertension *per se* that tends to cluster with T2DM in clinical settings. Cardiac complications of prediabetes in the GK rat have not yet been established but few studies have addressed functional changes in overt T2DM. These are signposted in the subsequent sections.

3.4.3 Aims and Scope of the Study

Although HF treatment has markedly improved, reversal of pathological changes and full restoration of function remains difficult. Consequently, identification of predisposing conditions and prevention of early cardiac injury is very desirable. Past studies, analyses of datasets from populations and theoretical mechanisms are consistent with the proposition that increasing glucose has a continuous association with risk for HF, even at concentrations below the cut-offs for a diagnosis of DM, but the underlying pathogenesis is unclear. Because IGT is a common and potentially treatable condition, information concerning how increasing glucose may contribute to other risk factors for HF is of particular clinical consequence.

As described in the first chapter of this thesis, failure of the heart, during either systolic and/or diastolic phases of the cardiac cycle, has its origins rooted in an adverse structural, biochemical, and molecular remodelling of myocardium that involves its cellular constituents and the ECM. In this work, focus is on the pathogenic role of dysglycemia beginning in prediabetes and progressing to overt mild T2DM, in contributing to adverse remodelling of the myocardium and the identification of potential molecular and transcriptional mechanisms that underlie this association. An intrinsic myocyte contractile dysfunction may supplement the remodelling process in contributing to the failure of the heart as a pulsatile muscular pump, underscored by changes in bioenergetics, myosin isoforms, cytoskeletal proteins, and ion transport systems. However, assessment of myocyte contractile function was not further pursued in the GK rat as earlier studies (in our laboratory) were unable to demonstrate any significant abnormalities in the contractile function of myocytes isolated from the GK LV for up to 18 months of untreated DM (Howarth *et al.*, 2007).

In the present work data regarding the development and progression of remodelling changes can be roughly divided into (1) that concerning the phenotype and (2) that concerning the mechanisms that govern the establishment of the phenotype. Specifically, the following issues have been addressed:

1. It has become clear that cardiac remodelling is attended by cardiac hypertrophy and interstitial fibrosis, leading to the loss of normal cardiac function and that dynamic structural remodelling is a milestone in HF progression. Using the GK rat as a model of prediabetes, (at 8 weeks of age), this study tests the hypothesis that dysglycemia of prediabetes may contribute to HF pathogenesis by stimulating myocyte hypertrophy and fibrosis proliferation in the LV. How mild HG *per se* impacts LV structure in the long term was also examined by studying remodelling changes at the other end of the dysglycemia continuum, i.e. in overt chronic (mild) T2DM in the GK rat. Moreover as ageing is an independent risk factor for HF, the study design enabled assessment of the combined effects of ageing and mild HG on the myocardium. Conventionally, a limit for advanced age in humans is set at 65 years and in the literature, a corresponding cut-off point for rats is set at age above 18 months (Ferrari *et al.*, 2003). This has been adopted in the present study in the choice of age groups.
2. In investigating the putative mechanisms that could underlie structural remodelling in the dysglycemic LV, this study has investigated the involvement of TGF β 1, cytokine activation being a pivotal mediator in cardiac remodelling in response

to myocardial overload or injury. Several lines of evidence point to the role of HG-induced TGF β 1 as a powerful initiator of tissue repair, sustained production of which underlies the development of myocardial fibrosis. Moreover, increased TGF β 1 expression has also been identified in the myocardium during cardiac hypertrophy and HF. Confirming the activation of TGF β 1 in dysglycemic states may highlight a role in HF pathogenesis and inversely, present therapeutic opportunities.

3. HF has come to be recognised as a disorder of cell signalling and several protein kinases and phosphatases are now seen as having especially cogent roles in HF pathogenesis. Of the labyrinthine maze of signal transduction events initiated by HG that lead up to HF, this work investigates alterations in Akt activity and its downstream signalling via the mTOR/p70S6K axis. The Akt-MTOR-p70S6k axis is a key mediator of the hypertrophic response and recent studies have suggested an HG-dependent TGF β 1 mediated activation of this pathway *in vitro*

4. As most signal transduction mechanisms that are involved in HF pathogenesis converge on the cell nucleus and long-term effects on virtually every aspect of cardiac function are exerted through the enforcement of altered gene expression, thus making it a logical target for therapeutic intervention. Therefore, a major objective of this study was to examine the occurrence of transcriptional reprogramming of key genes that execute hypertrophic/fibrotic gene programmes during pathological remodelling of the heart in response to dysglycemic states

Altogether, this study has utilized a broad transcriptomic and proteomic approach to provide an overview of the profound modifications that affect the heart at both ends of the dysglycemia continuum. An improved understanding of how HG can account for the causes of adverse myocardial remodelling carries with it the potential of identifying new biomarkers predictive of risk, onset and progression, and response to intervention(s) aimed at preventing and/or regressing the remodelling of myocardium in dysglycemic states.

CHAPTER 4

LEFT VENTRICLE STRUCTURAL REMODELLING IN THE PREDIABETIC GOTO-KAKIZAKI RAT

Left Ventricle Structural Remodelling in the Prediabetic Goto-Kakizaki Rat

4.1 Abstract

Background: This study tested the hypothesis that experimental prediabetes can elicit structural remodelling in the LV.

Methods: LV isolations from 8-week old male GK rats and age-matched male Wistar controls were used to assess remodelling changes and underlying TGF β 1 activity, pro-hypertrophic Akt-p70S6K signalling and gene expression profile of the extracellular ECM using histological, immunohistochemical, immunoblotting and quantitative gene expression analyses.

Results: Prediabetes in GK rats was confirmed by impaired glucose tolerance and modestly elevated fasting blood glucose. LV remodelling in the GK rat presented with marked hypertrophy of cardiomyocytes and increased ECM deposition that altogether translated into increased heart size in the absence of ultrastructural changes or fibre disarray. Molecular derangements underlying this phenotype included recapitulation of foetal gene phenotype markers BNP and α -SKA, activation of the Akt-p70S6K pathway and altered gene expression profile of key components (Collagen 1 α , fibronectin) and modulators (MMP2 and 9 and CTGF) of the ECM. These changes were correlated with parallel findings of increased TGF β 1 transcription and activation in the LV and elevated active TGF β 1 in plasma of GK rats compared to controls (*t* test, $p < 0.05$ vs. age-matched Wistar control for all parameters).

Conclusions: This is the first report describing LV structural remodelling in experimental prediabetes. Results suggest that ventricular decompensation pathognomonic of advanced diabetic cardiomyopathy may have possible origins in pro-fibrotic and pro-hypertrophic mechanisms triggered *before* the onset of T2DM. TGF β 1 activity may represent a key intermediary in this process.

4.2 Introduction

The high prevalence of HF seen in individuals with T2DM is partly accounted for by a diabetes-specific cardiomyopathy (Boudina and Abel, 2010). HG is the primary diagnostic feature of DM, the target for anti-diabetic therapy and together with HbA_{1c} the principal marker of glucose control (Schainberg *et al.*, 2010). It follows that several lines of epidemiological evidence have accumulated to suggest an independent effect of HG on HF, in the absence of confounding co-morbidities/risk factors. Indeed, previous work and theoretical mechanisms are consistent with the proposition that increasing glucose has a continuous association with risk for HF and adverse cardiovascular outcomes even at concentrations *below* the range defined for a diagnosis of diabetes; i.e. in the dysglycemia of IGT (also impaired fasting glucose), used interchangeably with the term ‘prediabetes’ (Nielsen and Lange, 2005; Bergman, 2010; Schainberg *et al.*, 2010).

The association between HG and HF may be mediated, in part by an effect of HG on LV structure. Structural remodelling of the LV characterised principally by myocyte hypertrophy and fibrosis proliferation is recognised as the pathological *sine qua non* of the failing heart. It is noteworthy that in recent years, HF has been redefined as the sustained progression of LV myocardial remodelling that precedes the impairment of chamber performance and overt clinical manifestation (Fedak *et al.*, 2005). One mechanism whereby HG can elicit unfavourable structural remodelling is via activation of the pro-fibrotic cytokine TGFβ₁. This concept is reinforced by previous clinical and experimental work highlighting the functional linkage of HG-stimulated increase of protein synthesis, in particular of ECM proteins with increased TGFβ₁ signalling, mainly in the kidney (Ziyadeh, 2004) but also in the heart (Ramos-Mondragon *et al.*, 2008), suggestive of systemic effects. Less established is the causal relationship of TGFβ₁ in provoking myocyte hypertrophy. As described in Chapter 1, recent *in vitro* work has demonstrated the capacity of HG to induce hypertrophic growth by TGFβ₁-mediated activation of the Akt-mTOR-p70S6K signalling, a canonical pathway in cell size regulation (Wu and Derynck, 2009). However, *in vivo* validation of this mechanism in a setting of moderate HG and in the context of the cardiomyocyte is pending.

Compelling epidemiological evidence notwithstanding, the role of HG in HF pathogenesis is unclear. The relationship of HG to HF is complicated by converse observations that improved glycaemic control does not improve cardiac function and

hence prevent HF (Nielsen and Lange, 2005) and also that HF can in turn, induce insulin resistance and DM (Schainberg *et al.*, 2010). Genetic heterogeneity of sample populations, intercurrent events such as acute coronary syndromes, sex-pooled analyses and environmental risk factors are amongst other caveats confounding interpretation of clinical studies. Experimental support is limited, with most work focussing on chemically induced Type 1 models of the disease that ultimately represent an extreme of the metabolic profile (rarely encountered in clinical practice) or Type 2 models burdened with the twin load of DM and other element(s) of the metabolic syndrome. Prediabetes was estimated to affect over 7 million in the UK population in 2009 (Diabetes UK, 2009) and considering prevalence is ever-burgeoning, the importance of assessing the myocardial consequences of mild-moderate HG in animal models that represent a pure diabetic aetiology cannot be overstated.

In light of the foregoing, the well characterized GK rat model (Goto *et al.*, 1975) was utilized to address whether LV structural remodelling begins in a state of IGT that precedes the onset of T2DM. Briefly, characteristics of the disease in the GK rat include a reduced β cell mass, hepatic and peripheral insulin resistance altogether culminating in mild basal HG, marked glucose intolerance that deteriorates over time to frank T2DM (Yasushi *et al.*, 2007). As the disease progresses untreated, the GK rat also manifests main features of metabolic, hormonal and vascular disorders described for T2DM (Howarth *et al.*, 2007). In this chapter, data are presented to substantiate the hypothesis that the HG of prediabetes is sufficient stimulus to induce LV remodelling characterised by myocyte hypertrophy and ECM proliferation concomitant with increased circulating active TGF β 1, alterations in TGF β 1-sensitive signalling events and the gene expression profile of the ECM.

4.3 Methods

As given in Chapter 3

4.4 Results

1. Characterisation of prediabetes in the Goto-Kakizaki rat

At 8 weeks of age, fasting blood glucose in GK rats was within the normal range (<125 mg/dL) but consistently higher than age-matched control animals (76.2 ± 5.73 vs. 107 ± 6.21 mg/dl, $p < 0.01$) (Fig 4.1 A). Glucose clearance capacity in diabetic and control animals was assessed using the glucose tolerance test (GTT) (Fig 4.1 B). Maximal response to glucose challenge was significantly higher in untreated diabetic animals versus control. Additionally, blood glucose levels following GTT were higher at all time points measured and did not return to baseline level indicating severely impaired glucose tolerance ($p < 0.01$). Two hour blood glucose of GK rats at 8 weeks was <200 mg/dL and when coupled with fasting blood glucose values (Fig 4.1 A), satisfied criteria for a diagnosis of IGT in accordance with current guidelines (WHO, 2006). Mean plasma insulin levels were not assessed in this study but glycemic status in GK animals were consistent with impaired secretion of insulin and peripheral insulin resistance previously reported in this model (Portha *et al.*, 1991).

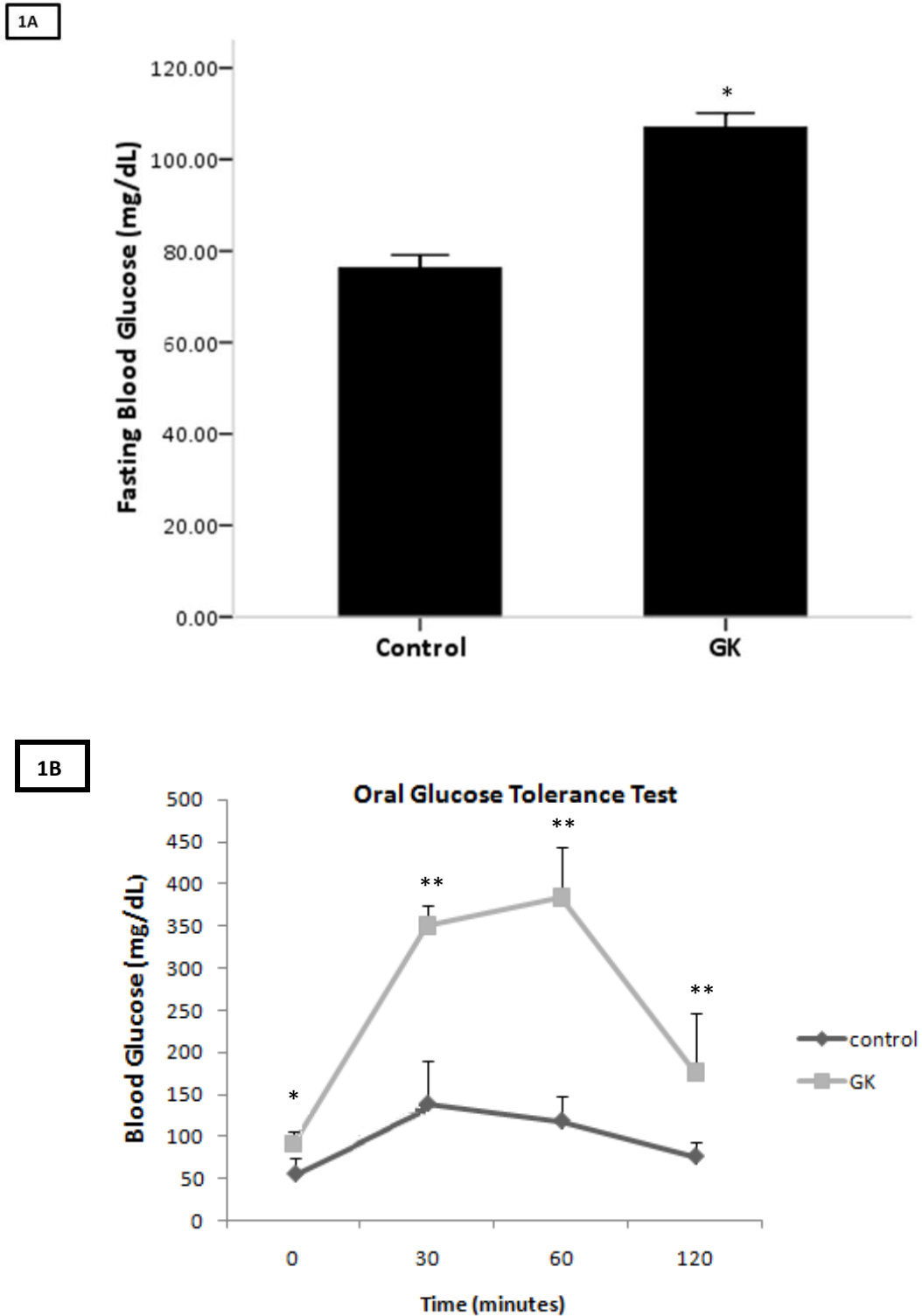


Fig 4.1: Glucometry data. Fasting Blood glucose (1A) and GTT (1B) demonstrating elevated fasting glucose and impaired glucose tolerance in GK rats compared to controls

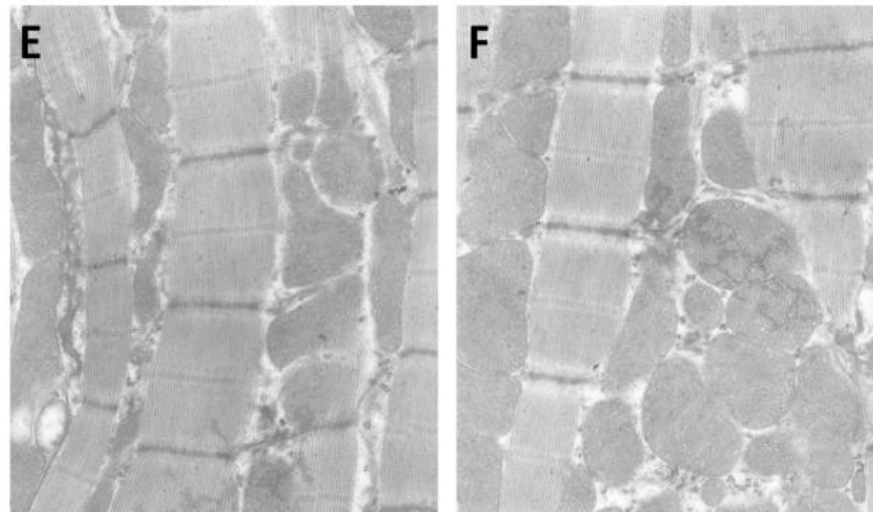
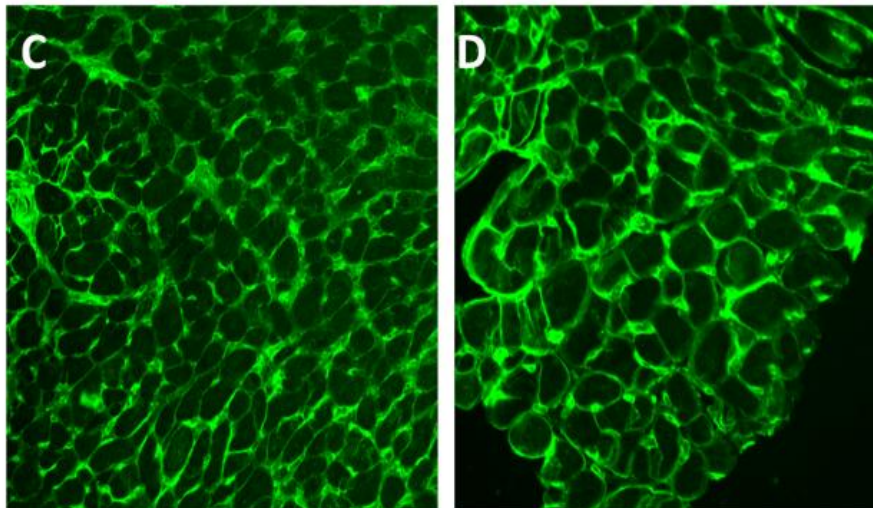
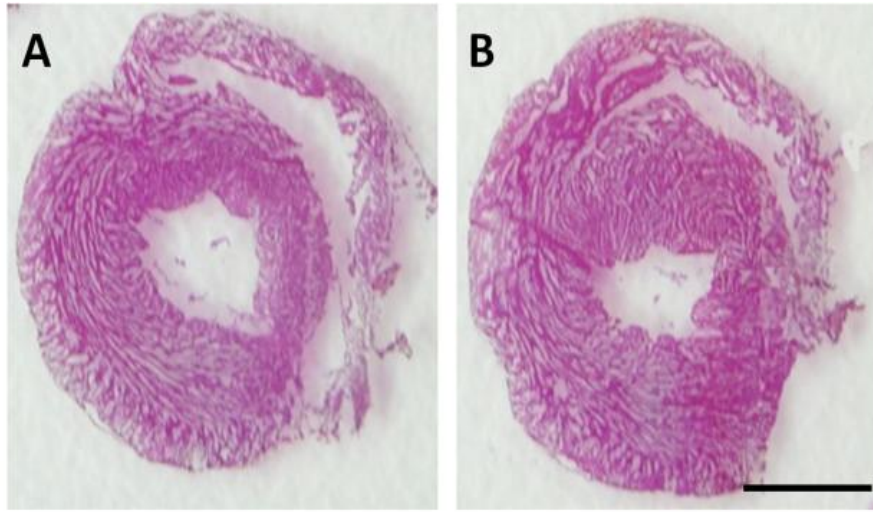
at 8 weeks (n=8/group). Data expressed as Mean±SEM. * $p < 0.05$, ** $p < 0.01$, unpaired t test.

2. Histopathology, gross morphology and gravimetry

Body weight (BW), whole heart weight (HW) and LV weight (LVW) was assessed in prediabetic GK and age-matched control animals at 8 weeks. No significant differences were found in BW among groups, whereas HW and LVW normalized to BW showed a modest but significant increase within the GK group (Table 4.1). Small increases in thickness of the LV free wall were also evident in GK rats (Fig 4.2 B) compared to age-matched controls (Fig 4.2 A) but this difference did not reach statistical significance ($p > 0.05$). At the cellular level however, a conspicuous increase in cardiomyocyte width was apparent in the GK group that was further confirmed by quantifying Lectin staining (Fig 4.2 D, Table 4.1). No major ultrastructural alterations were apparent on comparison of control and GK groups (Figs. 4.2 E and 4.2 F) and both groups showed comparable preserved sarcomeric structure within cardiomyocytes (i.e. within sarcoplasm, contractile apparatus and organelles). A subtle differentiating feature in prediabetic rats was the recurrent finding of altered intercalated disk presentation. Intercalated discs in the GK group frequently presented with dilation of fascia adherens and a zig-zag configuration (Fig 4.2 H) opposed to normal sinuous appearance within control animals (Fig 4.2 G). It has been suggested that this feature represents the brisk pace of sarcomerogenesis in the adapting myocardium much of which takes place at the intercalated disc and is reminiscent of normally growing hearts (Legato *et al.*, 1984)

Table 4.1: General characteristics of control and GK rats at 8 weeks. Values are expressed as mean±SEM. * unpaired *t* Test $p < 0.05$ versus age-matched control. BW: body weight; HW: heart weight; LVW: left ventricle weight

Animals	BW (g)	HW (g)	Hw/BW Ratio g/100g BW	LVW/BW (mg/g)	LV thickness (mm)	Myocyte Diameter (µm)
Control (n=8)	325±1.49	0.80±0.01	0.24±0.441	1.76±0.42	2.98±0.20 7	9.11±2.55
GK (n=8)	329±0.43	0.92±0.008*	0.28±0.002*	1.98±0.80 *	3.15±0.46	9.93±2.69 *



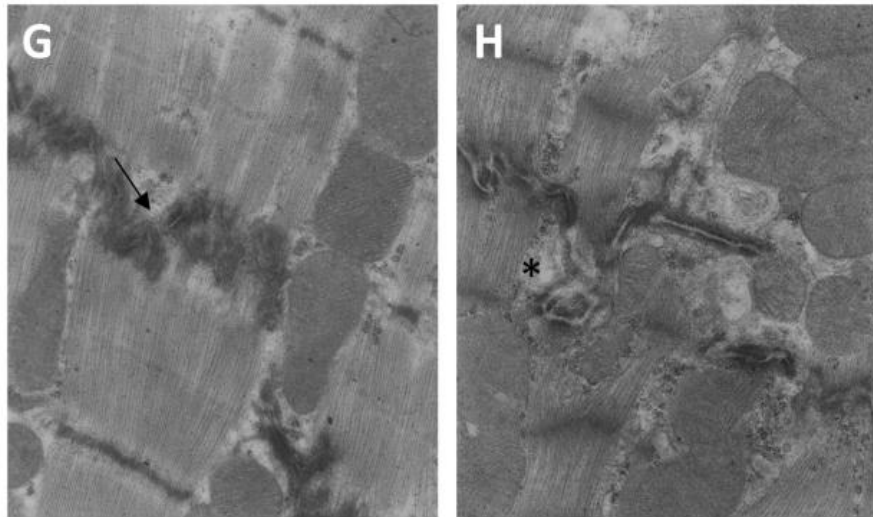


Fig 4.2: Left ventricle Hypertrophy and Myocyte Ultrastructure. Representative photomicrographs from 4-5 hearts showing slight increase in LV wall thickness in GK (2B) rats compared to controls (2A). Scale bar=3 mm. Typical FITC-conjugated Lectin staining showing increased myocyte diameter in GK rats (2D) vs. Control (2C) Magnification X400. Representative transmission electron micrographs of the LV in control and GK rats (n=4) (2E & 2F) showing comparable cytoarchitecture. Normal aspects of the A and I bands, M and Z discs, densely packed mitochondria and regular arrangement of sarcomere (Magnification x14, 000). Representative intercalated disc in control and GK rats (2H, 2G). Control showing characteristic sinuous aspect (2G), adherens junctions evidenced by arrow whereas typical intercalated disk in GK cell; note dilatation of fascia adherens indicative of sarcomerogenesis (*) (2H) (Magnification x18, 000).

The density of collagen protein was evaluated by Picosirius Red staining in control and GK rats (Fig 4.3). In control animals, fibrosis in the LV was negligible. Within the GK group, ECM proliferation was still limited but significantly more pronounced, wherein accretions were evident throughout the interstitium and distributed evenly throughout the thickness of the myocardium. Quantitatively, there was a 1.43-fold increase in collagenous matrix accumulation, occupying $1.44 \pm 1.02\%$ of the LV in GK animals vs. $1.006 \pm 0.13\%$ in controls $p < 0.05$ (Fig 4.3 C).

3

Picrosirius Red Staining

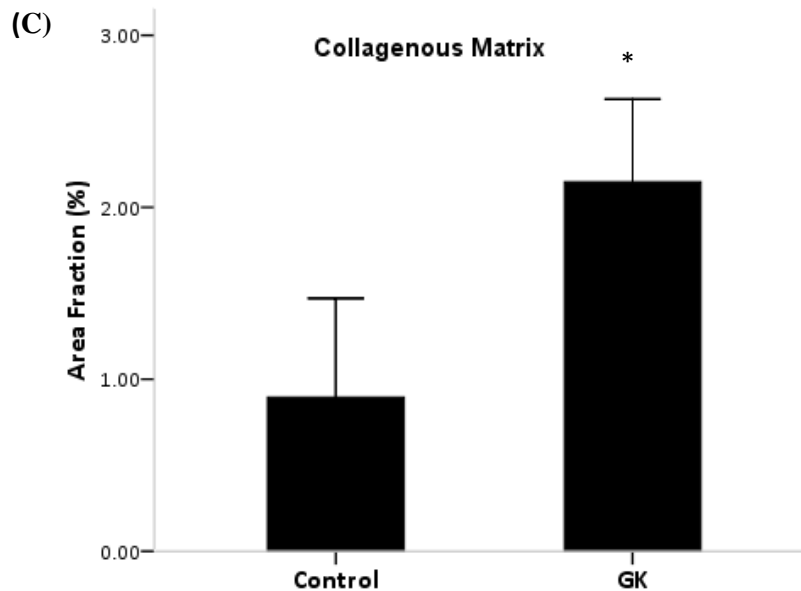
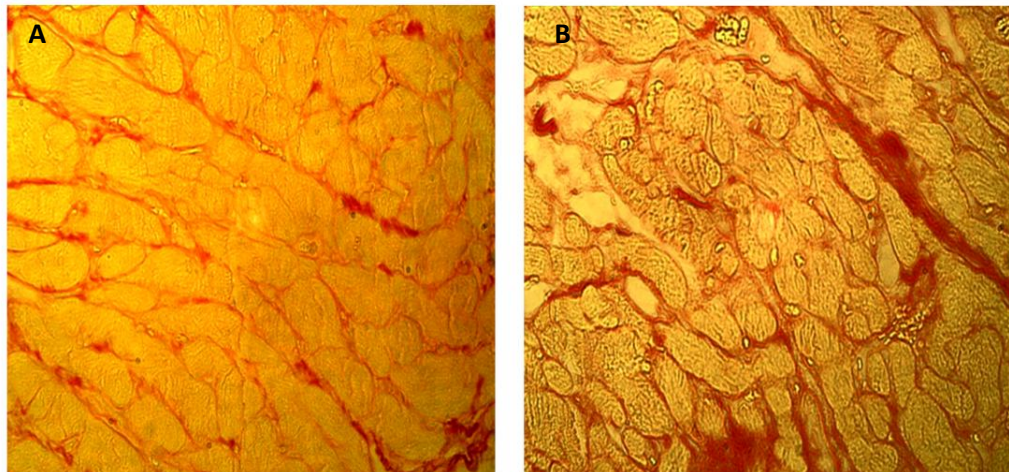


Fig 4.3: Collagenous matrix proliferation in the interstitium. Increased picrosirius red staining was evident in GK (3B) compared to control animals (3A) Magnification X400. Collagen protein area fraction quantified by image analysis (3C). Data presented as Mean+SEM. * unpaired t test $p < 0.05$, $n = 37-41$ fields from 5-6 rats in each group.

3. Molecular events characterising extracellular matrix proliferation in the prediabetic LV

a. Increased active TGF β 1 levels and mRNA expression in the prediabetic GK rat Plasma and LV samples from GK and control rats were used to evaluate total and active TGF β 1 concentration by ELISA (Fig 4.4). Active TGF β 1 levels increased in GK Plasma and LV relative to control animals (plasma: 2.55 ± 0.55 vs. 1.67 ± 0.11 ng/ml, $p < 0.05$; LV: 5.47 ± 1.48 vs. 2.89 ± 0.60 pg/mg of total protein, $p < 0.05$). Total TGF β 1 protein levels were also increased in the LV of GK rats relative to controls (10.32 ± 1.99

vs. 7.38 ± 0.50 pg/mg of total protein, $p < 0.05$) but remained largely unchanged in plasma (4.87 ± 0.84 vs. 4.46 ± 0.46 , $p > 0.05$). Increased LV TGF β 1 in was accompanied by a 1.4 fold transcriptional upregulation of TGF β 1 mRNA in GK LV relative to controls, as determined by quantitative RT-PCR (Fig 4.4 D).

4. Gene expression profile of the intersitium and connective tissue growth factor

Both HG and TGF β 1 activity are known to regulate gene expression of the ECM. Using RTqPCR, this study investigated whether fibrotic deposition in GK rats was paralleled by an altered ECM gene expression phenotype.

Collagen type 1 α (Co1 α) and fibronectin (Fn) expression were significantly increased in GK rats (Fig 4.5 A), whereas collagen type 3 α (Col3 α) expression was not altered ($p > 0.05$). Message levels for regulators of the ECM also changed in prediabetes. Notable increases in the expression of connective tissue growth factor (CTGF), a key mediator of fibroblast differentiation and activity (Fig 4.5 B) was found in GK LV. Metalloproteinases represent a group of enzymes that catalyze ECM degradation and in this study we found significant upregulation of MMP2 and MMP9 in GK rats compared to controls (Fig 4.5 B). Finally, mRNA expression levels of tumour necrosis factor α , elastin, vimentin, integrin α 1 and integrin α 5 were also assessed but no significant differences were detectable in GK rats vs. controls.

Table 4.2: Total and active TGF β 1 in plasma of control and GK rats. Data expressed as Mean+SEM. * unpaired t test, $p < 0.05$. (n=3)

	Total Plasma TGF β 1 (pg/ml)	Active Plasma TGF β 1 (pg/ml)
Control	4.46 ± 0.35	1.67 ± 0.09
GK	4.87 ± 0.65	$2.55 \pm 0.21^*$

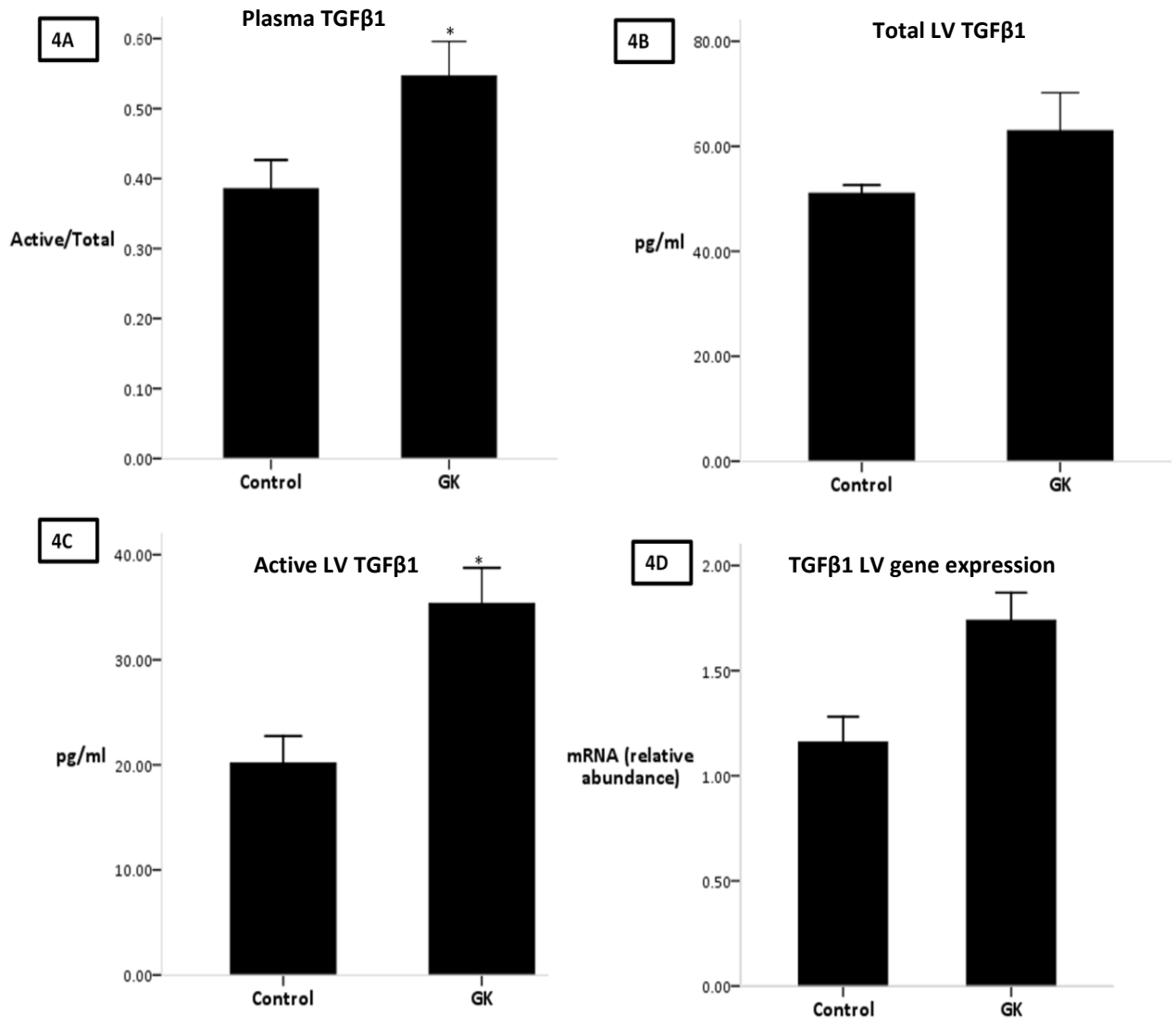


Fig 4.4: TGFβ1 protein level and expression. Results of ELISA showing increased ratio of active: total TGFβ1 protein (4A), total TGFβ1: total extracted LV protein (3B) and active TGFβ1: total extracted LV protein (4C) in LV samples of GK vs. control animals (n=3/group). LV mRNA expression of TGFβ1 (4D). RT-PCR amplification was normalized to that of GAPDH (n=8/group). Table showing Experiments for both ELISA and RTqPCR were conducted in triplicate. Data expressed as Mean+SEM. * unpaired t test, $p < 0.05$.

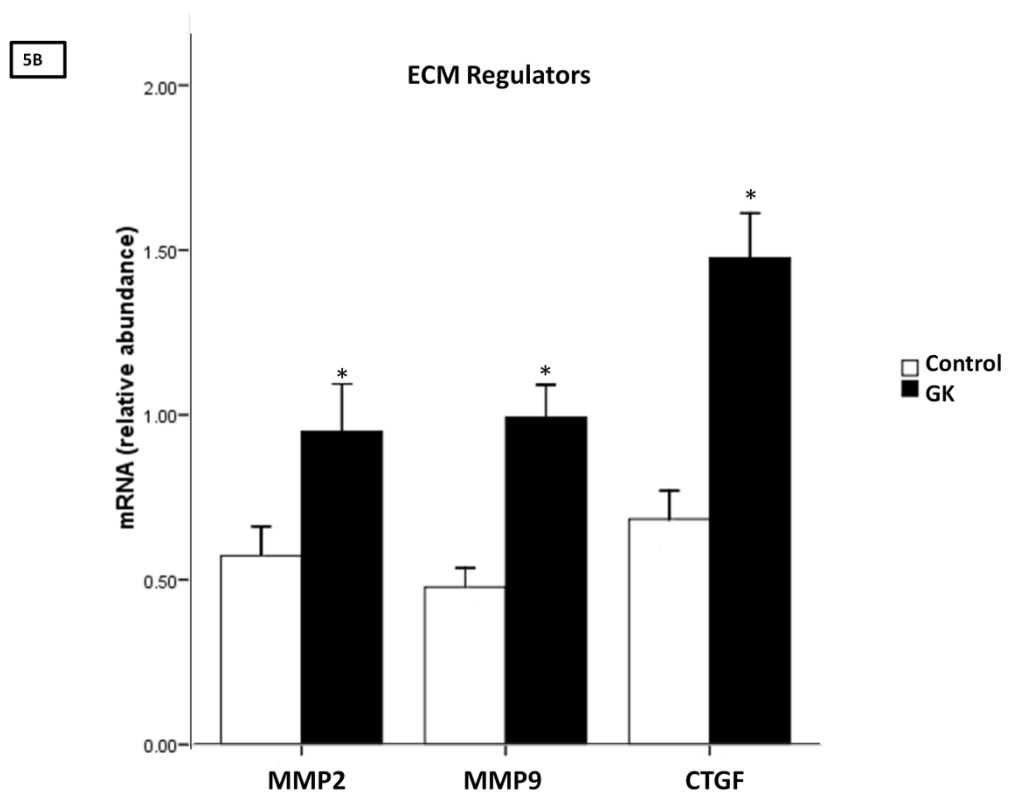
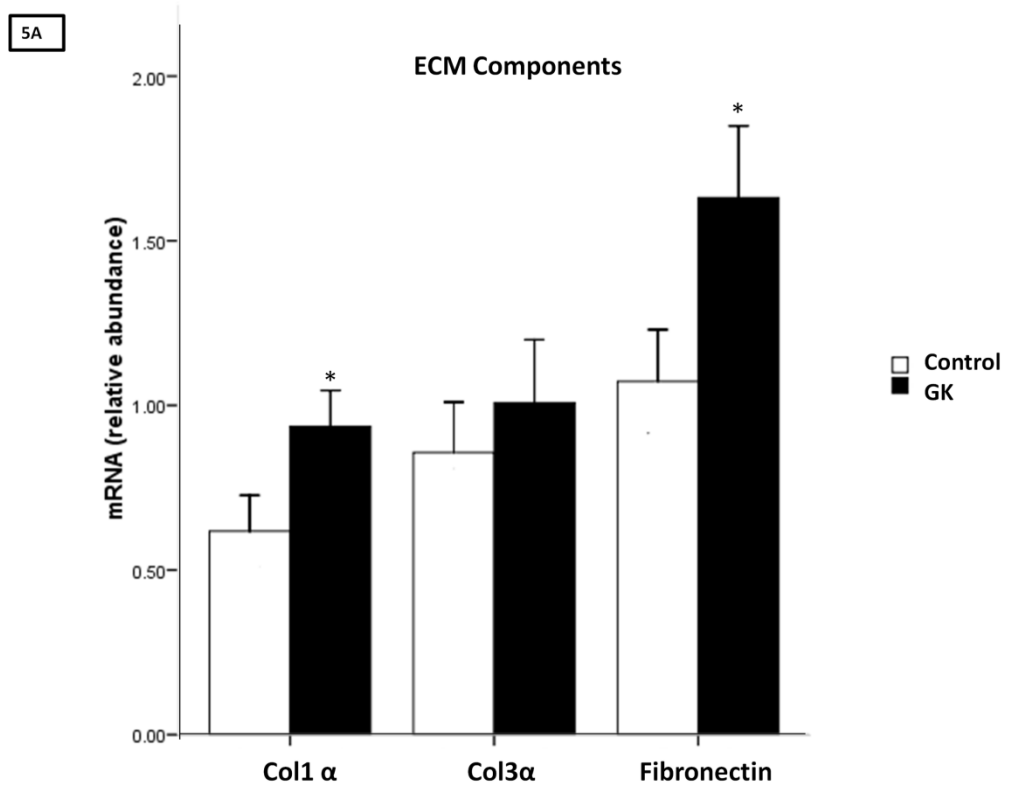
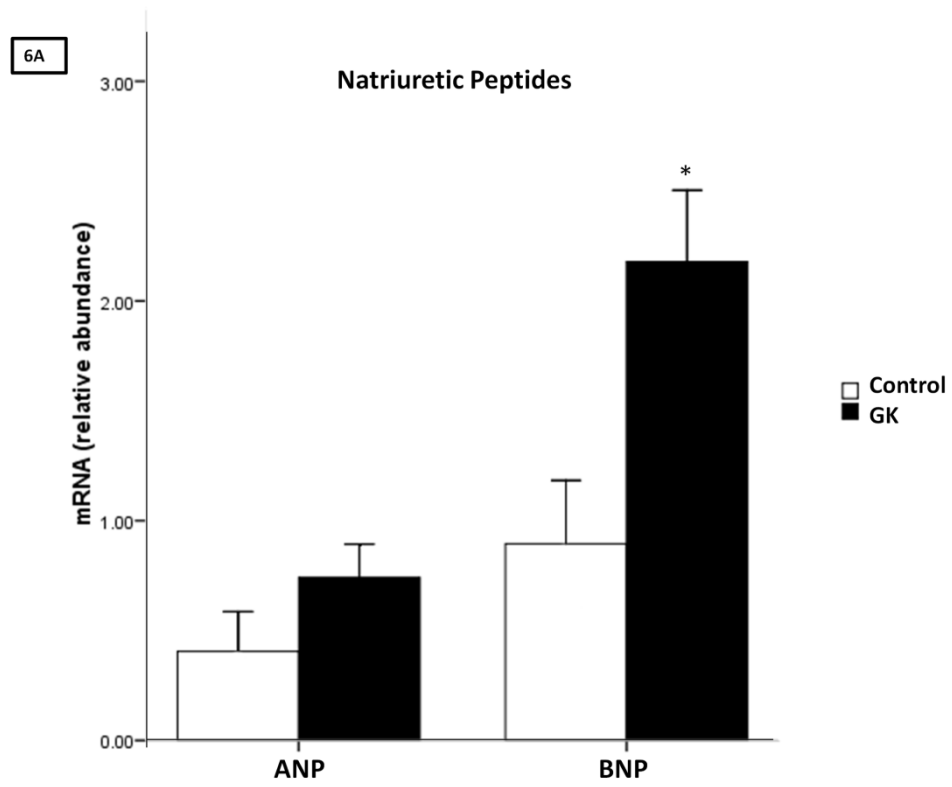


Fig 4.5: Gene expression profile of the extracellular matrix. Increased message levels for ECM components Coll α and Fn (5A) and regulators MMP2, MMP9 and CTGF (5B). RT-PCR amplification was normalized to that of GAPDH (n=8/group). Data expressed as Mean+SEM. * unpaired t test, $p<0.05$.

Molecular events underlying left ventricle hypertrophy in prediabetes

5. Recapitulation of a foetal gene phenotype

Increased expression of the natriuretic peptides ANP and BNP and of myofibrillar protein α SKA are considered sensitive biomarkers for cardiac hypertrophy. Furthermore, TGF β 1 has been demonstrated to stimulate recapitulation of fetal cardiac genes. Therefore, to investigate whether histologically-determined myocyte hypertrophy was concurrent with induction of corresponding molecular markers, this study quantified ANP and BNP mRNA by RTqPCR (n=8/group) and cellular α SKA by indirect immunofluorescence labelling. Cardiac hypertrophy in GK rats was accompanied by significant upregulation of cardiac BNP transcripts in the LV whereas ANP mRNA was unchanged (Fig 4.6 A). In this study, normalized pixel intensity measurements obtained by confocal imaging were used to determine cellular α SKA1 protein levels. This method demonstrated a significant increase in signal intensity of Anti- α SKA1 immunostaining in GK rats relative to age-matched control animals (24.12 ± 1.06 vs. 14.24 ± 1.42 , arbitrary units) (Fig 4.6 D) The distribution of α SKA1 immunostaining in GK rats was of a focal pattern similar to that in control animals, but both density and staining intensity of reactive fibres were greater in GK (Fig 4.6 C) vs. normal myocardium (Fig 4.6 B).



α Skeletal Actin Immunofluorescent Labelling

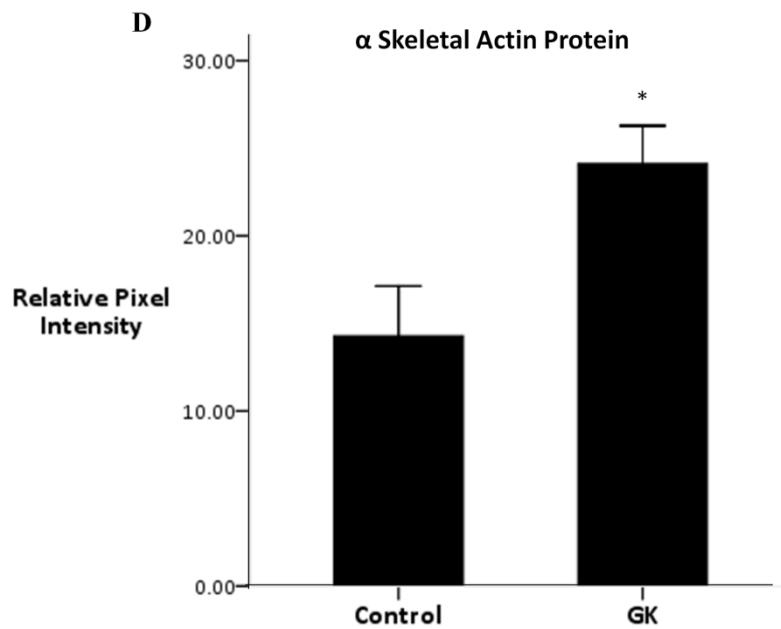
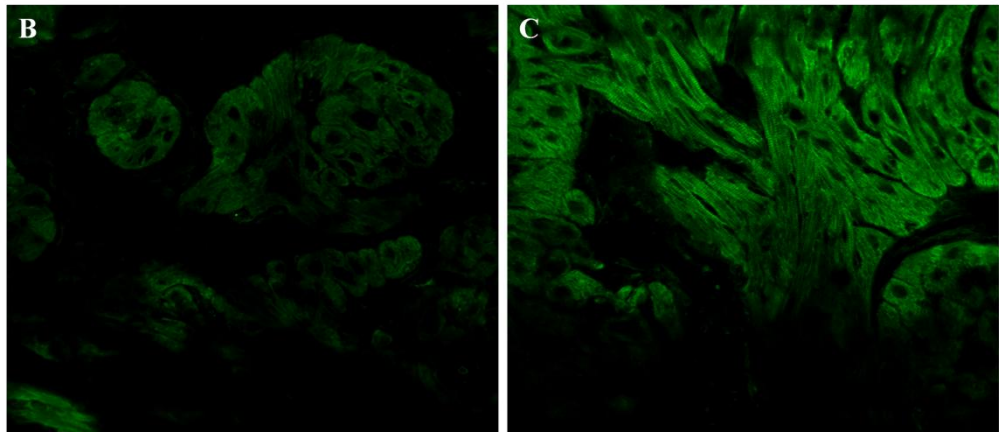


Fig 4.6: Expression of biomarkers for cardiac hypertrophy. mRNA expression of natriuretic peptides ANP and BNP (6A). RT-PCR amplification was normalized to that of glyceraldehyde-3-phosphate dehydrogenase (GAPDH). Data expressed as Mean+SEM. * $p<0.05$. Representative confocal photomicrographs demonstrating increased anti- α -SKA1 (green) immunoreactivity in GK LV (6C) relative to control (6B). Magnification X400. Quantitatively, α -SKA1 protein level (pixel intensity from immunofluorescence images) was consistently elevated in GK rats compared to controls (6D). Data expressed as Mean+SEM. * unpaired t test, $p<0.05$

6. Activation of Akt-p70S6K signaling in the prediabetic LV

To investigate hypertrophic signaling mechanisms possibly underlying myocyte hypertrophy in the prediabetic LV, this study focused on those pathways which are known targets of TGF β 1. A recent study has demonstrated that the capacity of HG to induce cellular hypertrophy *in vitro* is dependent upon MMP-dependent activation of TGF β 1 that regulates the activity of the akt-mTOR-p70S6K axis, a key cascade in protein synthesis upregulation (Wu and Derynck, 2009).

It was of particular relevance to test this theory, as all other determinants of this mechanism (i.e. HG, myocyte hypertrophy, increased circulating TGF β 1 and increased MMP expression in the LV) occurred simultaneously in this study. Thus, levels and activation (phosphorylation) of Akt (Ser473) and p70S6K (Thr389), a downstream marker of TOR activation were measured by immunoblot (Fig 4.7 A). The latter phosphorylation site is well-recognized to reflect actual mTOR activity (Wang *et al.*, 2005). Results indicate that there were significant increases in both Akt (Fig 4.7 D) and p70S6K phosphorylation (Fig 4.7 E) in GK relative to Wistar control hearts at 8 weeks (n=3/group). No differences in total Akt or total p70S6K were detectable within groups (Figs. 4.7 B, 4.7 C). Accordingly, ratio of normalised phosphorylated Akt:Total Akt and normalised phosphorylated p70S6K:total p70S6K were significantly increased in GK rats relative to age-matched controls (pAkt:Akt - 0.99 ± 0.02 vs 0.74 ± 0.06 , *t* test, $p<0.05$; pp70S6K:p70S6K - 1.33 ± 0.80 vs 0.98 ± 0.98 *t* test, $p<0.05$).

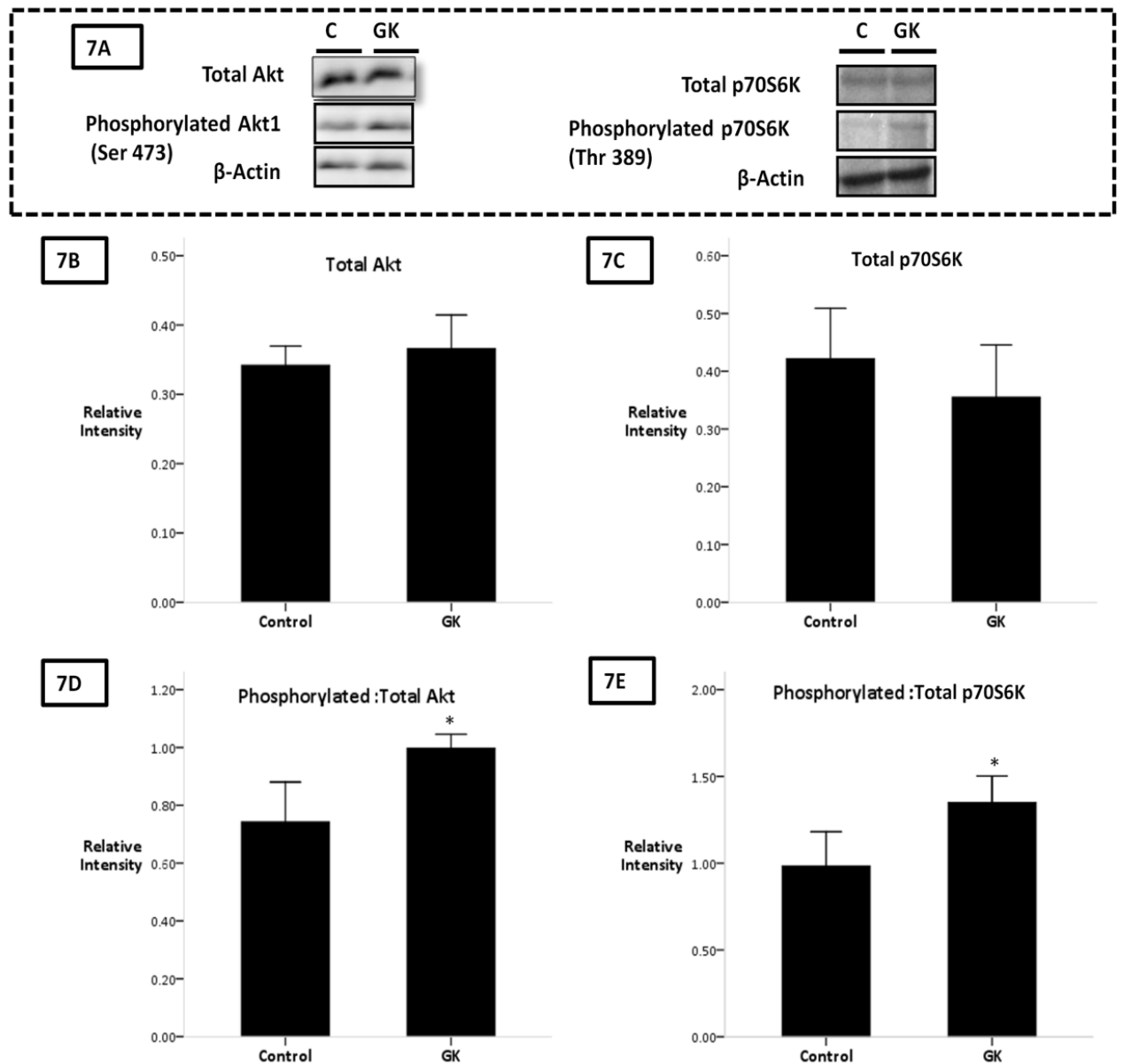


Figure 4.7: Activation of Akt-p70S6K signaling. Representative immunoblots of total LV protein extracts showed increased levels of phosphorylated Akt and phosphorylated p70S6K in GK hearts relative to controls (C in 7A). β -actin served as a loading control (7A). There were no significant differences in levels of total Akt (7C) or total p70S6K (7B) in either group. Quantitative densitometric analysis corrected for protein loading showed increased Akt phosphorylation normalized to total Akt in GK rats (7E) and p70S6K phosphorylation normalized to total p70S6K (7D). Values in graphs represent the average data obtained from 3 separate experiments from each group conducted in duplicate. Data expressed as Mean+SEM. * unpaired t test, $p < 0.05$

4.5 Discussion

In this study, the morphological and molecular consequences of prediabetes on the LV in the GK rat have been characterised. This is the first report of LV structural remodelling and underlying molecular events, in a state of IGT that precedes onset of T2DM in the GK rat. LV remodelling in the prediabetic GK rat presented with marked hypertrophy of cardiomyocytes and increased ECM deposition that altogether translated into increased heart size in the absence of ultrastructural changes, fibre disarray or wall thickening. Molecular derangements in this model of prediabetes included recapitulation of foetal gene phenotype markers BNP and α SKA, activation of the pro-hypertrophic Akt-p70S6K pathway and altered gene expression profile of key components (Col1, Fn) and modulators (MMP2, CTGF, MMP9) of the ECM. Finally, these changes were correlated with parallel findings of increased TGF β 1 transcription in the LV and elevated circulating active TGF β 1. Taken together, these findings are significant in that they demonstrate a possible role for the dysglycemia of IGT in the pathophysiology of developing cardiac complications via early effects on ventricle structural remodelling. This concept finds resonance in recent clinical reports of concentric remodelling and LVH in IGT (Fujita *et al.*, 2007; Schainberg *et al.*, 2010).

The GK rat as a model of prediabetes:

To the best of current knowledge, this is the first study to establish the utility of the adult GK rat as a model of prediabetes. For the duration of the experimental period, GK rats consistently demonstrated mild basal HG and IGT. Moreover, in the literature (and in previous experience), GK rats are described as non-obese, normotensive and normolipidemic (Gupte *et al.*, 2010) providing the valuable advantage of examining the effects of mild HG *per se* on development of cardiac hypertrophy and remodelling in the absence of the confounding effects of obesity/ hypertension that tend to cluster with glucose abnormalities in a clinical setting.

TGF β 1 in cardiac pathology

It is becoming increasingly apparent that TGF β 1 represents a key mediator of cardiac adaptation to a dysmetabolic environment and/or hemodynamic overload. An established effector of the detrimental outcomes of experimental and clinical HG,

TGF β 1 activation also has consistent implications in diabetic cardiomyopathy, MI, hypertension and HF pathogenesis accountable in the most part due to direct and potent actions in myocyte hypertrophy and matrix metabolism (Matsumoto-Ida *et al.*, 2006; Wu and Derynck, 2009)). Pharmaceutical intervention to antagonize the effects of TGF β 1 is therefore an important therapeutic target in heart disease. In this regard, it is notable that the *in vivo* inhibition of TGF β by Tranilast administration reverses myocyte hypertrophy and fibrotic deposition of DCM (Kelly *et al.*, 2007)

In this study, an overall increase in TGF β 1 activity in the LV of prediabetic GK rats was manifested by increased active TGF β 1 and upregulated *TGF β 1* gene expression in the LV, consistent with previous studies describing elevated *TGF β 1* at translational and protein levels, also correlated therein with hypertrophic growth, fibrosis and recapitulation of foetal cardiac genes (Schultz *et al.*, 2002). Increased circulating active TGF β 1 reported in this study is also particularly relevant considering the use of TGF β 1 as a risk stratification tool for myocardial fibrosis in HF pathogenesis post MI has been recently advocated (Sovari *et al.*, 2010). However, the correlation between events within the myocardium and markers in the circulation requires further clarification before the prognostic value of a snapshot measurement of TGF β 1 can be determined.

TGF β 1 in Fibrotic Remodelling:

In this work, exaggerated LV deposition of collagenous matrix that characterised the fibrotic process in GK rats was concomitant with the upregulation of Coll α , Fn and CTGF transcription. These results are comparable to previous observations of the ECM in prediabetes preceding onset of the metabolic syndrome (Yagi *et al.*, 1997) and T2DM (Kaminski *et al.*, 2009). Several lines of evidence suggest that an elevated LV TGF β 1 may underlie these findings; *In vitro* and gene transfer studies have demonstrated that TGF β 1 can stimulate myocardial fibrosis by increasing abundance of Coll α mRNA through intermediate Smad protein signalling (Verrecchia and Mauvel, 2007). Conversely, inhibition of myocardial fibrosis was observed on antagonism of TGF β 1 gene expression *In vivo*, providing further proof that increases in matrix protein production may indeed be mediated by TGF β 1 modulated gene expression (Lijnen *et al.*, 2000). Additionally, both *in vitro* and *in vivo* work demonstrates the ability of TGF β 1 to induce increased matrix production in fibroblasts. TGF β 1 activation may exert this pro-fibrotic influence by mediating C-TGF activation, considered a critical downstream mediator of fibroblast activation and proliferation (Leask, 2010).

TGF β 1 also exerts transcriptional control over endogenous collagenases of the LV including collagenase 1 and is intimately involved in MMP-2 and 9 activities although the latter associations appear to be reciprocal and are currently unclear (Van Linthout *et al.*, 2008; Wu and Derynck, 2009). Paradoxical findings of increased metalloproteinase(s) (i.e. MMP2, MMP9) transcription and MMP substrate, collagen, in this work maybe a direct reflection of a complex metabolic profile in the hyperglycaemic milieu. Upregulation of MMP2 has been previously reported in ischemic and dilated cardiomyopathies (Seeland *et al.*, 2002; 2009). Justification of this phenomenon is based on the premise that total matrix collagen content is a function of synthesis and degradation, and degraded products of matrix proteins may in turn stimulate collagen synthesis and deposition of poorly structured fibrotic tissue in the myocardium (Li *et al.*, 2000).

Altogether, current data are in agreement with a model wherein TGF β 1 activity is a major regulator of fibrosis in the myocardium. This postulation is confirmed and extended to a prediabetic setting wherein it appears that even the mild HG of IGT is capable of stimulating a pro-fibrotic phenotype in the LV possibly through increased TGF β 1 expression and activity which in turn could affect gene expression of ECM components and also ECM production by fibroblasts, the latter very likely through C-TGF activation.

TGF β 1 in hypertrophic remodelling:

Topical evidence from *in vitro* and transgenic studies suggests a pivotal role for TGF β 1 in mediating the association between hypertrophy and HG (Gorksha-Hicks and Rathmell, 2009; Wu and Derynck, 2009). In particular, a recent *in vitro* study demonstrated that hypertrophy in HG could be blocked by inhibiting TGF β 1 receptor signalling. Furthermore, HG strongly enhanced metalloproteinase2-and 9 mediated TGF β 1 activation which in turn activated the Akt-TOR-p70S6K pathway. Finally, HG-induced cell hypertrophy was inhibited by preventing MMP-2/9 activation or TGF induced Akt downstream signalling (Wu and Derynck, 2009). This study now reports that the genetically defined GK model faithfully recapitulates several features of this paradigm in the prediabetic stage, wherein increased TGF β 1 activity was coincident with myocyte hypertrophy, increased MMP2 & 9 gene expression and activation of Akt-p70S6K signalling in the LV. In such a perspective, it is possible to speculate that the mild HG of prediabetes can induce myocyte hypertrophy by the activation of TGF β 1

via increased MMP activity which in turn activates the Akt-mTOR-S6k pathway- a key regulator of protein synthesis (Manning and Cantley, 2007).

Undeniably, some considerations limit the literal interpretation of this theory- First, at present, it is not possible to exclude the possibility that TGF β 1 mediates parallel or proximal events that may govern the hypertrophic response of the LV in prediabetes. Second, the mitogenic actions of hyperinsulinemia also merit consideration as insulin stimulation is a known activator of Akt-p70S6K signalling. While this study did not evaluate incidence of hyperinsulinemia (HI), its contribution to Akt-p70S6K activation is possibly minimal given that insulin signaling through the PI3K α /Akt-1 pathway, upstream of mTOR and p70S6K is impaired in HI (Poornima and Parikh, 2006).

In this study, IGT was sufficient stimulus for the induction of a foetal gene program, i.e. upregulation of BNP mRNA and cellular α SKA – both features typically seen in TGF β 1 over-expression (Parker *et al.*, 1990) and also in pathological hypertrophy arising from hypertension or DM (Matsumoto-Ida *et al.*, 2006). The prevailing view is that recapitulation of foetal gene phenotype in HG reflects a compensatory adaptation of the stressed heart in response to altered metabolic flux to maintain the economy of muscular contraction (Taegtmeyer *et al.*, 2010). Differential expression of BNP and ANP, i.e. no change in ANP message levels observed in this work is comparable to previous studies of DCM (Fredersdorf *et al.*, 2004) as well as decompensated experimental HF (Langnickel *et al.*, 2000). Upregulation of BNP mRNA is regarded as a sensitive marker of hypertrophy, left ventricular dysfunction and is an approved marker for the detection of acutely decompensated HF (Lukowicz *et al.*, 2005). The significance of increased natriuretic peptide transcription is currently unclear in the clinical context. A recent study has shown a long-term, dose-dependent benefit of BNP administration in reversing cardiac hypertrophy *in vivo* with simultaneous TGF β 1 downregulation and disrupted downstream signalling (He *et al.*, 2010). An increased LV cellular α SKA is a phenomenon that has not been previously described in the prediabetic rodent. Upregulated α SKA is a prominent feature of the foetal gene phenotype and represents a well-accepted marker of myocyte hypertrophy. It has been postulated that the increased α SKA during hypertrophy reflects a temporary requirement for large quantities of striated muscle actin when muscle volume is increasing rapidly (Clement *et al.*, 1999).

Concluding remarks and clinical perspectives

Simultaneous myocyte hypertrophy and fibrosis proliferation usually represent the morphological correlate of LV functional insufficiency. Moreover, reactivation of the foetal cardiac gene programme is also considered a hallmark for progressive decline in cardiac function and poor prognosis (Stilli *et al.*, 2006). Nonetheless, data presented here do not allow us to conclude that hypertrophy, matrix deposition, altered signal transduction and gene expression are events in the development or progression of altered ventricle function in a dysglycemic milieu, warranting further functional assessments of the LV and an extended time-course study in the GK rat.

In summary, this work highlights the possibility that ventricular decompensation frequently reported in HF of diabetic origin may be linked to an early remodelling of cardiac parenchyma triggered by the cardiotoxic effects of moderate, early changes in glucose metabolism and presents the likelihood of TGF β 1 involvement in this process. From a clinical standpoint, the findings presented in this work are corroborated by emerging current recommendations encouraging a stringent degree of glycemic control to compensate for the low threshold of glucose perturbation that apparently engenders the onset of cardiac consequences (Nielsen and Lange, 2005; Bergman, 2010; Schainberg *et al.*, 2010). Finally, it is estimated that patients may be exposed to a decade of mild-moderate HG before a diagnosis of overt DM is made (Schainberg *et al.*, 2010). The potential pathological implications of the preceding provide considerable incentive for further experimental delineation of the singular role of early dysglycemia in promoting the adverse myocardial sequelae of T2DM.

CHAPTER 5

CHRONIC EFFECTS OF MILD HYPERGLYCEMIA ON LEFT VENTRICLE TRANSCRIPTIONAL PROFILE AND STRUCTURAL REMODELLING IN THE SPONTANEOUSLY DIABETIC GOTO-KAKIZAKI RAT

5.1 Abstract

Background: HF in chronic T2DM may be partly due to adverse structural remodelling of the LV but the contribution of HG *per se* in this process is controversial.

Methods: In this study, the LV from 18 month old, mildly diabetic, male GK rats and age-matched male Wistar controls was analysed with respect to remodelling processes and cognate transcriptional profile.

Results: Chronic mild T2DM produced LV hypertrophy in GK rats, underscored by increased myocyte size, expression of natriuretic peptides and Akt phosphorylation. In the absence of caspase-3 mediated apoptosis, fibrosis proliferation in the GK LV paralleled increased transcriptional and biologically active pro-fibrogenic TGF β 1 in the LV with upregulated mRNA abundance for key ECM components such as fibronectin, collagen type(s) 1 and 3 α and regulators including MMP 2 and 9, and TIMP4, Cx43 and integrin α 5. GK rats also presented with altered mRNA expression for cardiac SERCA2a, Na⁺/Ca²⁺ exchanger and the L-type Ca²⁺ channels which may contribute to the altered Ca²⁺ transient kinetics previously observed in this model at 18 months of age (*t* test, *p*<0.05 vs. age-matched Wistar control for all parameters).

Conclusions: The results indicate that chronic mild HG can produce a hypertrophic myopathy that recapitulates several aspects of the failing heart. Diffuse fibrotic deposition in this model is possibly a product of HG-induced TGF β 1 upregulation and altered transcriptional profile of the ECM.

5.2 Introduction

The aging diabetic patient is a potential case of CHF, (Verny, 2007; Jugdutt 2010) due in part to a decompensated myopathy characterised principally by progressive structural remodelling of the LV. As chronic HG may drive adverse tissue remodelling by inducing cardiotoxic effects, routine treatment for T2DM often targets tight glycemic control to delay and/or allay cardiac complications including DCM. However, in spite of robust epidemiological links substantiating the correlation between T2DM, advancing age and HF (Verny, 2007; Jugdutt 2010), the contribution of a *milieu* dominated by HG *per se* in HF pathogenesis is questionable for several reasons. Cardiac involvement in the elderly diabetic is usually multifactorial, frequently arising from co-morbid conditions including hypertension, obesity, ischemic events etc. Further ambiguity on the effect of HG proper on myocardial complications arises from incongruent epidemiological findings. While early data have suggested a protective effect of improved glucose control on cardiovascular-related mortality (UKPDS group, 1998) recent trials have reported no effect (Duckworth *et al.*, 2009) or increased risk (ACCORD study group, 2008) with intensive glucose control on major cardiovascular events. Finally, much of what is known of a DCM comes from experimental work utilizing models rendered diabetic with STZ/alloxan. Interpretations of studies employing this phenotype are rarely tempered by the fact that the degree of HG is very often supra-physiological, rarely encountered in clinical practice and that the diabetogen itself may exert direct cardiotoxic effects (Wold and Ren, 2004).

Of the several proposed mechanisms whereby HG may induce LV remodelling, the activity of pro-fibrotic and pro-hypertrophic cytokine TGF β 1 in the pathogenesis of cardiac complications has been the subject of much recent inquiry. The ability of TGF β 1 to induce an adverse remodelling in the LV appears to stem from (but not limited to) a capacity to provoke a pro-fibrotic programme in the heart. This in turn negatively affects the transcriptional profile of the ECM and key mediators of intracellular calcium [Ca²⁺]_i (Ramos-Mondragon *et al.*, 2008), which regulate expression of foetal genes (Kapoun *et al.*, 2004), including natriuretic peptide expression (Parker *et al.*, 1990) and also provoke pro-hypertrophic signalling via the akt-mTOR-p70S6K axis (Wu and Derynck, 2009). However, sufficient information on

these events in the long-term diabetic myocardium, uncomplicated by associated features of the metabolic syndrome is not available.

In such a perspective, the effects of chronic mild HG that represents an important and predictable metabolic derangement of this disease on ventricle structure are unknown. The non-obese, spontaneously diabetic GK rat is ideally suited to address this issue as it represents an aetiology dominated by mild HG. Much akin to the typical clinical presentation of T2DM, disease pathogenesis in this model includes a reduced β cell mass, hepatic and peripheral insulin resistance altogether culminating in mild basal HG, marked glucose intolerance that deteriorates over time to frank T2DM (Howarth *et al.*, 2007) Accordingly, this work examined fibrotic, hypertrophic and apoptotic events in the long-term GK myocardium to test the hypothesis that a modest elevation in HG is sufficient stimulus for the sustenance of geometric, cellular and molecular remodelling in the heart.

5.3 Methods

As described in chapter 3.

5.4 Results

1. General Characteristics of the Diabetic GK rat:

At 18 months, measurement of fasting blood glucose indicated that GK rats were mildly hyperglycaemic compared to Wistar control rats (Table 5.1). Glucose clearance capacity was significantly affected in diabetic GK animals as blood glucose levels following glucose tolerance tests were higher at all time points measured ($p < 0.01$) and did not return to baseline level within 3 hours (Fig 5.1). Mean plasma insulin levels were not assessed in this study, glycemic status in GK animals being consistent with impaired secretion of insulin and peripheral insulin resistance previously reported in this model (Portha *et al.*, 1991). GK rats presented with lower BW compared to controls but significantly higher but HW/BW ratio (Table 5.2). No obvious differences in subcutaneous fat distribution were evident between groups, nor were there any indications of overt congestive heart failure such as hepatomegaly, pleural effusion, or ascites on gross examination. Incidence of hypertension was not evaluated as previous studies have demonstrated that GK rats are normotensive and have slightly reduced resting heart rates at 18 months of age (Howarth *et al.*, 2007). No overt differences in the distribution of epicardial fat were noted.

Table 5.1 General Characteristics of GK and age-matched Wistar control rats at 18 months. Values are expressed as Mean±SEM. * unpaired *t* Test $p < 0.05$ versus age-matched control.

Animals	BW (g)	HW (g)	HW/BW ratio g/100g BW	Fasting blood glucose (mg/dL)
Control (<i>n</i> =8)	418±6.07	1.22±0.2	0.21±0.01	95±0.30
GK (<i>n</i> =8)	413±3.36	1.41±0.16*	1.41±0.16*	131±0.22*

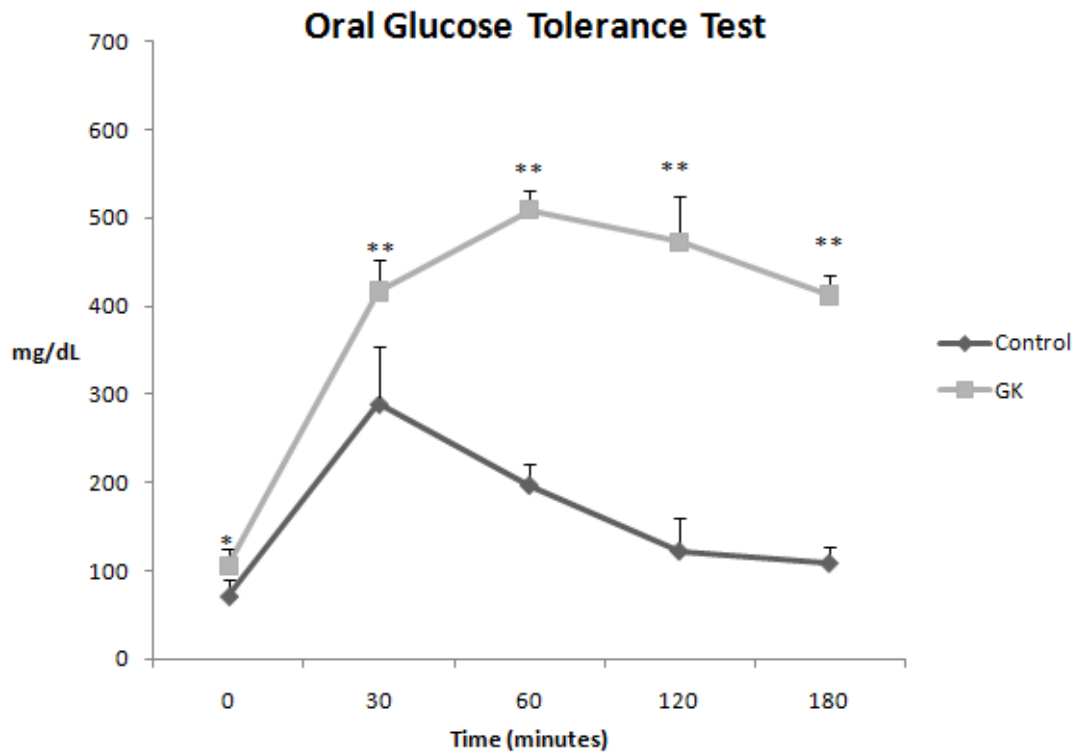


Fig 5.1: Oral glucose tolerance test. Impaired glucose tolerance in GK rats following intraperitoneal glucose challenge compared to age matched wistar controls at 18 months ($n=8$ /group). Data expressed as Mean+SEM. **unpaired *t* test, $p < 0.01$ for GK compared to Wistar controls.

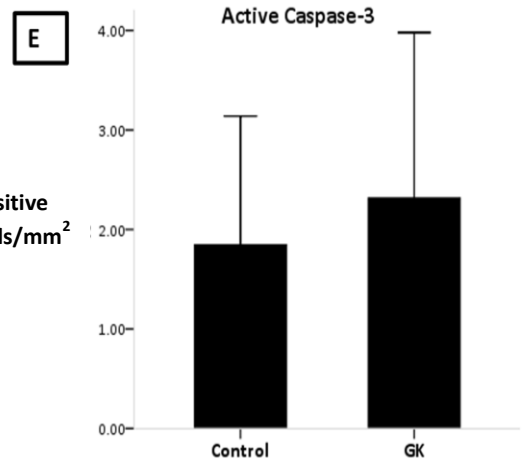
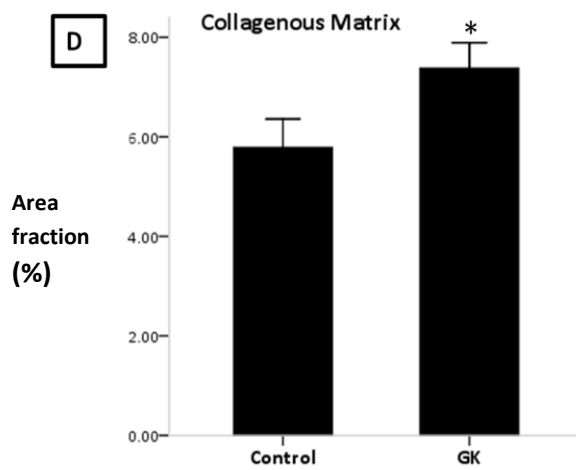
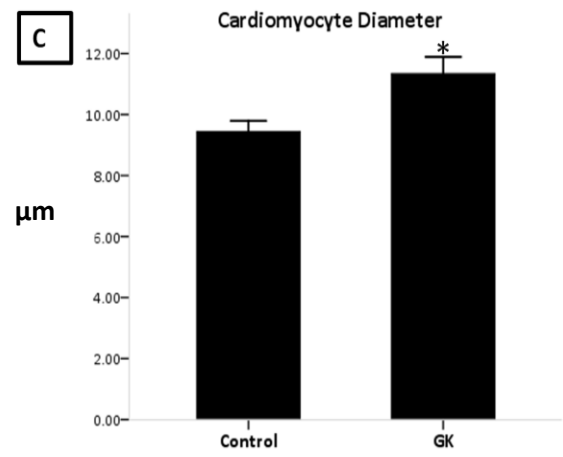
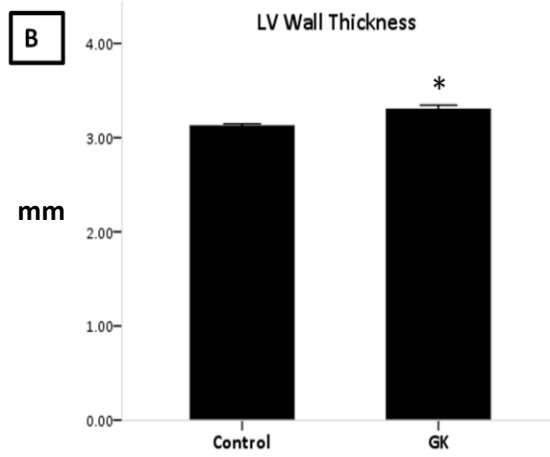
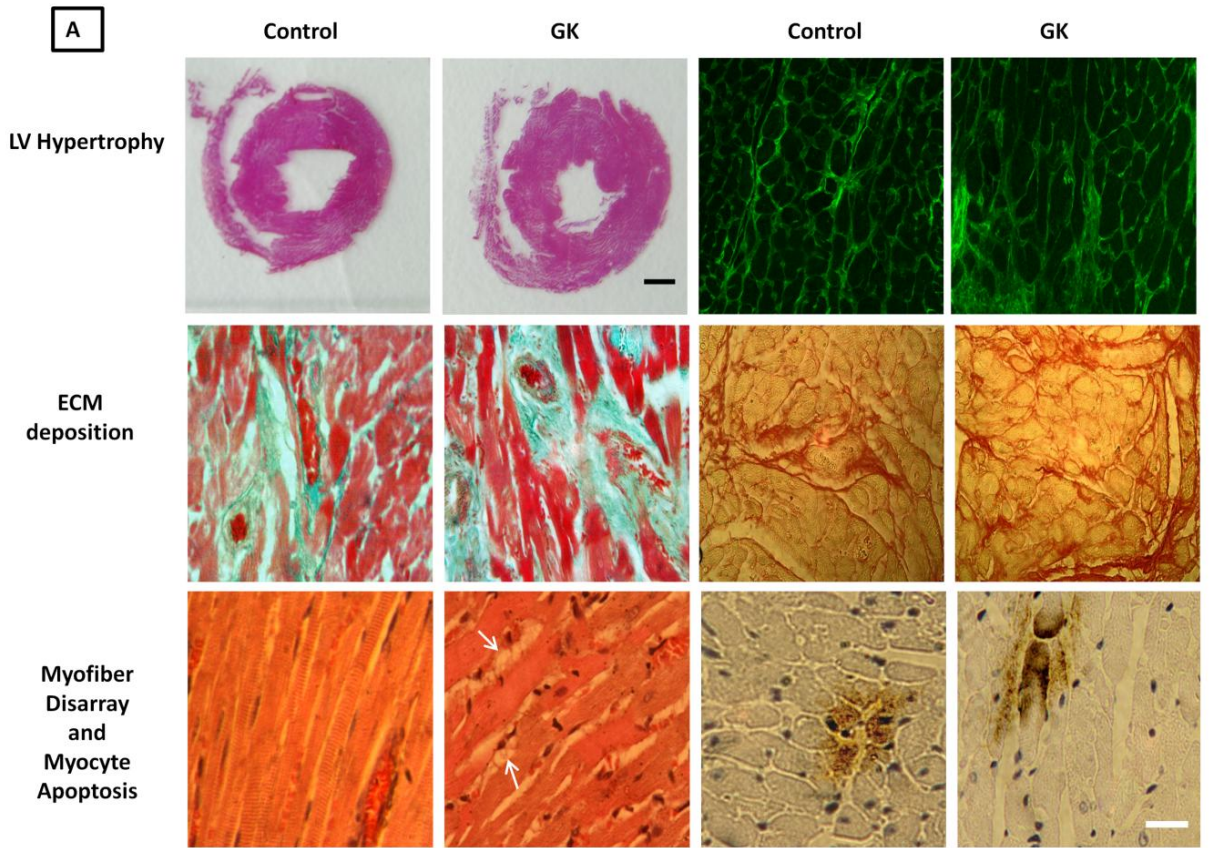
2. **Histopathology of the LV:** Chronic diabetes affected the weight and gross appearance of the LV. The analysis of surfaces of ventricular cross-sections with Image J demonstrated significantly increased wall thickness in diabetic animals relative to control (Fig 5.2 A, top left panels). LV wall thickness was 3.08 ± 2.39 mm in control vs.

3.35±0.17 mm in GK rats, $p<0.05$ (Fig 5.2 B). Masson's trichrome, Sirius red, Lectin and H/E staining were used to examine LV morphological changes. At the cellular level, LV wall thickness translated into increased cardiomyocyte diameter in GK rats (Fig 5.2 A, top right panels). Morphometric analysis of Lectin stained sections revealed a 20.25 % increase in myocyte diameter in GK rats (11.34±0.54 μm) compared to age-matched controls (9.43±0.35 μm) (Fig 5.2 C, $p<0.05$). Quantitatively, GK rats presented an increased ECM deposition in interstitial spaces, as stained by Sirius red (red-staining) and Masson's trichrome (green-staining) compared to controls (Fig 5.2 A, middle panels) and evaluated on Sirius red sections (5.87±0.54 % in control vs. 7.38±0.50 % in GK LV, Fig 5.2 D, $p<0.05$).

Overall, the myocardium from control animals showed normal structure (Fig 5.2 A, lower left panel). In addition to diffuse accumulation of fibrotic material and hypertrophic cardiomyocytes, myofibre disarray was also occasionally evident in GK rats (Fig 5.2 A, lower left panel). The effects of DM upon myofibre disarray were difficult to assess as it was largely non-uniform and frequently shared the same microscopic section with regions showing preserved architecture, (albeit with increased fibrosis). On H&E stained sections from GK rats, signs of impending cell death, marked by spongy and vacuolated cytoplasm, (arrows, Fig 5.2 A, lower left panel) were occasionally apparent. Therefore, this study investigated whether fibrosis proliferation and myocyte hypertrophy were related to HG-induced cell death by caspase-3 dependent mechanisms. Highlighted by cleaved (active) caspase-3 staining (Fig 5.2 A, lower right panels), long-standing mild DM produced small changes in apoptotic cell death in GK vs. control animals but incidence of apoptotic cardiomyocytes was low in both groups and the relation did not reach statistical significance. (1.84±1.29 in control LV vs. 2.31±1.66 positive myocytes/ mm^2 in GK LV, Fig 5.2 E, $p>0.05$)

Fig 5.2: Structural remodelling of the Left Ventricle

Representative ventricular cross-sections from control and GK rats (A, top left panels) and graph illustrating quantitatively increased wall thickness in GK rats *vs.* control (B). Scale bar indicates 3 mm. At the cellular level, FITC-conjugated Lectin staining demonstrated increased cell diameter in GK rats *vs.* control (A, top right panels), and graphically represented in (C). Representative photomicrographs demonstrating increased collagenous matrix deposition on Masson's trichrome (green) and Picrosirius red (red) stained sections in GK rats relative to age-matched controls (A, middle panels). Quantitative analysis of collagen deposits calculated from Sirius red stained sections after allowing specific separation of collagen fibres (red) against background (yellow) indicates significant elevation of cardiac collagen deposits in GK *vs.* control mice (D). At 18 months of age, control Wistar rats showed relatively normal myocardial architecture with preserved cross striation patterns (lower left panel), whereas GK rats occasionally presented with a disordered and irregular pattern of myofibrillar arrangement (A, lower left panel, arrow). Caspase-3 immunohistochemistry (brown staining) in the left ventricle of control and GK rats (A, lower right panels). Sections are counterstained with Haematoxylin (blue). Original magnification X400. Quantitatively, cleaved caspase-3 activity was unchanged in GK relative to age-matched Wistar control animals (E). Data in graphs expressed as Mean+SEM. * unpaired t test, $p < 0.05$; unless otherwise indicated, scale bar in panels indicate 20 μm and accounts for all photomicrographs. $n=4-5$ rats/group



3. Molecular events underlying structural remodelling

a. TGF β 1 levels and gene expression

Increasing evidence indicates that TGF β 1 induction by HG stimulates and sustains pro-hypertrophic and pro-fibrotic mechanisms in the heart. As such plasma and LV samples from GK and control rats were used to evaluate differences in total and biologically active TGF β 1 protein levels by ELISA and TGF β 1 gene expression in the LV by qRT-PCR (Fig 5.3). Long standing DM produced a significant increase in mRNA abundance of TGF β 1 (0.97 ± 0.14 in control *vs.* 1.92 ± 0.17 in GK LV, ratio units, Fig 5.3 D, $p<0.01$) in the LV of diabetic rats and this change paralleled an increased bioactive TGF β 1 protein level in the LV (5.4 ± 0.74 and 2.12 ± 0.54 pg/mg Total TGF β 1 protein, respectively, *vs.* control, Fig 5.3 C, $p<0.05$) although total LV TGF β 1 protein levels remained comparable (Fig 5.3 B, $p>0.05$). No changes in the ratio of active: total TGF β 1 levels were observed in GK plasma relative to control (0.46 ± 0.11 in control and 0.63 ± 0.17 in GK, ratio units, Fig 5.3 A, $p>0.05$)

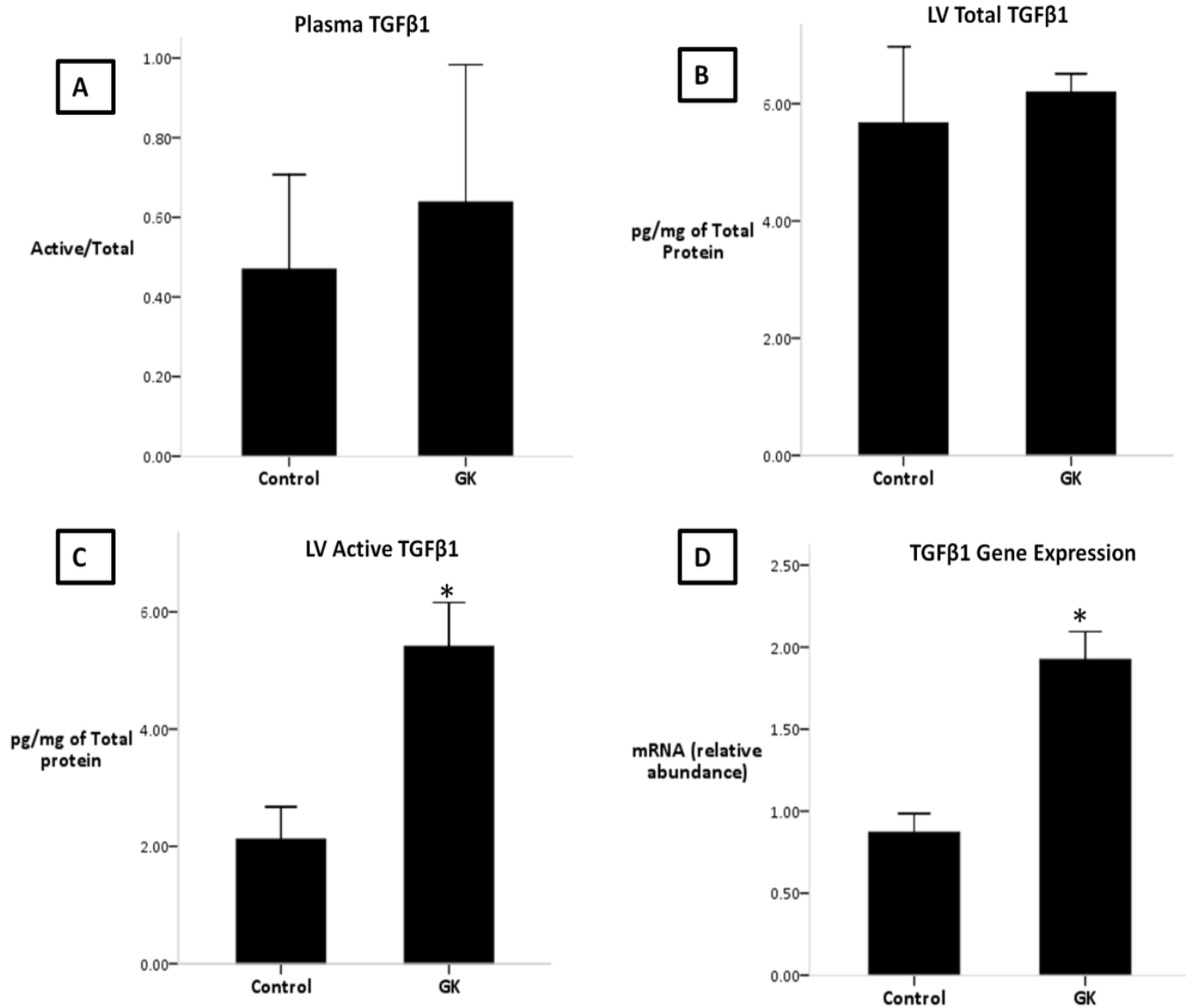


Fig 5.3: TGFβ1 protein level and gene expression

Summarised data from ELISA showing unchanged ratio of active: total TGFβ1 protein (A) and total TGFβ1: total extracted LV protein (B) in plasma of GK vs. control animals and increased active TGFβ1: Total extracted protein (C) in the LV of GK vs. control animals ($n=3/\text{group}$). mRNA expression of TGFβ1 (D). qRT-PCR amplification was normalized to that of glyceraldehyde-3-phosphate dehydrogenase (GAPDH) ($n=8/\text{group}$). The results of both ELISA and qRT-PCR are representative of 3 individual experiments conducted in triplicate. Data expressed as Mean+SEM. * unpaired t test, $p<0.05$.

b. Altered LV Gene Expression Profile in the Long-term diabetic GK**Transcriptional profile of the ECM**

A putative mechanism whereby HG (and TGF β 1) can induce a pro-fibrotic programme in the LV is via transcriptional regulation of key components of the ECM. Investigation of this effect in the long term diabetic GK LV by qRT-PCR demonstrated that increased ECM deposition and TGF β 1 were concurrent with transcriptional upregulation of Collagen type 1 α (Col1 α), collagen type 3 α (Col3 α) and fibronectin (Fn) expression (Col1 α : 0.66 \pm 0.99 in control vs. 1.37 \pm 0.17 in GK LV, Col3 α : 0.67 \pm 0.11 in control vs. 1.22 \pm 0.16 in GK LV, Fn: 0.68 \pm 0.12 vs. 1.36 \pm 0.091, Ratio units, Fig 5.4 A, p <0.05) but unaffected Elastin mRNA abundance relative to control (0.64 \pm 0.56 in control and 0.82 \pm 0.15 in GK LV, ratio units, Fig 5.4 A, p >0.05). Moreover, these changes were accompanied by distinct alterations in transcriptional activity of the regulators of the ECM. Notably, message levels for CTGF, the key downstream effector of TGF β 1 on fibroblast activity was significantly increased in the GK myocardium (1.55 \pm 0.19 in GK LV compared to 0.61 \pm 0.12 in control LV, ratio units, Fig 5.4 B, p <0.01). Diabetic animals also presented with increases in mRNA abundance of the MMP2 and 9 that catalyze ECM degradation (MMP2: 0.60 \pm 0.07 in control vs. 0.98 \pm 0.094 in GK; MMP9: 1.20 \pm 0.11 in GK LV vs. 0.68 \pm 0.09 in Control, Fig 5.4 B, p <0.05). Interestingly, mRNA abundance of endogenous MMP inhibitor, TIMP4 was also upregulated in the diabetic heart (GK: 1.46 \pm 0.14 vs. 0.68 \pm 0.08 in control, ratio units, Fig 5.4 B, p <0.05) whereas TIMP1 levels were unaffected by the disease (1.27 \pm 0.12 in control vs. 1.45 \pm 0.22 in GK LV, ratio units, p >0.05). A significant increase in message levels for gap in junctional protein Cx43 was also evident in diabetic rats (1.93 \pm 0.23 vs. 1.29 \pm 0.56, Fig 5.4 B, p <0.05). Cx43 is the dominant connexin in ventricular myocytes and activity and maintenance of the ECM in the ventricle are functionally coupled to its expression levels (Zhang *et al.*, 2008). Message levels for the integrins, a family of cell surface receptors known to attach cells to the ECM and involved in fibrotic protein deposition and proliferation were also altered by chronic mild HG (Hescheler and Fleischmann 2000). The α 1 and β 1 integrin heterodimers bind myocardial collagen to cardiomyocytes whereas α 5 binds fibronectin. Integin α 5 mRNA was upregulated in diabetic rats (1.38 \pm 0.10 vs. 0.64 \pm 0.08 in controls, Fig 5.4 B, p <0.05), whereas levels of

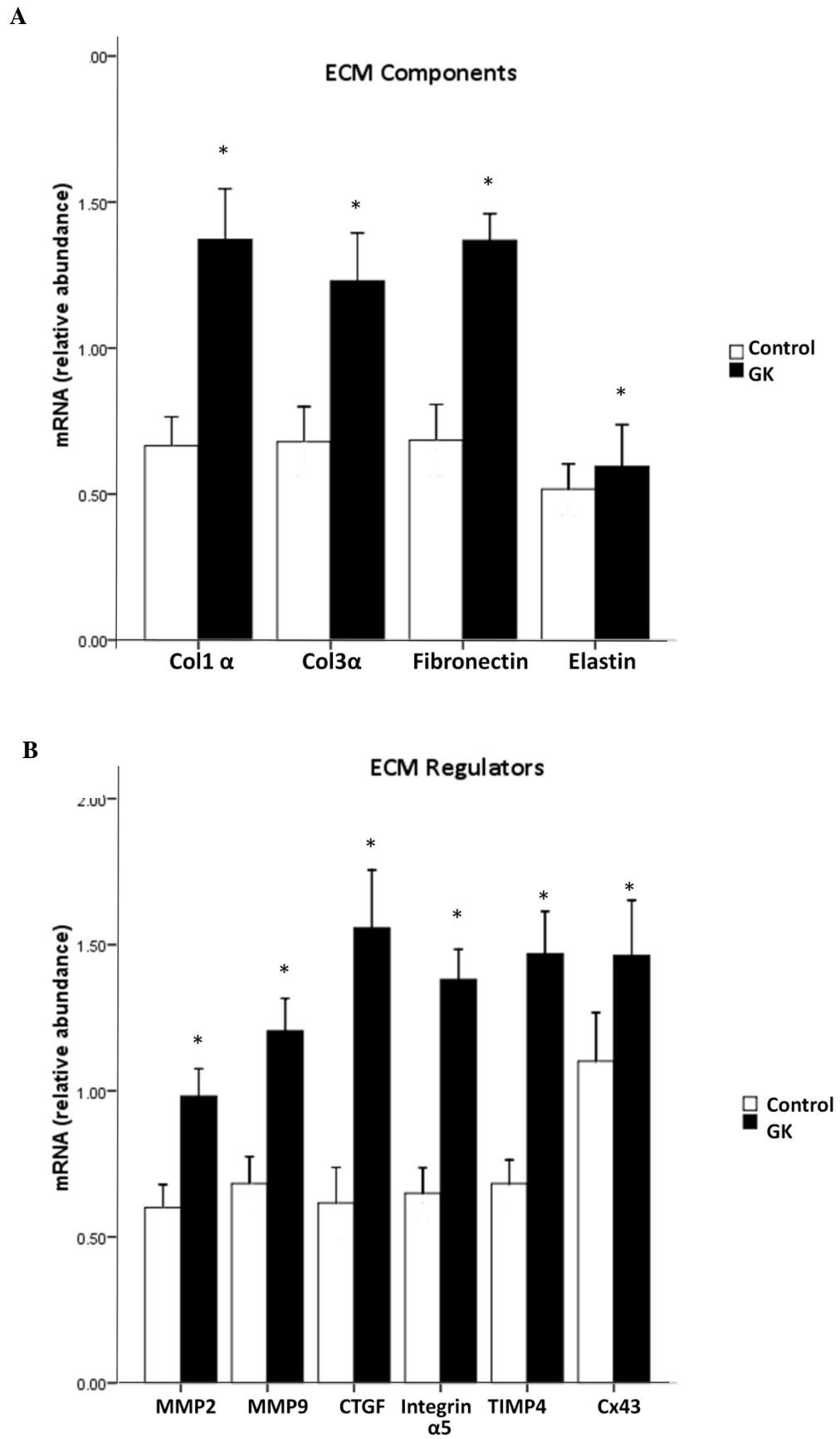
integrins $\alpha 1$ and $\beta 1$ remained unaffected ($p > 0.05$). Taken together, long term mild HG appeared to stimulate a complex gene expression profile in the ECM where alterations in message levels for secondary regulators (Integrin $\alpha 5$, Cx43), were concomitant with increased ECM components (Col1 α , Col3 α , Fn) and paralleled by increased transcription of ECM breakdown agents (MMP2 and MMP9) and their inhibitors (TIMP4) likely representing compensatory mechanisms in the LV. Finally, mRNA expression levels of pro-inflammatory marker tumour necrosis factor α and vimentin (a marker for fibroblasts), were also assessed but no significant differences were detectable in GK rats vs. controls ($p > 0.05$).

Recapitulation of a foetal gene phenotype

Gene expression of natriuretic peptides ANP and BNP, key indicators of hypertrophy and quantitative biomarkers for heart failure, was measured in GK and control LV (Fig 5.4 C). mRNA levels of ANP rose significantly in GK animals (10.15 ± 3.70 ratio units) compared to control (1.47 ± 0.28 ratio units, $p < 0.05$). BNP that has been shown to be independent risk marker for diastolic dysfunction and CHF in diabetic patients (Gaede *et al.*, 2005) was also significantly upregulated relative to controls (0.70 ± 0.07 vs. 1.23 ± 0.16 , ratio units, $p < 0.05$).

Gene expression of $[Ca^{2+}]_i$ mediators

Myocyte remodelling and contractility are known to be intimately interrelated and impaired Ca^{2+} handling is implicated as a fundamental mechanism for myocardial dysfunction, following pathological hypertrophy (Houser *et al.*, 2000). As these changes encoding key mediators of $[Ca^{2+}]_i$ i.e. sarcoplasmic reticulum Ca^{2+} ATPase (SERCA2a), phospholamban (Pln), ryanodine receptor (RyR2), Na^+/Ca^{2+} exchanger (NCX), and voltage-gated L-type calcium channels $Ca_v1.2$ and $Ca_v1.3$ were investigated. At 18 months of age, abundance of SERCA2a mRNA was significantly increased in GK hearts (0.99 ± 0.07 vs. 0.68 ± 0.10 , ratio units, Fig 5.4 D, $p > 0.05$). As is usually expected of a hypertrophic phenotype, NCX transcription was upregulated (1.77 ± 0.10 vs. 1.15 ± 0.11) as were genes encoding L-type calcium channels $Ca_v1.2$ (1.50 ± 0.16 vs. 0.90 ± 0.11 , Fig 5.4 D, $p < 0.05$), $Ca_v1.3$ (1.11 ± 0.19 vs. 2.40 ± 0.51) and finally, expression levels of Pln (1.50 ± 0.18 vs. 1.64 ± 0.16 in GK, Fig 5.4 D, $p > 0.05$) and RyR2 (1.61 ± 0.24 in control vs. 2.06 ± 0.06 in GK, Fig 5.4 D, $p > 0.05$) were unaffected by the disease



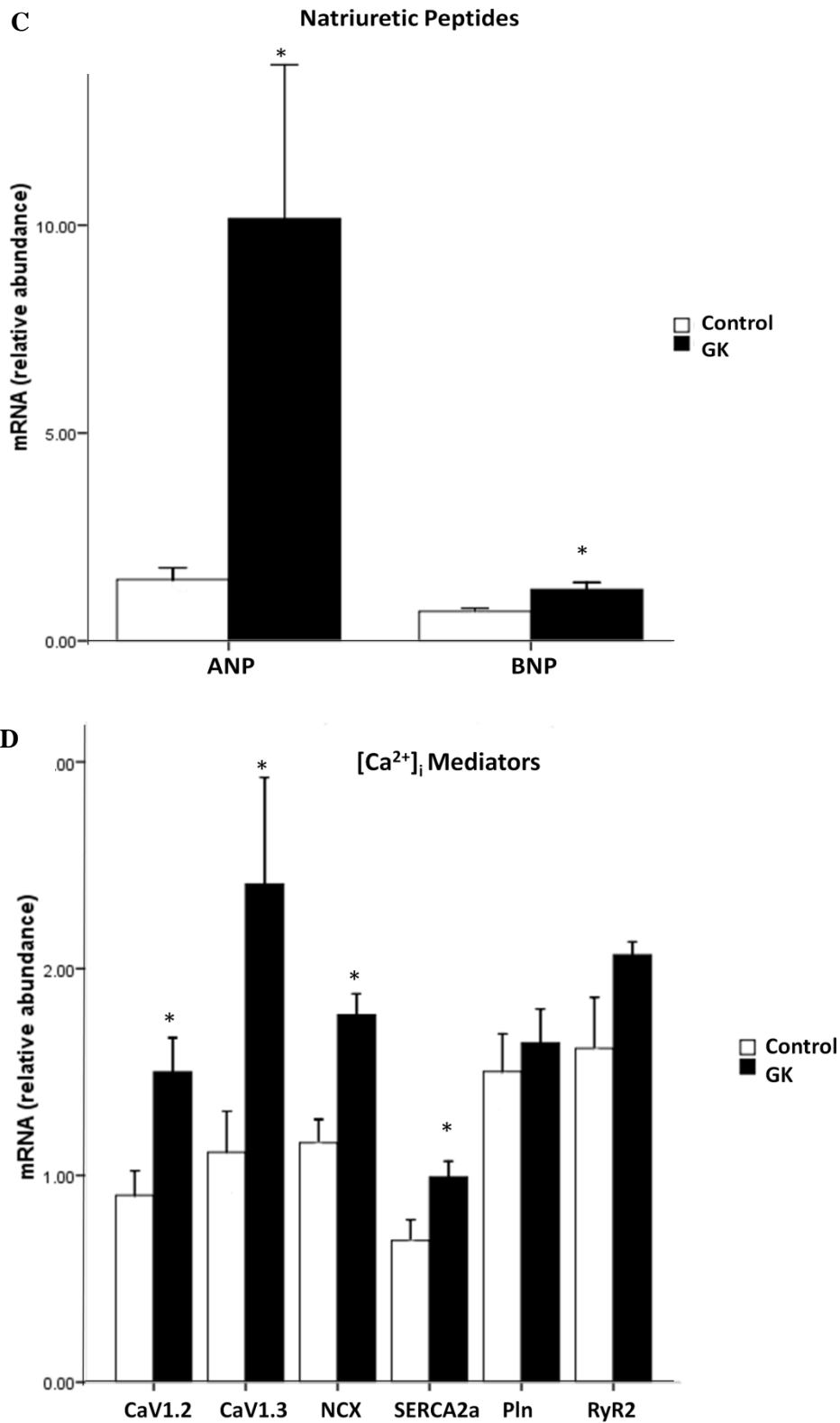


Fig 5.4: Transcriptional profile of the Left ventricle in chronic mild T2DM. Relative abundance of mRNA for various components (A) and regulators (B) of the interstitium, natriuretic peptides ANP and BNP (C) and mediators of $[Ca^{2+}]_i$ (D) in the

LV of control and GK animals. RT-PCR amplification was normalized to that of GAPDH. Bars indicate Mean+SEM, $n = 7-8$, of 2–3 independent experiments. $*p < 0.05$

c. Akt activity

To determine HG-sensitive signalling events in myocyte hypertrophy, this study investigated activation of the Akt-mTOR-p70S6K axis by western blotting. p70S6K, activated by upstream mTOR, is known to phosphorylate the ribosomal protein S6 enabling the up-regulation of TOP mRNA for encoding translational machinery and ribosomal proteins (Alessi *et al.*, 1998). Of particular interest, the Akt- mTOR-p70S6K axis is also a known target of HG-induced TGF β 1 activation and the association appears metalloproteinase (MMP2 and 9) -dependent (Wu and Derynck, 2009). Thus, levels and activation (phosphorylation) of Akt (Ser473) and p70S6K (Thr389), were measured by immunoblot (Fig 5.5 A). The latter phosphorylation site is well-recognized to reflect actual mTOR activity (Wang *et al.*, 2005).

Phosphorylated (Ser 437) Akt protein, indicative of functional activation, was increased significantly in GK rats relative to controls (0.23 ± 0.03 vs. 0.39 ± 0.03 ratio units, $p < 0.05$). p70S6K phosphorylation was not similarly influenced (0.31 ± 0.13 in control LV vs. 0.49 ± 0.19 in GK, ratio units, $p > 0.05$). Furthermore, as total protein levels of Akt and p70S6K were comparable in GK and control animals ($p > 0.05$), ratio of normalised pAkt:Total Akt was significantly increased in GK rats relative to age-matched controls (pAkt:Akt: 0.68 ± 0.99 vs. 1.06 ± 0.02 , Fig 5.5 B, $p < 0.05$;) but normalised pp70S6K:total p70S6K remained unchanged (pp70S6K:p70S6K, 1.55 ± 0.48 in GK vs. 0.60 ± 0.08 in control, Fig 5.5 C, $p > 0.05$).

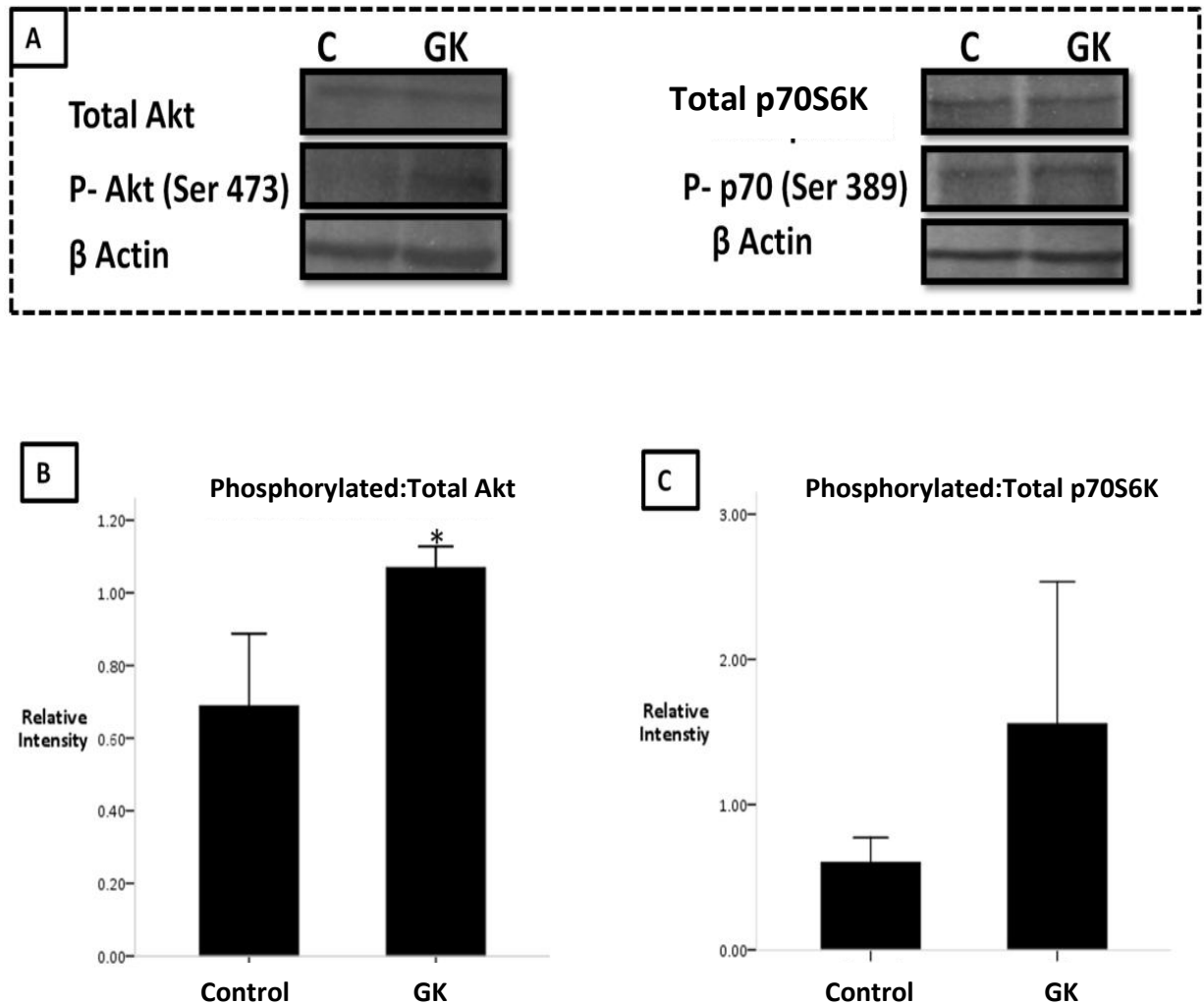


Fig 5.6: Akt-p70S6K signalling. Representative immunoblots of total cardiac protein extracts showed increased levels of phosphorylated Akt in GK hearts relative to controls (C in 5.6 A). β -actin served as a loading control (A). There was no significant difference in levels of total Akt or total p70S6K. Quantitative densitometric analysis corrected for protein loading demonstrated increased Akt phosphorylation normalized to total Akt in GK rats (B) whereas p70S6K phosphorylation were not statistically significant between groups (C). Values in graphs represent the average data obtained from 3 separate experiments from each group conducted in duplicate. Bars indicate Mean+SEM, * unpaired t test, $p < 0.05$

5.5 Discussion

Despite the prevalence of HF in the aging T2DM population, the influence of mild HG *per se* on long-term structural remodelling in the heart is not well established. The present study demonstrates that a *milieu* dominated by chronic mild HG is sufficient stimulus for the sustenance of a cardiomyopathic phenotype that recapitulates several molecular and structural aspects of the failing heart. These include myocyte hypertrophy and an increased ventricle wall thickness, natriuretic peptide expression with activation of Akt, diffuse fibrotic deposition in extracellular spaces, pro-fibrotic cytokine induction with altered transcriptional activity of the ECM and mediators of $[Ca^{2+}]_i$. Alterations of these key elements intrinsic to the normal function of the myocardium likely represent the structural and molecular substrates of electrical anisotropy and myocardial heterogeneity that accompany altered diastolic LV function frequently observed in chronic T2DM (Van Kujik *et al.*, 2010).

Caspase-3 Activity

LV hypertrophy and fibrosis proliferation are recurrent findings in ventricular decompensation of diabetic origin and are often associated with increased apoptotic cell death in the myocardium (Francis *et al.*, 2001; Chatham *et al.*, 1996). A critical step in the execution of the apoptotic program eliciting DNA fragmentation is cleavage of caspase-3 into 19 and 17 kDa fragments. In this study, the LV exposed to chronic mild HG did not present with altered caspase-mediated apoptosis. The apparent discrepancy between the present findings and those reporting increased apoptosis in experimental diabetic cardiomyopathy may reflect the severity of HG in those studies, often in the range of 250-650 mg/dL in the T1DM rat (Kajstura *et al.*, 2001; Fiordaliso *et al.*, 2000; Cai *et al.*, 2002). As such, current findings support the notion that severity of HG may be an important determinant in apoptotic responses evoked by the caspases. In addressing the limitations of this finding, it cannot be ruled out that apoptosis may have occurred independent of caspase-3 activation. Although histological signs of necrosis were not apparent, ubiquitin-related autophagic cell death still remains a possibility (Diwan and Dorn, 2007). However, likelihood is advanced that inconspicuous apoptosis in the mildly diabetic LV may be related to the obvious absence of LV dilation. Several lines of evidence indicate that caspase-mediated cardiac myocyte apoptosis is unambiguously the cause of transitioning from compensated hypertrophy to decompensated dilated cardiomyopathy (Diwan and Dorn, 2007) that is typically

antecedent to overt HF. Conversely, inhibition of apoptosis by pharmacological caspase inhibition prevents cardiomyopathic degeneration and reverses dilated cardiomyopathy (Hayakawa *et al.*, 2003). Nevertheless, whether unaffected caspase-3 activity is a direct indication of a compensated myopathy in the chronically diabetic GK rat is difficult to envision at the present time.

TGF β 1 and the extracellular matrix

In the relative absence of apoptotic cell death, an HG- upregulated TGF β 1 may underlie increased ECM proliferation in the long term T2 diabetic GK myocardium. Several mechanisms by which HG may activate TGF β 1 expression have been previously demonstrated. Of these, activation of a HG-sensitive glucose response element identified in the TGF β 1 promoter region and HG-activated Protein kinase C induced expression of TGF β 1 via thrombospondin (TSP-1) may act upstream of TGF β 1 in HG-induced fibrosis proliferation (Smoak, 2004). Once upregulated, the ability of TGF β 1 to exert profibrotic effects in the myocardium is well described and often via transcriptional control over the fibrillar collagens and fibronectin (Ramos-Mondragon *et al.*, 2008). Furthermore, TGF β 1 self amplifies its expression in myofibroblasts and can trigger fibroblast proliferation and phenotypic conversion to myofibroblasts that synthesize collagen types I and III (Berk *et al.*, 2007). This effect is often by induction of the key TGF β 1 downstream effector, CTGF, by acting on TGF β 1 response elements localized in the CTGF promoter site (Ramos-Mondragon *et al.*, 2008). The present study observed an upregulated TGF β 1 and CTGF mRNA in long-standing experimental DM and enhanced TGF β 1 LV activation concomitant with an increased collagenous matrix deposition, and transcriptional upregulation of major fibrillar collagens and FN. As such, it is possible to infer that activation of TGF β 1 may underlie the extracellular matrix deposition in the long-term mildly diabetic myocardium. It is noteworthy that in this study, plasma TGF β 1 levels were unaffected by diabetes and did not parallel transcriptional activity or biologically active TGF β 1 in the GK LV. As the use of TGF β 1 as a risk stratification tool for predicting the development of myocardial fibrosis resulting in heart failure has recently been advocated (Sovari and Dudley, 2010), current findings advice a degree of caution in assessing cardiac pathology based solely upon blood TGF β 1, which appears to be differentially regulated within the myocardium and in the circulation, at least in the diabetic milieu.

A co-ordinated response of opposing elements in cellular and stromal compartments

maintains the integrity of the remodelling programme in the heart. In this regard, cell surface bound and soluble MMPs, their natural tissue inhibitors (TIMPs) constitute important systems for regulating ECM turnover. In investigating the effect of chronic HG on the transcriptional profile of the regulators of the ECM, the present results indicate that collagen deposition in the LV was paralleled by transcriptional upregulation of MMP2 and 9 and attendant increase in endogenous MMP inhibitor TIMP4, which is the dominant cardiac isoform of the TIMPs. The exact role of the latter in the remodelling heart is presently unclear, as TIMPs can also facilitate MMP activation by stabilisation and/or localisation (Kurrelmeyer *et al.*, 1998). Interestingly, the activities of TGF β 1 and MMPs are known to be intertwined; Experimental evidence points towards the possibility that TGF β 1 can up-regulate MMP-2 and its cell surface activator MT-MMP in fibroblasts (Manso *et al.*, 2006). The reverse is also documented (Wu and Derynck, 2009), and moreover, Col type I, whose production is regulated by TGF β 1, may result in increased MMP-2 activity (Kurrelmeyer *et al.*, 1998). Regardless of activating processes, the net result of cardiac MMP activation is loss of the normal interstitial supporting structure (Francis, 2001), and upregulated MMP transcription observed in this study mirrors previous findings in severe congestive HF and in human cardiomyopathic hearts (Kurrelmeyer *et al.*, 1998; Manso *et al.*, 2006).

Additionally, data presented in this study indicate that long-term mild HG may influence expression pattern of the major ventricular transmembrane gap junction protein Cx43 and the membrane-spanning integrins, both of which co-ordinate ECM-myocyte interaction (Hescheler and Fleischmann, 2000; Manso *et al.*, 2006; Zhang *et al.*, 2008). Given the roles of integrins and Cx43 function on electrical integrity and ECM homeostasis in the myocardium, it is conceivable that HG-associated abnormalities in the expression of these molecules may be important in the pathogenesis of a DM-specific cardiomyopathy. Where dysregulated transcription may be the result of a complex interplay of mechanical/chemical signals in diabetic tissue microenvironment, consideration is given to the role of TGF β 1 in mediating this effect. In relation to Cx43, a recent *in vitro* study demonstrated HG-evoked TGF β 1 mediated increase in Cx43 expression and gap-junction mediated cell-cell communication (Hills *et al.*, 2009). Finally, TGF β 1 stimulation increased expression of α 5 β 1 integrins in fibroblasts and in turn, overexpression of the same integrin heterodimer increased TGF β expression (Manso *et al.*, 2006). Altogether, the present results have implicated a complex interplay of MMPs, integrins, cytokines and ECM components in the heart

exposed chronically to mild HG. While further comprehensive and temporal analyses are required to delineate causative from compensatory adaptations, translational upregulation of ECM components and regulators described in this study are a likely reflection of altered local synthesis response to chronic HG. It is also feasible that the alterations represent a response to the generation of inappropriate isoforms of the molecule (s), if DM were to alter alternative splicing patterns of specific genes (Roy *et al.*, 1990). Both these possibilities are hypothetical but realistic and warrant further experimental enquiry.

LV Hypertrophy

Coupled with ECM deposition, the finding of LV hypertrophy in GK rats parallels previous experimental (Arres-Carrasco *et al.*, 2009; Falcao-Pires *et al.*, 2009) and clinical (Fujita *et al.*, 2007; Van Heerebeek *et al.*, 2007) reports of the decompensating T2DM heart. The molecular basis of specific patterns of cardiac remodelling in DM (and the involvement of apoptotic processes herein) is uncertain as of this writing, but much evidence has extended the regulatory portfolio of HG-upregulated TGF β 1 to include cellular hypertrophy. In keeping with the phenotype observed in this study, TGF β 1 overexpression resulted in cardiac hypertrophy that was characterized by both interstitial fibrosis and myocyte hypertrophy (Rosenkranz *et al.*, 2002). In the same vein, expression of mRNA encoding TGF β 1 is increased in the LV myocardium of patients with LVH (Li *et al.*, 1997) and it is known to be specifically expressed in hypertrophic myocardium during the transition from stable hypertrophy to overt HF (Berk *et al.*, 2007).

Recent work underscores the pathophysiological significance of increased MMP-activated TGF β 1 induction as a contributing factor in the onset of HG-induced hypertrophy, mediated via modulation of Akt-mTOR-p70S6K axis (Wu and Derynck, 2009). However, increased Akt activity (phosphorylation) but unaffected phosphorylation of Akt target protein p70S6K in the chronically diabetic GK heart does not fully supplement this *in vitro* finding. In explanation, two inter-related possibilities that could contribute to this phenomenon are presented: Firstly, the hypertrophic targets of Akt and mTOR may not be uniquely restrained to p70S6K activation, and additional targets may be involved (Mc Mullen *et al.*, 2004; 2004). Moreover, previous work

demonstrates that short term Akt activation, deemed essential for physiological growth of the heart, activates mTOR and downstream p70S6K. On the contrary, chronic Akt activation was associated with a transition to decompensated myocyte hypertrophy and downregulation of signalling to S6K (Mc Mullen *et al.*, 2004; 2004b; O'Neill and Abel, 2005). Although this hypothetical effect has not yet been investigated in the diabetic milieu, the current findings provide strong indication of such an effect when coupled with previously presented observations in the prediabetic GK rat wherein myocyte hypertrophy and TGF β 1 increase were concomitant with upregulated activity of both p70S6K and Akt (unpublished data). Given this, the relation between Akt signal intensity and/or duration in determining early *vs.* late hypertrophic remodelling in the diabetic heart merits further enquiry.

The molecular signature of pathological hypertrophy was recapitulated in the long term diabetic GK rat, manifested by quantitative changes in gene expression of key mediators of $[Ca^{2+}]_i$ and the natriuretic peptides, the latter presumably upregulated as a compensatory mechanism to promote natriuresis and suppress myocyte hypertrophy, altogether aimed at reducing load (Olson and McKinsey, 2005). Once again, the involvement of upregulated TGF β 1 in these transcriptional changes cannot be disregarded. Of note, Kapoun *et al.* (2004) reported that BNP treatment produced a remarkable inhibition of TGF β 1-induced effects on human cardiac fibroblasts and opposed TGF β 1-regulated genes related to fibrosis including Coll1, Fn, CTGF, and the TIMPs. Similarly, TGF β 1 activation has implications in ionic remodelling of the failing ventricle, capable of altering myocyte shortening and Ca^{2+} kinetics and also NCX mRNA expression, that was observed in this study (Ramos-Mondragon *et al.*, 2008) TGF β 1 involvement notwithstanding, cardiac hypertrophy is associated with marked changes in myocardial contractility. These contractile abnormalities are frequently accompanied by alterations in $[Ca^{2+}]_i$ transient that have been previously reported in myocytes isolated from GK rats at 18 months of age (Howarth *et al.*, 2007). By means of extension, the results presented in this section indicate that increased $[Ca^{2+}]_i$ transient amplitude in the long term diabetic GK LV (Howarth *et al.*, 2007) may be due in part to increased transcription of the L-type calcium channels resulting in elevated Ca^{2+} influx at systole.

Concluding Remarks:

This study has demonstrated that cardiac remodelling in a diabetic setting can be viewed, at least in part, as a transcriptional disorder. As such, normalization of the gene expression patterns of through transcriptional therapies may represent a promising interventional approach in the treatment of DCM. The extents to which the remodelling changes described here contribute to LV functional impairment are the subject of ongoing enquiry. In the absence of apoptotic cell death, LV dilation and increased amplitude of the calcium transient associated with a compensated stage of hypertrophy (Wickenden *et al.*, 1998), it is perhaps to be expected that available data indicate preserved cardiac function in this model even at 18 months of age (Howarth *et al.*, 2007). In this sense, it is tempting to speculate that the addition of another stressor such as obesity/hypertension that frequently cluster with DM, especially in the elderly, may ‘tip-the-balance’ in favour of a dilated cardiomyopathy coupled with an overt decline in LV mechanical performance.

In its entirety, this study represents an exploration of the clinical relevance and suitability of the mildly diabetic GK rat for experimental delineation of HG-induced chronic cardiac remodelling and a cardiomyopathic phenotype. It is especially notable that the model that emerges from this study implicates complex interactions between the matrix and the myocyte, cytokine induction and potential electrical remodelling at fasting blood glucose levels that very closely skim the upper limit of optimal HbA1c goals for T2DM patients with persistent HG, as outlined by current consensus guidelines (Fasting glucose 70-130 mg/dL to achieve HbA1c of <7%) (McCulloch, 2010). Finally, when compared to results of Chapter 3, the relation between the severity of DM and the development of myocardial sequelae is especially highlighted as chronic HG of 131.4 ± 0.22 mg/dl (compared to a normoglycemia of 95.2 ± 0.3 mg/dl in control animals) produced remodelling changes in the LV that are identical in several respects to those reported in the short term, severely diabetic T1 model of the disease. In this regard, HG being the principal marker of DM in experimental studies, this work also emphasizes the importance of specifically defining disease severity in studies of the heart.

CHAPTER 6

IMPACT OF AGE ON STRUCTURAL REMODELLING IN THE LEFT VENTRICLE IN THE GOTO-KAKIZAKI RAT

6.1 Introduction

The cardiac effects of T2DM are known to be most pronounced in the elderly (Verny, 2007). Chronic HG may underlie this process, by producing structural changes that alter LV compliance and by extension, function. However, major difficulties arise in studying DM-related complications in the ageing heart. Ageing imposes unique conditions on cardiac adaptation to cardiac stress and cardiac involvement in the ageing is usually multi-factorial, with increased frequency of arterial hypertension and coronary damages due to accumulation of vascular risk factors. Beyond these issues, how chronic HG affects the heart specifically and potentially accelerates the effects proper to ageing are relatively unknown. In the laboratory, the STZ-induced type 1 rat model remains the ‘work horse’ for studying cardiomyopathic changes in the diabetic heart, in spite of obvious limitations in translational value and relatively short study periods. Because the HG that dominates the pathophysiology and clinical course of T2DM is potentially modifiable, information concerning how increased glucose may contribute to other risk factors for HF, notably advanced age, is of particular clinical consequence as no effective treatment serves to reverse HF once established (Strahrenberg *et al.*, 2010). In response to these issues, this study represents an investigation of the effect of ageing on dysglycemia-related myocardial remodelling changes, based on the hypothesis that chronic mild HG accentuates the effects of ageing in the heart. In examining the additive effects of HG and cardiac ageing, an experimental protocol was chosen in which each of these two conditions in isolation were likely to produce only modest remodelling changes. As such, GK rats were examined at 2 ends of the dysglycemia continuum to allow comparison across a wide age range while also approximating the typical clinical course of the disease during progression from IGT to overt T2DM.

6.2 Methods

As described in Chapter 2

6.3 Results

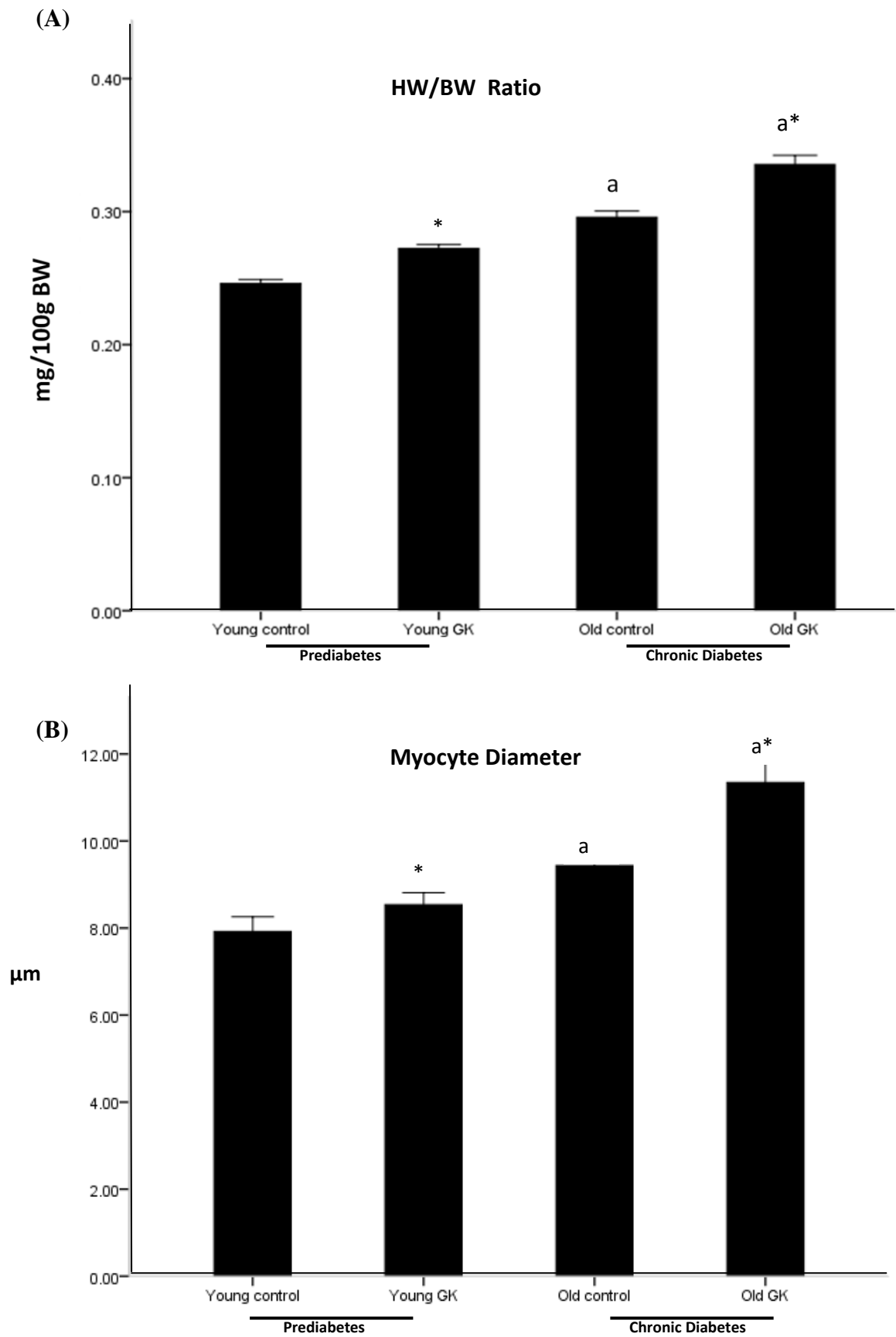
Data described in graphs below are from young Wistar (young control), young GK, old Wistar (old control) and old GK groups as outlined in Chapter 2 and as given in

Chapters 4 and 5 respectively. The letter 'a' indicates a significant ageing effect, *significant dysglycemia effect, a* indicates interaction of ageing and T2DM. 2-way ANOVA, level of significance is set at $p < 0.05$.

Represented in Fig 6.1, mean HW/BW ratio (A), LV wall thickness (B) and myocyte diameter (C) demonstrated a trend towards greater LV hypertrophy with ageing, and the effect was accentuated by the presence of T2DM. (HW/BW ratio: $F(3,32)=66.8$, $p < 0.05$; LV wall thickness: $F(3,17)=17.86$, $p < 0.01$; myocyte diameter: $F(3,82)=14.39$, $p < 0.05$). A significant consequence of age-induced remodelling of the heart is the accumulation of connective tissue and old Wistar rats also displayed markedly higher ECM deposition in interstitial spaces than the LV from young control animals (D) ($F(3,153)=67.712$, $p < 0.05$).

Mechanisms that possibly underlie remodelling changes in the LV were also compared across groups for age-related interactions. A positive correlation between level of HG and TGF β 1 activity was observed with levels of active protein increasing in parallel with HG increase (Fig 6.2 C). An interesting observation was that although Total TGF β 1 protein levels in the LV were significantly reduced with ageing in GK groups (Fig 6.2 A, $F(3, 17)$, $p < 0.05$), active LV TGF β 1 showed a significant increase (Fig 6.2 B). This suggests that the mechanisms that mediate TGF β 1 activation in the LV, notably HG and MMP induction (Wu *et al.*, 2009) may be upregulated in the GK myocardium, as is the case in the present study. Within the control group, age-related effects were not statistically significant for either parameter ($p > 0.05$). Finally, phosphorylation levels of Akt protein (and p70S6K in the prediabetic group) were only significantly upregulated by dysglycemia ($F(3, 35)$, $p < 0.05$) and there was no apparent trend towards alteration with increasing age in both control and GK groups ($p > 0.05$), (Fig 6.3).

Fig 6.1



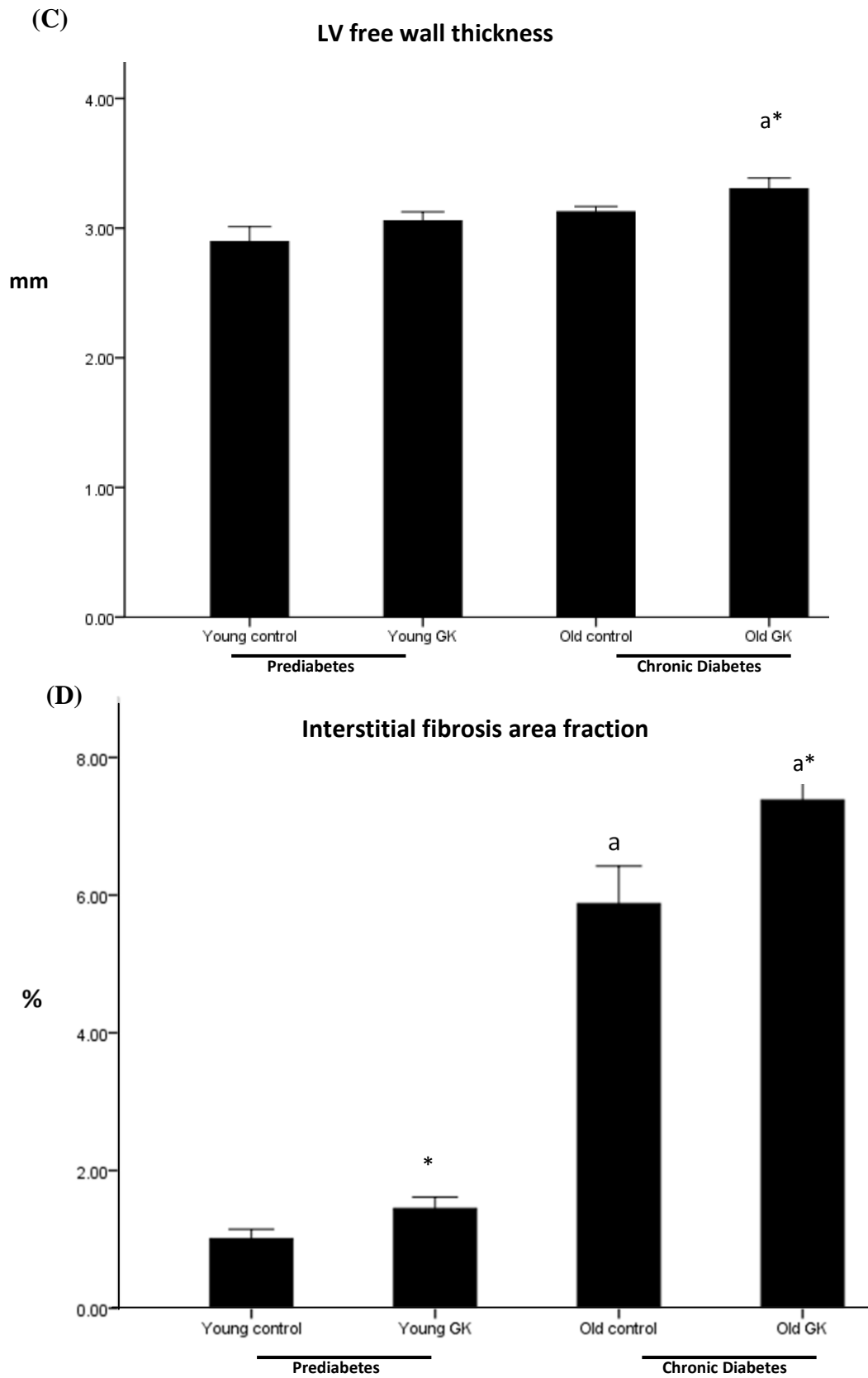
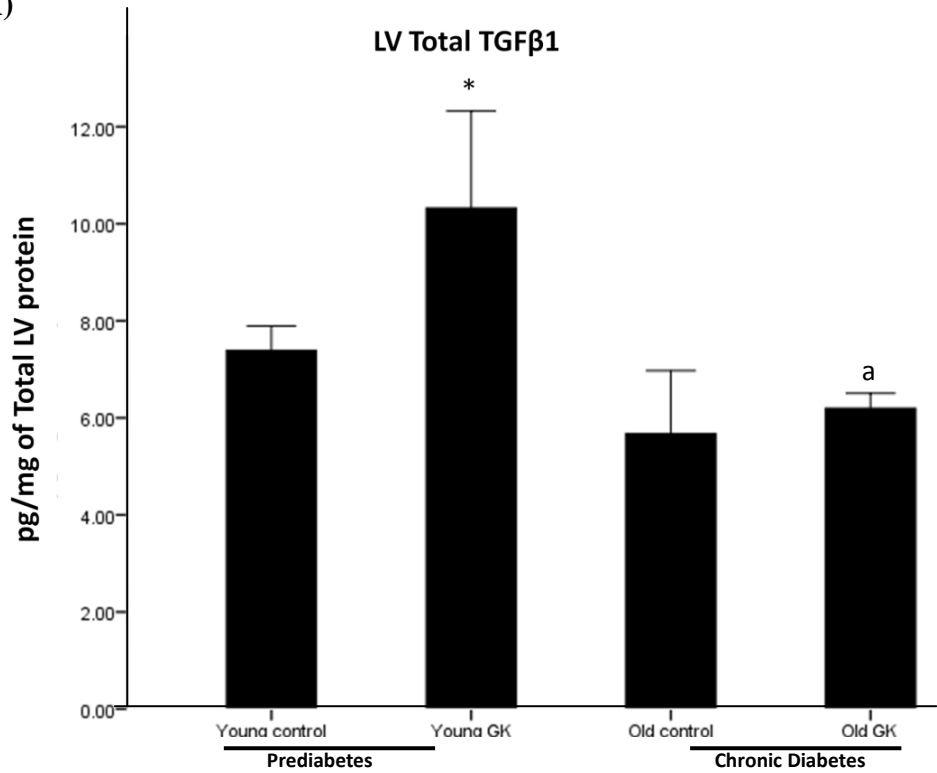
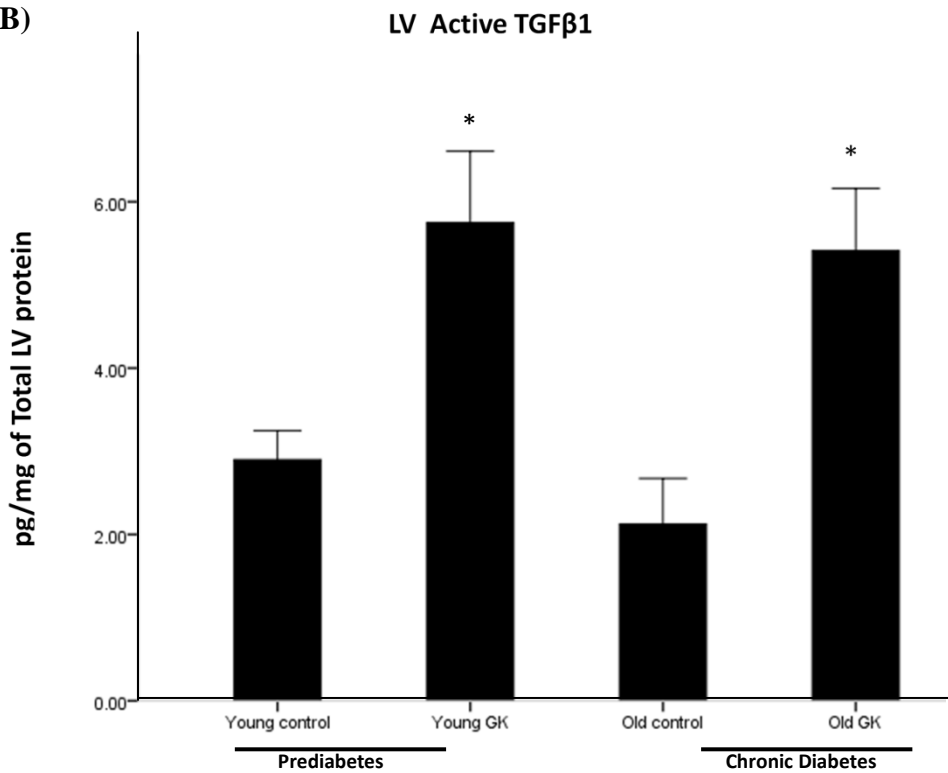


Fig 6.1: Age-dependent structural remodelling in the LV. HW/BW ratio (A), LV wall thickness (B) Myocyte diameter (C) and ECM (interstitial) area fraction (D) were determined using LV histological sections from young and old diabetic and age-

matched Wistar control groups. $n= 4-5$ in each group. The letter 'a' indicates a significant ageing effect *significant dysglycemia effect. 2-Way ANOVA, $p<0.05$

Fig 6.2**(A)****(B)**

(C)

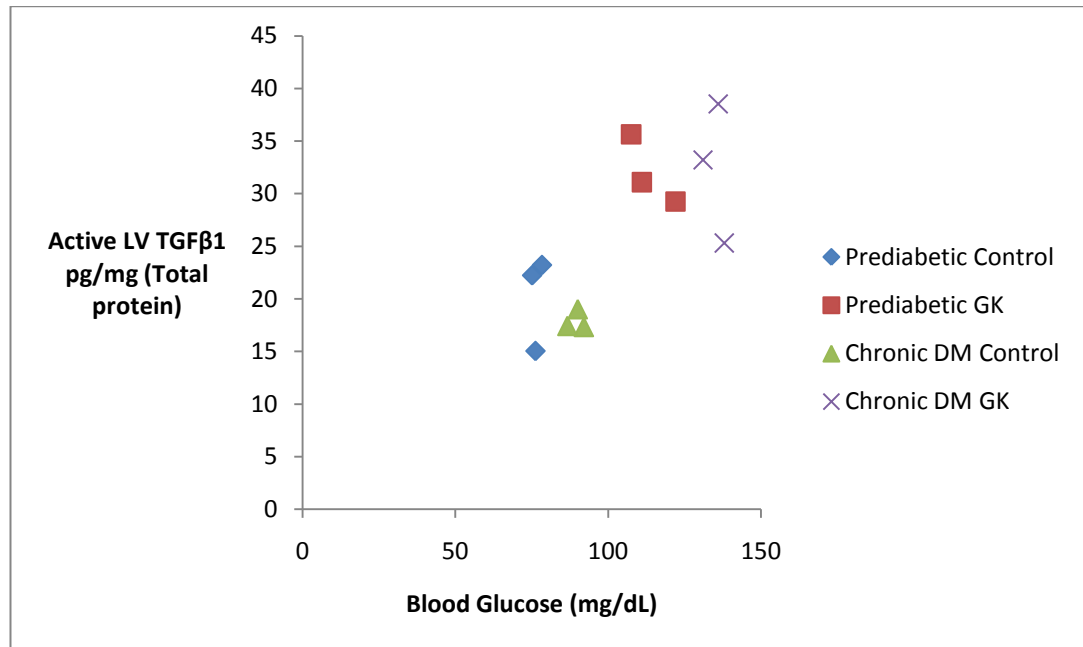
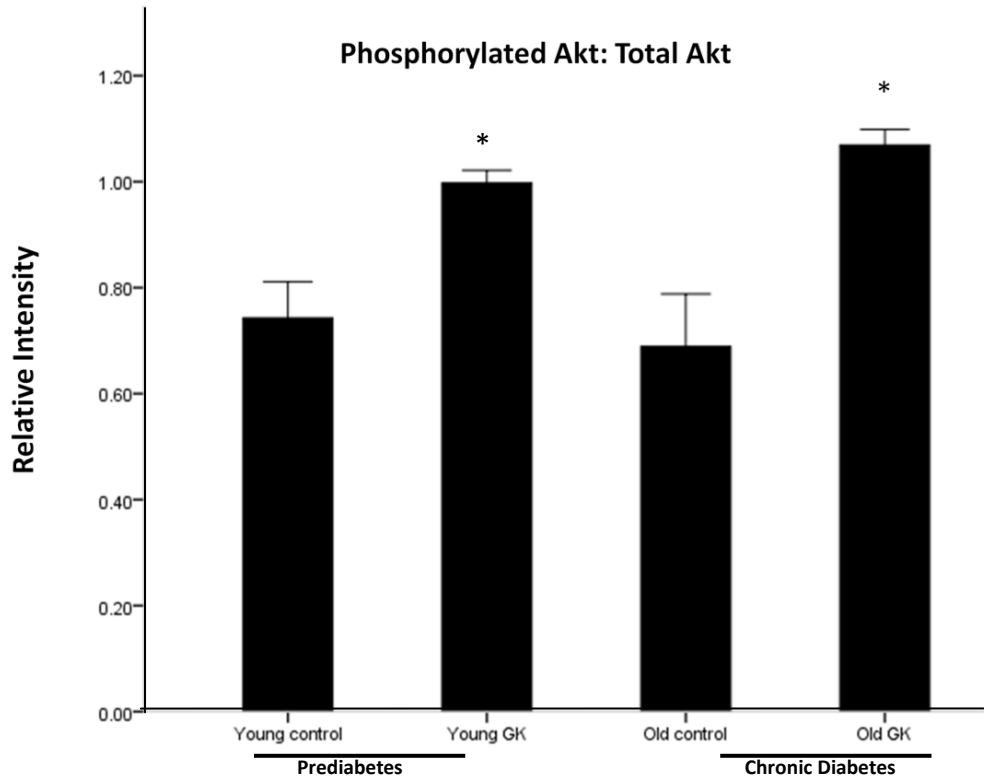


Fig 6.2: Age-related effects on LV TGFβ1 concentration. Total TGFβ1 (A) and Active TGFβ1 protein (B) in control and GK rats determined by ELISA. The letter 'a' indicates a significant ageing effect *significant dysglycemia effect. 2-Way ANOVA, $p < 0.05$. $n = 3$ in each group. Correlation between blood glucose and active TGFβ1 in the LV.

Fig 6.3

(A)



(B)

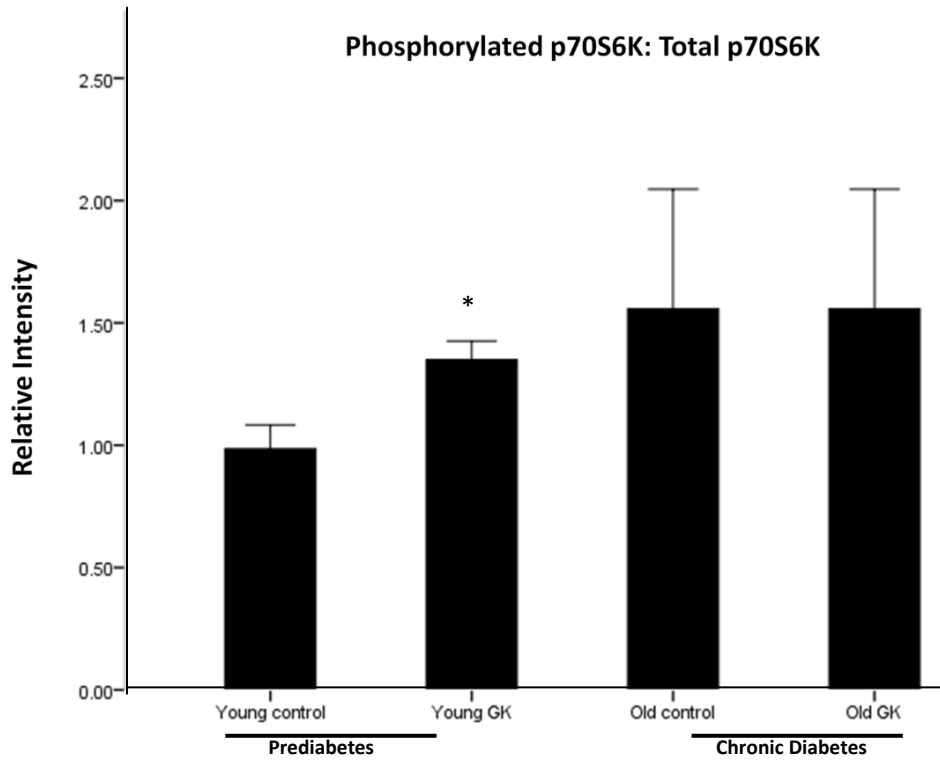


Fig 6.3: Effect of age on Akt (A) and p70S6K (B) phosphorylation in the LV. *significant dysglycemia effect. 2-Way ANOVA, * $p < 0.05$. $n=3$ in each group

6.4 Discussion

Ageing is often associated with a progressive decline of the cardiovascular system, characterized in part by an increase in wall thickness of the ventricles (Burgess *et al.*, 2001). Aged rodents are also known to present with ventricular hypertrophy in association with excess ECM accumulation (Thomas *et al.*, 1992; Lin and Bissell, 1993; Seccia *et al.*, 1999). In concord, from the combined results of this study, it can be inferred that ageing results in structural remodelling of the LV in the Wistar heart. As given, modestly increased HW in ageing control rats was reflected by a small increase in LV mass and significantly increased myocyte dimensions. Moreover, differences in ECM accumulation between young and ageing Wistar control rats also reached statistical significance, further suggesting a qualitative loss of structural integrity at 18 months of age, in keeping with clinical observations at comparable age groups (Lakhan and Harle, 2008). This work also demonstrates that chronic but modest elevations in HG can aggravate age-induced remodelling changes in the GK heart. As hypothesised, the effects of ageing on structural remodelling were far more prominent in the GK myocardium, presenting with significantly elevated wall thickness, myocyte size and ECM deposition relative to younger GK rats as well as age-matched Wistar controls. Since myocardial architecture accounts for efficient pump function at the global level of the heart, distribution of interstitial fibrosis and myocyte hypertrophy during LV remodelling are critical factors for adverse prognosis in heart diseases and often represent the structural correlate of LV functional deficit (Buckberg *et al.*, 2008). It is particularly noteworthy that this marked remodelling occurred in response to fasting blood glucose levels (131mg/dL) that very closely skim the upper limit of optimal HbA1c goals for T2DM patients with persistent HG, as outlined by current consensus guidelines. Indeed, the American Diabetes Association and the European Association for the Study of Diabetes consensus guidelines for pharmacotherapy to control HG in T2DM recommends fasting glucose values of 70-130 mg/dL to achieve an optimal HbA1c treatment goal of <7% (McCulloch, 2010). Moreover, fasting plasma glucose has recently been shown to be prognostic of incident HF in a large randomised trial of patients at high CV risk (Held *et al.*, 2007) and worryingly, epidemiological studies by Poirier and colleagues (2001) and Redfield *et al.*, (2003) have reported that the

prevalence of asymptomatic diastolic dysfunction in patients with type 2 diabetes to be between 52 and 60%, despite meeting clinical criteria for acceptable glycemic control. Taken together, it can be argued that present definitions for dysglycemic states may be inadequate and thereby underestimate the implications of the disease, supplementing recent articles addressing the need to redefine optimal HbA1c levels (Bergman *et al.*, 2010; Schainberg *et al.*, 2009), and perhaps ‘individualise’ targets in patient populations that may require special considerations, especially those with other risk factors for HF. On the flipside, another line of reasoning is that if HG drives the pathogenesis of a diabetes-specific cardiomyopathy, one would expect intensive glycemic control in diabetic patients to translate into meaningful morbidity and mortality benefits. However, as mentioned previously, it is disconcerting to note that recent clinical trials targeting tight glycemic control have indicated no such effect or the possibility of worsening results (Montori *et al.*, 2009). The answer to this conundrum may lie in a better understanding of the relationship between dysglycemia and cardiac structure with an emphasis on the importance of early subtle changes in glucose levels, as provided by the preceding chapters and discussed in the next section.

CHAPTER 7

GENERAL DISCUSSION

7.1 Perspectives

It is stressed that a majority of studies dealing with LV remodelling changes in DM are focussed primarily at the end point of what is undoubtedly a dynamic process of change, with likely origins in prediabetes and IGT as given in Chapter 4. Therefore, morphological/functional assessment of remodelling changes in response to HG following several weeks of exposure provides a description ‘after the fact’, in the process missing the temporal relation of the remodelling process that may perhaps be all important. Such information can only be obtained from studies like the present, of which there is sparsity.

As described in Chapter 4, T2DM in the GK rat was preceded by a prediabetic phase during which cardiomyocyte hypertrophy and modest fibrosis proliferation were already apparent in the LV. This finding provides novel experimental support for the clinical contention that HG may reflect a risk for HF even in the absence of DM, at least in part, by initiating early LV structural remodelling. It is well established that in the longer term, hypertrophy and fibrosis progress to a maladaptive state, and become important blood pressure-independent predictors of myocardial infarction, HF and cardiovascular mortality (Cohn, 2000; Lips *et al.*, 2003) Although association does not equate causality, the data presented in Chapter 3 are corroborated by robust epidemiological evidence suggesting that IGT and IFG are not only indications of risk for progression to T2DM, but also to have independent pathophysiologic significance that includes mortality and cardiac functional deficit (Nielsen and Lange, 2005). It has been previously hypothesised that the structural manifestations of DCM consist of two major components; the first being a compensatory adaptation to HG-related metabolic alterations, while the other represents degenerative changes for which the myocardium may have only a limited capacity for repair (Thompson, 1988). Underlying this supposition is the fact that compensatory mechanisms activated during the initial remodelling process have the paradoxical role of serving simultaneously as adaptive, compensatory changes, and as major contributing elements to the progression of CHF (Cohn, 2000). When supplemented with previous work, the same concepts may also be applied to remodelling changes as described in this work, in the GK rat. As such, in the following section it is argued that initial compensatory molecular adaptations triggered in response to the mild dysglycemia of prediabetes may have become deleterious when sustained in the long term and may underscore the worsening phenotype as the T2DM

progressed untreated. Comments are limited to molecular events in hypertrophy and fibrosis proliferation relevant to data presented in the preceding chapters.

First, early transcriptional remodelling of the ECM in the GK rat was characterised by increased message levels of the gelatinases MMP 2 and 9. These changes in MMP expression, likely indicators of activity, were further sustained in the long-term, an effect that has been previously correlated with onset of apoptotic processes, defective angiogenesis and contractile dysfunction (Reinhardt *et al.*, 2002; Yaras *et al.*, 2008). Previous work has demonstrated the temporal role of MMPs in which MMP2 levels were increased on compensatory concentric remodelling as a protective response to ECM proliferation. However, in decompensation and eccentric remodelling, MMP2 and 9 are known to remain activated, suggesting a role for the MMPs in the teleological function of the heart's structure (Nishikawa *et al.*, 2003).

Second, another key example is that of TGF β 1, potent stimulus for hypertrophy, collagen synthesis, matrix accumulation and organization, that was found to be upregulated in both pre-and overt T2DM in the GK myocardium. Several lines of evidence confirm that continuous over-expression of pro-inflammatory cytokines including TGF β 1 within the myocardium contribute to the progression of cardiac remodelling, the hallmark of heart failure by sustaining cardiac hypertrophy, cardiac fibrosis and cell death (Sivasubramanian *et al.*, 2001; Dai *et al.*, 2004). While excessive TGF β 1 may be deleterious by promoting collagen deposition, increased myocardial stiffness and diastolic dysfunction, how acute activation of TGF β 1 impacts the myocardium is less well established. A baseline level of TGF β signalling has been deemed necessary to preserve cardiac structure and to protect the pressure-overloaded myocardium from uncontrolled matrix degradation that could result in cardiac dilation (Dobaczewski *et al.*, 2010). Furthermore, short-term cardioprotective effects may be associated with the preservation of endothelium-dependent relaxation, prevention of free radical generation, a decrease in TNF- α release and attenuation of ischemia-reperfusion injury (Lefer *et al.*, 1990; 1993).

Third, involvement of Akt, a protein kinase that regulates a broad range of physiological responses in the heart, including metabolism, gene transcription, cell size and survival (O'Neill and Abel, 2005) cannot be discounted. The finding that Akt- and p70S6K phosphorylation were increased in prediabetic GK rats in association with LV hypertrophy is mirrored in previous work in cardiac-specific doxycycline-dependent inducible Akt1-transgenic mice that developed adaptive hypertrophy following short-

term induction that was reversible on doxycycline treatment (Shiojima *et al.*, 2005). Akin to the chronic T2DM rat described in this study, long term sustained Akt activation induced extensive hypertrophy. Furthermore, prolonged induction led the progression to a dilated phenotype and cardiac dysfunction that was not attenuated but further exacerbated by transgene repression with doxycycline. Interestingly, rapamycin treatment that inhibits MTOR signalling inhibited Akt-mediated cardiac growth in both acute and chronic stages. However, in direct concurrence with the results of this work, phosphorylation levels of S6K in DTG hearts were not altered in the chronic phase of Akt induction, corroborating the supposition that Akt to S6K signaling is impaired following prolonged Akt. Altogether, these findings reiterate the supposition that the fine-tuning of the Akt signalling pathway, reflected in level and duration of Akt signaling may modulate compensated vs. decompensated remodelling (Nagoshi *et al.*, 2005) and current data extend this postulation to the HG-stressed heart.

Altogether, these alterations at the level of the genome/proteome may represent early adaptations in the HG-stressed heart that have the capacity to become deleterious in the long term and adversely affect myocardial structure and function. The possibility exists that the molecular changes described above may not only persist in response to uncontrolled HG like in the present study, but also with glucose control becoming myocardial representations of the ‘legacy effect’ or ‘metabolic memory’ of HG, (DCCT Research group, 1993; Nathan *et al.*, 2005) a concept that has arisen from evidence of ongoing vascular injury as a result of prior transient episodes of poor glycemic control, that is today gaining momentum in pathogenesis of diabetic complications. Very briefly, the prevailing view in this fledgling field is that that gene–environment interactions not only represent current glycemic status, but also include precedent HG, which could transmit conserved epigenetic fates that are spatially and temporally consistent with persistent gene activities (Cooper and El Osta, 2010). Occurrence of a HG-mediated metabolic memory was documented over 20 years ago in a series of cell culture experiments where transient exposure of endothelial cells to HG followed by a return to normoglycemia was associated with persistent upregulation of various ECM proteins including fibronectin and type IV collagen (Roy *et al.*, 1990). When applied to the vasculature, epigenetic changes as a result of HG are held accountable a structural fixation due to endothelial damage up to a “point of no return”, when a regression of vascular disease progression is no longer possible (Jax, 2010). Extrapolated to the present setting, the possibility arises that the myocardium exposed to early transient HG

may also present with limited capacity for repair owing not only to the metabolic memory in endothelial cells but in the myocardium itself? However, as of this writing, an in-depth understanding of the genomic effects of HG and how epigenetic pathways may be interrupted for therapeutic benefit is far from realised and the onus is still on the early identification and treatment of DM as opposed to intensification at a later stage to achieve any meaningful long-lasting cardio-therapeutic benefit.

7.2 Limitations and future scope of the study

In addressing the limitations of the findings reported in this thesis, the following admonishments are due, but in the process have also raised several clinically relevant questions worthy of further experimental pursuit.

First, this work is primarily descriptive by design, the overall outcome being the assessment of the interactive effects of ageing and chronic uncontrolled HG on remodelling processes in the LV. While the demonstration of HG-related cellular and molecular perturbations provides insight into the nature of disease, the data presented do not allow us to conclude that hypertrophy, matrix deposition, altered signal transduction and gene expression are events in the development or progression of altered ventricle function in the diabetic milieu uncomplicated by traditional cardiovascular risk factors. The true test for determining compensated *vs.* decompensated remodelling lies in the assessment of LV function that was outside the remit of the present thesis. However, previous functional data in the GK rat provide some insight: In GK rats upto 12 weeks of age, cardiac function appears to be preserved at resting physiological conditions, wherein diastolic dysfunction was undetectable without an added insult of salt overload and could be corrected by pharmacological intervention directed at the renin-angiotensin and the neutral endopeptidase system (Gronholm *et al.*, 2005). Using isolated Langendorff-perfused hearts, El-Omar *et al.* (2004) demonstrated that no significant functional changes can be found in GK rat hearts under normoxic conditions while after a brief exposure to hypoxia a marked contractile defect could be seen both in systolic and diastolic LV function. Reports of LV function at later stages of T2DM in the GK rat are not directly forthcoming. On the one hand, the structural phenotype is reminiscent of chronic mechanical stress with pressure overload where cardiomyocyte hypertrophy is often observed in association with myocardial fibrosis. The LV undergoes concentric hypertrophy without chamber dilatation, and cardiac function is usually preserved. The global accumulation of collagen alters the material properties of

the myocardium, resulting in a stiffer, less compliant chamber. In some cases, LV filling and diastolic function are reduced. DHF ensues, accompanied with progression of ECM accumulation in the absence of LV dilatation (Mandinov *et al.*, 2000). Direct evidence is lacking however and the contention can only be affirmatively resolved with measures of diastolic function. In the absence of the latter, other indices are perhaps suggestive of unaffected mechanical activity that is associated with a compensated remodelling phenotype even at 18 months of age; These include unaltered resting heart rate and LV action potential duration, normal heart rate variability, QRS and QT duration and preserved contractile kinetics in isolated ventricular myocytes (Howarth *et al.*, 2004; 2007). Moreover, unchanged apoptosis index and absence of LV dilation may be interrelated findings that further supplement this stance as transition to CHF have been associated primarily with an elevated degree of apoptosis (Fedak *et al.*, 2005). Although focussed investigation into LV function in this model is warranted, and is a key avenue of future exploration, the available data encourages the possibility that mild HG elevation and moderately deranged carbohydrate metabolism alone *may not* be sufficient to produce overt changes in cardiac function. By extension, a paradigm arises wherein HG in DM potentially promotes a setting in which addition of another stressor (obesity, hypertension, hypoxia) is poorly tolerated and ‘tips the balance’ in favour of a cardiomyopathy with well recognized anatomic, molecular and functional landmarks reminiscent of the failing heart. This perspective is reiterated in numerous reports of the combined effects of DM and hypertension and/or obesity, ischemic events etc in experimental T2DM. At this juncture, the utility of the GK rat comes to the fore as it represents a clinically relevant HG-dominated aetiology, providing a *tabula rasa* setting onto which additional ‘stressors’ or comorbidities can be added and cumulative CV outcomes measured. As such, the present study has presented an important rationale for the commencement of experiments wherein adult diabetic GK rats are fed a high sucrose diet, to assess the combined effects of mild T2DM and diet-related obesity on cardiac function, structure and remodelling.

Second, in the absence of an interventional approach, this study is by necessity, correlative in nature. The demonstration that the myocardial bioactive TGF β 1 is upregulated in early in T2DM and can potentially result in many of the features of myocardial remodelling that are associated with HF (e.g., myocyte hypertrophy, interstitial fibrosis, and induction of a foetal pattern of gene expression) suggests that TGF β 1 signalling plays a central role in the pathophysiology of myocardial failure.

However, at present it remains to be determined whether myocardial TGF β 1 mediates (or modulates) remodeling of the myocardium in response to a dysglycemic environment. Moreover, where experimental evidence has demonstrated that the TGF β 1-inhibitor Tranilast can reverse the diastolic dysfunction and histopathological features of DCM in T1DM (Kelly *et al.*, 2007), translation of these findings in diabetic patients is currently hampered by challenges arising from an incomplete understanding of TGF β 1 activation patterns and dissection of fibrogenic vs. immunomodulatory or homeostatic effects of TGF β 1 signalling (Dobacewski *et al.*, 2010), altogether representing an exciting area of future research with several unanswered questions. These include addressing whether TGF β 1 simply represents one of several peptides activated in response to HG that act in concert, or does it occupy a particularly focal position as a distal convergence point for other pathways? Where most experimental observations of TGF β 1 in diabetes are derived from studies performed in young animals, current demonstration of upregulated TGF β 1 in the ageing T2DM rat highlights the importance of understanding the consequences of ageing on the TGF β system. Dissection of the relative roles of TGF β 1, β 2 and β 3 and receptor subtypes and their activation effects on different cell types in the myocardial remodelling process will further determine whether inhibition of TGF β 1 signalling proves to be an effective therapeutic intervention for preventing and ameliorating the development of myocardial failure in DM. In the same vein, analysis of the pro-hypertrophic Akt signalling pathway as an offshoot of TGF β 1 activation in the present study also highlights gaps in present understanding of the that signals converge on such a nodal control point and what HG-sensitive effector pathways may operate downstream. Advancements in the field are not at a stage to allow the full comprehension of how closely related, HG-sensitive kinases such as PKC, AMPK interact or whether their individual properties may be exploited clinically. Nevertheless, the results of the present study do implicate the activation of Akt and its downstream effector p70 in association with a hypertrophic phenotype, proffering the theoretical basis for such a demand.

Third, the primary focus of this work has been on molecular events triggered by HG as an endpoint. While HG is clearly an important prognostic indicator of poor clinical outcome, it may ultimately represent but one proponent of the remodelling process in DM. The same theme is reiterated in previous work suggesting that the direct metabolic changes caused by diabetic HG may not be the only targets in the treatment of DCM (Falcão-Pires *et al.*, 2009). In interpreting the results of this or any other study of DM,

it is important to bear in mind that sequelae, including cardiomyopathy, must be considered a mosaic of both primary and secondary alterations (Thompson, 1988). In this sense, insulin resistance and hyperinsulinemia are key mechanisms outside HG-conditional events in the onset of remodelling changes if the direct actions of insulin upon such processes as the transport of glucose and amino acids across cellular membranes, the regulation of both anabolic and catabolic enzymes, and the stimulation of DNA translation and mRNA transcription are taken into account. Nevertheless, one must appreciate that the involvement of T2DM in HF pathogenesis is associated with a panoply of complementary and intricately interrelated triggers not limited to the effects of HG and altered insulin signalling resulting in oxidative stress, nitrosative stress, signal transduction defects, alterations in $[Ca^{2+}]_i$ handling and mitochondrial dysfunction often acting on a substrate of inherited mutations. As such, it is unlikely that a series or a series of series of experimental studies can fully encompass disease pathophysiology. However, by focussing on the most practical options for intervention, studies like the present have important implications for understanding the basic mechanisms responsible for the myocardial response to HG and for the development of new treatment strategies for DCM and HF. These are briefly summarised below.

7.3 Concluding remarks

Clinical Perspectives

Previous studies have linked favourable changes in ventricular geometry to improved survival (Packer *et al.*, 1991; Pfeffer *et al.*, 1992; Waagstein *et al.*, 1993; Colucci *et al.*, 1996; MERIT-HF study group, 1999; Konstam *et al.*, 1992;1993; Cohn and Ferrari, 2000; Linde and Daubert, 2010), suggesting that remodelling may be a suitable surrogate endpoint for intervention. Although the issue of whether the ageing GK rat represents a decompensated functional phenotype cannot be affirmatively resolved at the present time, the results of this study are still significant in as much as they demonstrate the remodelling effects of chronic HG *per se*. Extrapolated to the clinic where HG almost always clusters with features of the metabolic syndrome, it is likely that the impact of DM on ventricle structure is amplified by high blood pressure and dyslipidemia, compounded by an accelerated atherosclerosis and impaired collateral formation that together exacerbate the existing phenotype. In this regard, further delineation of the role HG as a fundamental cause of nonischemic cardiomyopathy should allow for the development of new therapies aimed at metabolic modulation. The transcriptional alterations that underscored the remodelling phenotype in this study may

also be of particular therapeutic importance. Transcriptional reprogramming has been shown to correlate with loss of cardiac function and, conversely, improvement in cardiac function in response to drug therapy or implantation of a left ventricular assist device is accompanied by normalization of cardiac gene expression (Abraham *et al.*, 2002; Lowes *et al.*, 2002; Blaxall *et al.*, 2003; McKinsey and Olson, 2005). Strategies to control cardiac gene expression, therefore, represent attractive, albeit challenging, approaches for HF therapy in T2DM.

The study design employed here demonstrated that remodelling changes originate in the prediabetic phase that is today understood to be typical of the clinical course of T2DM and for which greatest uncertainty exists regarding impact on the heart and the need for intervention. The results described in this thesis demonstrate that prediabetes represents a morphological intermediate between normal and diabetic states, highlighting a graded effect of IGT on ventricle structure along the type 2 diabetic continuum. When coupled with recently published studies demonstrating an increased prevalence of diastolic dysfunction in prediabetic participants (Stahrenberg, 2010), current data favour the assumption that early preventive measures for good metabolic control may mediate a long term benefit in the diabetic patient. As a corollary, targeting HG and HG-sensitive remodelling mechanisms may represent one possible approach to combat diastolic dysfunction and diastolic heart failure. Ultimate proof-of-concept is a test of blood glucose lowering and is the subject of ongoing trials. A trial of great interest in this perspective is the Outcome Reduction with an Initial Glargine Intervention (ORIGIN) due to end in late 2011, that has recruited 12,612 patients with type 2 DM or impaired glucose tolerance and concomitant CVD, randomizing them to insulin glargine (and omega 3-fatty acids) with the dose titrated to achieve normoglycaemia to assess effects on 5 year incidence of CV events (Gerstein *et al.*, 2008). Another awaited trial is the Acarbose Cardiovascular Evaluation (ACE) trial (Holman and Pan, 2007), a randomised, placebo-controlled trial that investigates the effect of anti-diabetic medication acarbose on secondary prevention of cardiovascular events in approximately 7,500 prediabetic patients with established CVD for a minimum of 4 years. It is anticipated that analyses of these trials may demonstrate that restoration of normoglycemia in prediabetes allays development of remodelling in the myocardium, thus consolidating the present argument for early tight glycemic control.

Conclusion

In conclusion, this study endorses the likely detrimental influence of long-term subtle glucose abnormalities on HF pathogenesis, and extends these observations to the prediabetic range. Because prevention of HF is a major public health goal and no clear improvement in event rates have been noted in the recent past (Recchia and Lionetti, 2010), the present work presents another basis to suggest that targeting HG at early stages is a medical imperative. Further elucidation of the information generated from cellular and molecular models like the present may result in the provision of optimal therapy at an appropriate time to retard HF progression in the dysglycemic patient. Future work with judicious use of experimental models and parallel studies of the human disorder holds great promise in this regard

BIBLIOGRAPHY

Abel DE (2005) Myocardial Insulin Resistance and Cardiac Complications of Diabetes. Current Drug targets- Immune, Endocrine and Metabolic Disorders 5:219-226

Abraham WT, Gilbert EM, Lowes BD et al (2002) Coordinate changes in Myosin heavy chain isoform gene expression are selectively associated with alterations in dilated cardiomyopathy phenotype. Mol Med 8:750-760

Action to Control Cardiovascular Risk in Diabetes Study Group (2008) Effects of intensive glucose lowering in type 2 diabetes. N Engl J Med. 358:2545-2559

Adeghate E, Howarth FC, Rashed H et al (2006) The effect of a fat-enriched diet on the pattern of distribution of pancreatic islet cells in the C57BL/6J mice. Ann N Y Acad Sci 1084: 361–370

Albert NM, Eastwood CA, Edwards ML (2004) Evidence-based practice for acute decompensated heart failure. Critical Care Nurse 24:14-29

Alessi DR, Kozlowski MT, Weng QP et al (1998) 3-phosphoinositide-dependent protein kinase 1 (PDK1) phosphorylates and activates the p70S6 kinase in vivo and in vitro, Current Biology 8: (2): 69–81

Animals (Scientific Procedures) Act 1986 Online
<http://www.homeoffice.gov.uk/science-research/animal-research/>
http://www.opsi.gov.uk/acts/acts1986/pdf/ukpga_19860014_en.pdf
Accessed 12 Feb 2008

Annes JP, Munger JS, Rifkin DB (2003). Making sense of latent TGFbeta activation. J Cell Sci 116(Pt 2):217-224

Anselmino M, Malmberg K, Mellbin L et al (2010) Overview of the importance of glycaemic control for cardiovascular events in the in-and out-patient setting. Rev Endocr Metab Disord 11:87–94

Anversa P, Hiler B, Ricci R et al (1986) Myocyte cell loss and myocyte hypertrophy in the aging rat heart. J Am Col Cardiol 8: 1441–1448

Aronow WS and Ahn C (1999) Incidence of heart failure in 2737 older persons with and without diabetes mellitus. Chest 115: 867–868

Ares-Carrasco S, Picatoste B, Benito-Martin A et al (2009) Myocardial fibrosis and apoptosis, but not inflammation, are present in long-term experimental diabetes. Am J Physiol Heart Circ Physiol 297: H2109–H2119

Asghar O, Al-Sunni A, Khavandi K et al (2009) Diabetic cardiomyopathy. Clin Sci 116:741-760

Ban CR and Twigg SM (2008) Fibrosis in diabetes complications: Pathogenic mechanisms and circulating and urinary markers. Vasc Health Risk Manag 4(3): 575-596

- Bandyopadhyay P (2006) Cardiovascular disease and diabetes mellitus. *Drug news Perspect* 19(6): 369-375
- Banerjee I, Yekkala K, Borg TK et al (2006) Dynamic interactions between myocytes, fibroblasts, and extracellular matrix. *Ann N Y Acad Sci* 1080: 76–84
- Banerjee I, Fuseler JW, Price RL et al (2007) Determination of cell types and numbers during cardiac development in the neonatal and adult rat and mouse. *Am J Physiol* 293: H1883–H1891
- Barr ELM, Zimmet PZ, Welborn TA et al (2007) Risk of Cardiovascular and All – Cause Mortality in Individuals with Diabetes Mellitus, Impaired Fasting Glucose, and Impaired Glucose tolerance. The Australian Diabetes, Obesity, and Lifestyle Study (AusDiab). *Circulation* 116: 151-157
- Baum VC, Clark WA, Pelligrino DA (1989). Cardiac myosin isoenzyme shifts in non-insulin treated spontaneously diabetic rats. *Diabetes Res* 10: 187-190
- Bauters C, Lamblin N, McFadden E et al (2003) Influence of diabetes mellitus on heart failure risk and outcome. *Cardiovasc Diabetol* 2:1
Available via: <http://www.cardiab.com/content/2/1/1> Accessed 8th February 2009
- Begum N and Ragolia L(1998) Altered regulation of insulin signaling components in adipocytes of insulin-resistant type II diabetic Goto-Kakizaki rats. *Metabolism* 47:54-62
- Bell DS (2003) Diabetic cardiomyopathy. *Diabetes Care* 26: 2949–2951
- Benjamin IJ and Schneider MD (2005) Learning from failure: congestive heart failure in the postgenomic age. *J Clin Invest* 115(3):495–499
- Bergman M (2009) Inadequacies of absolute threshold levels for diagnosing prediabetes. *Diabetes Metab Res Rev* 26:3-6
- Berk B, Fujiwara K and Lehoux S (2007) ECM remodelling in hypertensive heart disease. *J Clin Invest* 117(3):568-575
- Bertoni AG, Goff DC, D’Agostino RB et al (2006) Diabetic cardiomyopathy and subclinical cardiovascular disease: the Multi-Ethnic Study of Atherosclerosis (MESA). *Diabetes Care* 29:588–594
- Bertrand L, Horman S, Beauloye C and Vanoverschelde JL (2008) Insulin signalling in the heart. *Cardiovasc Res* 79(2):238-248
- Bianchi C, Miccoli R, Penno G et al (2008) Primary prevention of cardiovascular disease in people with dysglycemia. *Diabetes Care* 31:S208-S214
- Bidasee KR, Zhang Y, Hong Shao C et al(2004) Diabetes Increases Formation of Advanced Glycation End Products on Sarco(endo)plasmic Reticulum Ca^{2+} -ATPase. *Diabetes* 53(2):463-473

Blaxall BC, Tschannen-Moran BM, Milano CA et al (2003) Differential gene expression and genomic patient stratification following left ventricular assist device support. *J Am Coll Cardiol* 41:1096-1106

Boudina S, Sena S, O'Neill BT et al (2005). Reduced mitochondrial oxidative capacity and increased mitochondrial uncoupling impair myocardial energetics in obesity. *Circulation* 112: 2686–2695

Boudina S and Abel DE (2007) Diabetic Cardiomyopathy Revisited. *Circulation* 115:3213-3223

Boudina A and Abel DE (2010) Diabetic cardiomyopathy, causes and effects. *Rev Endocr Metab Disord* 11:31–39

Bowers SLK, Banerjee I, Baudino TA (2010) The extracellular matrix: At the centre of it all. *J Mol Cell Cardiol* 474-482

Bracken NK, Qureshi MA, Singh J et al (2003) Mechanism underlying contractile dysfunction in streptozotocin induced type 1 and type diabetic cardiomyopathy. In: *Atherosclerosis, Hypertension and Diabetes* (Eds. N.S. Dhalla et al) Kluwer Academic Publishers, pp 387-408

British heart foundation statistic website. Morbidity from heart failure. Available via <http://www.heartstats.org/datapage.asp?id=1595> Accessed 9 February 2010

British heart foundation statistics website. Survival after initial diagnosis of heart failure, around 2002, London. Available via <http://www.heartstats.org/atozpage.asp?id=2392> Accessed 9 February 2010

British Medical Association, 2004. *Diabetes Mellitus: An update for healthcare professionals*. London: BMA 2004 Available via <http://www.bma.org.uk/ap.nsf/Content/Diabetes> Accessed 5 April 2008

Brownlee M (2001) Biochemistry and molecular cell biology of diabetic complications. *Nature* 414:813–820

Brownlee M (2005) The pathobiology of diabetic complications: a unifying mechanism. *Diabetes* 54:1615 –1625

Brownlee M, Cerami A, Vlassara H (1988) Advanced glycosylation end products in tissue and the biochemical basis of diabetic complications. *N Engl J Med* 318:1315-1321

Brownlee M (2005) The pathobiology of diabetic complications: a unifying mechanism. *Diabetes* 54:1615 –1625

Buchanan J, Mazumder PK, Hu P et al (2005) Reduced cardiac efficiency and altered substrate metabolism precedes the onset of hyperglycemia and contractile dysfunction in two mouse models of insulin resistance and obesity. *Endocrinology* 146: 5341–5349

Buckberg G, Hoffman JI, Mahajan A et al (2008) Cardiac mechanics revisited: the relationship of cardiac architecture to ventricular function. *Circulation* 118:2571–2587

Burnette WN (1981) "Western blotting": electrophoretic transfer of proteins from sodium dodecyl sulfate--polyacrylamide gels to unmodified nitrocellulose and radiographic detection with antibody and radioiodinated protein. *Anal Biochem* 112(2):195-203

Burgess ML, McCrea JC, Hedrick HL (2001) Age-associated changes in cardiac matrix and integrins. *Mech Ageing Dev* 122(15):1739-1756

Cai L and Kang JY (2001) Oxidative stress and diabetic cardiomyopathy. *Cardiovasc Toxicol* 1:181–193

Cai L and Kang JY (2003) Cell Death and Diabetic Cardiomyopathy. *Cardiovasc Toxicol* 3(3):219-228

Cai L, Li W, Wang G et al (2002) Hyperglycemia-Induced Apoptosis in Mouse Myocardium: Mitochondrial Cytochrome *c*-Mediated Caspase-3 Activation Pathway. *Diabetes* 51:1938–1948

Cameron J and Cruikshank JK (2007) Glucose, Insulin, diabetes and mechanisms of arterial dysfunction. *Clin Exp Pharm Physiol* 34:677-682

Cefalu WT and Watson K (2008) Intensive glycemic control and cardiovascular disease: observations from the ACCORD study. Now what can a clinician possibly think? *Diabetes* 57:1163-1165

Chandrashekar Y, Sen S, Anway R et al (2004) Long-term caspase inhibition ameliorates apoptosis, reduces myocardial troponin-I cleavage, protects left ventricular function, and attenuates remodeling in rats with myocardial infarction. *J Am Coll Cardiol* 43:295-301

Chattou, S, Diacono J and Feuvray D (1999) Decrease in sodium-calcium exchange and calcium currents in diabetic rat ventricular myocytes. *Acta Physiol Scand* 166: 137-144

Choi KM, Zhong Y, Hoit BD et al (2002) Defective intracellular (Ca²⁺) signaling contributes to cardiomyopathy in Type 1 diabetic rats. *Am J Physiol (Heart Circ Physiol)* 283: H1398–H1408

Clement S, Chaponnier C and Gabbiani G (1999) A Subpopulation of Cardiomyocytes Expressing α -Skeletal Actin Is Identified by a Specific Polyclonal Antibody. *Circ Res* 85(10): e51

Cohn JN (1995) Structural basis for heart failure: ventricular remodeling and its pharmacological inhibition. *Circulation* 91:2504 –2507

Cohn JN, Archibald DG, Ziesche S et al (1986) Effect of vasodilator therapy on mortality in chronic congestive heart failure. Results of a Veterans Administration Cooperative Study. *N Engl J Med* 314:1547–1552

Cohn JN and Ferrari R (2000) Cardiac remodelling-concepts and clinical implications: a consensus paper from an international forum on cardiac remodelling. *J Am Coll Cardiol* 35:569-582

Colucci WS, Packer M, Bristow MR et al (1996) Carvedilol inhibits clinical progression in patients with mild symptoms of heart failure. *Circulation* 94:2800–2806

Cooper ME and El-Osta A (2010) Mechanisms and implications for diabetic complications. *Circ Res* 107:1403-1413

Cosyns B, Droogmans S, Weytjens C et al (2007) Effect of streptozotocin-induced diabetes on left ventricular function in adult rats: an in vivo Pinhole Gated SPECT study. *Cardiovasc Diabetol* 6: 30

Coutinho M, Gerstein HC, Wang Y et al (1999) The relationship between glucose and incident cardiovascular events: a metaregression analysis of published data from 20 studies of 95,783 individuals followed for 12.4 years. *Diabetes Care* 22:233–240

Dai RP, Sheen ST, He BP et al (2004) Differential expression of cytokines in the rat heart in response to sustained volume overload. *Eur J Heart Fail* 6 (6): 693-703

Darmellah A, Baetz D, Prunier F (2007). Enhanced activity of the myocardial Na⁺/H⁺ exchanger contributes to left ventricular hypertrophy in the Goto-Kakizaki rat model of type 2 diabetes: critical role of Akt. *Diabetologia* 50: 1335–1344

Davidoff AJ, Pinault FM, Rodgers RL (1990) Ventricular relaxation of diabetic spontaneously hypertensive rat. *Hypertension* 15: 643-651

Definition and diagnosis of diabetes mellitus and intermediate hyperglycemia: report of a WHO/IDF consultation (2006). Available via http://www.who.int/diabetes/publications/Definition%20and%20diagnosis%20of%20diabetes_new.pdf, Accessed: 10 January 2010

De Tombe PP (1998) Altered contractile function in heart failure. *Cardiovasc Res* 37(2):367-380

Devereux RB, Roman MJ, Paranicas M et al (2000) Impact of diabetes on cardiac structure and function: the strong heart study. *Circulation* 101: 2271–2276

Dhalla AK, Hill MF, Singal PK (1996) Role of oxidative stress in transition of hypertrophy to heart failure. *J Am Coll Cardiol* 28: 506–514

Dhalla NS, Liu X, Panagia V et al (1998) Subcellular remodeling and heart dysfunction in chronic diabetes. *Cardiovasc Res* 40: 239–247

Dhalla NS, Pierce GN, Innes IR & Beamish RE (1985) Pathogenesis of cardiac dysfunction in diabetes mellitus. *Can J Cardiol* 1: 263–281

Diabetes Control and Complications Trial Research Group (1993) The effect of intensive treatment of diabetes on the development and progression of long-term complications in insulin-dependent diabetes mellitus. *N Engl J Med* 329:977-986

Diaz R, Paolasso EA, Piegas LS, et al (1998) Metabolic modulation of acute myocardial infarction: the ECLA glucose-insulin-potassium pilot trial. *Circulation* 98: 2227–2234

Di Bonito P, Moio N, Cavuto L et al (2005) Early detection of diabetic cardiomyopathy: usefulness of tissue Doppler imaging. *Diabet Med* 22: 1720–1725

Diabetes UK (2010). Diabetes in the UK 2010. Key statistics on diabetes. Available via http://www.diabetes.org.uk/Documents/Reports/Diabetes_in_the_UK_2010.pdf Accessed 4th November 2010

Diabetes UK Report (2009) Prediabetes; Preventing the type 2 diabetes epidemic. Available via <http://www.diabetes.org.uk/Documents/Reports/PrediabetesPreventingtheType2diabetesEpidemicOct2009report.pdf> Accessed: 10 Jan 2010

Dillmann WH (1989) Diabetes and thyroid-hormone-induced changes in cardiac function and their molecular basis. *Annu Rev Med* 40: 373-394

Diwan A and Dorn GW (2007) Decompensation of Cardiac Hypertrophy: Cellular Mechanisms and Novel Therapeutic Targets. *Physiology* 22: 56-64

Dobaczewski M, Chen W, Frangogiannis NG (2010) Transforming growth factor signalling in cardiac remodelling. *J Mol Cell Cardiol* doi: [doi:10.1016/j.yjmcc.2010.10.033](https://doi.org/10.1016/j.yjmcc.2010.10.033)

Dokken BB (2008) The Pathophysiology of Cardiovascular Disease and Diabetes: Beyond Blood Pressure and Lipids. *Diabetes Spectrum* 21(3):160-165

Douglas PS, Morrow R, Ioli A et al (1989). Left ventricular shape, afterload, and survival in idiopathic dilated cardiomyopathy. *J Am Coll Cardiol* 13:311–315

Duckworth W, Abraira C, Moritz T et al (2009) Glucose control and vascular complications in veterans with type 2 diabetes. *N Engl J Med* 360:129-39

El-Omar MM, Yang Z-K, Philips AO et al (2004) Cardiac dysfunction in the Goto-Kakizaki rat A model of Type 2 diabetes mellitus. *Basic Res Cardiol* 99(2):133-141

Falcão-Pires I, Gonçalves N, Moura C et al (2009) Effects of Diabetes Mellitus, Pressure-Overload and Their Association on Myocardial Structure and Function. *Am J Hypertens* 22(11): 1190–1198

Fang ZY, Prins JB, Marwick TH (2004) Diabetic cardiomyopathy: evidence, mechanisms, and therapeutic implications. *Endocr Rev* 25: 543–567

- Farah MCK, DeCastro CRP, Moreira VM, Riso ADM et al (2009) The Myocardium in Tetralogy of Fallot: a Histological and Morphometric Study *Arq Bras Cardiol* 92(3):160-167
- Fedak PW, Verma S, Weisel RD et al (2005) Cardiac remodeling and failure: From molecules to man (Part II) *Cardiovasc Pathol* 14 (2005) 49– 60
- Fein FS (1996) Diabetic Cardiomyopathy. In: *The heart in Diabetes*. (Eds: Chatham JC, Forder JR, McNeill JH) Norwell, MA, Kluwer, pp 1-36
- Fein FS, Kornstein LB, Strobeck JE, Capasso JM, et al (1980). Altered myocardial mechanics in diabetic rats. *Circ Res* 47: 922-933
- Fein FS and Sonnenblick EH (1985). Diabetic cardiomyopathy. *Prog Cardiovasc Dis* 27:255-270
- Ferrari AU, Radaelli A and Centola M (2003) Aging and the cardiovascular system *J Appl Physiol* 95(6): 2591-2597
- Fiordaliso F, Li B, Latini R et al (2000) Myocytes death in streptozotocin-induced diabetes in rats is angiotensin II-dependent. *Lab Invest* 80:513–527
- Foo RS, Mani K, Kitsis RN (2005) Death begets failure in the heart. *J Clin Invest* 115:565-571
- Forero MG, Pennack JA, Learte AR et al (2009) DeadEasy Caspase: Automatic Counting of Apoptotic Cells in *Drosophila* 4(5):e5441
- Fox CS, Coady S, Sorlie PD et al (2007) Increasing cardiovascular disease burden due to diabetes mellitus: The Framingham Heart Study. *Circulation* 115(12):1544-50
- Francis GS (2001) Diabetic cardiomyopathy: fact or fiction (Editorial)? *Heart* 85:247 – 248
- Francis GS (2001) Pathophysiology of chronic heart failure. *Am J Med* 110 (suppl 7A): 37S–46S
- Fredersdorf S, Thumann C, Ulucan C et al (2004) Myocardial hypertrophy and enhanced left ventricular contractility in Zucker diabetic fatty rats. *Cardiovasc Pathol* 13(1): 11-19
- Fujii M, Wada A, Tsutamoto T et al (2002). Bradykinin improves left ventricular diastolic function under long-term angiotensin-converting enzyme inhibition in heart failure. *Hypertension* 39: 952–957
- Fujita M, Asanuma H, Kim J et al (2007) Impaired glucose tolerance: a possible contributor to left ventricular hypertrophy and diastolic dysfunction. *Int J Cardiol* 118(1):76-80

Gaede P, Hildebrandt P, Hess G et al (2005) Plasma N-terminal pro-brain natriuretic peptide as a major risk marker for cardiovascular disease in patients with type 2 diabetes and microalbuminuria. *Diabetologia* 48:156-163

Gao F, Gao E, Yue TL, Ohlstein EH (2002) Nitric Oxide Mediates the Antiapoptotic Effect of Insulin in Myocardial Ischemia-Reperfusion: The Roles of PI3-Kinase, Akt, and Endothelial Nitric Oxide Synthase Phosphorylation. *Circulation* 105:1497-1502

Galderisi M (2006) Diastolic dysfunction and diabetic cardiomyopathy: evaluation by Doppler. *J Am Coll Cardiol* 48:1548–1551

Gauguier D, Froguel P, Parent V et al (1996) Chromosomal mapping of genetic loci associated with non-insulin dependent diabetes in the GK rat. *Nat Genet* 12:38–43

Gerstein HC, Miller ME, Byington RP et al (2008) Action to Control Cardiovascular Risk in Diabetes (ACCORD) Study Group Effects of intensive glucose lowering in type 2 diabetes. *N Engl J Med* 358:2545-2559

Gill PS, Davis R, Davies M et al (2009) Rationale and study design of a cross sectional study documenting the prevalence of Heart Failure amongst the minority ethnic communities in the UK: the E-ECHOES Study (Ethnic - Echocardiographic Heart of England Screening Study) *BMC Cardiovasc Disord* 9:47

Goldfine AB and Beckman JA (2008) Life and death in Denmark: lessons about diabetes and coronary heart disease. *Circulation* 117(15):1914-1917

Goodfellow J (1997) Microvascular heart disease in Diabetes mellitus. *Diabetologia* 40:S130-S133

Goraksha-Hicks P and Rathmell JC (2009) TGF- β : A New Role for an Old AktTOR. *Dev Cell* 17(1):6–8

Goto Y, Kakizaki M and Masaki N (1975) Spontaneous diabetes produced by selective breeding of normal Wistar rats. *Proc Jpn Acad* 51: 80–85

Gottdiener JS, Arnold AM, Aurigemma GP et al (2000) Predictors of congestive heart failure in the elderly: the Cardiovascular Health Study. *J Am Coll Cardiol* 35:1628–1637

Graham HK, Horn M and Trafford AW (2008) Extracellular matrix profiles in the progression to heart failure. European Young Physiologists Symposium Keynote Lecture- Bratislava. *Acta Physiol. (Oxf)* 194: 3–21

Graham HK and Trafford AW (2007) Spatial disruption and enhanced degradation of collagen with the transition from compensated ventricular hypertrophy to symptomatic congestive heart failure. *Am J Physiol* 292(3):H1364-H1372

Grönholm T, Cheng ZJ, Palojoki E et al (2005) Vasopeptidase inhibition has beneficial cardiac effects in spontaneously diabetic Goto–Kakizaki rats. *Eur J Pharmacol* 519(3):267-276

- Gudjonsson T and Rahko PS (2002) Relation of "inotropic reserve" to functional capacity in heart failure secondary to ischemic or nonischemic cardiomyopathy. *Am J Cardiol* 89: 1057–1061
- Guerra S, Leri A, Wang X et al (1999) Myocyte death in the failing human heart is gender dependent. *Circ Res* 85:856–866
- Gupta S, Prahash AJ and Anand IS (2000) Myocyte contractile function is intact in the post-infarct remodeled rat heart despite molecular alterations. *Cardiovasc Res* 48:77–88
- Gupte S, Labinskyy N, Gupte R et al (2010) Role of NAD(P)H Oxidase in Superoxide Generation and Endothelial Dysfunction in Goto-Kakizaki (GK) Rats as a Model of Nonobese NIDDM. *PLoS One* 25(7):e11800
- Gustafsson I, Kistorp CN, James MK et al (2007) OPTIMAAL Study Group. Unrecognized glycometabolic disturbance as measured by hemoglobin A1c is associated with a poor outcome after acute myocardial infarction. *Am Heart J* 154:470-476
- Gutierrez C, Blanchard DG (2004) Diastolic heart failure: challenges of diagnosis and treatment. *Am Fam Phys* 69:2609–2616
- Hamby RI, Zoneraich S, Sherman L (1974) Diabetic cardiomyopathy. *JAMA* 229(13):1749–1754
- Hansen A, Haass M, Zugck C et al (2001) Prognostic value of Doppler echocardiographic mitral inflow patterns: Implications for risk stratification in patients with chronic congestive heart failure. *J Am Coll Cardiol* 37: 1049-1055
- Hayakawa Y, Chandra M, Miao W et al (2003) Inhibition of cardiac myocyte apoptosis improves cardiac function and abolishes mortality in the peripartum cardiomyopathy of $\alpha(q)$ transgenic mice. *Circulation* 108: 3036–3041
- Wells C and Gordon E (2008) Geographical variations in premature mortality in England and Wales. *Health Statistics Quarterly* 2008. In Office for National Statistics. Available via: http://www.statistics.gov.uk/downloads/theme_health/HSQ38
Accessed: 19th April 2010
- Held C, Gerstein HC, Yusuf S et al (2007) ONTARGET/TRANSCEND Investigators. Glucose levels predict hospitalization for congestive heart failure in patients at high cardiovascular risk. *Circulation* 115:1371–1375
- He JG, Chen YL, Chen BL et al (2010) B-type natriuretic peptide attenuates cardiac hypertrophy via the transforming growth factor- β 1/smad7 pathway *in vivo* and *in vitro*. *Clin Exp Pharmacol Physiol* 37(3) 283-289
- Hermida N, Lopez B, Gonzalez A et al (2009). A synthetic 666 peptide from transforming growth factor-beta1 type III receptor prevents myocardial fibrosis in spontaneously hypertensive rats. *Cardiovasc Res* 81: 668 601–609
- Hescheler J and Fleischmann BK (2000) Integrins and cell structure:powerful determinants of heart development and heart function. *Cardiovasc Res* 47(4) 645-647

Hilfiker-Kleiner D, Landmesser U, Drexler H (2006) Molecular Mechanisms in Heart Failure *J Am Coll Cardiol* 48:56-66

Hills CE, Bland R, Benett J et al (2009) TGF-beta1 mediates glucose-evoked up-regulation of connexin-43 cell-to-cell communication in HCD-cells. *Cell Physiol Biochem* 24(3-4):177-186

Hobbs FDR, Kenkre JE, Roalfe AK et al (2002) Impact of heart failure and left ventricular systolic dysfunction on quality of life: a cross-sectional study comparing chronic cardiac and medical disorders and a representative adult population. *Eur J Heart Fail* 23:1867-1876

Hobbs R and Boyle A (2010) Heart failure. In *Cleveland Clinic: Current Clinical Medicine*, 2nd edition, Saunders Ltd.

Available via: <http://www.mdconsult.com/books/page.do?eid=4-u1.0-B978-1-4160-6643-9..00026-6&isbn=978-1-4160-6643-9&type=bookPage&from=content&uniquId=234180712-4>

Accessed 5th September 2010

Holman RR and Pan CY (2007) Acarbose Cardiovascular Evaluation (ACE) trial in prediabetic subjects. Presented at the 2nd International Congress on Prediabetes and the Metabolic Syndrome, April 25–28, 2007. *Diabetes & Vascular Disease Research* 4(1) S128

Horst D, Rau H, Walfish PJ et al (1997) CTLA4 Alanine-17 Confers Genetic Susceptibility to Graves' Disease and to Type 1 Diabetes Mellitus. *J Clin Endo Metab* 82(1): 143-146

Houser SR and Marguiles KB (2003) Is Depressed Myocyte Contractility Centrally Involved in Heart Failure? *Circ Res* 92:350

Houser SR, Piacentino V, Weisser J (2000) Abnormalities of calcium cycling in the hypertrophied and failing heart. *J Mol Cell Cardiol* 32:1595-1607

Howarth FC, Adem A, Adeghate EA et al (2005) Distribution of atrial natriuretic peptide and its effects on contraction and intracellular calcium in ventricular myocytes from streptozotocin-induced diabetic rat. *Peptides* 26:691 –700

Howarth FC, Shafiullah M and Qureshi MA (2007) Chronic effects of type 2 diabetes mellitus on cardiac muscle contraction in the Goto-Kakizaki rat. *Exp Physiol* 92:1029-1036

Howarth FC, Qureshi MA, Bracken NK et al (2001) Time-dependent effects of streptozotocin-induced diabetes on contraction of ventricular myocytes from rat heart. *Emirates Med J* 19: 35–41

Howarth FC, Qureshi MA, White E (2002) Effects of hyperosmotic shrinking on ventricular myocyte shortening and intracellular Ca²⁺ in streptozotocin-induced diabetic rats. *Pflugers Arch* 444:446 –451

Howarth FC, Qureshi A, Singh J (2004) Effects of acidosis on ventricular myocyte shortening and intracellular Ca^{2+} in streptozotocin-induced diabetic rats. *Mol Cell Biochem* 261: 227–233

Howarth FC, and Qureshi MA (2006) Effects of carbenoxolone on heart rhythm, contractility and intracellular calcium in streptozotocin-induced diabetic rat. *Mol Cell Biochem* 289 :21-29

Hunt SA, Abraham WT, Chin MH et al (2005) ACC/AHA 2005 guideline update for the diagnosis and management of chronic heart failure in the adult: a report of the American College of Cardiology/American Heart Association Task Force on Practice Guidelines (Writing Committee to Update the 2001 Guidelines for the Evaluation and Management of Heart Failure). *Circulation* 112:e154-e235

Hutchinson KR, Stewart JA and Lucchesi PA (2010) Extracellular matrix remodelling during the progression of volume overload-induced heart failure. *J mol Cell Cardiol* 48:564-569

Ingelsson E, Sundstrom J, Arnlov J et al (2005). Insulin resistance and risk of congestive heart failure. *294:334-341*

Ishihara M, Inoue I, Kawagoe T et al (2001) Diabetes mellitus prevents ischemic preconditioning in patients with a first acute anterior wall myocardial infarction. *J Am Coll Cardiol* 38(4):1007-1011

Ishitani T, Hattori Y, Sakuraya F, Onozuka H et al (2001) Effects of calcium sensitizers on contraction, calcium transients and myofilament sensitivity in the diabetic rat myocardium: potential usefulness as inotropic agents. *J pharmacol Exp Ther* 298: 613-622

Iribarren C, Karter AJ, Go AS et al (2001) Glycemic Control and Heart Failure Among Adult Patients With Diabetes. *Circulation*. 103:2668-2673

Jackson CV, McGrath GM, Tahiliani AG et al (1985) A functional and ultrastructural analysis of experimental diabetic rat myocardium. *Diabetes* 34:876-883

Jax TW (2010) Metabolic memory: a vascular perspective. *Cardiovasc Diabetol* 9:51
doi: 10.1186/1475-2840-9-51. Available via
<http://www.ncbi.nlm.nih.gov/pmc/articles/PMC2946275/> Accessed 12th Dec 2010

Jessup M and Brozena S (2003) Heart failure. *N Engl J Med* 348:2007-2018

Jonassen AK, Brar BK, Mjos OD, et al (2000) Insulin administered at reoxygenation exerts a cardioprotective effect in myocytes by a possible antiapoptotic mechanism. *J Mol Cell Cardiol* 32: 757–764

Jugdutt BI (2010) Aging and heart failure: changing demographics and implications for therapy in the elderly. *Heart Fail Rev* 15 (5):401-405

Kahn RC (2005) Ed. Joslin's Diabetes Mellitus. Lippincott Williams and Wilkins pp 89-91

Kajstura J, Fiordaliso F, Andreoli AM et al (2001). IGF-1 overexpression inhibits the development of diabetic cardiomyopathy and angiotensin II-mediated oxidative stress. *Diabetes* 50: 1414–1424

Kaminski M, Szepietowska B, Bonda T et al (2009) CCN2 protein is an announcing marker for cardiac remodeling following STZ-induced moderate hyperglycemia in mice. *Pharmacol Rep* 61(3):496-503

Kannel WB, Hjortland M, Castelli WP (1974) Role of diabetes in congestive heart failure: The framingham study. *Am J Cardiol* 34:29–34

Kapoun AM, Liang A, O'Young G et al (2004) B-type natriuretic peptide exerts broad functional opposition to transforming growth factor-beta in primary human cardiac fibroblasts: fibrosis, myofibroblast conversion, proliferation, and inflammation. *Circ Res* 94:453–461

Kawaguchi M, Asakura T, Saito F et al (1999) Changes in diameter size and F-actin expression in the myocytes of patients with diabetes and streptozotocin-induced diabetes model rats. *J Cardiol* 34:333–339

Kawano K, Hirashima T, Mori S et al (1991) New inbred strain of Long-Evans Tokushima lean rats with IDDM without lymphopenia. *Diabetes* 40:1375-1381.

Kawano K, Hirashima T, Mori S (1992) Spontaneous long-term hyperglycemic rat with diabetic complications. Otsuka Long-Evans Tokushima Fatty (OLETF) strain. *Diabetes* 41:1422-1428

Kelly DJ, Zhang Y, Connelly et al (2007) Trilast attenuates diastolic dysfunction and structural injury in experimental diabetic cardiomyopathy. *Am J Physiol (Heart Circ Physiol)* 293: H2860-H2869

Khaw KT, Wareham N, Bingham S et al (2004) Association of hemoglobin A1c with cardiovascular disease and mortality in adults: The European prospective investigation into cancer in Norfolk. *Ann Intern Med* 141:413-420

Kita Y, Shimizu M, Sugihara N, Shimizu K et al (1991) Correlation between histopathological changes and mechanical dysfunction in diabetic rat hearts. *Diabetes Res Clin Pract* 11(3):177-188

Koeppen BA and Stanton BM (2008) In: Berne and Levy Physiology with STUDENT CONSULT online access. Mosby International, London. pp 256-267

Knollmann BC and Roden DM (2008) A genetic framework for improving arrhythmia therapy *Nature* 451:929-936

Available via: <http://www.nature.com/nature/journal/v451/n7181/full/nature06799.html>

Accessed: 08/09/2010

Komajda M, Wimart MC and Thibout E (1994) The ATLAS study (Assessment of Treatment with Lisinopril and Survival); justification and objectives. *Arch Mal Coeur Vaiss* 87:45–50

Konstam MA, Kronenberg MW, Rousseau MF, et al (1993) Effects of the angiotensin converting enzyme inhibitor enalapril on the long-term progression of left ventricular dilatation in patients with asymptomatic systolic dysfunction. 88:2277–2283

Konstam MA, Rousseau MF, Kronenberg MW, et al (1992) Effects of the angiotensin converting enzyme inhibitor enalapril on the long-term progression of left ventricular dysfunction in patients with heart failure. *Circulation* 86:431–438

Kotsanas G, Delbridge LM, Wendt IR (2000) Stimulus interval-dependent differences in Ca^{2+} transients and contractile responses of diabetic rat cardiomyocytes. *Cardiovasc Res* 46:450-462

Kumar P and Clarke ML (2009) In. Kumar and Clark's clinical medicine, 7th edition. Saunders Ltd, pp:1069-1123

Kurrelmeyer K, Kalra D, Bozkurt B, Wang F et al (1998) Cardiac remodeling as a consequence and cause of progressive heart failure. *Clin Cardiol* 12(1):114-119

Kwak HB, Song W and Lawler JM (2006) Exercise training attenuates age-induced elevation in Bax/Bcl-2 ratio, apoptosis and remodelling in the rat heart. *FASEB J* 20(6):791-793

LaFramboise WA, Bombach KL, Dhir RJ et al (2005) Molecular dynamics of the compensatory response to myocardial infarct. *J Mol Cell Cardiol* 38:103 -117

Lagadic-Gossman D, Buckler KJ, Le Prigent K and Feuvray D (1996) Altered Ca^{2+} handling in ventricular myocytes isolated from diabetic rats. *Am J Physiol* 270: H1529–H1537

Lakhan S and Harle L (2008) Cardiac fibrosis in the elderly, normotensive athlete:case report and review of the literature. *Diagnostic Pathol* 3:12

Langenickel T, Pagel I, Hobnel K et al (2000) Differential regulation of cardiac ANP and BNP mRNA in different stages of experimental heart failure. *Am J Physiol Heart Circ Physiol* 278:HI500-HI506

Leask A, Abraham DJ (2004) TGF-beta signaling and the fibrotic response. *FASEB J* 18:816–827

Leask A (2010) Potential therapeutic targets for cardiac fibrosis: TGF β , angiotensin, endothelin, CCN2 and PGDF, partners in fibroblast activation. *Circ Res* 106:1675

Legato MJ, Mulieri LA, Alpert NR (1984) The ultrastructure of myocardial hypertrophy: Why does the compensated heart fail? *Eur Heart J* 5(F):251-259

Lefter AM, Ma XL, Weyrich AS (1993) Mechanism of the cardioprotective effect of transforming growth factor beta 1 in feline myocardial ischemia and reperfusion. *Proc Natl Acad Sci USA* 90:1018–1022

- Lefer AM, Tsao P, Aoki N et al (1990) Mediation of cardioprotection by transforming growth factor-beta. *Science* 249(4964):61-64
- Lenzen S (2008) The mechanisms of alloxan- and streptozotocin-induced diabetes. *Diabetologia* 51:216–226
- Lijnen PJ, Petrov VV, Fagard RH (2000) Induction of cardiac fibrosis by transforming growth factor β 1. *Mol Genet Metab* 71:418-435
- Linde C and Daubert C (2010) Cardiac resynchronization therapy in patients with new York heart association class I and II heart failure: An approach to 2010. *Circulation* 122:1037:1043
- Lin C and Bissell M (1993) Multi-faceted regulation of cell differentiation by extracellular matrix. *FASEB J* 7:737–743
- Li RK, Li G, Mickle D et al (1997) Overexpression of transforming growth factor-beta1 and insulin-like growth factor-I in patients with idiopathic hypertrophic cardiomyopathy. *Circulation* 96:874-881
- Lionetti V and Recchia FA (2002) New therapies for the failing heart: trans-genes versus trans-cells. *156(3):130-135*
- Lips DJ, DeWindt LJ, Van Kraaj et al (2003) Molecular determinants of myocardial hypertrophy and failure: alternative pathways for beneficial and maladaptive hypertrophy. *Eur Heart J* 24 (10): 883-896
- Liu JE, Palmieri V, Roman MJ et al (2001) The impact of diabetes on left ventricular filling pattern in normotensive and hypertensive adults: the Strong Heart Study. *J Am Coll Cardiol* 37: 1943–1949
- Li YY, Feng YQ, Kadokami T et al (2000) Myocardial Extracellular matrix remodelling in transgenic mice overexpressing tumour necrosis factor alpha can be modulated by anti-tumour necrosis factor alpha therapy. *PNAS* 97(23) 12746-12751
- Lowes BD, Gill EA, Abraham WT, et al (1999) Effects of carvedilol on left ventricular mass, chamber geometry and mitral regurgitation in chronic heart failure. *Am J Cardiol* 83:1201–1205
- Lowes BC, Minobe W, Abraham WT et al (1997) Changes in gene expression in the intact human heart. Downregulation of alpha-myosin heavy chain in hypertrophied, failing ventricular myocardium. *J Clin Invest* 100:2315–2324
- Lowry OH, Rosebrough NJ, Farr AL et al (1951) Protein measurement with the Folin phenol reagent. *J Biol Chem* 193(1):265-275
- Lowes BD, Gilbert EM, Abraham WT et al (2002) Myocardial gene expression in dilated cardiomyopathy treated with beta-blocking agents. *N Engl J Med* 346:1357-1365

Lukowicz TV, Fischer M, Hense HW et al (2005) BNP as a marker of diastolic dysfunction in the general population: Importance of left ventricular hypertrophy. *Eur J Heart Fail* 7(4): 525-531

MacDonald MR, Petrie MC, Hawkins NM (2008) Diabetes, left ventricular systolic dysfunction, and chronic heart failure. *Eur Heart J* 29 (10): 1224-1240

Mak KH, Moliterno DJ, Granger CB et al (1997) Influence of diabetes mellitus on clinical outcome in the thrombolytic era of acute myocardial infarction. GUSTO-I Investigators. Global Utilization of Streptokinase and Tissue Plasminogen Activator for Occluded Coronary Arteries. *J Am Coll Cardiol* 30:171–179

Mandinov L, Eberli FR, Seiler C et al (2000) Diastolic heart failure. *Cardiovasc Res* 45:813–825

Mann DL (1999) Mechanisms and Models in Heart Failure: A Combinatorial Approach *Circulation* 100:999-1008

Manning BD and Cantley LC (2007) AKT/PKB signaling: navigating downstream. *Cell* 129:1261–1274

Manso AM, Elsherif L, Kang SM et al (2006) Integrins, membrane-type matrix metalloproteinases and ADAMs: potential implications for cardiac remodeling. *Cardiovasc Res* 69:574-584

Matsumoto-Ida M, Takimoto Y, Aoyama T et al (2006) Activation of TGF- β 1-TAK1-p38 MAPK pathway in spared cardiomyocytes is involved in left ventricular remodeling after myocardial infarction in rats *Am J Physiol (Heart Circ Physiol)* 290: H709-H715

Matsusaka H, Tomomi I, Matsushima S et al (2006) Targeted deletion of matrix metalloproteinase 2 ameliorates myocardial remodeling in mice with chronic pressure overload. *Hypertension* 47:711-717

Maytin M and Colucci WS (2002) Molecular and cellular mechanisms of myocardial remodeling *J Nucl Cardiol* 9:319 –327

Marso SP and Stern DM (2003) Diabetes and cardiovascular disease: integrating science and clinical medicine. Lippincott Williams and Wilkins, pp 56-74

Marwick TH (2006) Diabetic heart disease. *Heart* 92:296–300

Mazumder PK, O'Neill BT, Roberts MW et al (2004). Impaired cardiac efficiency and increased fatty acid oxidation in insulin-resistant ob/ob mouse hearts. *Diabetes* 53: 2366–2374

McCulloch DK (2010). Management of persistent hyperglycemia in type 2 diabetes mellitus. In: UpToDate online textbook. Available via <http://www.uptodate.com>

Accessed 24th September 2010

McKelvie RS, Yusuf S, Pericak D et al (1999) Comparison of candesartan, enalapril, and their combination in congestive heart failure: randomized evaluation of strategies

for left ventricular dysfunction (RESOLVD) pilot study. The RESOLVD Pilot Study Investigators. *Circulation* 100:1056–1064

McKinsey TA and Olson EN (2005) Toward transcriptional therapies for the failing heart: chemical screens to modulate genes. *J Clin Invest* 115(3):538–546

McMullen JR, Shioi T, Zhang Li et al (2004) Deletion of ribosomal S6 kinases does not attenuate pathological, physiological, or insulin-like growth factor 1 receptor-phosphoinositide 3-kinase-induced cardiac hypertrophy. *Mol Cell Biol* 24:6231-6240

McMullen JR, Sherwood MC, Tarnavski O et al (2004) Inhibition of mTOR signaling with rapamycin regresses established cardiac hypertrophy induced by pressure overload. *Circulation* 109:3050-3055

McNeill JH (1999) Experimental models of diabetes. Informa Health Care, UK. pp 41-68

MERIT-HF Study Group (1999) Effect of metoprolol CR/XL in chronic heart failure: metoprolol CR/XL randomized intervention trial in congestive heart failure. *Circulation* 100:2001–2007

Metzger JM, Wahr PA, Michele DE, Albayya F et al (1999) Effects of myosin heavy chain isoform switching on Ca²⁺-activated tension development in single adult cardiac myocytes. *Circ Res* 84: 1310-1317

Miner EC and Miller WL (2006) A Look Between the Cardiomyocytes: The Extracellular Matrix in Heart Failure. *Mayo Clinic Proceedings* 81(1): 71-76

Mizushige K, Yao L, Noma T et al (2000). Alteration in left ventricular diastolic filling and accumulation of myocardial collagen at insulin resistant prediabetic stage of a type II diabetic animal model. *Circulation* 101:899-1009

Montori VM and Fernández-Balsells M (2009) Glycemic Control in Type 2 Diabetes: Time for an Evidence-Based About-Face? *Diabetes Care* 150(11):803-808

Movassat J, Le Bailbe D, Lubrano-Berthelie C et al (2008) Follow-up of GK rats during prediabetes highlights increased insulin action and fat deposition despite low insulin secretion. *Am J Physiol Endocrinol Metab* 294: E168–E175

Nathan DM, Cleary PA, Backlund JY et al (2005) Intensive diabetes treatment and cardiovascular disease in patients with type 1 diabetes. *N Engl J Med* 353:2643-2653

Nathan DM, Davidson MR, DeFronzo RA et al (2007) Impaired fasting glucose and impaired glucose tolerance. *Diabetes Care* 30(3): 753-759

National Horizon Scanning Centre Clinical guidelines CG108 (2010). Available via: <http://guidance.nice.org.uk/CG108> Accessed 22nd December 2010

National heart lung and blood institute working group on cellular and molecular mechanisms of diabetic cardiomyopathy (1998) Available via: <http://www.nhlbi.nih.gov/meetings/workshops/diabmin.htm> Accessed 2nd July 2009

Nagoshi T, Matsui T, Aoyama T et al (2005) PI3K rescues the detrimental effects of chronic Akt activation in the heart during ischemia/reperfusion injury. *J Clin Invest* 115(8):2128–2138

Narula J, Haider N, Virmani R (1996) Apoptosis in myocytes in end-stage heart failure. *N Engl J Med* 335:1182–1189

National Institute for Health and Clinical Excellence (2003). Management of chronic heart failure in adults in primary and secondary care. Clinical guideline CG5. London: NICE; July 2003

Available via: <http://www.nice.org.uk/nicemedia/pdf/CG5NICEguideline.pdf>
Accessed 22nd May 2010

Nemoto O, Kawaguchi M, Yaoita H, Miyake K et al (2006) Left ventricular dysfunction and remodeling in streptozotocin-induced diabetic rats. *Circ J* 70:327-334

Nielsen C and Lange T (2005) Blood glucose and heart failure in nondiabetic patients. *Diabetes Care* 28:607-611

Neubauer S, Horn M, Naumann A et al (1995) Impairment of energy metabolism in intact residual myocardium of rat hearts with chronic myocardial infarction. *J Clin Invest* 95:1092–1100.

Nichols GA, Hillier TA, Brown JB (2008) Normal Fasting Plasma Glucose and Risk of type 2 Diabetes Diagnosis. *Am J Med* 121:519-524

Nichols GA, Hillier TA, Erbey JR et al (2001) Congestive heart failure in type 2 diabetes: prevalence, incidence, and risk factors. *Diabetes Care* 24:1614–1619

Nishikawa N, Yamamoto K, Sakata Y et al (2003) Differential activation of matrix metalloproteinases in heart failure with and without ventricular dilatation. *Cardiovasc Res* 57:766-774

Noda N, Hayashi H, Satoh H, Terada H et al (1993) Ca²⁺ transients and cell shortening in diabetic rat ventricular myocytes. *Jpn Circ J* 57: 449-457

Nukatsuka M, Yoshimura Y, Nishida M, Kawada J (1990) Allopurinol protects pancreatic beta cells from the cytotoxic effect of streptozotocin: in vitro study. *J Pharmacobiodyn* 13:259–262

Office for National Statistics, Mortality statistics: Deaths registered in 2008, DR_08. Newport: Office for National Statistics, 2008 Available via: http://www.statistics.gov.uk/downloads/theme_health/DR2008/DR_08.pdf
Accessed 22nd May 2010

Okayama H, Hamada M and Hiwada K (1994) Contractile dysfunction in the diabetic-rat heart is an intrinsic abnormality of the cardiac myocyte. *Clin Sci (Colch)* 86:257–262

O'Neill BT and Abel ED (2005) Akt1 in the cardiovascular system: friend or foe? *J Clin Invest* 115(8): 2059–2064

Olivetti G, Abbi R, Quaini F et al (1997) Apoptosis in the failing human heart. *N Engl J Med* 336:1131–1141

Olson EN and McKinsey TA (2005) Toward transcriptional therapies for the failing heart: chemical screens to modulate genes. *J Clin Invest* 115(3):538-546

Ostenson CG, Khan A, Abdel-Halim SM et al (1993). Abnormal insulin secretion and glucose metabolism in pancreatic islets from the spontaneously diabetic GK rat. *Diabetologia* 36: 3–8

Owan TE, Hodge DO, Herges RM et al (2006) Trends in prevalence and outcome of heart failure with preserved ejection fraction. *N Engl J Med* 355(3):251-259

Packer M, Carver JR, Rodeheffer RJ et al (1991) Effect of oral milrinone on mortality in severe chronic heart failure. *N Engl J Med* 325:1468–1475

Packer M (1992) The neurohormonal hypothesis: a theory to explain the mechanism of disease progression in heart failure. *J Am Coll Cardiol* 20:248-254

Packer M (2002) The impossible task of developing a new treatment for heart failure. *J Card Fail* 8:193–196

Parker TG, Packer SE, Schneider MD (1990). Peptide growth factors can provoke "fetal" contractile protein gene expression in rat cardiac myocytes. *J Clin Invest* 85: 507–514

Parving HH, Tarnow L, Nielsen FS, Rossing P, Mandrup-Poulsen T, Osterby R and Nerup J (1999) Cyclosporine nephrotoxicity in type 1 diabetic patients: A 7-year follow-up study. *Diab Care* 22:478-483

Peter R and Evans MC (2008) Management of diabetes in cardiovascular patients. *Heart* 94:369-375

Available via: <http://heart.bmj.com/cgi/content/extract/94/3/369?maxtosresourcecityCI>
Accessed 31 May 2008

Peterson JT, Hallak H, Johnson L et al (2001) Matrix metalloproteinase inhibition attenuates left ventricular remodeling and dysfunction in a rat model of progressive heart failure. *Circulation* 103:2303-2309

Pfeffer MA, Braunwald E, Moye LA, et al (1992) Effect of captopril on mortality and morbidity in patients with left ventricular dysfunction after myocardial infarction. Results of the Survival and Ventricular Enlargement Trial. *N Engl J Med* 327:669–677

Pierce GN, and Dhalla NS (1985) Heart mitochondrial function in chronic experimental diabetes in rats. *Can J Cardiol* 1: 48-54

Pieske B and Houser SR (2003) $[Na^+]_i$ handling in the failing human heart. *Cardiovasc Res* 57:874-886.

- Pierce GN and Russell JC (1997) Regulation of intracellular Ca^{2+} in the heart during diabetes. *Cardiovasc Res* 34:41-47
- Poirier P, Bogaty P, Garneau C et al (2001). Diastolic dysfunction in normotensive men with well-controlled type 2 diabetes: importance of manoeuvres in echocardiographic screening for preclinical diabetic cardiomyopathy. *Diabetes Care* 24: 5–10
- Poornima IG, Parikh P, Shannon RP (2006) Diabetic cardiomyopathy: the search for a unifying hypothesis. *Circ Res* 98(5):596-605
- Portha B, Serradas P, Bailbe D et al (1991) Beta-cell insensitivity to glucose in the GK rat, a spontaneous nonobese model for type II diabetes. *Diabetes* 40:486–491
- Prediabetes, The silent pandemic (2009) In: The Press and Journal. Available via: <http://www.pressandjournal.co.uk/Article.aspx/1469394?UserKey> Accessed 19th March 2010
- Rakieten N, Rakieten ML, Nadkarni MV (1963) Studies on the diabetogenic action of streptozotocin (NSC-37917). *Cancer Chemother Rep* 29:91–98
- Ramos-Mondragon R, Galindo CA, Avila G (2008) Role of TGF- β on cardiac structural and electrical remodelling. *Vasc Health Risk Manag* 4 (6) 1289-1300
- Regan TJ, CF Wu, Yeh CK et al (1981) Myocardial composition and function in diabetes: The effects of chronic insulin use. *Circ Res* 49:1268-1277
- Redfield MM, Jacobsen SJ, Burnett JC Jr et al (2003). Burden of systolic and diastolic ventricular dysfunction in the community: appreciating the scope of the heart failure epidemic. *JAMA* 289: 194–202
- Reinila A and Akerblom HK (1984) Ultrastructure of heart muscle in short-term diabetic rats: influence of insulin treatment. *Diabetologia* 27: 397–402
- Reinhardt D, Sigusch HH, Hensse J et al (2002) Cardiac remodelling in end stage heart failure: upregulation of matrix metalloproteinase (MMP) irrespective of the underlying disease, and evidence for a direct inhibitory effect of ACE inhibitors on MMP. *Heart* 88:525-530
- Ren J and Bode MA (2000) Altered cardiac excitation-contraction coupling in ventricular myocytes from spontaneously diabetic BB rats *Am J Physiol Heart Circ Physiol* 279: H238-H244
- Ren J and Davidoff AJ (1997) Diabetes rapidly induces contractile dysfunctions in isolated ventricular myocytes. *Am J Physiol* 41: H148–H158
- Ren J, Walsh MF, Hamaty M et al (1998) Altered inotropic response to IGF-I in diabetic rat heart: influence of intracellular Ca^{2+} and NO. *Am J Physiol Heart Circ Physiol* 275: H823-H830
- Ritter O and Ludwig N (2003) The molecular basis of myocardial hypertrophy and heart failure. *Trends Mol Med* 9 (7) 313-321

Riva E, Andreoni G, Bianchi R, Latini R et al (1998) Changes in diastolic function and collagen content in normotensive and hypertensive rats with long-term streptozotocin-induced diabetes. *Pharmacol Res* 37:233–240

Rosenkranz S, Flesch M, Amann K et al (2002) Alterations of beta-adrenergic signaling and cardiac hypertrophy in transgenic mice over-expressing TGF-beta(1) *Am J Physiol Heart Circ Physiol* 283:H1253–1262

Rota M, Lecapitaine N, Hosoda T, Boni A et al (2006) Diabetes promotes cardiac stem cell aging and heart failure, which are prevented by deletion of the p66shc gene. *Circ Res* 99:1–2

Roy S, Sala R, Cagliero E et al (1990) Overexpression of fibronectin induced by diabetes or high glucose: phenomenon with a memory. *Proc Natl Acad Sci U S A* 87:404–408

Rubler S, Dluglash J, Yuceogly YZ et al (1972) New type of cardiomyopathy associated with diabetic glomerulosclerosis. *Am J Cardiol* 30:595–602

Russ, M, Reinauer H, Eckel J (1991) Diabetes-induced decrease in the mRNA coding for sarcoplasmic reticulum Ca²⁺-ATPase in adult rat cardiomyocytes. *Biochem Biophys Res Commun* 178: 906-912

Sabbah Hn (2000) Apoptotic cell death in heart failure. *Cardiovasc Res* 45 (3): 704-712

Sack MN (2009) Type 2 diabetes, mitochondrial biology and the heart *J Mol Cell Cardiol* 46:842-849

Sakaguchi M, Isono M, Isshiki K et al (2006) Inhibition of mTOR signalling with rapamycin attenuates renal hypertrophy in the early diabetic mice. *Biochem Biophys Res Comm* 340(1):296-301

Saraste A, Pulkki K, Kallajoki M, Heikkilä P et al (1999) Cardiomyocyte apoptosis and progression of heart failure to transplantation. *Eur J Clin Invest* 29:380–386

Savabi F and Kirsch A (1992) Diabetic type of cardiomyopathy in food restricted rats. *Can J Physiol Pharm* 70:1040–1047

Schaffer SW, Mozaffari MS, Artman M, Wilson GL (1989) Basis for myocardial mechanical defects associated with non-insulin-dependent diabetes. *Am J Physiol Endocrinol Metab* 256: E25-E30

Schaper J, Froede R, Hein S et al (1991) Impairment of myocardial ultrastructure and changes of the cytoskeleton in dilated cardiomyopathy. *Circulation* 83:504–514

Schainberg A, Riberio-Oliveira Jr A, Riberio JM (2010) Is there a link between glucose levels and heart failure? An update. *Arq Bras Endocrinol Metab* 54(5):488-497

Schannwell CM, Schneppenheim M, Perings S et al (2002) Left ventricular diastolic dysfunction as an early manifestation of diabetic cardiomyopathy. *Cardiol* 98:33 –39

- Schiller M, Javelaud D, Mauviel A (2004) TGF-beta-induced SMAD signaling and gene regulation: consequences for extracellular matrix remodeling and wound healing. *J Dermatol Sci* 35:83–92
- Schultz J, Witt SA, Glascock BJ et al (2002) TGFβ1 mediates the hypertrophic cardiomyocyte growth induced by angiotensin II. *J Clin Invest* 109(6):787–796
- Scrutinio D, Napoli V, Passantino A et al (2000) Low-dose dobutamine responsiveness in idiopathic dilated cardiomyopathy: relation to exercise capacity and clinical outcome. *Eur Heart J* 21: 927–934
- Seccia M, Bettini E, Vulpis V et al (1999) Extracellular matrix gene expression in the left ventricular tissue of spontaneously hypertensive rats. *Blood Press* 8(1):57–64
- Seeland U, Kouchi I, Zolk O et al (2002) Effect of ramipril and furosemide treatment on interstitial remodeling in post-infarction heart failure rat hearts. *J Mol Cell Cardiol* 34:151–163
- Seeland U, Selejan S, Engelhardt S (2007) Interstitial remodeling in beta1-adrenergic receptor transgenic mice. *Basic Res Cardiol* 102:183–193
- Selvetella G, Hirsch E, Notte A et al (2004) Adaptive and maladaptive hypertrophic pathways: points of convergence and divergence. *Cardiovasc Res* 63:373-380
- Semeniuk LM, Kryski AJ, Severson DL (2002) Echocardiographic assessment of cardiac function in diabetic db/db and transgenic db/db-hGLUT4 mice. *Am J Physiol (Heart Circ Physiol)* 283: H976–H982
- Sharma K, Dhingra S, Khaper N and Singal PK (2007) Activation of apoptotic processes during transition from hypertrophy to heart failure in guinea pigs. *Am J Physiol (Heart Circ Physiol)* 293: H1384-H1390
- Shaw JE, Zimmet PZ, Hodge AM (2000) Impaired Fasting Glucose: How Low Should it Go? *Diabetes Care* 23:34-39
- Sherwood L (2008) *Human physiology: from cells to systems* (7th edition). Brooks/Cole, Belmont, USA, Pp 303-333.
- Shi SR, Key ME, and Kalra KL (1991) Antigen retrieval in formalin-fixed, paraffin-embedded tissues: An enhancement method for immunohistochemical staining based on microwave oven heating of tissue sections. *J Histochem Cytochem* 39: 741–748
- Shiojima I, Sato K and Izumiya Y et al (2005) Disruption of coordinated cardiac hypertrophy and angiogenesis contributes to the transition to heart failure. *115(8):2108–2118*
- Sidell RJ, Cole MA, Draper NJ et al (2002) Thiazolidinedione treatment normalizes insulin resistance and ischemic injury in the Zucker fatty rat heart. *Diabetes* 51: 1110–1117
- Singh J, Chonkar A, Bracken N, Adeghate E et al (2006) Effect of streptozotocin-induced type 1 diabetes mellitus on contraction, calcium transient, and cation contents in the isolated rat heart. *Ann N Y Acad Sci* 1084:178 –190

- Sivasubramanian N, Coker ML, Kurrelmeyer KM et al (2001) Left ventricular remodeling in transgenic mice with cardiac restricted overexpression of tumor necrosis factor. *Circulation* 104:826-831
- Skern R, Frost P and Nilsen F (2005) Relative transcript quantification by QPCR: roughly right or precisely wrong? *BMC Mol Biology* 6:10
- Smoak IW (2004) Hyperglycemia-induced TGF β and fibronectin expression in embryonic mouse heart. *Dev Dyn* 231(1):179-189
- Solomon SD, StJohn SM, Lamas GA et al (2002) Survival and Ventricular Enlargement (SAVE) Investigators. Ventricular remodeling does not accompany the development of heart failure in diabetic patients after myocardial infarction. *Circulation*. 106:1251–1255
- Song LS, Sobie EA, McCulle S et al (2006) Orphaned ryanodine receptors in the failing heart. *Proc Natl Acad Sci USA* 103:4305–4310
- Sovari AS and Dudley SC (2010) Using Serum transforming growth factor- β to predict myocardial fibrosis. *Circ Res* 106:e3
- Spinale FG (2007). Myocardial matrix remodeling and the matrix metalloproteinases: influence on cardiac form and function. *Physiol Rev* 87:1285–1342
- Spinale FG, Coker ML, Krombach SR et al (1999) Matrix metalloproteinase inhibition during the development of congestive heart failure: effects on left ventricular dimensions and function. *Circ Res* 85:364-376
- Spinetti G, Kraenkel N, Emanuelli C et al (2008) Diabetes and vessel wall remodelling: from mechanistic insights to regenerative therapies. *Cardiovasc Res* 78(2): 265-273
- Stahrenberg R, Edelmann F, Mende M et al (2010) Association of glucose metabolism with diastolic function along the diabetic continuum. *Diabetologia* 53(7): 1331–1340
- Stilli D, Bocchi L, Berni R et al (2006) Correlation of α -skeletal actin expression, ventricular fibrosis and heart function with the degree of pressure overload cardiac hypertrophy in rats. *Exp Physiol* 91:571-580
- Stone PH, Muller JE, Hartwell T et al (1989) MILIS Study Group. The effect of diabetes mellitus on prognosis and serial left ventricular function after acute myocardial infarction: contribution of both coronary disease and diastolic left ventricular dysfunction to the adverse prognosis. *J Am Coll Cardiol* 14: 49–57
- Stratton IM, Adler AI, Neil HA et al (2000) Association of glycaemia with macrovascular and microvascular complications of type 2 diabetes (UKPDS 35): prospective observational study. *BMJ* 321:405-412
- Swedberg K, Cleland J, Dargie H et al (2005) Guidelines for the diagnosis and treatment of chronic heart failure: Executive summary (Update 2005). *Eur Heart J* 26: 1115-1140
- Swynghedauw B, Delcayre C, Samuel JL et al (2010) Molecular mechanisms in evolutionary cardiology failure. *Ann NY Acad Sci* 1188:58-67

Syrový I and Hodný Z (1992) Non-enzymatic glycosylation of myosin: effects of diabetes and ageing. *Gen Physiol Biophys* 11(3):301–307

Tamada A, Hattori Y, Houzen H, Yamada Y et al (1998) Effects of beta adrenoceptor stimulation on contractility, intracellular calcium and calcium current in diabetic rat cardiomyocytes. *Am J Physiol* 43:H1849-H1853

Tan SM, Zhang Y, Connelly KA (2010), Targeted inhibition of activin receptor-like kinase 5 signaling attenuates cardiac dysfunction following myocardial infarction. *Am J Physiol Heart Circ Physiol*; 298: H1415-425

Taegtmeyer H, Sen S, Vela D (2010) Return to the fetal gene program. *Ann NY Acad Sci* 1188: 191–198

Tellez JO, Dobrzynski H, Greener ID et al (2006). Differential expression of ion channel transcripts in atrial muscle and sinoatrial node in rabbit. *Circ Res* 99(12):1384-1393

The SOLVD Investigators (1991) Effect of enalapril on survival in patients with reduced left ventricular ejection fractions and congestive heart failure. *N Engl J Med*.325:293–302

Thomas D, McCormick R, Zimmerman S et al (1992) Aging and training induced alterations in collagen characteristics of rat left ventricle and papillary muscle. *Am J Physiol (Heart Circ Physiol)* 32(263) H778–H783

Thompson EW (1988) Structural manifestations of diabetic cardiomyopathy in the rat and its reversal by insulin treatment. *Am J Anat* 182:270–282

Thrainsdóttir IS, Aspelund T, Thorgeirsson G et al (2005) The association between glucose abnormalities and heart failure in the population based Reykjavik study. *Diabetes Care*. 28:612-616

Tominaga M, Eguchi H, Manaka H et al (1999) Impaired glucose tolerance is a risk factor for cardiovascular disease, but not impaired fasting glucose: The Funagata Diabetes Study. *Diabetes Care*. 22:920-924

Tschope C, Walther T, Koniger J et al (2004) Prevention of cardiac fibrosis and left ventricular dysfunction in diabetic cardiomyopathy in rats by transgenic expression of the human tissue kallikrein gene. *FASEB J* 18:828–835

Turk J, Corbett JA, Ramanadham S et al (1993) Biochemical evidence for nitric oxide formation from streptozotocin in isolated pancreatic islets. *Biochem Biophys Res Commun* 197:1458–1464

UK Prospective Diabetes Study (UKPDS) Group (1998) Effect of intensive blood-glucose control with metformin on complications in overweight patients with type 2 diabetes (UKPDS 34) *Lancet* 352:854-654

Vander AJ, Sherman JH, Luciano DS (2007) *Human physiology: the mechanisms of body function*. McGraw Hill, Columbus, OH, USA, pp 701-830

Van Heerebeek L, Hamdani N, Handoko L et al (2008) Diastolic Stiffness of the Failing Diabetic Heart Importance of Fibrosis, Advanced Glycation End Products, and Myocyte Resting Tension Circulation 117:43-51

Van Linthout S, Seeland U, Riad A et al (2008) Reduced MMP-2 activity contributes to cardiac fibrosis in experimental diabetic cardiomyopathy. Basic Res Cardiol 103:319-327

Van Melle JP, Bot M, De Jonge P et al (2010) Diabetes, Glycemic Control, and New-Onset Heart Failure in Patients with Stable Coronary Artery Disease: Data from the Heart and Soul Study. 33(9) 2084-2089

Van Kujik J, Jan Flu W, Valentijn TM and Chonchol M (2010) Influence of Left Ventricular Dysfunction (Diastolic Versus Systolic) on Long-Term Prognosis in Patients With Versus Without Diabetes Mellitus Having Elective Peripheral Arterial Surgery. Am J Cardiol 106 (6):860-864

Vasan RS, Larson MG, Benjamin EJ et al (1997) Left ventricular dilation and the risk of congestive heart failure in people without myocardial infarction. N Engl J Med 336:1350-1355

Verny C (2007) Congestive heart failure in the elderly diabetic. Diabetes Metab 33(1) S32-S39

Verrecchia F and Mauvel A (2007) Transforming growth factor beta and fibrosis. World J Gastroenterol 13(22):3065-3062

Villar AV, Cobo M, Llano M et al (2009) Plasma levels of transforming growth factor-beta1 reflect left ventricular remodeling in aortic stenosis. PLoS ONE 4:e8476

Waagstein F, Bristow MR, Swedberg K et al (1993) Beneficial effects of metoprolol in idiopathic dilated cardiomyopathy. Lancet 342:1441-1446

Walker AC and Spinale FG (1999) the structure and function of the cardiac myocyte: a review of fundamental concepts. J Thorac Cardiovasc Surg 118:375-382

Wang X, Beugnet A, Murakami M et al (2005) Distinct signalling events downstream of mTOR cooperate to mediate the effects of Amino acids and insulin on initiation factor 4E-Binding proteins. Mol Cell Biol 25 (7):2558-2752

Wang J, Song Y, Wang Q et al (2006) Causes and Characteristics of Diabetic Cardiomyopathy Rev Diabet Stud 3(3):108-117

Wasserstrom JA, Sharma R, Kapur S et al (2009) Multiple Defects in Intracellular Calcium Cycling in Whole Failing Rat Heart. Circulation: Heart Failure 2: 223-232

Weir GC, Clore ET, Zmachinski CJ and Bonner-Weir S (1981) Islet secretion in a new experimental model for non-insulin dependent diabetes. Diabetes: 30:570-595

Wencker D, Chandra M, Nguyen K et al (2003) A mechanistic role for cardiac myocyte apoptosis in heart failure. J Clin Invest 111:1497-1504

Wold LE and Ren J (2004) Streptozotocin directly impairs cardiac contractile function in isolated ventricular myocytes via a p38 map kinase-dependent oxidative stress. *Biochem Biophys Res Commun* 318 (4):1066-1071

Wong AKF, Donnelly L, Doney A et al (2010) Glycaemic control and the development of heart failure and its importance in diabetic patients with established heart failure. Abstracts from the European Society of Cardiology 2010 Congress
Available via: www.escardio.org/congresses/esc-2010/ Accessed: 22nd December 2010

Wu L, Derynck (2009) Essential role of TGF- β signalling in glucose-induced cell hypertrophy. *Dev Cell* 17:35-48

Wickenden AD, Kaprielian R, Kassiri Z et al (1998) The role of action potential prolongation and altered intracellular calcium handling in the pathogenesis of heart failure. *Cardiovasc Res* 37 (2):312-323

Xia Z, Kuo KH, Nagareddy PR, Guo FWX et al (2007) N-acetylcysteine attenuates PKC β_2 overexpression and myocardial hypertrophy in streptozotocin-induced diabetic rats *Cardiovas Res* 73(4):770-782

Yagi K, Shokei K, Wanibuchi H et al (1997) Characteristics of diabetes, blood pressure and cardiac and renal complications in otsuka long-evans tokushima fatty rats. *Hypertension* 29:728-735

Yamamoto M, Jia DM, Fukumitsu KI et al (1999) Metabolic abnormalities in the genetically obese and diabetic Otsuka Long-Evans Tokushima Fatty rat can be prevented and reversed by alpha-glucosidase inhibitor. *Metabolism* 48:347-354.

Yanni J, Tellez JO, Sutyagin PV et al (2010) Structural remodelling of the sinoatrial node in obese old rats. *J Mol Cell Cardiol* 48(4):653-662

Yang Y, Wang J, Qin L et al (2007) Rapamycin Prevents Early Steps of the Development of Diabetic Nephropathy in Rats. *Am J Nephrol* 27:495-502

Yaras N, Ugur M, Ozdemir S, Gurdal H, Purali N et al (2005) Effects of diabetes on ryanodine receptor Ca release channel (RyR $_2$) and Ca $^{2+}$ homeostasis in rat heart. *Diabetes* 54:3082–3088

Yasushi A, Tomoda M, Murata Y, Inui H et al (2007) Antidiabetic effect of long-term supplementation with *Siraitia grosvenori* on the spontaneously diabetic Goto–Kakizaki rat. *Br J Nutr* 97:770-775

Yu Z, Tibbits GF, McNeill JH (1994) Cellular functions of diabetic cardiomyocytes: contractility, rapid-cooling contracture, and ryanodine binding. *Am J Physiol* 266: H2082–H2089

Zannad F, Braincon S, Juilliere Y et al (1999) Incidence, clinical and etiologic features, and outcomes of advanced chronic heart failure: the EPICAL Study. *Epidemiologie de l'Insuffisance Cardiaque Avancee en Lorraine. J Am Coll Cardiol* 33:734-742

Zhang H, Chen X, Gao E et al (2010) Increasing Cardiac Contractility After Myocardial Infarction Exacerbates Cardiac Injury and Pump Dysfunction. *Circ Res* 107:800-809

Zhang Y, Kanter EM, Laing JG, Aprhys C et al (2008) Connexin43 expression levels influence intercellular coupling and cell proliferation of native murine cardiac fibroblasts. *Cell Commun Adhes* 15(3):289-303

Zheng H, Mayhan WG, Bidasee KR et al (2005) Blunted nitric oxide-mediated inhibition of sympathetic nerve activity within the paraventricular nucleus in diabetic rats. *Am J Physiol Regul Integr Comp Physiol* 290: R992–R1002

Zhou YP, Ostenson C, Ling ZC and Grill V (1995) Deficiency of pyruvate dehydrogenase activity in pancreatic islet cells of diabetic GK rats. *Endocrinology* 136:3546-355

Zhou YT, Grayburn P, Karim A et al (2000) Lipotoxic heart disease in obese rats: implications for human obesity. *Proc Natl Acad Sci U S A* 97: 1784–1789

Zimmet PZ and Alberti KG (2006) Globalisation and the non-communicable disease epidemic. *Obesity* 14(1): 1-3

Ziyadeh FN (2004). Mediators of diabetic renal disease: the case for TGF- β as the major mediator. *J Am Soc Nephrol* 15 (1):S55–S57



COMMUNICATIONS**Papers**

D'Souza A, Hussain M, Howarth FC, Woods NM, Bidasee K, Singh J (2009) Pathogenesis and pathophysiology of accelerated atherosclerosis in the diabetic heart. *Mol Cell Biochem* 331(1-2) 89-116.

D'Souza A, Howarth FC, Yanni J, Boyett MR, Dobryznski H, Bidasee KR & Singh J. Left Ventricle Structural Remodelling in the Prediabetic Goto-Kakizaki Rat. (Accepted for publication, *Exp Physiol*).

D'Souza A, Howarth FC, Yanni J, Boyett MR, Dobryznski H, Bidasee KR & Singh J. Chronic Effects of Mild Hyperglycemia on Left Ventricle Transcriptional Profile and Structural Remodelling in the Spontaneously Diabetic Goto-Kakizaki Rat. (In peer review process, *Biochemical Pharmacol*, submitted 1/05/2011)

Abstracts in Edited Conference Proceedings

D'Souza A, Woods NM and Singh J (2008) Cation contents in the isolated rat heart and aorta during STZ-induced type-1 DM. *Fundam Clin Pharmacol*, Abstracts of the EPHAR 2008 Congress, 22:9

D'Souza A, Woods NM and Singh J (2009) Investigation of histological and physiological alterations underlying cardiomyopathy in the STZ-induced type-1 diabetic rat heart. *Proceedings of the 6th annual conference for medical students in the GCC countries*. 67

D'Souza A, Woods NM and Singh J (2009) Temporal Characteristics of Phenotypic Alteration and its Functional Correlate in the STZ-induced Diabetic Rat Heart: Preliminary Observations. *Proc Physiol Soc* 15, PC104

Al Kitbi M, Howarth FC, Singh J, **D'Souza A** (2010) Effects of type 1 and type 2 diabetes on contractile proteins of the isolated rat heart. *Proceedings of the 7th annual conference for medical students in the GCC countries*. 67.

D'Souza A, Boyett M, Dobryznski H, Yanni J and Singh J (2010) Remodelling of the left ventricle in the Goto-Kakizaki rat. *Proc Physiol Soc* 15, OC20 [Winner of the Best Presentation Prize at the metabolism and endocrinology themed meeting of the Physiological Society, AstraZeneca, Macclesfield, July 2010]
